Functional diversity of extracellular matrix components during vessel migration, endothelial sprouting and blood vessel stabilization

Denise Stenzel

University College London

and

Cancer Research UK London Research Institute

PhD supervisor: Dr. Holger Gerhardt

A thesis submitted for the degree of

Doctor of Philosophy,

University College London, 2009

Meinen Eltern,

Erika und Holger

I, Denise Stenzel confirm that the work presented in this thesis is my own. Where information has been derived from other sources, I confirm that this has been indicated in the thesis.

1 Abstract

The formation of mature blood vessels requires recruitment of mural cells (MC) and generation of an extracellular matrix in order to stabilize and support the nascent vessel. The precise sequence of basement membrane protein expression and function during initiation, elongation and stabilization of the angiogenic sprout remains unclear.

The first project describes a function of astrocytic Fibronectin (FN) in guided vessel migration. Integrin-binding is dispensable for fibrilliar FN assembly but mediates endothelial cell adhesion *in vivo*. VEGF-A dependent migration of retinal vessels requires PI3K activity and astrocytic FN possibly functions to retain VEGF protein on the astrocytic matrix.

In a second project we discovered endothelial tip cells-specific expression of laminin alpha4 (*Lama4*) and provide first evidence for an influence of laminin α4 on endothelial Dll4/Notch signalling in sprouting angiogenesis. Loss of *Lama4* leads to increased filopodia formation, tip cell numbers and consequently increased vessel density, resembling the phenotype of disturbed Dll4/Notch signalling. Loss of *Lama4* leads to reduced *Dll4* and Notch target gene expression, whereas gain-of-function results in increased *Dll4* expression *in vitro*. Preliminary results suggest that laminin α4 induced *Dll4* expression involves both VEGFR2 and integrin signalling.

The third project addresses the cell-autonomous requirement of heparan sulfate (HS) production by MCs during mouse embryonic vascular development. Conditional deletion of HS synthesis in MC caused severe vascular defects and embryonic lethality. Unexpectedly, distinct regions of vascular growth showed selective requirement for MC HS production: whereas MC recruitment in peripheral skin vascularization is severely disrupted, MCs during brain angiogenesis appear unaffected. Similarly, PDGF-B and TGF-β signalling are impaired in the peripheral vessels, but not in the brain.

These data suggest that cell-autonomous HS is essential for MC recruitment in the skin vasculature, where induction and differentiation of local progenitor cells from the mesenchymal cell lineage is mediated by TGF-β signalling. (299 words)

2 Acknowledgment

First and most importantly, I would like to thank my parents who I dedicated this thesis to- you mean the world to me.
Ich widme diese Arbeit meinen Eltern, Erika und Holger Stenzel. Und danke meiner Familie, insbesondere meinem Bruder, Stefan sowie meinen Eltern für ihre endlose Geduld, Grenzenüberschreitende Unterstützung und lieben, aufmunternden Worte. Ihr seid die treibende Kraft und ohne Euch und eure ununterbrochene Motivation wäre es mir nie möglich gewesen diesen Weg zu gehen. Ich liebe euch aus tiefsten Herzen. Danke, dass ihr immer für mich da seid.

I would like to express a huge thank you to my supervisor Holger Gerhardt. You have been without doubt a great teacher and an inspiration throughout my PhD. You taught me endurance, patience and persistence with attention to detail, -"The devil lies in the detail"-. I am extremely grateful for the opportunity working with you and have been fortunate to receive your encouragement and support. I couldn't have asked for a better mentor.
I would like to extend my deepest gratitude to the past and current members of the vascular biology lab, Andrea Lundkvist, Per Lindblom, Li-Kun Phng, Marta Busse, Jane Babbage, Dominique Sauvaget, Claudio Franko, Lars Jakobsson, Giovanni Mariggi and 'part-lab member' Mariona Graupera for scientific discussion but most of all, for the great fun and sociable environment. A very big thank you as well to our 'sister lab', the lymphatic development lab and to many other LRI-based labs for sharing exciting meetings, for extremely helpful input and for reagents urgently needed in last minute, spontaneous experiments.
In particular, I'd like to thank Giovanni, Lars and Sophie. You helped me far beyond understanding my scientific data, you cheered me up at dark stressful days and I'll take your invaluable worldly wisdom wherever I go. Unquestionably, you coped with the worst mood swings possible and I thank you from the bottom of my heart. You certainly brightened up my days.
Thanks Giovanni for teaching me the essential Italian. It surely will be remembered.
Sophie, I thank you for sharing my bad taste in 80s-music. And Dominique, you taught me the basics of molecular biology and genetics, but also introduced me to the best exercise and work out ('body pump').

I thank Cancer Research UK for the generous sponsorship and the support during the whole time of my PhD. I feel fortunate to work in such a prestigious institute with many talented scientists.
I would like to acknowledge several facilities that helped my enormously and considerately contributed to my research: Experimental Pathology, in particular Emma Nye; Peter Jordan from the Light Microscopy and the Electron Microscopy Lab.
A huge thank you to Sue Watling, Craig Thrussell and Claire Darnbrough at the Animal Unit (Portacabin 2) in Clare Hall for helping me with the mouse experiments and taking care of the little fellows. In this aspect, I would like to mention the hundred of mice that scarified their lives.

I would like to thank my collaborators: Maya Nisancioglu, Ralf Adams, Yu Yamaguchi, Vassiliki Kostourou**,** Anna Domogatskaya**,** Sergey Rodin, Karl Tryggvason, Lydia Sorokin, Aarjan van der Flier, Mariette Vogelzang, Richard Hynes, Stephen Robinson and Kairbaan Hodivala-Dilke.
I am thankful for the constructive criticism and advice received from my thesis committee David Ish-Horowicz and Sharon Tooze.

Lastly I would like to thank all the people who have made London my home for almost 5 years. In particular a heartfelt thanks to my flatmates, Jack and Joanne for feeding me and challenging my resistance to spices but most importantly, for all the laughter.
I am extremely thankful to Dan (the best host I've ever met, your dinner and house-parties will be unforgotten), Steffi (the greatest Squash partner I could asked for although still unbeaten), Micha, Denis, Sean, Linda, Tim, Heiko, Thomas…
I also want the express my gratitude to my friends Susan, Yvonne, Mandy, Sabine and Katja –you are surely the best. Danke, dass ihr immer ein offenes Ohr für mich habt und mich auf dem Boden der Tatsachen haltet während der wohl bisher herausfordensten Zeit meines Lebens. Ihr seid grossartig!

Table of Content

Table of Figures

List of Tables

3 Abbreviation

AKT/PKB	protein kinase B
Ang	Angiopoitin
BM	basement membrane
Cdc42	cell division cycle 42
CNS	central nervous system
CSL	CBF/Suppressor of Hairless/LAG2
Dll4	Delta-like 4
DSL	Delta, Serrate and LAG2
E	embryonic day
EC	endothelial cell
ECM	extracellular matrix
ERK1/2	extracellular-signal-regulated kinase-1/2
FA	focal adhesion
FGF	fibroblast growth factor
FN	fibronectin
GFP	green fluorescent protein
Hes	Hairy/ Enhancer of Split
Hey	Hes-related proteins
HGF	Hepatocyte growth factor
HS	heparan sulfate
HSPG	heparan sulfate proteoglycan
IF	immunofluorescence
ILK	integrin linked kinase
ISH	*in situ* hybridization
Itg	integrin
Jag1	Jagged-1
LN	laminin
MAPK	mitogen-activated protein kinase
MC	mural cell
MMP	matrix metalloproteinase
N-cadherin	neuronal cadherin
NG2	chondroitine sulfate proteoglycan 4

NICD	notch intracellular domain
Nrarp	Notch-regulated ankyrin repeat protein
P	postnatal day
PC	pericytes
PDGF	platelet-derived growth factor
PECAM/CD31	platelet/endothelial cell adhesion molecule-1
PI3K	Phosphoinositide 3-kinases
PKA	Protein kinase A
PLC-γ	Phospholipase C gamma
qPCR	quantitative polymerase chain reaction
Rac1	Ras-related C3 botulinum toxin substrate 1
Rho	Ras homolog gene family
RT	room temperature
RTK	receptor tyrosine kinase
siRNA	small interference ribonucleic acid
TGF	transforming growth factor
VE-cadherin	vascular endothelial cadherin
VEGF	vascular endothelial growth factor
VEGFR	vascular endothelial growth factor receptor
vSMC	vascular smooth muscle cell

4 Introduction

4.1 Vascular development and circulatory system

Living organisms must have the ability to transport nutrients, gases and waste to and from cells. Single-cell organisms exchange and interact with their outside environment via their cell surface. Multicellular but primitive-structured organisms, such as the hydra lack specialized organs like blood vessels and hearts, therefore exchanging biological materials through their skin.

Higher developed organisms have developed a circulatory system to sufficiently supply cells with nutrients and oxygen and to remove metabolic waste and carbon dioxide. Insects and arthropods evolved an open circulatory system, pumping blood into cavities, so called hemocoels with blood, lymph and interstitiual fluids diffusing back to the circulatory system between cells. In contrast, vertebrates have a closed circulatory system, i.e. blood does not circulate through cavities but is closed at all times within vessels of different size and wall thickness.

In 1628, William Harvey discovered that the heart pumps the blood around the body through arteries and that veins return blood to the heart {Carmeliet, 2005 #501}. The vascular system of higher vertebrates and humans consist of two main routes, including a heart. Firstly, the pulmonary circulation pumping blood to and from the heart to lungs to exchange gases in the lungs. And secondly, the systematic circulation pumping blood away from the heart out to the body. Both circulatory systems consist of a network of arteries, capillaries, and veins. The pulmonary circulation transports oxygen-depleted blood away from the heart (pulmonary arteries) to the lungs, and returns oxygenated blood back to the heart (pulmonary veins). Arteries of the systematic circulation pump oxygenated blood away from the heart to provide the rest of the body with oxygen and nutrients and deoxygenated blood is returned to the heart by veins.

Artery walls are composed of multiple layers of smooth muscle cells (SMC) and elastic fibres controlling vessel expansion and contraction to regulate the blood pressure. Arteries connect to a complex bed of smaller vessels, so called capillaries that function in the actual exchange of oxygen/CO_2, nutrients and hormones carried by the blood to surrounding cells and tissues. The circulatory loop of the vascular system is completed via veins, carrying deoxygenated blood from the capillaries to the heart.

A network of coronary vessels supplies the heart itself with oxygen and nutrients to maintain cardiac muscle function.

In addition, a secondary circulatory system the so-called lymphatic system collects interstitial fluid that transports materials between cells. Because of the blood hydrostatic and osmotic pressure, blood plasma continuously leaks from the capillaries and lymph vessels return this fluid back to the blood circulation {Carmeliet, 2005 #501}. Lymph flows from small lymphatic capillaries into lymph vessels, connecting to the lymph nodes, lymph organs or the cardiovascular system via the thoracic duct (Purves 2002).

The complex networks of blood and lymphatic vessels not only effective nutrient supply and fluid homeostasis during physiology but are also required for organ growth during development and repair of wounded tissues.

Given the importance of the vascular system in physiology, it is not surprising that vascular dysfunction contributes to many pathologic conditions. The most common disabling and fatal complications of the vascular systems are atherosclerotic injuries. Arthrosclerosis describes a condition of progressive, narrowing and hardening of the arteries that leads to ischemia, cardiovascular infarct or stroke. Ischemia, the lack of blood supply to an organ or tissue is caused by constriction or obstruction of blood vessels. In a wide variety of pathologies, vascular dysfunction causes tissue ischemia followed by new vessel formation. The newly formed vessels are often poorly patterned and leaky vessel, leading to further complications. Cancerous growth requires new vessel formation, and dysfunctional tumour vessels and the presence of lymphatic vessels accelerate metastatic spreading of tumour cells. In cancer, metastasis is the migration and spreading of tumour cells from an original tumour site to other tissues in the body via body and lymph.

4.2 Angiogenesis in pathological condition

Understanding how blood vessels form could lead to great advances in treating vascular diseases such as ischemia by inducing vessels growth and stimulating myocardial angiogenesis (Carmeliet and Jain 2000). However, the majority of pathological conditions are a result of excessive and uncontrolled vessel growth such as cancer and diabetic retinopathy. Is there a possibility to interfere with the mechanism of vessel formation by targeting the molecular key players to suppress vessel growth?

Pathological retinal neovascularization in patients with diabetes is a result of the

imbalance of pro-angiogenic and anti-angiogenic factors, such as the accumulation of vascular endothelial growth factor (VEGF, for detailed description see 4.7) leading to microvascular retinal changes (Campochiaro 2004). Hyperglycemia impaired insulin signalling and adipose-derived adipokines are characteristic features of diabetes playing a pivotal role in diabetes-associated microvascular complications (Bakker, Eringa et al. 2009). Hyperglycemia, an excessive amount of glucose circulating in the blood plasma - induces pericyte apoptosis and thickening of the basement membrane (BM) leading to incompetence of the vascular walls. These damages change the formation of the blood-retinal barrier and also make the retinal blood vessels become hyper-permeable, eventually leading to retinal micro-hemorrhaging.

Sima et al. report on the vascular endothelium in artherosclerosis, pointing out that the activation of endothelial cells may involve the modulation of permeability and of the biosynthesis activity with respect to the synthesis of BM components (Sima, Stancu et al. 2009).

The existence of tumour-derived factors responsible for promoting neovascularization was postulated 70 years ago (Ide et al., 1939) and tumour growth was proposed to be crucially dependent on the development of neovascular supply (reviewed in (Ferrara and Kerbel 2005)). Judah Folkman hypothesized the inhibition of angiogenesis as a concept for anti-tumour therapy in 1971 (Folkman, Merler et al. 1971). Most investigations over the last decades focused on finding inducers and inhibitors as an effective treatment for tumour onset and progression. However, recent data highlight the reciprocal relationship between tumour endothelial cells and its surrounding microenvironment. Endothelial cells (EC) play a critical role in defining the local immune response and provide support for tumour growth and metastasis (reviewed in (Nikitenko 2009) and (Aird 2009)). EC origin has been widely discussed and accepted that ECs derive from either pre-existing vessels or from endothelial progenitor cells (EPCs). In general, EPCs are cells that have the potential to differentiate into ECs receiving pro-angiogenic stimuli. EPCs are mobilized from the bone marrow and/or differentiate from mesenchymal stem cells.

Endothelial cell progenitors and hematopoietic cells share a common bone marrow derived progenitor, putatively termed haemangioblast (Figure 4.1). VEGF family members stimulate these cells to develop into ECs. The microenvironment of various tissues provide the signal for EPC mobilization from original sources (e.g. bone marrow and/ or mesenchymal stem cell) and the niche for their differentiation into mature endothelium during embryogenesis or neovascularization of the adult organism

under physiological and pathological conditions. Likewise to vascular development during embryogenesis, the induction of angiogenesis in the tumour is a consequence of an imbalance between multiple inhibitory and stimulatory molecules, referred as "angiogenic switch". Pro-and anti-angiogenic stimuli trigger tumour vascularization and may be provided and released by tumour cells, EC, stromal cells, blood and extracellular matrix (reviewed in (Nikitenko 2009)).

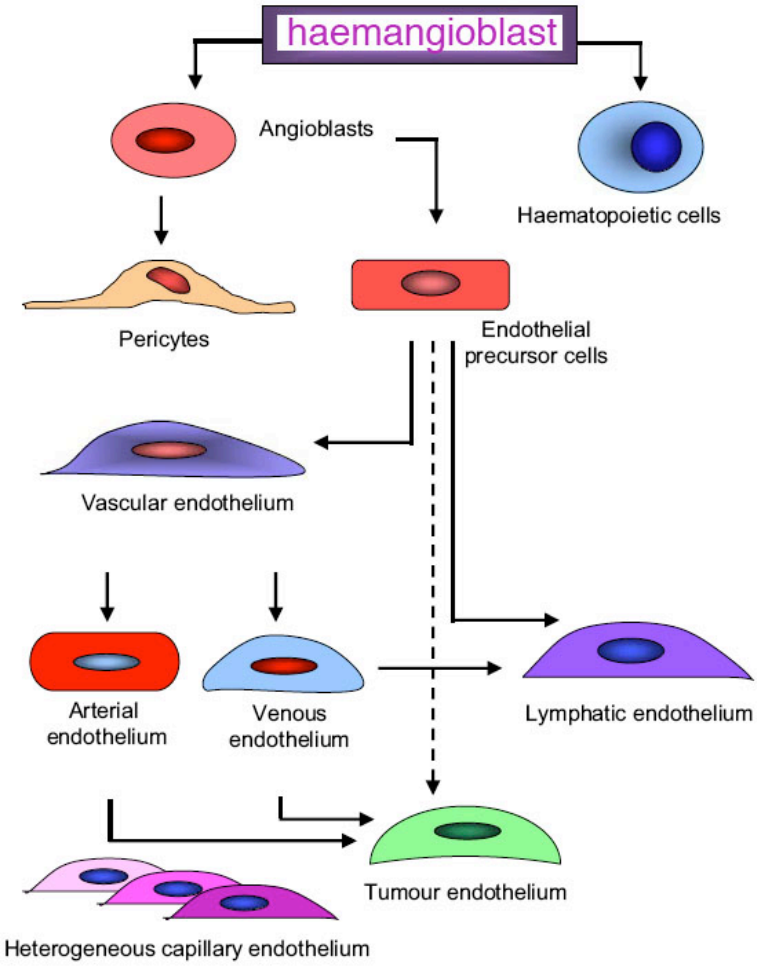

Figure 4.1 Putative pathway of normal and tumour endothelial cell differentiation

Normal endothelial cells are derived from progenitor cells (haemangioblast) that can give rise to both endothelial and blood cells. Angioblasts can give rise to pericytes and smooth-muscle cells, which form the outer walls of most blood vessels, or to endothelial precursor cells. These are committed to becoming either vascular ECs ("endothelioblasts", which are then capable of undergoing arterio-venous specification) or "lymphangioblasts" (committed to becoming lymphatic endothelium). Lymphatic ECs can also trans-differentiate from venous endothelium. "Tumour endothelial cells" in "non-endothelial" tumours derive from either normal endothelium or from endothelial progenitors that acquire specific properties and express specific markers that are not expressed in normal endothelium or tumour endothelial markers (adapted from (Nikitenko 2009)).

The balance of these factors determines the intensity of the vascular response and varies between different types of tumours. A greater vascular density often correlates with metastasis and spreading of tumour cells by gaining access to the circulatory system (Langley and Fidler 2007). The presence of functional lymphatics around the tumour is sufficient for lymphatic metastasis and these tumours do not require intratumour lymphatic for cancer dissemination (Nikitenko 2009).

4.3 Angiogenesis during development

The vascular system is the first organ that arises during embryonic development. Apart from the nutritive function, vessels also provide instructive trophic signals to promote organ morphogenesis (Carmeliet 2005).

Development of the vascular system begins with the aggregation of mesoderm derived angioblast precursors in the embryo and the formation of blood islands in the visceral yolk sac (Rossant and Howard 2002). A close association between the primitive hematopoietic cells and the developing endothelium exists in the yolk sac, suggestive of a common precursor, the so-called haemangioblast. Within the embryo itself, the first blood vessels form in the absence of haematopoiesis, indicating that these precursors are exclusively endothelial precursors or angioblast. The early blood vessels in the embryo or yolk sac develop by aggregation of *de novo* forming angioblasts into a primitive network of simple endothelial tubes- a process known as vasculogenesis (Figure 4.2).

Hierarchical organization and development of a mature vascular system involves a complex process of remodelling and refining the initial pattern by endothelial cell proliferation and sprouting of new vessels from existing ones- the process of angiogenesis (Rossant and Howard 2002). The establishment of a highly organized and functional vascular network is far more complex than suggested by this frequently used division in vasculogenesis and angiogenesis. As vessels start to remodel into a circulatory vascular system, they undergo localized migration into different parts of the body, regulated branching into capillary plexus, proliferation to expand the vessel network as well as vessels regression and pruning (Figure 4.2).

Depending on their function, ECs need to be specialized, vessel calibre will be determined and differentiation of vessels into arteries, veins, capillaries and lymph vessels takes place. Maturation and stabilization of newly formed vessels is

accompanied by the recruitment of mural cells (MC) and the formation of basement membrane (BM).

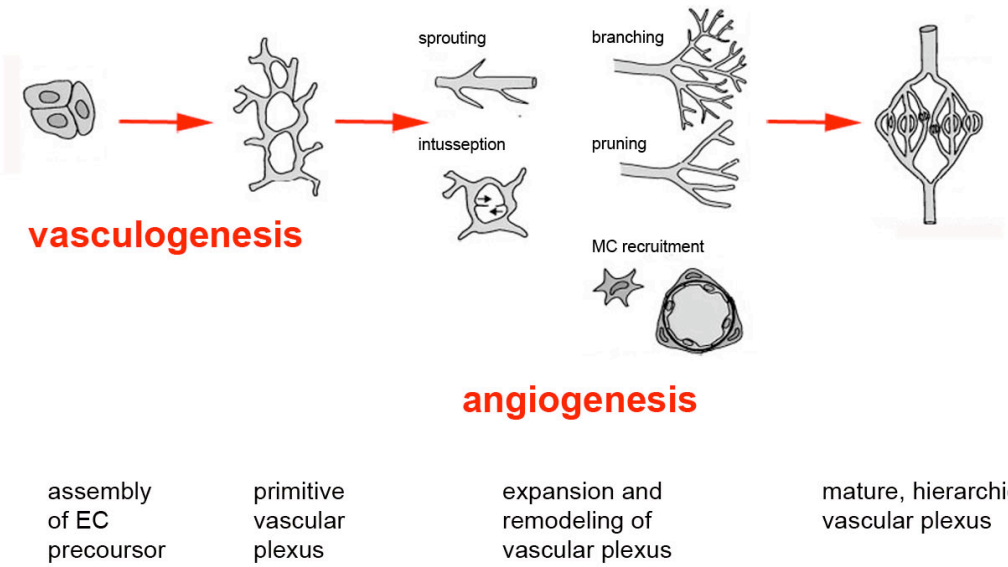

Figure 4.2 Development of a vascular plexus by vasculogenesis and angiogenesis
Development of the vascular system occurs by vasculogenesis and subsequent angiogenesis. Endothelial progenitors assemble and give rise to a primitive vascular labyrinth which further expands during angiogenesis; mural cells (MC) are recruited and the vascular network remodels in a hierarchical plexus consisting of arteries, veins and capillaries (adapted and modified from (Carmeliet 2000)).

Although great efforts were undertaken to understand these processes in more detail within the last decades, we still know very little about the spatial and temporal cues that leads to an a functional mature vascular plexus. Are these processes genetically programmed? What signalling pathways are involved in vascular patterning? Are angiogenic processes coordinated by multiple signalling pathways that interact and interfere with each other? Or is proliferation regulated by one signalling pathway while an other directs migration? What determines branching morphogenesis? How is the fine balance between stimulatory and inhibitory signals controlled? And how do other cell types and matrix components influence vessel formation and patterning?

Angiogenesis in its simplest description is the expansion of the vascular plexus from existing vessels. Expansion and remodelling of the vascular plexus may occur by intussusceptive, collateral and guided angiogenesis and these events likely occur under different circumstances including the absence or presence of blood flow and external stimuli. Remodelling of the vascular plexus by intussuseptive growth involves the enlargement of venules, which sprout or become divided by pillars of periendothelial

cells or by transendothelial cell bridges, which then split into individual capillaries. Collateral growth denotes the expansive growth of pre-existing vessels, forming collateral bridges between arterial networks (reviewed by (Carmeliet 2000)).

Guided angiogenic sprouting involves the specialization of ECs within the growing vessels and requires external stimuli as well as a patterned environment (reviewed in (Roca and Adams 2007);(Gerhardt, Golding et al. 2003); (Hellstrom, Phng et al. 2007)).

4.4 The retinal vasculature -a model system to study sprouting angiogenesis

The idea of precise guidance and directional migration during angiogenesis arose from observations of filopodia rich leading cells (Marin-Padilla 1995) and analogies to other pervasive organ systems such as the axonal guidance by attractive and repulsive forces. Axonal guidance requires the formation of growth factor gradients and axon outgrowth relies on guidance of cells and subcellular processes along predefined tracks, characteristics that have been implicated during guided angiogenesis.

Further, the formation of the insect tracheal system shares many signalling pathways navigating sprouting cells through the tissue that may function in vascular morphogenesis. Additionally both the tracheal system as wells as axonal guidance share structurally and functionally similarities to the vertebrate vasculature (reviewed in (Affolter and Caussinus 2008)). Several cellular and molecular paradigms in *Drosophila* tracheal system, such as cell migration, competition and rearrangement, as well as the elaboration of a complex apical luminal environment might serve related roles in the formation of other branched organs or tissues, such as the retinal vasculature.

VEGF-A controls angiogenic sprouting by guiding filopodial extensions from specialized endothelial cells situated at the tip of vascular sprouts that is rather similar to tracheal cell navigating through the developing embryo. Further studies have shown the distinction of leading tip cells and the following stalk cells in growing angiogenic sprouts that involves notch signalling via the Delta-like 4 (Dll4) ligand. The control of tip cell formation in branching tubules such as the tracheal branches, malpighian tubules and intersegmental vessels of zebrafish are also linked to Delta-Notch signalling (Affolter and Caussinus 2008); (Roca and Adams 2007).

Each angiogenic sprout is composed of two different endothelial cell (EC) types, see

Figure 4.3. The sprouting tip consists of a single, highly polarized EC that extends long actin-rich filopodia. This cell is referred to as tip cell (T), whereas the following ECs trailing the angiogenic tip cell are referred to as stalk cells (S). Stalk cells line the vascular lumen, form firm EC junction and extend comparably less filopodia protrusion. Interestingly, the morphological differences of tip and stalk cells are also reflected in their function and behaviour. Figure 4.4 summarize the characteristics of endothelial tip and stalk cells.

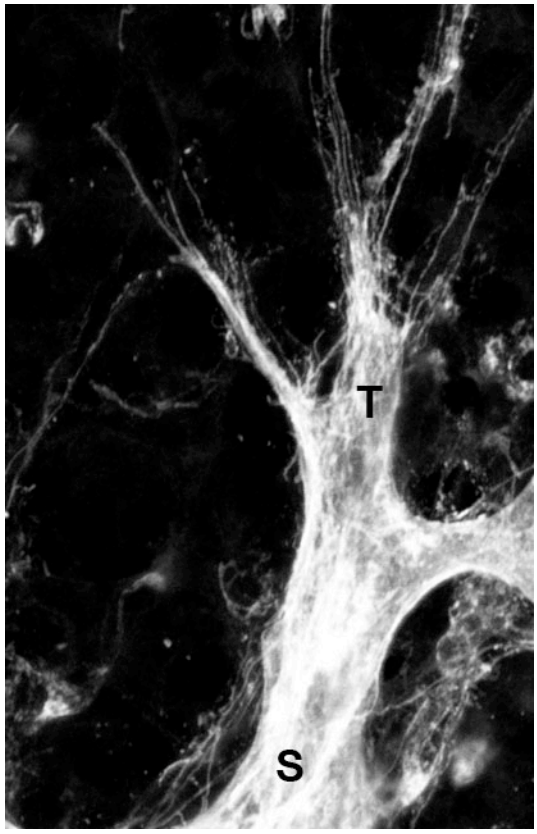

Figure 4.3 Angiogenic sprout

The leading angiogenic sprout consists of two endothelial cell types that differ in their cell morphology, behaviour and gene expression. T- tip cell, S- stalk cell

The tip cell is active, expressing a motile and invasive behaviour in order to migrate in an avascular tissue and to respond in a polarized manner and by directed migration to attractive cues such as growth factor gradients. In contrast, stalk cells are less dynamic but highly proliferative to expand vessel growth in diameter and length. In addition, endothelial stalk cells are polarized cells with an apical surface orientated towards the lumen and a basal surface that is enclosed by BM, indicating that endothelial stalk cell primarily contribute to BM formation (Figure 4.4).

Endothelial tip and stalk cells also differ in their gene expression profile. Tip

cells strongly express the following genes but their expression is not exclusive and therefore, can not considered as truly unique tip cell markers: *Pdgfb*, *Dll4*, *Unc5b*, *Vegfr2* and *Vegfr3* (Gerhardt, Golding et al. 2003); (Claxton and Fruttiger 2004); (Lu, Le Noble et al. 2004); (Tammela, Zarkada et al. 2008). Whereas stalks cells express higher levels of *Robo4* (Huang, Yu et al. 2009) and *Vegfr1*. Thus, the endothelial cell population is heterogeneous in their morphology, cell behaviour and gene expression (quantitatively) but should not be mistaken with a stable cell fate or terminal cell differentiation.

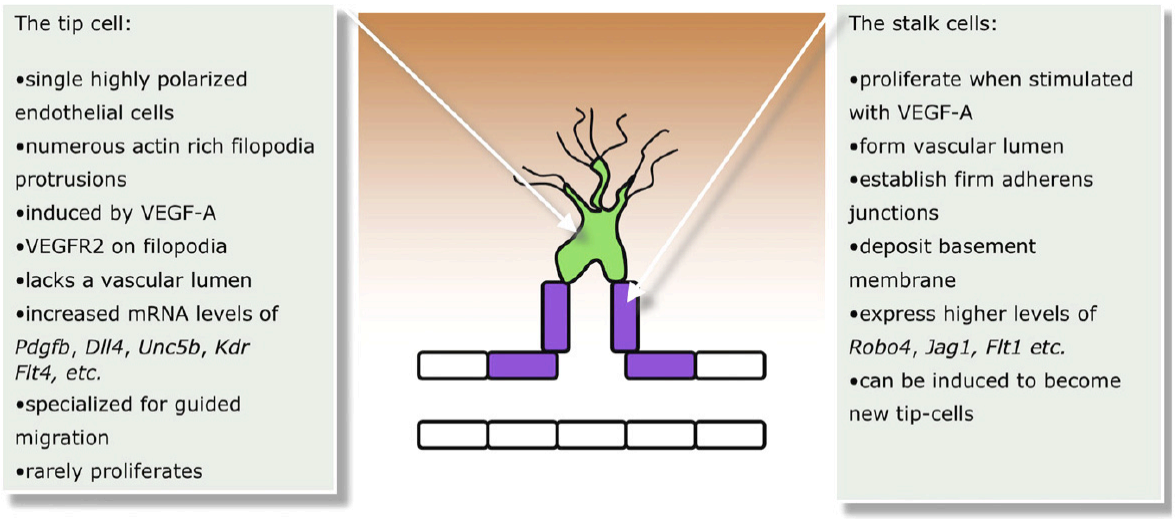

Figure 4.4 Phenotypic and molecular differences between endothelial tip and stalk cells

Tip cells (green) head each vascular sprout stimulated by an extracellular VEGF-A gradient (orange). Following endothelial cells (purple) form the lumenized stalk (Phng and Gerhardt 2009).

Most observations described above addressing angiogenesis on a cellular level are derived from the retinal vasculature. Well-defined patterning events as well as simultaneous vascular sprouting at the periphery and remodelling at the centre, allows to study different aspects of vessel formation, maturation and gene expression in a single preparation. This system, preferably used in our lab, is easily accessible and an ideal structure for visualization and high resolution imaging (Gerhardt, Golding et al. 2003).

The cup-like mouse retinas starts out as an avascular tissue in the embryo. Retinal vascularization begins in the most superficial (or inner) retinal layer at the optic

nerve head and radiates outwards from this central point. It reaches the retinal periphery during the first week of birth (Gariano and Gardner 2005). Similar to the central nervous system (CNS), angiogenic sprouting is the predominant mechanism of vessels growth in the retina however; vessel expansion by intussusception cannot be excluded. The growth pattern facilitates the analysis of the initially planar, two-dimensional vasculature in the retina at great detail (Roca and Adams 2007). Previous work has shown that this rapid and highly directional growth of blood vessels is controlled by a spatial concentration gradient of matrix-anchored vascular endothelial growth factor A (VEGF-A) released by astrocytes in response to local hypoxia (Stone, Itin et al. 1995); (Forsythe, Jiang et al. 1996); (Gerhardt, Golding et al. 2003). VEGF-A is a very potent chemo attractive signal for ECs and promotes the polarized sprouting of specialized endothelial tip cells, at the leading edge of the vascular plexus (Figure 4.5). Whereas the explorative, invasive nature of tip cells leads to an extension of the endothelial network along the VEGF-A gradient, a second process, tubulogenesis, is required for the generation of patent, blood-carrying vessels.

Although angiogenic growth in the retina, like in most other tissues, has so far not been observed dynamically, tip cells can be frequently seen in close contact with other tips, suggesting that the interaction of filopodial processes and, subsequently, cell bodies leads to bridge-like structures in which ECs lack long filopodia and no longer display tip cell features. It may be at this stage that sprouts are converted into new tubules, form anastomoses, and become part of a simple, plexus-like network at the vascular perimeter (Roca and Adams 2007). Each new sprout eventually connects via the leading tip cell with neighbouring sprouts to form continuous lumen and thus, establish blood flow in the new vascular loop (Blum, Belting et al. 2008). The emergence of new endothelial tip cells from the stalk plexus will promote further extension of the vascular network so that growth of the vasculature is presumably achieved through repeated cycles of EC sprouting and tubulogenesis.

Recent data provide support for a model in which the formation and intracellular and intercellular fusion of endothelial vacuoles drives vascular lumen formation (Kamei, Saunders et al. 2006). Using high-resolution time-lapse two-photon imaging of transgenic zebrafish, Kamei and colleagues examined how endothelial tubes assemble *in vivo*, comparing results with time-lapse imaging of human endothelial-cell tube formation in three-dimensional collagen matrices *in vitro*. Their observation proposed a model of pinocytic vesicles formation, followed by fusion and enlargement of intracellular vacuoles and eventually fusion of intercellular vacuolar compartments to

form a patent lumen. *In vitro* data support this model, Bayless and colleagues showed that intracellular vacuoles arise from integrin-dependent and cdc42/Rac1-dependent pinocytic events downstream of integrin-extracellular-matrix signalling interactions (Bayless, Salazar et al. 2000). Although not shown for murine vascular development, it is likely that vacuole fusion is also favourably model for lumen formation during sprouting angiogenesis.

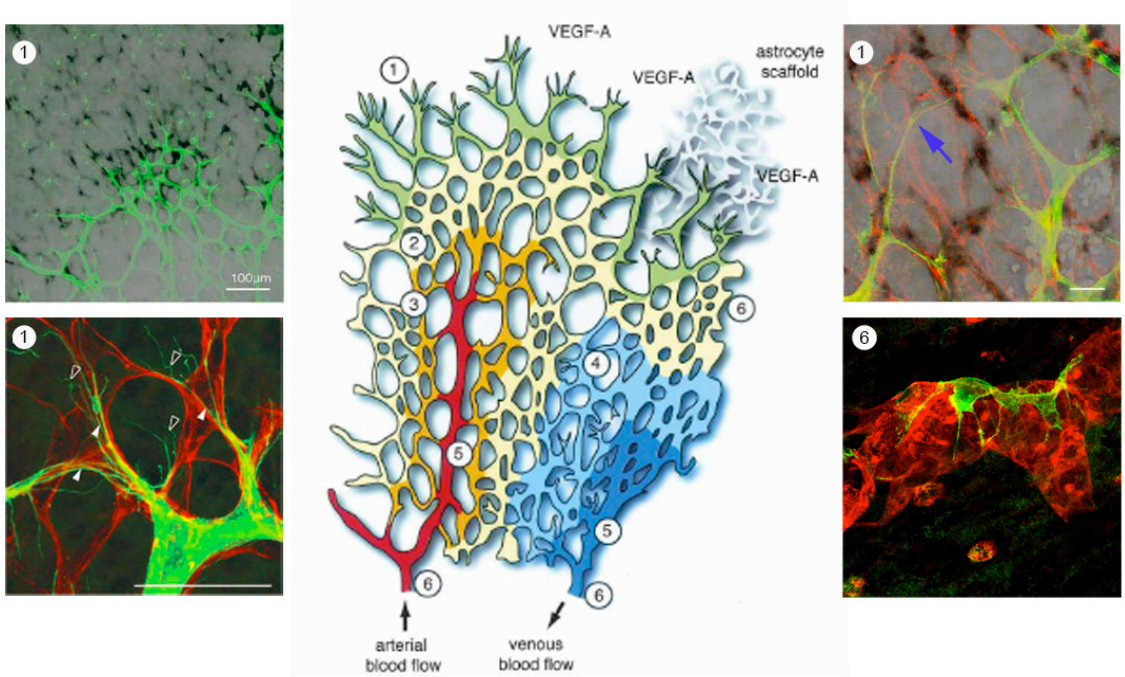

Figure 4.5 Mouse retinal vascular development

In the sprouting zone (1), directional extension of tip cells and filopodia promote vascular growth along a gradient of matrix bound VEGF-A, which is released by astrocytes in response to hypoxia. Upper panel demonstrates *Vegfa* expression (black) by astrocytes (red) ahead of the growing vasculature (green). Lower panel, left: Tip cell extends filopodia (green) that closely align to and follow the astrocytic network (red). Interaction of sprouting tips (blue arrow) and anastomosis generates a plexus of patent but non-hierarchically organized vessels (2). Pruning (3) and secondary sprouting in a perpendicular direction (4) leads to vascularization and remodelling of the retinal vascular plexus. Differentiation of vessels in arteries and veins (5) as well as the recruitment of pericytes (6) occurs; lower panel, right: Close association of pericyte (green) to the blood vessel (red). Adapted and modified from (Roca and Adams 2007); (Gerhardt, Golding et al. 2003)

Extensive angiogenic remodelling in the retinal plexus converts the primary capillary plexus into arteries, veins, and capillary beds. While growth into the periphery continues, the region of the plexus that is closer to the centre of the retina is remodelled by pruning and secondary sprouting processes. Pruning is most pronounced in areas in close proximity to arteries so that the periarterial vasculature is relatively sparse and contains only few branchpoints. This remodelling correlates with reduced VEGF-A messenger RNA (mRNA). Presumably, relative hyperoxia surrounding arteries and flow-dependent tissue oxygenation negatively regulates VEGF-A production. In contrast, the perivenous vasculature remodels at a much slower rate, is a site of extensive EC proliferation, retains a higher density of vessels and branchpoints, and contains numerous secondary sprouts emerging from capillaries. Although it is unclear whether these regional features are caused by hemodynamic factors (i.e., differences in the pressure and speed between arterial and venous blood flow), the concentration of oxygen in the blood stream, differential gene expression in arteries and veins, or a combination of all three, angiogenic remodelling around the arterial branch appears to strongly favour tube formation over new sprouting whereas the perivenous vasculature is permissive for both processes (Roca and Adams 2007).

Astrocyte precursors enter the retina through the optic nerve and radiate towards the periphery. Vascularization subsequently follows the pre-existing astrocytic meshwork, suggesting a function in guidance and scaffolding for growing vessels. Consistent with this, filopodia extension of the growing endothelial tip often align with process of the underlying astrocytes that secret VEGF-A (Figure 4.5).

In addition to close astrocyte- endothelial cell interaction during angiogenic sprouting, mural cell (MC) intimately associate with the developing blood vessels. MC consist of pericytes (PC) that envelope capillaries and vascular smooth muscle cells (vSMC) which tightly wrap around bigger vessels such as arteries and veins (Figure 4.5). In the retina, pericytes recruitment is dependent on paracrine platelet derived growth factor B (PDGF-B) signalling. Endothelial cells at the sprouting vascular front express *Pdgfb*. CNS-derived pericytes express the receptor, *Pdgfrb* and by sensing the growth factor invest the growing vessels by longitudinal migration. The establishment of mature blood vessels by formation of firm adhesion junction, pericyte recruitment, and deposition of BM components restricts vessels growth. However, are there other limiting factors? What initiates endothelial specification? And how are tip cells selected? And what determines growth arrest?

4.5 Notch signalling in sprouting angiogenesis

Recent studies highlighted the importance on Notch signalling in the process of tip cell selection and the induction of angiogenic sprouts. The Notch pathway is an evolutionary conserved signalling system that has multiple roles in cell fate specification, tissue patterning and morphogenesis through effects on differentiation, proliferation, survival and apoptosis (Phng and Gerhardt 2009).

The Notch receptor is a single-pass transmembrane protein consisting of a single peptide, an extracellular domain that is responsible for ligand interaction, and a transmembrane domain that is in involved in receptor activation and an intracellular signalling domain {Dufraine, 2008 #506}. Notch signalling is initiated when the extracellular domain of the receptor engages ligand found on neighbouring cells that are in close proximity to one another (Figure 4.6). Thus, Notch signalling depends on cell-contact dependent interaction (Dufraine, Funahashi et al. 2008). In mammals, there are four Notch receptors, Notch1, Notch2, Notch3 and Notch4 and five canonical DSL (Delta, Serrate, LAG-2) ligands: Delta-like (Dll) 1, Dll3, Dll4 and Jagged-1 (Jag1) and -2 (Jag2). These ligands are type I cell surface proteins with multiple tandem epidermal growth factor (EGF) repeats in their extracellular domains. Several Notch receptors and ligands as well as signalling components have been identified in ECs, including Notch1 and -4, and ligands Dll1, Dll4 and Jag1 and -2. Global knockout studies and endothelial specific deletion of Notch and/ or their ligands highlighted the importance in proper construction of the vascular system and it become clear that Notch signalling is indispensable for vascular development during embryogenesis.

Notch-ligand binding leads to a cascade of proteolytic cleavages, first by a member of the disintegrin and metalloproteases (ADAM) family within the juxtamembrane region releasing the extracellular domain, followed by γ-secretase within the transmembrane domain. The final cleavage releases the Notch intracellular domain (NICD) and translocates to the nucleus where it interacts with CSL (CBF1, Su(H) and Lag-2) transcriptional repressors and converts them to transcriptional activators (Figure 4.6).

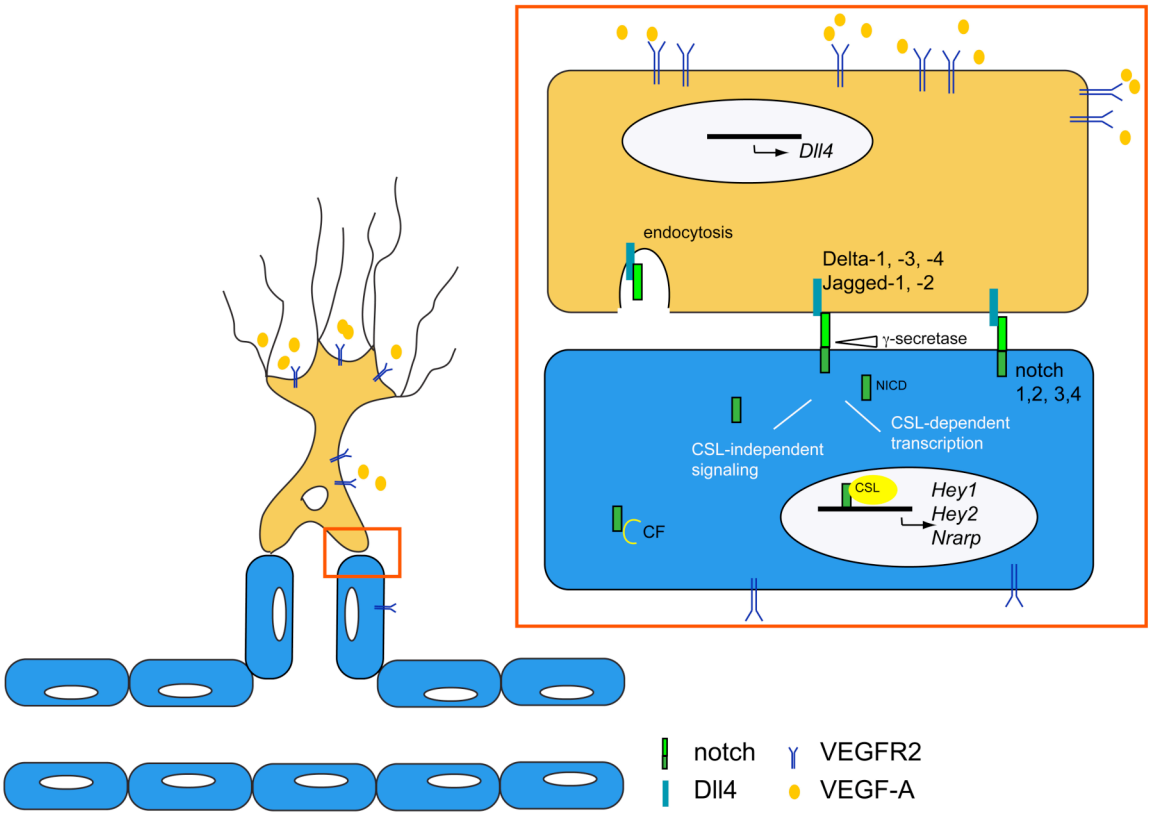

Figure 4.6 Dll4/ Notch signalling during angiogenic sprouting

Notch receptors are expressed on the cell surface. Upon binding and interaction with Notch ligand, Delta and Jagged, notch intracellular domain (NICD) becomes released by γ-secretase cleavage. NICD translocates to the nucleus to trigger transcriptional activation of Notch target genes. Notch ligand, Dll4 is strongly upregulated and expressed by endothelial tip cells (yellow) stimulated by VEGF-A gradient. Interaction with adjacent stalk cell (blue) results in induction and activation of mature quiescent stalk cell phenotype.
CSL (CBF1, Su(H) and Lag-2) transcriptional repressors are converted into transcriptional activators upon interaction with NICD. CSL dependent and independent activation occurs. The latter, requires cytoplasmic factors (CF) such as MAGP.

In the absence of NICD, CSL represses transcription through interaction with co-repressor complex. Upon binding of NICD, the co-receptor complex is replaced by transcriptional activator complex including NICD, mastermind-like and histone acetyltransferases that turns on expression of Notch targets such as the basic helix-loop helix proteins *Hairy/Enhancer of Slit (Hes)*, *Hes-related proteins* and *Notch-regulated ankyrin repeat proteins* (*Nrarp*). *Hes* and *Hey* genes are, in turn, transcriptional repressors of their own transcription and further downstream target genes (Phng and Gerhardt 2009); (Dufraine, Funahashi et al. 2008). Notch signalling controls multiple aspects of endothelial specification, e.g. the role of Dll4/ Notch signalling in arterial differentiation has been well established. At approximately E9.5-E11.5 of murine

embryogenesis the primary vascular plexus remodels leading to the establishment of a hierarchical vascular network consisting of arteries and veins. This process coincides with Notch1 and -4 expression, as well as notch ligand Dll4 expressing around the developing vasculature, however by E13.5, expression of these genes is restricted to the arterial endothelium. At the same time, members of the Eph signalling pathway, ephrinB2 and EphB4, are expressed and serve as markers of arterial and venous identity, respectively. Studies in mouse and zebrafish illustrated that Notch functions upstream of ephrinB2, promoting arterial specification. Targeted deletion of several members of the Notch family and Notch ligands result in deregulation of arterial and venous specification of ECs and deformation of arteries and veins *in vivo*.

As outlines in chapter 4.4 of this thesis, guided angiogenic sprouting requires the induction of a motile leading tip cell to migrate and expand the growing vasculature. Recent studies in mouse retina, in zebrafish intersegmental vessels (ISV) and tumour angiogenesis models highlighted that the specification of endothelial tip and stalk cells, both spatially and temporally is regulated by Dll4/Notch signalling. Tip cells express high levels of *Dll4* (Claxton and Fruttiger 2004) while Notch activity is predominantly observed in stalk cells (Hellstrom, Phng et al. 2007). Disruption of Dll4 or endothelial specific loss of *Notch1*, as well as suppression of Notch activity by pharmacological inhibitor γ-secretase inhibitor results in increased vessels density of the vascular plexus and excessive vessel sprouting. Increased and widespread expression of tip cell gene *Pdgfb* as well as aberrant filopodia induction in stalk ECs indicated dramatically augmented tip cell formation and sprouting (Hellstrom, Phng et al. 2007); (Suchting, Freitas et al. 2007).

In summary, *Dll4*-expressing endothelial tip cell activates Notch signalling in the adjacent, proliferating stalk cell (Figure 4.6). Loss of Notch signalling is associated with increased vascular endothelial growth factor receptor (VEGFR) *VEGFR2* expression (Suchting, Freitas et al. 2007); (Lobov, Renard et al. 2007), suggesting the following model: Dll4 signals through Notch1 in the adjoining cell to initiate a VEGF-feedback loop, limiting sprouting by downregulation of VEGFR2 (Figure 4.6), likely through direct binding of *Hey1* to the VEGFR2 promoter (Holderfield, Henderson Anderson et al. 2006). The tip cell phenotype is the default acquired in the absence of Notch signalling, whereas the stalk cell phenotype is acquired by Notch signalling (Hellstrom, Phng et al. 2007). Thus, Dll4 functions in restricting tip cell formation and excessive sprouting and therefore, has an anti-angiogenic capacity (Dufraine, Funahashi et al. 2008).

Dll4 expression is increased in ECs of murine and human tumours and its expression is regulated by VEGF-A (Thurston et al., 2007). Blockade of Dll4 in tumours resulted in overgrowth of tumour vasculature, similar to increased vessel density in mouse retinas after suppression of Notch signalling. Despite the increased tumour vasculature, Dll4 inhibition led to decreased tumour growth (Noguera-Troise, Daly et al. 2006). Perfusion studies revealed that Dll4 blockade resulted in abnormal non-functional tumour vessels that could not efficiently deliver blood to the tumour leading to hypoxic tumours negatively affecting tumour growth (Thurston, Noguera-Troise et al. 2007).

Notch receptor activation can also be mediated by non- DSL ligands, such as microfibril-associated glycoprotein family, MAGP-1 and -2, small glycoprotein that specifically associate with fibrillin-containing microfibrils to promote cell adhesion by binding to integrin αvβ3 (Gibson, Leavesley et al. 1999). Integrins are heterodimeric transmembrane cell adhesion molecules that mediate cell-matrix interactions and are discussed in chapter 4.18 .

MAGP-Notch interactions induce γ-secretase-dependent NICD generation and CSL-dependent activation of reporter constructs. MAGP-2 only activates Notch when expressed in the same cell as the receptor, suggestive of autocrine signalling. MAGP-2 can have an inhibitory effect on Notch in several EC lines and promotes angiogenic cell sprouting by blocking Notch signalling in ECs *in vitro* (Albig, Becenti et al. 2008); reviewed in (D'Souza, Miyamoto et al. 2008).

Increasing studies reveal Notch- ECM interaction and that Notch can influence matrix production during sprouting angiogenesis. Endothelial specific overexpression of *Dll4* (*mDll4*) resulted in increased expression of Notch effectors such as *Hey1*, *Hey2* and *Hes5* and vascular defects leading to embryonic lethality. Further, *mDll4* showed increased expression and transcription of fibronectin, laminin and CollagenI and -IV but reduced expression of matrix degrading enzymes, matrix metalloproteases (MMP) MMP-1, -2 and -9 (Trindade, Kumar et al. 2008).

Conversely, Benedito and colleagues showed that *Dll4-/-* mutants display a defective BM around the forming aorta and increased EC migration from the dorsal aorta to peripheral regions, which constitute the main causes of arterial lumen reduction in these embryos (Benedito, Trindade et al. 2008).

Notch activation in ECs increases the affinity of β1–integrin for fibronectin, collagens I and IV, and vitronectin, which in turn allows cells to adhere to β1 integrin substrates and prevents cell migration, endothelial sprouting and, angiogenesis (Leong,

Hu et al. 2002). Overexpression of intracellular domain of *Notch 4* in ECs results in a β1 integrin mediated increase in matrix adhesion and a reduced sprouting response to VEGF-A *in vivo* and *in vitro* (Leong, Hu et al. 2002).

Notch-mediated integrin activation is independent of the abundance of β1 integrin, but rather due to changes in the activation status of β1 integrin. The Ras family of small guanosine triphosphate (GTP) binding proteins and their downstream effectors are key players in the regulation of integrin activation. R-Ras enhances integrin-mediated cell adhesion by increasing integrin affinity and avidity, whereas H-Ras and its downstream effector Raf-1, a mitogen-activated protein kinase (MAPK), inhibit integrin activity. Hodkinson and colleagues show that the intracellular domain of mammalian Notch-1 activates integrins without affecting integrin expression. Integrin activation is dependent on γ –secretase mediated intra-membranous cleavage of membrane bound Notch releasing intracellular Notch which activates R-Ras, independent of CSL-transcription. Notch activation reversed H-Ras-and Raf-mediated suppression of integrin affinity. Membrane-bound Notch mutants that are inefficiently cleaved or intracellular Notch mutants lacking the ankyrin repeat sequence do not activate R-Ras or integrins. Notch ligand, Dll4 stimulates R-Ras dependent α5β1 integrin -mediated adhesion, demonstrating the physiological relevance of this pathway (Hodkinson, Elliott et al. 2007).

Dll4/Notch induced restriction of vascular sprouting via downregulation of VEGFR2 is based on endothelial specific interaction. *Dll4* –expressing ECs signal to neighbouring EC activating Notch signalling. However, recent studies implicated Notch signalling to neighbouring cells including vSMC during embryogenic vascular development and to tumour cells during tumour angiogenesis. In particular, endothelial specific deletion of *Jag1* results in embryonic lethality and cardiovascular defects, recapitulating the *Jag1* null phenotype. These embryos show striking deficits in vSMCs, whereas endothelial Notch activation and arterial-venous differentiation appear normal. Endothelial *Jag1* mutant embryos are phenotypically distinct from embryos in which Notch signalling is inhibited in endothelium (High, Lu et al. 2008). Further, Jag1-selective Notch signalling induces SMC differentiation via a RBP-Jkappa-dependent pathway. Overexpression of NICD promoted SMC- specific gene expression in mesenchymal 10T1/2 cells but not non-mesenchymal cells (Doi, Iso et al. 2006).
Further analyses suggest vSMC-autonomous function for Notch signalling in patterning

and collateral formation within the cerebral arterial circulation (Proweller, Wright et al. 2007).

Mutations in *Notch3* are associated with CADASIL, a stroke and dementia syndrome with vSMC dysfunction. Jin and colleagues linked Notch signalling to PDGF-B signalling, a major pathway in vSMC recruitment, differentiation and proliferation and showed that PDGFR-β is a novel immediate Notch target gene. PDGFR-β expression is upregulated upon Notch activation, depending on the CSL pathway. Conversely, PDGFR-β expression is strongly reduced in *Notch3* deficient mice and embryonic stem cells (Jin, Hansson et al. 2008).

Branching of blood vessels to form a tube-like vascular network is equally important as angiogenic sprouting and the restriction of new sprouts.
Notch is among the pathways crucial for branching morphogenesis. During *Drosophila* tracheal development, cross talk between Notch and Wnt/wingless, TGF-β/Dpp and receptor tyrosine kinase (RTK)/FGFR pathway generates branch patterning through the cooperative specification of cell fate. In vertebrates, Notch cross-talk functions in epithelial bud formation and branching of the developing prostate gland. Specifically, Notch/TGF-β antagonizism regulates branching (Grishina, Kim et al. 2005). Further, when murine embryonic ECs are in contact, ligand-depending Notch signalling is activated, and BMP/TGF-β- mediated migration is inhibited, suggesting a mechanism for contact-depending cross-talk regulating endothelial migration (Itoh, Itoh et al. 2004).

4.6 Sensing oxygen levels - Hypoxia induced angiogenic responses

Angiogenesis is mostly an adaptive response to tissue hypoxia, referring to oxygen levels that are reduced due to rapid oxygen consumption and/ or poor circulation. This process occurs in a wide variety of physiological and pathological conditions such as embryonic development and tumour growth, situations in which the rate of tissue expansion outpaces the accompanying angiogenesis leading to inadequate supply of blood and therefore, generating an highly hypoxic environment.

Angiogenesis is dependent on the accumulation of hypoxia-induced factors (HIFs), which are heterodimeric transcription factors of α- and β-subunits (reviewed in (Fong 2008)). During normal oxygen concentrations, intracellular HIF levels are low, due to rapid degradation mediated by oxygen-dependent prolyl hydroxylases (PHD), polyubiquitination, and proteosomal degradation of α-subunits. However, under hypoxia, PHD activity is suppressed, resulting in increase levels of HIFs, stabilization of α-subunits and the formation of heterodimers with HIF-1β, which is not subject to oxygen dependent regulation.

The accumulation of HIFs under hypoxia allows them to activate the expression of many angiogenic genes, such as *phosphoglycerate kinase* (*PGK*) and *Vegfa* and thereby, initiates an angiogenic response. As a result, glycolysis is increased, which partially compensate for reduced oxidative phosphorylation. Likewise, increased VEGF-A facilitates the adaptation to hypoxia, due to improved oxygen delivery as a result of angiogenesis (reviewed in (Fong 2008)).

HIF-1α and HIF-2α both activate the transcription of target genes by binding to hypoxia response elements (HRE) or similar sequence elements. The presence of HRE has been demonstrated for many angiogenic genes such as *Vegfa* and *Vegfr2* (Marti, Bernaudin et al. 2000). In contrast to HIF target genes, many other angiogenic genes like *Pdgfb, angiopoietin* and *Tgfb* lacking HRE are also upregulated by hypoxia or HIF-1α overexpression (Nilsson, Shibuya et al. 2004). Hypoxia also regulates endothelial cell-cell junctions and vascular permeability. In the brain, tissue hypoxia disrupts the blood brain barrier. Elevated VEGF-A levels under hypoxia are responsible for increased vascular leakage (Schoch, Fischer et al. 2002).

In EC as well as vSMC cultures, moderate hypoxia promotes expression of

angiogenic genes *Vegfa* and *Pdgfb*, respectively promoting cell proliferation and survival (LeCouter, Kowalski et al. 2001). However, hypoxia near anaerobic conditions reduces proliferation and triggers apoptosis, suggesting that the functional outcome depends on severity of hypoxia. Hypoxia may also regulate vSMC migration and adhesion properties (Schultz, Fanburg et al. 2006). Overexpression of HIF-1α significantly reduced FAK (focal adhesion kinase) phosphorylation and diminished vSMC adhesion to ECM. Since sprouting angiogenesis requires loosening of vSMCs from BM and ECs, reduced vSMC adhesion to ECM may favour angiogenesis (Corley, Taylor et al. 2005).

4.7 VEGF-VEGFR signalling in angiogenesis

In the yolk sac, the initial ECs associated with the blood islands fuse together to form a primitive capillary plexus, a honeycomb network of developing vessels. Within the embryo, dispersed angioblasts start to join together to form a capillary network in the head mesenchyme and posterior lateral plate mesoderm. In the developing cardiac crescent, endothelial progenitors form the primitive endocardial lining of the developing cardiac tube. These initial phases of vascular development are known as vasculogenesis and are largely dependent on vascular endothelial growth factor (VEGF) signalling (reviewed in (Rossant and Howard 2002). The VEGF family members are secreted, dimeric glycoproteins of approximately 40kDa. In mammals, the VEGF family consist of five members, VEGFA, -B, -C, -D and placenta growth factor (PlGF).

The *Vegf* gene consists of nine alternatively spliced exons, resulting in five VEGF-A isoforms in humans; the mouse *Vegf* gene produces at least three isoforms of 120, 164 and 188 amino acids (aa). The VEGF isoforms are denoted VEGF120, VEGF164 and VEGF188 and differ in their ability to interact with VEGFR co-receptors, such as neuropilins (Nrp) and heparan sulfate proteoglycans (HSPG), see Figure 4.7.

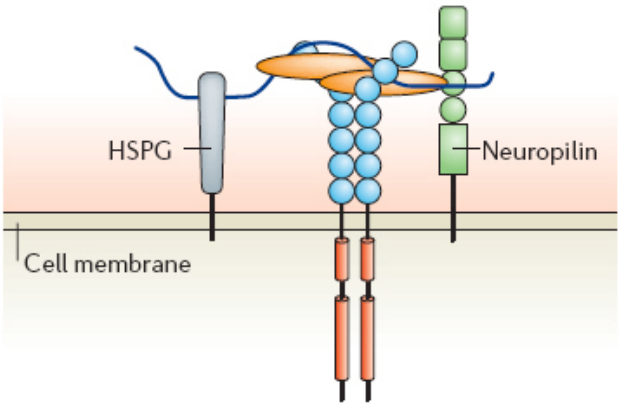

Figure 4.7 VEGF receptor signalling is modulated by different co-receptors

VEGFs as well as VEGFRs bind to co-receptors such as heparan sulfate proteoglycans (HSPGs) and Neuropilins. These interactions can influence VEGFR-mediated responses (Olsson, Dimberg et al. 2006).

The bioactivity of VEGF family members is regulated by proteolytic processing, suggesting specific interaction with different receptors and co-receptors (Lee, Jilani et al. 2005). VEGF164 and -188 can bind heparin, and associate with the ECM and is therefore retained in close vicinity to the secreting cell. In contrast, the short isoform VEGF120 lacks the HSPG- and Nrp- binding domains generating a freely diffusible VEGF variant. Recently, a new model has been proposed for Nrp interactions with VEGF isoforms. Pan and colleagues suggest that VEGF121 binds directly to neuropilin 1 (Nrp1); however, unlike VEGF165, VEGF121 is not sufficient to mediate the Nrp1-VEGFR2 complex (Pan, Chathery et al. 2007). Protease cleavage of matrix-bound VEGF188 results in release of an active, freely diffusible fragment.

Recent studies showed that heparin enhances VEGF165 induced phosphorylation of VEGFR2 but not VEGF120. Depletion of cell surface heparan sulfate results in reduction of the phosphorylation. Therefore it is likely that a heparin-like domain of heparan sulfate/heparin forms a complex with VEGF165 and VEGFR2 via the exon 7-encoded region, thereby enhancing VEGF165-dependent signalling (Ashikari-Hada, Habuchi et al. 2005). Further, biochemical studies indicate that heparin/ HS form a complex by simultaneously binding growth factor and receptor and thereby prolonging the half-life of the receptor complex (Ibrahimi, Zhang et al. 2004). Similar findings revealed a stabilization function for VEGF/VEGFR2 by co-receptors neuropilin when expressed by adjacent cells (Miao and Klagsbrun 2000).

Most cells however, produce multiple VEGF isoforms simultaneously with VEGF164 and VEGF120 being predominantly expressed.

The functional relevance of VEGF isoform has been studied in the retinal vasculature, expressing solely one isoform. While *VEGF164/164* mice exhibit no vascular defects, the *VEGF120/120* mice lacking heparin-binding, and therefore ECM interaction domains, displayed decreased vessel density and branch formation. Instead of being recruited into additional branches, nascent ECs were preferentially integrated within existing vessels to increase lumen calibre. Embryos harbouring only a heparin-binding isoform of VEGF-A (*VEGF188/188*) developed opposing defects, including excess endothelial filopodia and abnormally thin vessel branches in ectopic sites. Therefore, differential VEGF-A isoform localization in the extracellular space provides a control point for regulating vascular branching and guided migration towards a growth factor gradient (Ruhrberg, Gerhardt et al. 2002).

The VEGF ligands bind in an overlapping pattern to three receptor tyrosine kinases, denoted as VEGF receptor 1 (VEGFR1, Flt1), VEGFR2 (Kdr, Flk1) and VEGFR3 (Flt4). The VEGFR1 and -2 are primarily expressed in the vascular system and their expression is mainly restricted to the endothelial and lymphatic cell lineage, implying crucial function during vascular development. However, expression and perhaps function in other tissues have been described. VEGF and VEGFR2 are expressed by neurons during development, and VEGF has a direct effect on neuronal growth and maturation mediated by VEGFR2 (Khaibullina, Rosenstein et al. 2004). VEGFR1 is expressed in macrophages and is involved in their migration (Sawano, Iwai et al. 2001). VEGFR3 is expressed in early blood vessels but expression becomes later restricted to the developing lymphatic vasculature.

VEGFR2 binds VEGF-A, -C and –D, while VEGFR1 binds VEGF-A, -B and PlGF and VEGFR3 binds VEGF-C and –D. VEGF receptor binding properties are illustrated in Figure 4.8.

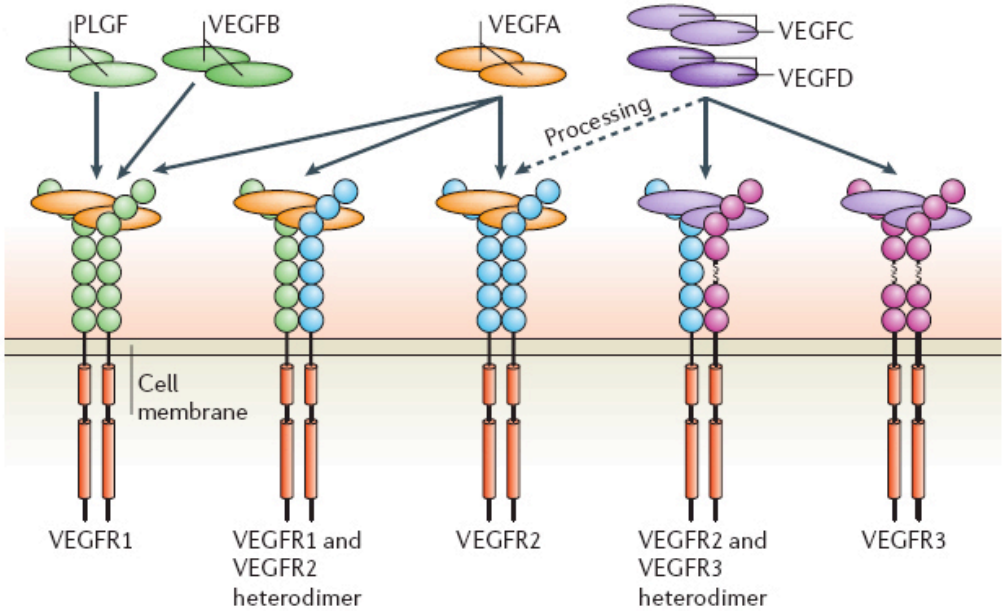

Figure 4.8 VEGF/ VEGFR family and its binding properties

Mammalian vascular endothelial growth factors (VEGFs) bind to the three VEGF receptor (VEGFR) tyrosine kinases, leading to the formation of VEGFR homodimers and heterodimers. Proteolytic processing of VEGFC and D allows binding to VEGFR2 (Olsson, Dimberg et al. 2006).

VEGF binding induces receptor dimerization, followed by activation of tyrosine kinase leading to autophosphorylation and subsequently activation of the downstream signalling cascade. Guided by the binding properties of the ligands, the receptors can form homodimers and heterodimers.

Interestingly, VEGFR1 has a 10-fold higher affinity to VEGF-A than VEGFR2 but VEGFR1 undergoes little detectable phosphorylation when bound to VEGF-A, whereas VEGF binding to receptor 2 results in autophosphorylation in several phosphorylation sites. VEGFR1 acts as a positive and negative regulator of VEGFR2 signalling capacity. Negative regulation of VEGFR2 is exerted, at least in part, by an alternatively spliced soluble variant of VEGFR1 that binds to VEGF and thereby prevents VEGF from binding to VEGFR2.

The requirements and importance of VEGF signalling during cardiovascular and lymphatic development has been illustrated by knockout studies. Inactivation of a single *Vegfa* allele resulted in early embryonic lethality due to severe reduction and calibre of the developing vessels. VEGF-A is haploinsufficient; homozygous embryos were produced by aggregation of homozygous mutant ES cells with tetraploid wildtype embryos revealing an even more severe phenotype and impaired vessel formation

(Carmeliet, Ferreira et al. 1996), indicating a tight dose-dependent regulation of embryonic vessel development by VEGF. The importance of regulated VEGF signalling is illustrated by the fact that a 2-3fold overexpression of *Vegfa* from its endogenous locus results in aberrant heart development and embryonic lethality (Miquerol, Langille et al. 2000). Induced deletion of VEGF-A in neonatal and adult mice as well as short-term withdrawal of VEGF-A by pharmalogical inhibitors leads to endothelial apoptosis and regression of blood vessels (Gerber, Hillan et al. 1999).

Deletion of *Vegfr2* leads to early embryonic lethality at E8.5 displaying a similar phenotype to *Vegfa-/-* but additionally, embryos developed early defect in the development of haematopoietic and ECs. Yolk-sac blood islands were absent at 7.5 days, organized blood vessels could not be observed in the embryo or yolk sac at any stage, and haematopoietic progenitors were severely reduced (Shalaby, Rossant et al. 1995). In contrast, *Vegfr1* deficient embryos die at E9.0 due to excessive endothelial proliferation and impaired lumen formation. The development and expansion of ECs in *Vegfr1*-/- animals is possibly a consequence of increased accessibility of VEGF-A for binding and activation of VEGFR2, implicating VEGFR1 as a negative regulator. Several studies have highlighted that VEGFR1 negatively influences VEGFR2 signalling. VEGFR2 mediated proliferation of ECs can be suppressed by VEGFR1, dependent on phosphoinositide 3-kinases (PI3K) activity and signalling while migration is unaffected (Zeng, Dvorak et al. 2001).

Activation of VEGFR2 signalling regulates multiple EC functions including proliferation, migration and survival. Knockout studies and inhibition of VEGFR2 has elucidated that VEGFR2 is essential in all aspects of normal and pathological vascular development. Targeting VEGFR2 by small-molecular-weight tyrosine kinase inhibitors has become in focus of current anti-angiogenic tumour therapies. However, understanding the specific signal transduction pathways of VEGFR2 and downstream signalling pathways may help targeting precise endothelial functions in tumours. The positions of several phosphorylation residues in VEGFR2 have been mapped and are summarized in Figure 4.9.

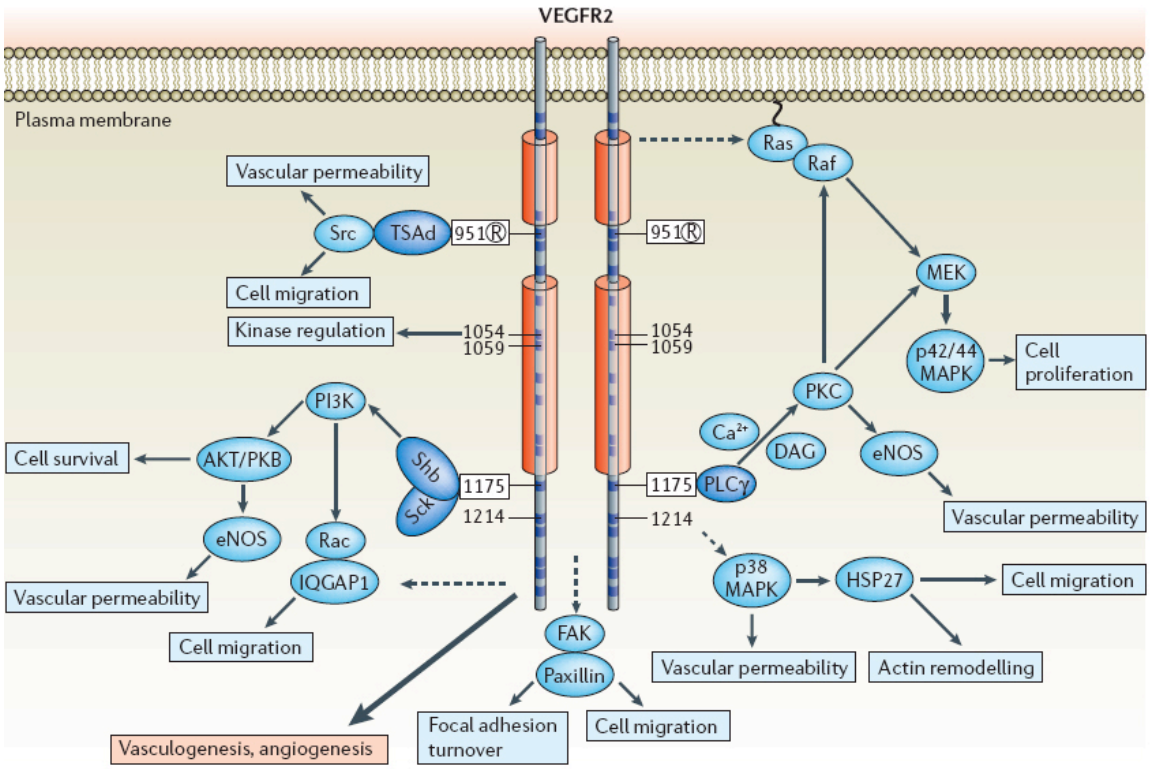

Figure 4.9 VEGFR phosphorylation sites and signal transduction

Intracellular domain and activated VEGFRs are shown with tyrosine phosphorylation sites that are indicated by numbers. Circled R indicates that use of the phosphorylation site is regulated dependent on the angiogenic state of the endothelial cell (for VEGFR2). Dark blue squares in the receptor molecules indicate positions of tyrosine residues. Binding of signalling molecules (dark blue ovals) to certain phosphorylation sites (boxed numbers), initiates signalling cascades (light blue ovals), which leads to the establishment of specific biological responses (pale blue boxes). The mode of initiation of certain signalling chains is unclear (dashed arrows). Final biological outcomes that are coupled to the respective receptors are indicated in pink boxes. DAG, diacylglycerol; EC, endothelial cell; eNOS, endothelial nitric oxide synthase; FAK, focal adhesion kinase; HPC, haematopoietic progenitor cell; HSP27, heat-shock protein-27; MAPK, mitogen-activated protein kinase; MEK, MAPK and ERK kinase; PI3K, phosphatidylinositol 3′ kinase; PKC, protein kinase C; PLCγ, phospholipase C-γ; Shb, SH2 and β-cells; TSAd, T-cell-specific adaptor (Olsson, Dimberg et al. 2006).

Phospholipase C gamma (PLCγ) binds to phosphorylated tyrosine residue 1175 (Tyr1175) and mediates the activation of MAPK/ ERK1/2 inducing EC proliferation. Mice expressing mutated Tyr1173Phe VEGFR2 die at E8.5-9.5 because of vascular defects resembling *Vegfr2*-/- mice, indicating an essential function of this particular phosphorylation residue (Takahashi, Yamaguchi et al. 2001); (Sakurai, Ohgimoto et al. 2005). The serine/threonine kinase AKT/PBK is activated downstream of PI3K and mediates survival of ECs (Fujio and Walsh 1999). Tyrosine residue 951 is a binding site

for the signalling adaptor TSAd (T-cell specific adaptor). Mutation of Y951 to F and introduction of phosphorylated Y951 peptide or TSAd siRNA into ECs blocked VEGF-A-induced actin stress fibers and migration, but not mitogenesis. Tumour vascularization and growth was also reduced in TSAd-deficient mice, indicating a critical role of Y951-TSAd signalling in pathological angiogenesis (Matsumoto, Bohman et al. 2005). The same study reported differential phosphorylation patterns of VEGFR2 within developing blood vessels in mouse embryoid bodies (Matsumoto, Bohman et al. 2005). More developed patent vessels associated with mural cells lacked Y951 VEGFR2 phosphorylation.

In addition to the VEGFR binding properties discussed above (Figure 4.9), VEGF receptors can bind and interact with a variety of molecules that do not necessarily act as co-receptors. Vascular endothelial cadherin (VE-cadherin) localized at adhesion junction forms a complex with VEGFR2 and thereby modulates its signalling properties (Lampugnani and Dejana 2007), see Figure 4.10.

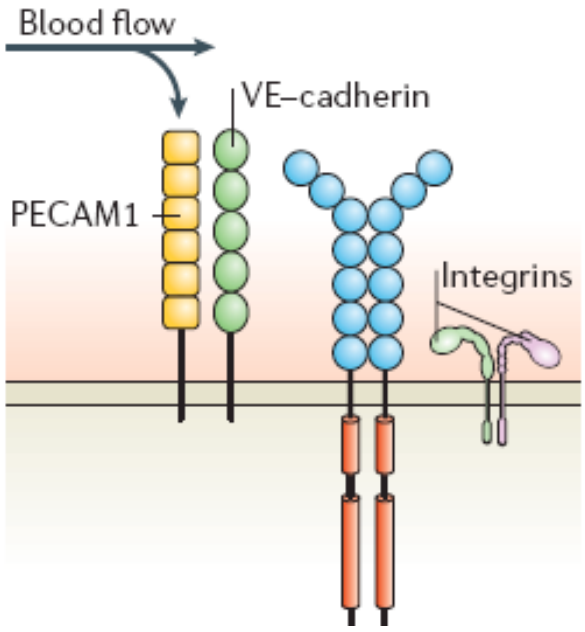

Figure 4.10 Mechanosensory complex formation

Blood flow might activate VEGFRs in a ligand-independent manner, by the formation of mechanosensory complexes that consist of platelet-endothelial-cell adhesion molecule-1 (PECAM1), vascular endothelial (VE)–cadherin, VEGFRs and integrins (Olsson, Dimberg et al. 2006).

Shear stress and blood flow determine at least to some extend vascular remodelling and homeostasis. Previous work showed that the conversion of integrins to a high-affinity state mediates a subset of shear responses, including cell alignment and gene expression. However, platelet/endothelial cell adhesion molecule-1 (PECAM-1, which directly transmits mechanical force), VE-cadherin (which functions as an adaptor) and VEGFR2 (which activates PI3K) comprise a mechanosensory complex that functions upstream of integrin activation (Figure 4.10). Together, this receptor complex is sufficient to confer responsiveness to flow in heterologous cells (Tzima, Irani-Tehrani et al. 2005).

Integrin signalling will be discussed in more detail but at this point it is worth mentioning that αvβ3 integrin directly interacts with VEGFR2 and its engagement promotes phosphorylation and activation of VEGFR2 (Soldi, Mitola et al. 1999). In addition, this interaction appears to be synergistic, as VEGFR2 activation induces β3 integrin tyrosine phosphorylation that in turn, is crucial for VEGF-induced VEGFR2 phosphorylation (Mahabeleshwar, Feng et al. 2007). These findings are in agreement with the *in vivo* data, deletion of the *integrin beta 3* chain in mice results in elevated expression levels of VEGFR2 (Reynolds, Reynolds et al. 2004).

4.8 PI3 kinase activity in angiogenesis

The PI3K signalling pathway has been implicated in many diverse cellular aspects, including cell growth, proliferation, differentiation, motility, survival and intracellular trafficking. Many of these functions relate to the ability of PI3-kinases to activate AKT, also known as protein kinase B (PKB), a regulator of small GTPases and scaffolding proteins. Upstream components of AKT signalling pathway such as PI3K, PTEN, and Ras are commonly mutated in many human cancers.

Class IA PI3Ks are composed of a p110 catalytic subunit (p110α, -β and –γ) bound to one of five regulatory subunits, known as p85s. Under unstimulated conditions, p85 stabilizes the labile p110 protein, while inhibiting its catalytic activity. Recruitment of the p85–p110 complex to receptors and adaptor proteins via the p85 SH2 (Src homology 2) domains alleviates this inhibition, leading to PI3K activation and production of PIP3 (phosphatidylinositol 3,4,5-trisphosphate). PIP3 formation is required to translocate AKT to the cell membrane (Figure 4.11). At PIP3, AKT becomes phosphorylated at specific serine (473) and threonine (308) residues and

thereby is activated (review by (Geering, Cutillas et al. 2007))

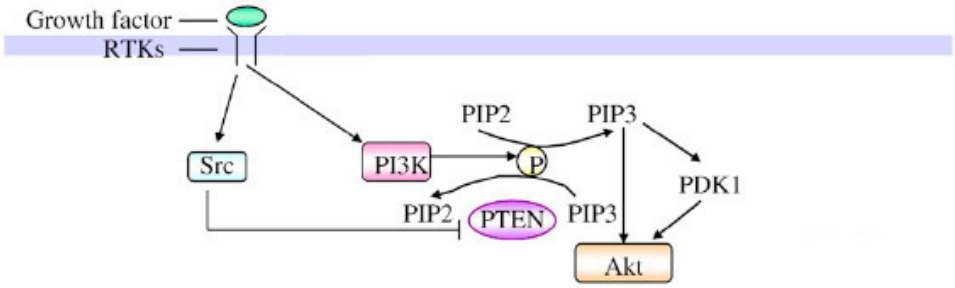

Figure 4.11 Schematic representation of PI3K/AKT signalling

Activation of receptor tyrosine kinases (RTKs) initiates receptor dimerization, and activates the intracellular pathways to increase PI3K activity. PI3K produces phosphatidylinositol-3,4-diphosphate (PIP2) and phosphatidylinositol-3,4,5-triphosphate (PIP3), which activates PDK1 and Akt (adapted and modified from (Jiang and Liu 2008)).

As discussed previously, PI3K signals downstream of VEGFR2 and has been implicates in angiogenesis, e.g. EC survival and regulation of VEGF and HIF-2 expression in human tumours by AKT activation (Fujio and Walsh 1999); (Jiang, Jiang et al. 2001); (Jiang and Liu 2008).

Graupera and colleagues showed that p110α isoform is selectively required for angiogenesis. Ubiquitous or EC-specific inactivation of p110α led to embryonic lethality at mid-gestation because of severe defects in angiogenic sprouting and vascular remodelling. p110α exerts this critical EC-autonomous function by regulating VEGF-A induced EC migration through the small GTPase RhoA (Graupera, Guillermet-Guibert et al. 2008).

PTEN is an important tumour suppressor gene, upregulated in many tumours (Li, Yen et al. 1997). PTEN functions as a multifunctional phosphatase whose major substrate is phosphatidylinositol-3,4,5-trisphosphate (PIP_3). By using its lipid phosphatase activity to dephosphorylate PIP_3, PTEN negatively regulates the PI3K–AKT pathway. Endothelial specific deletion of PTEN results in embryonic lethality at E11.5 due to bleeding and cardiac failure caused by impaired recruitment of PC and vSMCs to blood vessels, and of cardiomyocytes to the endocardium. These phenotypes depend strongly on p110γ rather than on p85α and were associated with increased expression of angiogenic factors, such as VEGF-A and VEGFRs (Hamada, Sasaki et al. 2005). Endothelial deficient PTEN mice displayed enhanced tumourigenesis due to an

increase in angiogenesis driven by vascular growth factors suggesting an indispensable role in normal cardiovascular morphogenesis and post-natal angiogenesis, including tumour angiogenesis (Hamada, Sasaki et al. 2005).

4.9 Stabilization of vessels by endothelial junctions

Vessel growth requires the formation of tight junctional complexes between ECs in order to form functional vessels. Cell-to-cell contacts control critical endothelial functions both in quiescent and activated conditions during angiogenesis. Junctional proteins restrain cell migration, contact inhibition of EC proliferation and apoptosis, and maintenance of apical-basal cell polarity (reviewed in (Dejana, Orsenigo et al. 2009)). Junctional signals counteract to angiogenesis and therefore, cell-to cell junctions need to be sufficiently dynamic to allow vessels to respond to an angiogenic switch and return the endothelium to a mature, quiescent state. In the endothelium, junctional complexes comprise tight junctions, adherent junction and gap junctions. These structures are formed by distinct transmembrane proteins that promote homophilic cell-to-cell interactions and the transfer of intracellular signals (Dejana, Orsenigo et al. 2009).
Depending on functional requirements of vessels, EC junctions vary considerably between tissues, e.g. tight junction in CNS are enriched controlling strict permeability whereas junctions in venules are dynamic and specialized in allowing plasma leakage and leukocyte migration.

Endothelial junctions generally consist of transmembrane and cytoplasmic components. At junctions, dimeric adhesive proteins bind to other identical dimers present on the adjacent cell, resulting in lateral clustering of adhesive complexes at cell-to-cell contact; the complex then organizes into zipper-like structures by lateral adhesion along cell borders. Several transmembrane adhesive proteins have been identified including vascular endothelial (VE-) and neural (N-) cadherin at adherent junctions (Lampugnani and Dejana 1997), occluding and members of the claudin family (Nitta, Hata et al. 2003) and junctional adhesive molecules (JAM) at tight junctions (Ebnet, Aurrand-Lions et al. 2003). Adherent junction of the endothelium are formed by transmembrane adhesive protein VE-cadherin, which is directly or indirectly bound intracellularly to β-catenin, p120, plakoglobin and others (Bazzoni and Dejana 2004). Targeted inactivation of VE-cadherin or truncation of the β-catenin-binding cytosolic domain of the VE-cadherin gene was found not to affect assembly of ECs in vascular plexi, but to impair their subsequent remodelling and maturation, causing lethality at 9.5

days of gestation. Deficiency or truncation of VE-cadherin induced endothelial apoptosis and abolished transmission of the endothelial survival signal by VEGF-A to AKT kinase and Bcl2 via reduced complex formation with VEGF receptor-2, β-catenin, and PI3K (Carmeliet, Lampugnani et al. 1999). The p85 subunit of PI3K can associate with VE-cadherin/ β-catenin complex and PI3K and AKT phosphorylation are activated by VE-cadherin clustering, leading to inhibition of EC apoptosis.

Endothelial-specific deletion of β catenin leads to embryonic lethality due to abnormal development of the vascular system with enlarged and irregular lumen and multiple hemorrhages (Cattelino, Liebner et al. 2003). The molecular mechanism of VE-cadherin/ β-catenin is complex and may involve multiple signalling pathways. Lampugnani and colleagues showed that the association of VE- cadherin with VEGFR2 contributes to density-dependent growth inhibition by de-phosphorylation of VEGFR2 by DEP-1 and other phosphatase associated with this complex (Lampugnani, Orsenigo et al. 2006). VE- cadherin limits cell proliferation by retaining VEGFR2 at the membrane and preventing its internalization into signalling compartments, in turn the lack of internalization is accompanied by the inhibition of MAPK activation and cell proliferation (Lampugnani, Orsenigo et al. 2006).

Further, endothelial adherent junction might be required for the formation of tight junctions. Endothelial VE-cadherin at adherent junctions upregulates the gene encoding the tight junction adhesive protein claudin-5. This effect requires the release of the inhibitory activity of *forkhead box factor FoxO1* and the Tcf-4-beta-catenin transcriptional repressor complex. VE-cadherin acts by inducing the phosphorylation of FoxO1 through AKT activation and by limiting the translocation of β-catenin to the nucleus (Taddei, Giampietro et al. 2008).

N-cadherin, although expressed by many ECs does not appear to be involved in endothelial cell-to-cell junctions in cultured ECs and mature vessels *in vivo* (Bazzoni and Dejana 2004). N-cadherin localizes to endothelial cell-cell junctions in addition to its well-known diffusive membrane expression. Loss of N-cadherin in ECs results in embryonic lethality at mid-gestation due to severe vascular defects. Intriguingly, loss of N-cadherin caused a significant decrease in VE-cadherin and its cytoplasmic binding partner, p120ctn, indicating that N-cadherin regulates angiogenesis, in part, by controlling VE-cadherin expression at the cell membrane (Luo and Radice 2005). The same study revealed that N-cadherin controls the level of β1 integrin in ECs.
In addition, N-cadherin might be important in pericyte-endothelial cell interaction.

Pluripotent embryonic stem cells (ES cells) genetically null for N-cadherin can differentiate normally into ECs. In addition, sprouting angiogenesis was unaltered, suggesting that N-cadherin is not essential for the early events of angiogenesis including EC migration and proliferation. However, the lack of N-cadherin led to impairment in pericyte covering of endothelial outgrowths, suggesting a function in subsequent maturation of endothelial sprouts by interacting with PC (Tillet, Vittet et al. 2005). Likewise, blocking N-cadherin function during chicken embryogenesis resulted in defective pericyte adhesion, increased pericyte recruitment and disturbed vascular morphogenesis including hemorrhaging (Gerhardt, Wolburg et al. 2000).

4.10 Vessel regression and endothelial cell apoptosis

Regression of vessels occurs under a variety of settings and is tightly controlled with apoptosis. Withdrawal of pro-angiogenic factors such as VEGF and FGF resulted in regression of newly formed vessels. It is possible that vessel regression is a consequence of cell apoptosis, but it is also possible that apoptosis temporally follows regression. With loss of cell-cell and cell-matrix contacts as the vessels begins to regress precipitating apoptosis of cells. Degradation of the ECM surrounding tubes led to the collapse of capillary tubes and subsequent apoptosis of ECs, Saunders and colleagues demonstrated that MMP-1 zymogen activation is mediated by multiple serine proteases and MMP-10, and that these events are central to EC-mediated collagen degradation and capillary tube regression in 3D collagen matrices (Saunders, Bayless et al. 2005). Depolymerization of microtubule component of the cytoskeleton and interference with cell spreading and attachment resulted in collapse of vessels and subsequent apoptosis (Bayless and Davis 2004); reviewed in (Im and Kazlauskas 2006). Using an *in vitro* angiogenesis model, Im and Kazlauskus discovered that PI3K was essential for tube formation, whereas PLCγ promoted regression. The underlying mechanism by which PLCγ antagonized tube formation appeared to be by competing with PI3K for their common substrate, phosphatidylinositol-4,5-bisphosphate. This study identified signalling enzymes involved with vessel regression, and reveal that the angiogenic program can be coordinated by the availability of a membrane (Im and Kazlauskas 2006), suggesting that regression is not merely a default of EC apoptosis.

4.11 Lymphatic vessel development during embryogenesis

Lymphatic vessels are generally found closely associated with and, in many cases, ensheathing major blood vessels. Present in almost all tissues, with the exception of the CNS, cartilage and cornea and epidermis, the lymphatic vasculature forms a complex network of vessels to maintain fluid homeostasis. Unlike the cardiovascular system, the lymphatic vasculature is not a closed circulatory system and has no central pump. Interstitial proteins and water, extravasated from capillary blood vessels are absorbed by lymphatic capillaries and transported to the blood circulation by the peristalsis of collecting lymphatic vessels and contractions of surrounding skeletal muscles. Despite the main function in maintaining tissue fluid balance and uptake of fat and fat-soluble vitamins via the lacteal vessels in the digestive tract, lymphatic vessel provide a route for immune cell trafficking and antigen delivery (reviewed in (Hosking and Makinen 2007). In addition to their role in homeostasis, lymphatic vessels are involved in several human diseases, such as tumour metastasis, lymphedema and inflammation. While tumour cells escape to regional lymph nodes via peritumoural lymphatic vessels promoting spreading of tumour cells, blockage and lack of proper lymphatic vessels causes lymphedema, suggesting important functions of lymphatic vasculature in pathological conditions and human diseases.

The lymphatic systems develops mid gestation during mouse embryonic development after the establishment of blood vasculature. Lymphatic ECs arise at specific locations of embryonic veins when a subset of venous ECs becomes committed to lymphatic endothelial lineage and sprout from the major veins in jugular and perimesonephric area to form primitive lymphatic sacs (Figure 4.12). The homeodomain transcription factor Prox-1 has been identified as a critical regulator of lymphatic endothelial cell (LEC) differentiation. Induction of polarized expression of Prox-1 in cardinal vein leads to upregulation of lymphatic-specific genes, such as vascular endothelial growth factor receptor 3 (VEGFR-3) and LYVE-1 (Wigle, Harvey et al. 2002).

Lymphatic vessels further sprout and migrate from jugular lymph sacs to form a primary lymphatic plexus.

VEGFR-3, one of the genes upregulated by Prox-1 in lymphatic endothelium, is a key regulator of lymphangiogenesis. Continuous signalling via VEGFR-3 is required not only for the growth but also for the survival of LECs and for the maintenance of the

vessels. Inhibition of VEGFR-3 signalling resulted in apoptosis of LECs and regression of lymphatic vessels during embryogenesis (Makinen, Jussila et al. 2001). The two known ligands for VEGFR-3, VEGF-C and VEGF-D, can induce lymphagiogenesis *in vivo* and stimulate proliferation, migration, and survival of LECs *in vitro* (Makinen, Veikkola et al. 2001). Genetic ablation of VEGF-C leads to failure in the migration and proliferation of the LECs, and as a result the embryos do not develop lymphatic vessels (Karkkainen, Haiko et al. 2004).

Remodelling of the primary lymphatic plexus produces a hierarchically organized network consisting of lymphatic capillaries and collecting lymph vessels. Both vessel types differ in morphology and function: the lymphatic capillaries are valveless endothelial tubes which have discontinuous BM, overlapping EC junctions and lack PC and SMCs, making them highly permeable to large macromolecules.

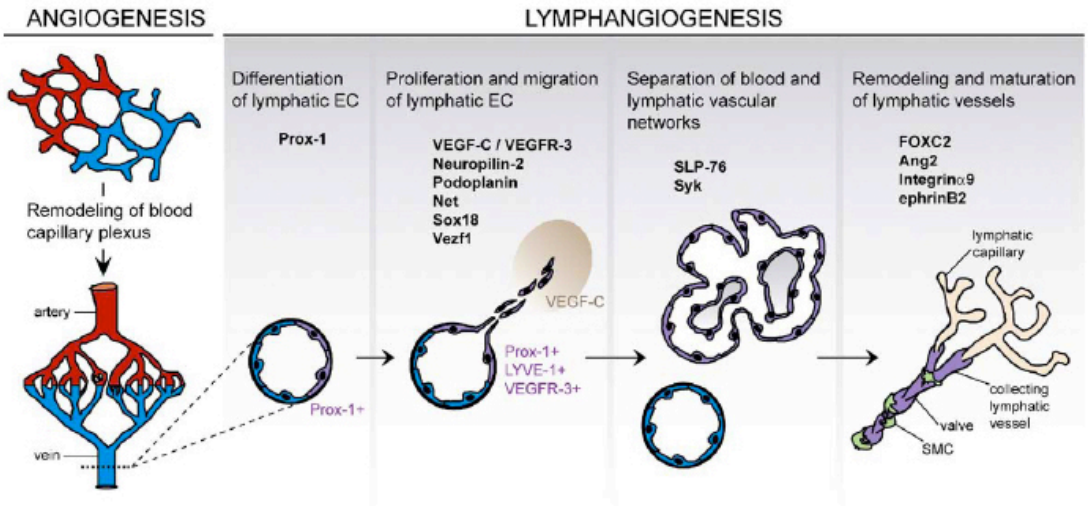

Figure 4.12 Development of lymphatic vasculature during embryogenesis

After the remodelling of the blood vasculature, lymphatic endothelial cells differentiate and sprout from the major veins to form lymphatic capillary plexus. Further maturation involves establishment of collecting lymphatic vessel versus lymphatic capillary identities and acquisition of SMC coverage as well as formation of luminal valves in the collecting vessels. Proteins involved in different processes in lymphatic development are shown below each section (Karpanen and Makinen 2006).

In contrast, collecting lymphatic vessels have sparse SMC coverage, which helps in propelling lymph forward, and numerous, irregularly located valves, which prevent backflow.

Maturation of lymphatic vessels correlates with the formation of luminal valves, the attachment of SMCs and PC, as well as the deposition of BM components and the assembly in a continuous matrix (Figure 4.12). In turn, lymphatic vessels may receive additional survival signals from the ECM, which can promote LEC survival *in vitro* by modulating integrin signalling (reviewed in (Karpanen and Makinen 2006).

Integrin $\alpha5\beta1$ can associate with VEGFR-3 and thereby regulate VEGFR-3 phosphorylation and function upon stimulation with VEGFR-3 ligands or ECM (Zhang, Groopman et al. 2005); (Wang, Zhang et al. 2001). In addition, integrins may have more direct functions in lymphangiogenesis. Integrin $\alpha9\beta1$, which is required for normal lymphatic development *in vivo*, was shown to directly bind VEGF-C and VEGF-D and thereby promote EC adhesion and migration (Huang, Wu et al. 2000).

Deficient valve formation and impaired SMC recruitment have severe effects on the functionality of lymphatic vessels, resulting in retrograde backflow and lymphedema. Substantial progress in understanding the development and molecular mechanism of the lymphatic vasculature has been made in the recent years and led to new insights into the role of lymphatic vessels in many diseased and might be beneficial in future therapeutics.

4.12 Stabilization of vessels by mural cells

Maturation of newly formed vessels during embryonic development and angiogenesis in general, is accompanied by the recruitment of mural cells (MC). MC consist of pericytes (PC) and vascular smooth muscle cells (vSMC) that associate with the vessel. MC may contribute to physical stability upon attachment, however recent studies suggest a major function of MC in EC differentiation, growth cessation and vessel stabilization.

While PC closely attach to the endothelium and are embedded in the BM of capillaries, vSMCs reside at arteries and veins. Their localization at the interface between ECs and the surrounding tissue makes them a key player in the interaction of the vessel and the extracellular space, therefore they may not only function in deposition and degradation of ECM components but also in sensing and shaping growth factor gradients.

In contrast to PC, vascular SMCs are enveloped by a continuous BM rich in collagen and elastin fibers. Smooth muscle cells can form up to several layers surrounding the endothelium of larger vessels, such as the dorsal aorta. Therefore, vSMCs are not in direct cell-cell contact with ECs and are separated by BM and in larger arteries by a tissue layer called the intima. Smooth muscle cells are highly contractile, regulating hemodynamic processes as a consequence of their high content of myofilaments and their strong smooth muscle alpha-actin (αSMA) expression.

PC instead express low levels of αSMA but can be detected using markers such as NG2 (chondroitin sulphate proteoglycan), desmin, regulator of G-protein signalling - 5 (RGS5) and PDGFR-β. Characteristically, PCs extend long processes and one single PC often contacts several ECs through specialized contacts, suggesting that PC facilitate and integrate cell communication. In areas where BM is absent between ECs and PCs, different types of endothelial-pericyte contacts have been described. In adhesion plaques, the intercellular space between two cells types is maintained and contains fibronectin deposits. Focal contacts called peg-socket-contacts represent membrane invaginations extending from either cell type, which contain tight-, gap- and adherent junctions (reviewed in (Armulik, Abramsson et al. 2005).

Pericyte coverage varies extensively between microvessels in different organs, with highest number of PC in the CNS and the lowest in skeletal muscle. These differences much likely reflect their function: while prevalent PC coverage contributes to the establishment of blood-brain-barrier in the CNS whereas PC coverage is low in

vessels surfaces engaged in exchange of gas and metabolites. Likewise PC morphology differs in distinct organs, adapting to their specific function in the organ.

In contrast to ECs, PC have a more complex ontogeny, as they can develop from various cells, as a function on their location in the embryo. In the CNS, PCs are derived from neural crest whereas PC enveloping coronary vessels arise from epicardial cells of the cardiac tract. Most commonly, however, PC originate from the mesenchyme. De Ruiter and colleagues demonstrated that embryonic ECs may transdifferentiate into vSMCs (reviewed in (Lamagna and Bergers 2006).

Recent studies identified PDGFRβ+ perivascular progenitor cells in tumours that are partly recruited from the bone marrow. These PDGFRβ+ cells differentiated into mature PC expressing pericyte markers NG2 and SMA and are able to elicit vascular stabilization, maturation and survival during adult angiogenesis (Song, Ewald et al. 2005).

PCs have the ability to modulate and differentiate in vSMCs and vice versa in conjunction with vessel growth and remodelling. In addition, PC may also give rise to other cell types of mesenchymal origin such as fibroblasts (Armulik, Abramsson et al. 2005). In the following chapters, I will summarize major findings, as well as signalling pathways, ECM components and junctional molecules functioning in mural cell recruitment. Pericyte–endothelial interactions are controlled by a host of different molecules, including platelet-derived growth factor (PDGF)-BB/PDGF receptor (PDGFR) β, membrane type (MT) 1-matrix metalloproteinase (MMP), Heparan sulphate proteoglycans (HSPG), N-cadherin, Ang1/Tie-2, transforming growth factor (TGF) β, hepatocyte growth factor (HGF), EphrinB2 and vascular cell adhesion molecule (VCAM) 1/α4-integrin (Gerhardt and Semb 2008). Figure 4.13 illustrates the principles of pericyte/ endothelial interaction and mural cell recruitment during development.

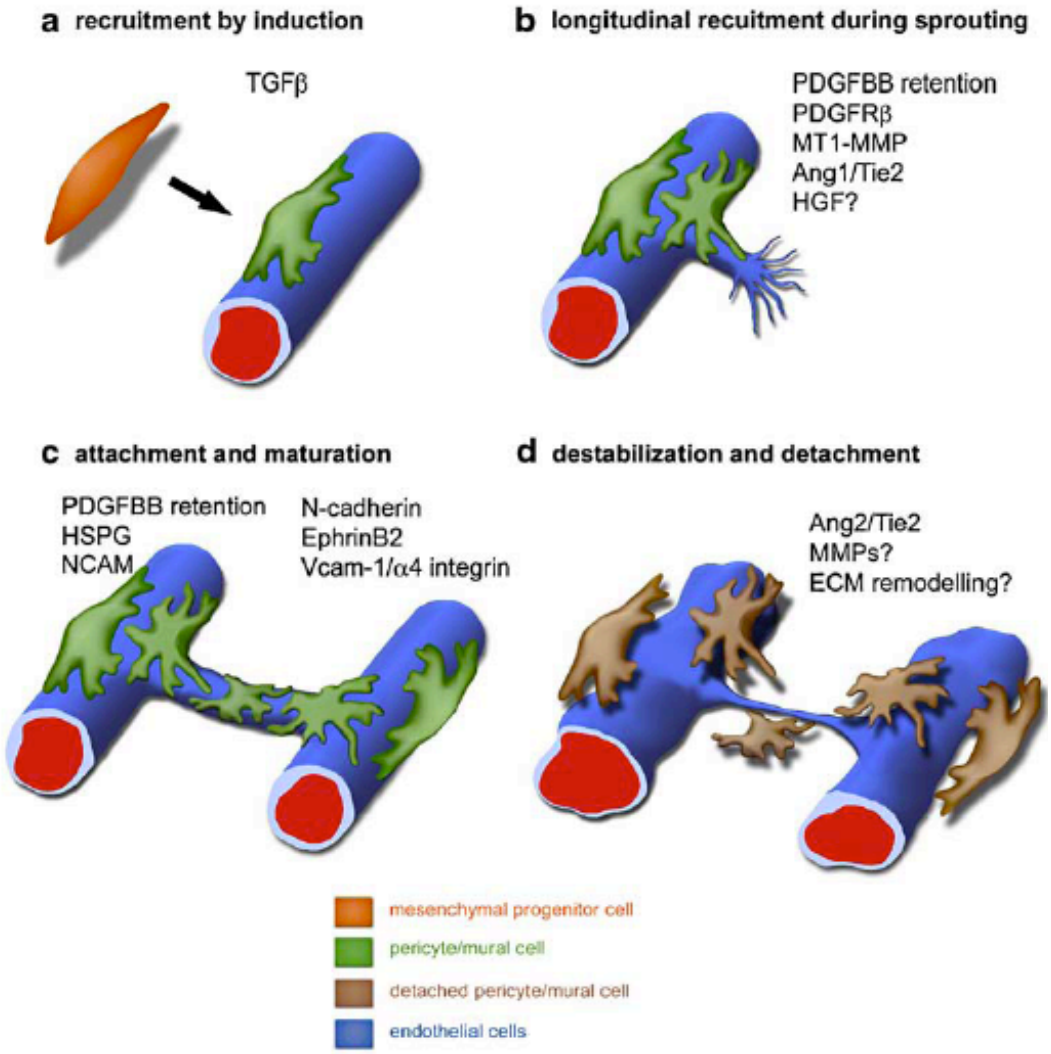

Figure 4.13 Schematic model of pericyte recruitment, attachment and detachment

Genes listed in the figure positively regulate pericyte recruitment and attachment; a) TGF-β dependent induction of mesenchymal progenitor cells to differentiate into pericytes; b) during sprouting angiogenesis, recruitment, proliferation and migration of pericytes requires endothelial PDGF-BB signalling to pericytes expressing PDGFR-β; MT1-MMP enhances this effect by direct interaction with PDGFR-β; Ang1 activates the endothelial Tie2 receptor, leading to endothelial HGF secretion, which increases pericyte motility. c) Vascular maturation requires firm pericyte adhesion regulated by endothelial–pericytic N-cadherin junctions, EphrinB2 and integrin signalling. HSPG and PDGF-BB retention are essential for attachment. NCAM expression by surrounding tissue enhances pericyte recruitment and attachment in a PDGF-BB dependent manner. d) Detachment of pericytes destabilizes the vasculature and leads to loss of diameter control. Ang2 counteracting the effect of Ang1 can lead to pericyte detachment. ECM degradation through either MMPs or alteration of HSPG may also contribute to this process (Gerhardt and Semb 2008).

4.13 De novo induction of vSMCs depends on TGF-β

Members of the TGF-β superfamily exert their effect by binding to specific serine/threonine kinase type I and type II receptor complexes. In mammals, seven type I, also termed activin receptor-like kinase (ALK) 1 to 7, and five type II receptors have been identified. TGF-β has high affinity for the TGF-β type II receptor (TβRII), and upon binding a specific TGF-β type I receptor (TβRI) is recruited. In ECs, TGF-β has been shown to bind and signal via both, ALK1 and ALK5. On heteromeric complex formation between type I and type II receptors, the TβRI is transphosphorylated by TβRII (Figure 4.14). This results in a conformational change in and activation of the type I receptor, which can subsequently propagate the signal inside the cell by the phosphorylation of specific effectors.

Endoglin, a third type of transmembrane TGF-β receptor, acts as a co-receptor and participates in TGF-β mediated ALK1 and ALK5- signalling in ECs. After receptor activation and phosphorylation, receptor-regulated Smads (R-Smads) are recruited and presented to the TβRI, which become phosphorylated and form a complex with common mediator (Co-)Smad 4, accumulate in the nucleus and regulate the expression of specific target genes. In ECs, ALK1 activation leads to phosphorylation of Smads1/5/8, while catalytic engagement of ALK5 results in phosphorylation of Smads2/3 (reviewed in (Bertolino, Deckers et al. 2005);(Goumans, Liu et al. 2009).

Genetic inactivation of members of the TGF-β signalling pathway including *TGFb1, TbRII, Alk1, Alk5, endoglin* and *Smad5* revealed that TGF-β signalling is essential for vascular development. Mice carrying loss of function mutations in any of these genes die at mid gestation between E9.5- E11.5 during embryonic development due to disrupted vasculogenesis in the yolk sac. Detailed analyses demonstrated TGF-β components to be crucial for several steps of the angiogenic process, including the maintenance of the integrity of the vessel wall, the recruitment of SMCs, the deposition of ECM, as well as the differentiation of ECs into a more specialized endothelium such as arteries and veins.

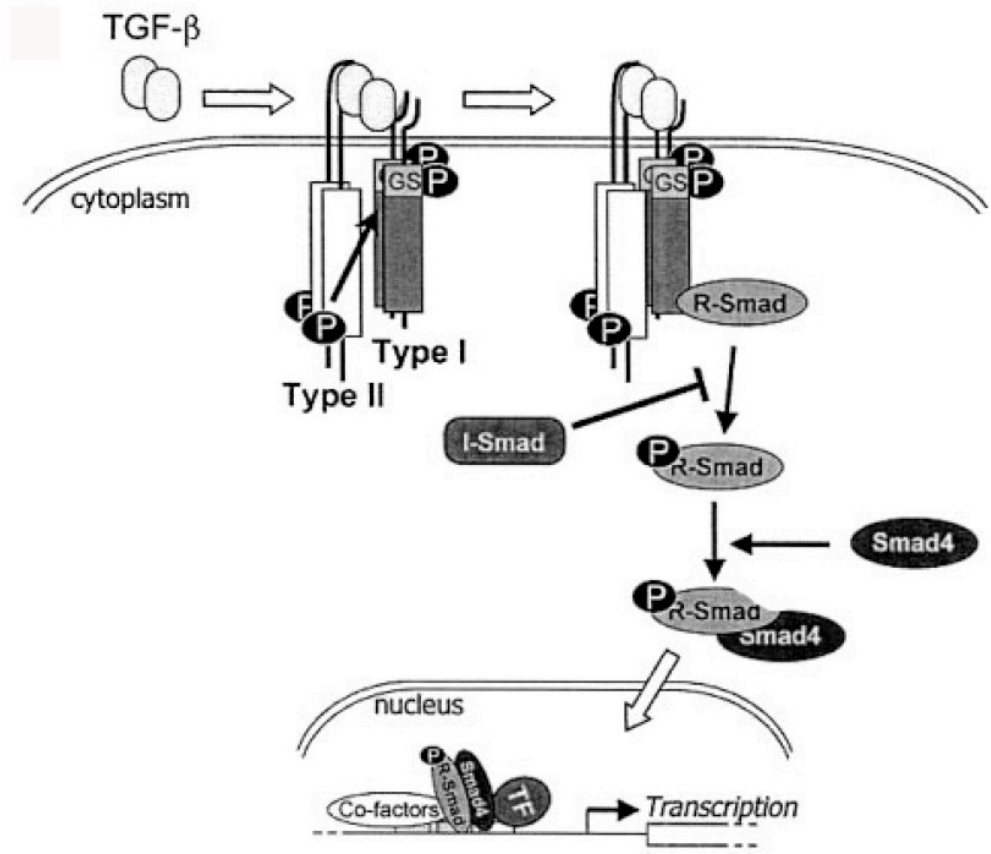

Figure 4.14 Schematic representation of TGF-β/SMAD signal transduction pathway

TGF-β induces a heteromeric complex of type I and type II serine/threonine kinase receptors. On ligand binding, a type II receptor interacts with a type I receptor and phosphorylates the GS domain of the type I receptor. Then, the activated type I receptor activates R-Smads by phosphorylating their C-terminus. On phosphorylation, R-Smads form heteromeric complexes with Smad4 that translocate into the nucleus. Within the nucleus, the heteromeric Smad complexes, in collaboration with transcription factors (TFs), cofactors (*ie*, coactivators and corepressors) participate in the regulation of target gene expression (Bertolino, Deckers et al. 2005).

Mutations in endoglin and ALK1 result in the human autosomal-dominant disorder called hereditary hemorrhagic telangiectasia (HHT) displaying vascular malformation including fragile and leaky vessels with defects in MC recruitment.

The primary target cell for TGF-β is the EC since endothelial-specific deletion of ALK5 and TβRII phenocopied the complete loss of TβRII or ALK5, indicating that the defects in the recruitment or differentiation of SMCs in these knockout mice are likely to be an indirect consequence of the primary defect in the ECs (Carvalho, Itoh et al. 2007).

Dependent on context and dosage, TGF-β has a stimulatory or inhibitory effect

on blood vessel formation. TGF-β signalling via ALK1 promotes endothelial proliferation, tube formation and migration while TGF-β/ALK5 signalling inhibits these responses. ALK1 and ALK5 physically interact, and their cross-talk provides ECs with a TGF-β dependent switch to fine tune endothelial function. ALK5, for example induces the expression of fibronectin and plasminogen activator inhibitor type 1 (PAI-1), a negative regulator of EC migration. ALK5 signalling has been proposed to regulate TGF-β-induced vascular permeability and actin cytoskeleton remodelling. Clustered VE-cadherin recruits TβRII and may promote TGF-β signalling by enhancing TβRII/ALK5 assembly in an active receptor complex. Elevated TGF-β-induced Smad2/3 activation by VE-cadherin indicates a positive and endothelial specific role for VE-cadherin in TGF-β/ALK5-induced vessel stabilization. Taken together, TGF-β/ALK5 signalling plays an important role in keeping the endothelium quiescent (Rudini, Felici et al. 2008).

Although the EC appears to be the primary target for TGF-β signalling during early blood vessel assembly, there is ample evidence for signalling from the EC to the MC important for maturation and stabilization of vessels. TGF-β is a potent stimulator for vSMC differentiation and vSMC express endoglin and multiple type I and II receptors, activating the expression of SMC differentiation genes such as SM22α. TGF-β-induced growth inhibition of vascular SMCs was found to be ALK5- mediated via both Smad3-dependent and p38 MAPK-dependent signalling pathways. *Smad3*-deficient vascular SMCs demonstrated reduced growth inhibition by TGF-β, but did not show any attenuated TGF-β-mediated migratory response (Feinberg, Watanabe et al. 2004). ECs produce latent TGF-β that upon EC-SMC interaction can be activated and induce SMC differentiation and function (Ding, Darland et al. 2004). Hirschi and colleagues identified that gap junction communication between endothelial and mesenchymal cells mediates TGF-β activation and subsequent MC differentiation (Hirschi, Burt et al. 2003). Cook et al. report that TGF–β induces rearrangement of the adherent junction complex by separating VEGFR2 from VE-cadherin and increasing β-catenin association with both VEGFR2 and VE-cadherin. This rearrangement requires VEGF signalling through VEGFR2 in ECs, highlighting a new mechanism in VEGF-TGF-β interaction (Cook, Ferrari et al. 2008).

The functional relevance of TGF-β expression and MC development *in vivo* has been demonstrated by gene inactivation in mice. *Alk1* and *endoglin* deficient mice display defective remodelling of the primary capillary plexus of the yolk sac and

aberrant development of SMCs. Mice lacking *TbRII, Smad5, Smad1* and *TGFb1* show defects in vasculature structure or blood vessel organization indicative of a defect in EC lining and impaired SMC development (reviewed by (Goumans, Liu et al. 2009)). Taken together, TGF-β signalling is important for vascular development and depending on the context acts pro-or anti-angiogenic on EC functions and controls SMC differentiation.

4.14 PDGF-B/PDGFRb signalling in pericyte recruitment

Similar to the VEGF growth factor family, platelet derived growth factor (PDGF) are dimers of disulfide-linked polypeptide chains. In mammals, four different genes encode for PDGF chains, PDGF-A, PDGF-B, PDGF-C and PDGF-D. All four ligands, which are inactive in their monomeric form, assemble intracellularly to form disulfide-linked homodimers. One heterodimer PDGF-AB has been demonstrated in human platelets, however, PDGF homodimers dominate, at least during development. Also, the endogenous expression of *Pdgfa* and *Pdgfb* are generally non-overlapping, suggesting that heterodimers are infrequent. All members of the PDGF/ VEGF family carry a growth factor core domain containing a conserved set of cysteine residues. The core domain is necessary and sufficient for receptor binding and activation. Classification into PDGFs and VEGFs is based on receptor binding, assuming selectivity for their cognate receptors (reviewed in(Andrae, Gallini et al. 2008). Recent studies showed however, that VEGF-A might bind to and activate PDGF receptors in bone-marrow-derived mesenchymal stem cells (Ball, Shuttleworth et al. 2007). Further challenges to functional distinctions come from the finding of VEGFR2/ PDGFRβ complexes (Greenberg, Shields et al. 2008).

PDGFs act via two membrane-bound receptor tyrosine kinases, PDGF receptor α and –β, with common domain structures. Ligand binding initiates receptor dimerization and subsequently autophosphorylation and activation of downstream signalling cascade. Phosphotyrosine residues provide docking sites for SH2-domain containing signalling molecules such as PI3K, PLCγ, Ras GTPase-activating protein (Ras-GAP) and Src family kinases, which initiate signal transduction.

Tallquist and colleagues generated mice that bear a PDGFR-β that can no longer activate PI3K or PLCγ and showed that that loss of PI3K and PLCγ activation does not fully incapacitate the β-receptor, but rather quantitatively represses the ability of the

receptor to carry out normal functions (Tallquist, Klinghoffer et al. 2000).

Depending on ligand configuration and the pattern of receptor expression, different receptor dimers may form. However, *in vivo* there is functional evidence for only few interactions, i.e. PDGF-AA and PDGF-CC via PDGFR-α and PDGF-BB via PDGFR-β. PDGFs act primarly as paracrine growth factors. Both PDGF and PDGFR expression patterns are spatio-temporally regulated *in vivo*, and several factors induce PDGFR expression, including TGF-β and basic fibroblast growth factor (bFGF) (reviewed in (Andrae, Gallini et al. 2008)). *Pdgfb* is mainly expressed in vascular ECs, whereas *Pdgfrb* is expressed in the mesenchyme, particularly in PC and vSMCs. As described for VEGF-A, binding to ECM components regulates diffusion of PDGFs in the tissue interstitium. For PDGF-B such binding is accomplished in part by the positively charged C-terminal motifs, referred to as retention motif, containing a conserved sequence of basic amino acid residues. The presence or absence of the retention motif is determined by alternative C-terminal proteolytic processing of the PDGF-B chain (reviewed in (Andrae, Gallini et al. 2008)).

Combined expression and loss of function studies of *Pdgfb* and *Pdgfrb* suggest that PDGF-B is released from the endothelium and promotes recruitment and proliferation of adjacent MC.

A detailed analysis of *Pdgfb* expression in the CNS revealed a heterogeneous endothelial *Pdgfb* expression pattern. At E11.5 and E14.5, *Pdgfb* expression occurred in most vascular EC recognized in the brain, while at later embryonic stages and postnatally *Pdgfb* expression is restricted to few, immature ECs (Hellstrom, Kalen et al. 1999). *Pdgfb* expression is strongest in leading endothelial tip cell of the retinal vasculature (Gerhardt, Golding et al. 2003), and endothelial specific ablation of *Pdgfb* results in cardiovascular defects resembling the *Pdgfb* null mice, indicating that the endothelium is the main source of PDGF-BB expression (Bjarnegard, Enge et al. 2004). Deletion of *pdgfb* in two other major cellular sources of PDGF-B, neurons, and hematopoietic cells had no effect on the vasculature (Enge, Bjarnegård et al. 2002); (Kaminski, Lindahl et al. 2001).

In mid-to-late gestational embryos, developing PC are normally seen as solitary PDGFR-β-positive cells in close proximity to capillaries (Lindahl, Johansson et al. 1997). Developing vSMC of arteries/arterioles are likewise PDGFR-β positive, and occur in single or multiple layers around the endothelial tube (Lindahl, Johansson et al. 1997). Hellstrom and colleagues confirmed the presence of abundant PDGFR-β-

positive vSMC/PC progenitors in a wide range of organs, including brain, skin and heart with the exception of the liver (Hellström, Kalén et al. 1999).

Pdgfb and *Pdgfrb* -deficient mice both displayed substantial loss of MC investment of capillary vessels due to reduced MC proliferation, suggesting a role of PDGF-B in vSMC/PC cell proliferation during vascular growth. Their findings led to a model in which PDGFR-β-positive vSMC/PC progenitors initially form around certain vessels by PDGF-B-independent induction. Subsequent angiogenic sprouting and vessel enlargement involves PDGF-B-dependent vSMC/PC progenitor co-migration and proliferation, and/or PDGF-B-independent new induction of vSMC/PC, depending on tissue context (Hellström, Kalén et al. 1999).

The degree of MC loss differs between different organs, reflecting a role of PDGF-B/PDGFR-β as a selective rather than inductive signal in PC/vSMC development. Induction of MC differentiation from the perivascular mesenchyme around the early aorta occurs independent of PDGF-B/PDGFR-β signalling. In contrast, the recruitment of MCs from a pre-existing pool of such cells, by means of co-migration and proliferation, is completely dependent on PDGF-B/PDGFR-β signalling, which would explain the almost complete loss of CNS MCs in the absence of PDGF-B or PDGFR-β (Hellström, Kalén et al. 1999).; reviewed in (Andrae, Gallini et al. 2008) and (Armulik, Abramsson et al. 2005).

Detailed analysis of the vasculature in CNS of *Pdgfb* and *Pdgfrb* deficient mice revealed that the absence of PCs correlates with endothelial hyperplasia, increased capillary diameter, abnormal EC shape and ultrastructure, changed cellular distribution of certain junctional proteins, and morphological signs of increased transendothelial permeability (Hellstrom, Gerhardt et al. 2001). These findings suggest that MC investment negatively controls EC proliferation and promotes vessel stabilization by maturation of ECs and the establishment of firm junctions. Despite severe MC defects and hypoplasia starting from embryonic day 10, *Pdgfb* and *Pdgfrb* null mice developed until E16-19.5. Although PC deficiency appears to have direct effects on EC number before E13.5, the subsequent increased VEGF-A levels may further aggravate defective microvessel architecture, promote vascular permeability, and contribute to the formation of the edematous and widespread hemorrhagic phenotype causing embryonic lethality in late gestation *Pdgfb* and *Pdgfrb* knock out embryos (Hellstrom, Gerhardt et al. 2001).

PDGF-B/PDGFR-β signalling also controls mesangial cell development in

kidney glomeruli. In *Pdgfb* and *Pdgfrb* knockout kidneys, mesangial cells are not properly recruited into the developing glomerular tufts, and as a consequence capillary branching fails. These data identified PDGFR-β positive mesangial cells as a primary target for endothelium-derived PDGF-BB (Lindahl, Hellstrom et al. 1998). Conversely, blocking PDGFR-β by administration of neutralizing antibodies resulted in severe disruption of the glomerular structure, whereas no apparent deformation was observed in the collecting ducts. In the disrupted glomeruli, the number of the mesangial cells was reduced markedly and capillary ECs of the glomeruli in the outer cortex region underwent apoptosis (Sano, Ueda et al. 2002).

Wagner and colleagues further established that mitogenic signalling is mediated by PDGFR-β in metanephric mesenchymal cells. PDGF signalling stimulates proliferation and migration of metanephric mesenchymal cells, from which mesangial cells are derived and PI3K is an important regulator of PDGF-induced DNA synthesis. Activation of ERK1/2 is partially dependent on PI3K, and both the PI3K and MEK-ERK1/2 pathways contribute to PI3K–dependent mitogenesis (Wagner, Ricono et al. 2007).

PDGF-B/PDGFR-β signalling also affects vessel formation and PC recruitment in the labyrinthine layer of the mouse placenta. Normally, the placenta develops a complex network of capillaries that generates a large surface for excretion and absorption. The reduced numbers of PC and trophoblasts in mutants of *Pdgfb* and *Pdgfrb* null embryos correlates with specific vascular defects including dilated vessels and an abnormal ratio of the surface area of maternal and fetal blood vessels in the placental labyrinth. Therefore, PDGF-BB acts locally to contribute to MC recruitment in the placenta and PC possibly control capillary branching through intussusceptive vessel splitting (Andrae, Gallini et al. 2008); (Ohlsson, Falck et al. 1999).

Recent results indicate a role for PDGF-B/PDGFR-β signalling in epicardial epithelial-to-mesenchymal transition (EMT) and recruitment of epicardium derived mesenchymal cells into the myocardium (Van den Akker, Winkel et al. 2008). *Pdgfb* and *Pdgfrb* deficient embryos displayed perimembranous and muscular ventricular septal defects, maldevelopment of the atrioventricular cushions and valves, impaired coronary arteriogenesis, and hypoplasia of the myocardium and cardiac nerves. The abnormalities correspond with models in which epicardial development is impaired and with neuronal neural crest-related innervation deficits. This implies a role for PDGF-B/PDGFR-β-signalling specifically in the contribution of these cell lineages to cardiac

development (Van den Akker, Winkel et al. 2008).

VEGF-A, FGF-2 and PDGF-B are pro-angiogenic factors that play essential roles during vascular development and pathological conditions. However, their precise interplay or potential synergysm is not well established. Using the matrigel plug assay, an *in vivo* angiogenesis model, Kano and colleagues showed enhanced intercellular PDGF-B signalling in a cell-type specific manner: VEGF-A enhances endothelial *Pdgfb* expression, whereas FGF-2 enhances mural *Pdgfrb* expression. Co-stimulation with VEGF-A and FGF-2 caused significant MC recruitment *in vitro* and formation of functional neovasculature *in vivo*, compared with single-agent stimulation, suggesting a synergistic effect by co-stimulation with growth factors (Kano, Morishita et al. 2005).
VEGF and PDGF stimulate proliferation and migration of EC and MC, respectively and thereby promote vessel growth and stabilization of newly formed sprouts. One would expect that both act synergistically during angiogenesis, however, a recent study revealed that combination of both growth factors completely suppressed angiogenesis.
Greenberg and colleagues found that under conditions of VEGF/PDGF stimulation VEGFR2 negatively regulates neovascularization (Greenberg, Shields et al. 2008). Stimulation of tissues with VEGF/PDGF results in a reduction of vascular pericyte coverage, but VEGFR2 inhibition restored pericyte coverage and neovascularization, suggesting that MC VEGFR2 negatively regulates this response.
Further *in vitro* studies demonstrated that VEGF-mediated activation of VEGFR2 suppresses PDGFR-β signalling in vSMC through the formation of a VEGFR2/ PDGFR-β complex. Therefore, Greenberg et al. identified VEGF-A as an angiogenic inhibitor by disrupting vSMC function. However, crucial expression studies are missing in this study. The authors have not demonstrated VEGFR2 expression in mural cells and the study lacks *in vivo* evidence for a function of VEGFR2 in SMC coverage. One could address this aspect by Cre-lox mediated deletion of VEGFR2 in mural cells.

Several isoforms of the growth factors PDGF and VEGF contain long C-terminal stretches of positively charged amino acids that mediate the binding to the ECM. This domain is referred to as retention motif and promotes binding to heparan sulfate (HS) proteoglycans.
In PDGF-A and PDGF-B, the HSPG-binding motifs do not affect receptor binding or biological activity of the recombinant proteins. However, in transfected cells, these motifs confer retention of the secreted growth factor to the surface of the producing

cells. Conversely, absence of the retention motif leads to increased secretion of a diffusible protein that readily accumulates in the cell culture medium. Deletion of the PDGF-B retention motif *in vivo* by gene targeting (*Pdgfb*$^{ret/ret}$) resulted in defective investment of PC in the microvessel wall. Although *Pdgfb*$^{ret/ret}$ mice survived into adulthood, the phenotype strongly resembled defects observed in *Pdgfb/ Pdgfrb* null mice including abnormal formation of the renal glomerulus mesangium. Detailed analysis suggested that retention of PDGF-B in microvessels is essential for proper recruitment and organization of PC and for renal and retinal function in adult mice (Lindblom, Gerhardt et al. 2003).

4.15 Heparan sulfate interaction during angiogenesis

The heparan sulfate (HS) complexity, their ubiquitous and evolutionary conserved expression pattern as well as their enormous spectrum of interaction may reflect the importance of HS during embryonic development and pathological condition.
Heparan sulfate glycosaminoglycans are members of the glycosaminoglycan (GAG) family, which are complex polysaccharides that are characterized by a repeat disaccharide unit of uronic acid linked to a glucosamine, also referred to as HS. These HS chains are unbranched and of variable length, with one end covalently bound to a core protein via serine residues. Their structural complexity arises from the differential modification of the saccharide backbone including N-and O-sulfations, as well as N-acetylation or unmodified N-residues. HSPG are classified into several families based on the core protein structure. Glypicans and Syndecans are two major cell surface HSPGs, and are linked to the plasma membrane by a glycosylphosphatidylinositol (GPI) linkage or a transmembrane domain, respectively. Perlecans are secreted HSPGs that are mainly distributed in the ECM (Figure 4.15). In contrast, to glypicans and perlecans, the syndecan family contains chondroitin sulftate in addition to the heparan sulfate chain (reviewed in (Lin 2004)).

HS chain biosynthesis takes place in the Golgi and can be divided in three major sequential processes: chain initiation, polymerization and modification. Figure 4.16 summarizes a simplified three-step process of HS chain synthesis.

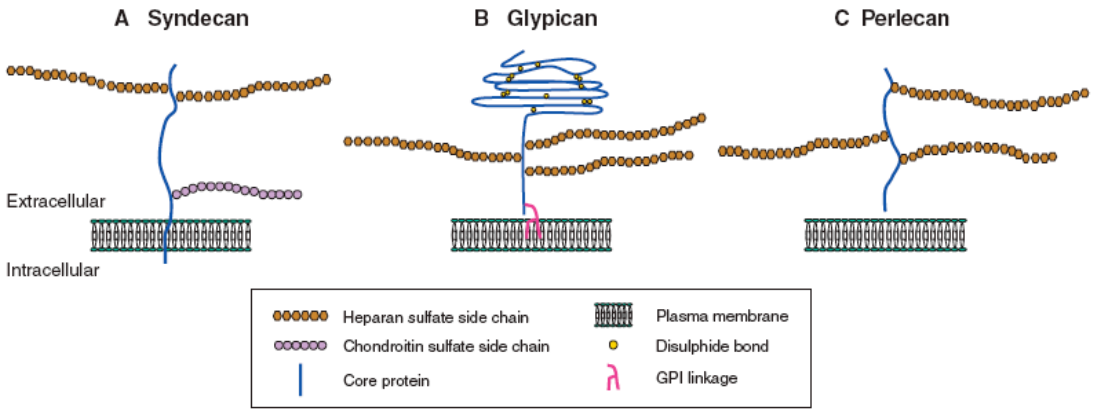

Figure 4.15 The three main classes of cell-surface heparan sulfate proteoglycans (HSPGs)

(A) Syndecan core proteins are transmembrane proteins that contain a highly conserved C-terminal cytoplasmic domain. Heparan sulfate (HS) chains attach to serine residues distal from the plasma membrane. Some syndecans also contain a chondroitin sulfate (CS) chain(s) that attaches to a serine residue(s) near the membrane. (B) The glypican core proteins are disulphide-stabilized globular core proteins that are linked to the plasma membrane by a glycosylphosphatidylinositol (GPI) linkage. HS chains link to serine residues adjacent to the plasma membrane. (C) Perlecans are secreted HSPGs that carry HS chains (Lin 2004).

HS chain synthesis begins with the assembly of a linkage tetrasaccharide (glucuronic acid-galactose-glactose xylose) at the GAG attachment site(s) of the core protein, which contains two to four Ser-Gly sequences. After addition of an N-acetylglucosamin residue, the HS polymer is generated by alternating addition of N-acetylglucosamin and glucuronic acid catalyzed by glycosyl transferase encoded by *EXT*.

As the chain grows, modifying enzymes introduce sulfate groups at various positions, and some of the glucuronic acid residues are converted into iduronic acid (epimerization). Any of the four NDST enzyme (glucosaminyl Ndeacetylase/ N-sulfotransferase 1-4) can replace the acetyl group in N-acetylglucosamine with a sulfate group. 2O-, 3O- and 6O-sulfotransferases (OST) attach additional sulfate groups. The addition of negatively charged sulfation groups results in a highly negatively charged, hydrophilic HS product that contains clusters of N-and O-sulfated sugar residues separated by non-sulfated regions (Figure 4.16). The negative charge contributed by carboxyl and sulfate groups is essential for interactions between HS and basic amino acid residues in proteins such as VEGF-A and PDGF-B.

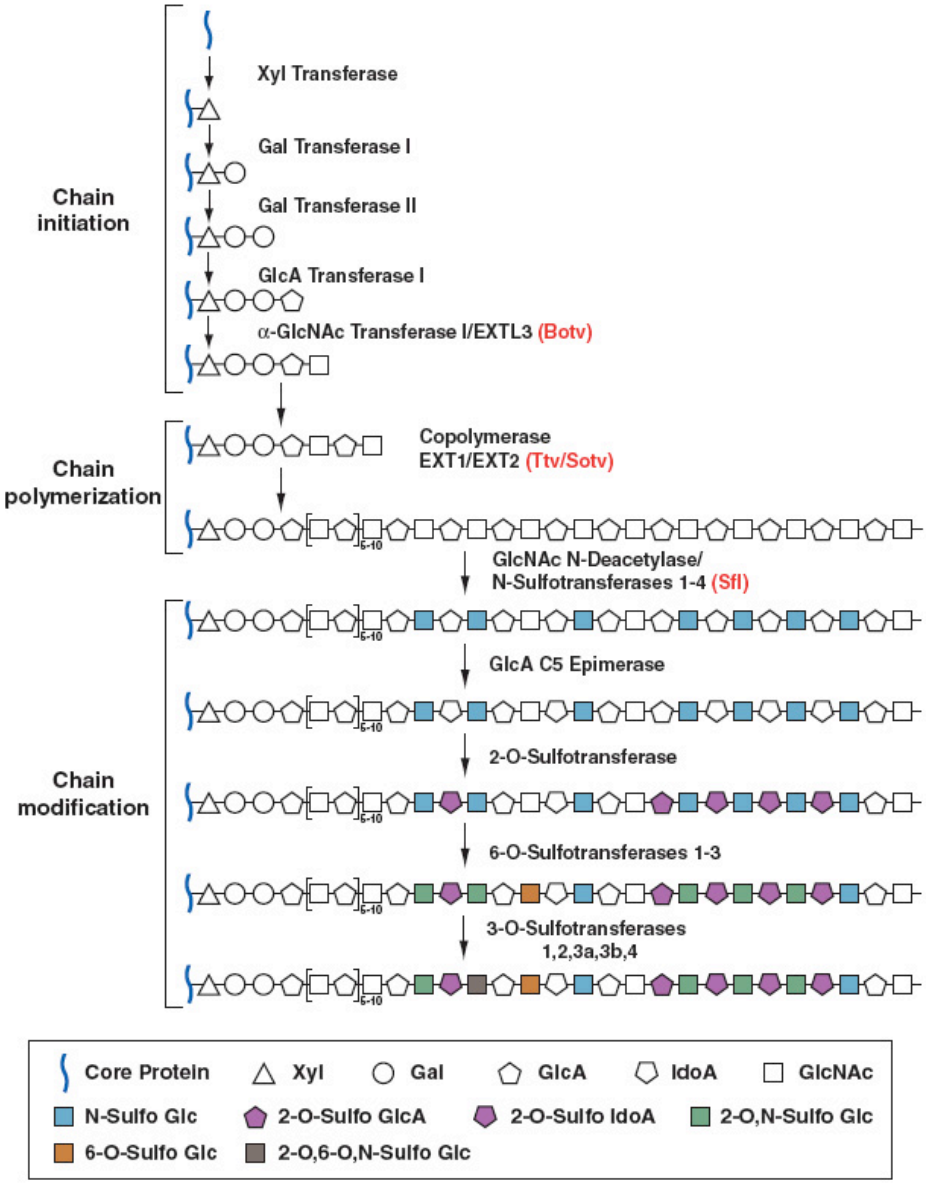

Figure 4.16 Heparan sulfate chain biosynthesis

Heparan sulfate (HS) glycosaminoglycan (GAG) chains are synthesized on a core protein by the sequential action of individual glycosyltransferases and modification enzymes, in a three-step process involving chain initiation, polymerization and modification. HS chain synthesis begins with the assembly of a linkage tetrasaccharide on serine residues in the core polypeptide. This process is catalyzed by four enzymes (Xyl transferase, Gal transferase I-II and GlcA transferase I), which add individual sugar residues sequentially to the non-reducing end of the growing chain. After the assembly of the linkage region, one or more α-GlcNAc transferases add a single α1,4-linked GlcNAc unit to the chain, which initiates the HS polymerization process. HS chain polymerization then takes place by the addition of alternating GlcA and GlcNAc residues, which is catalyzed by the EXT family proteins. As the chain polymerizes, it undergoes a series of modifications that include GlcNAc N-deacetylation and Nsulfation, C5 epimerization of GlcA to IdoA, and variable *O*-sulfation at C2 of IdoA and GlcA, at C6 of GlcNAc and GlcNS units, and, occasionally, at C3 of GlcN residues. The HS GAG chains are ~100 or more sugar units long and have numerous structural heterogeneities. Gal, galactose; GlcNAc, Nacetylglucosamine; GlcA, glucuronic acid; GlcNS, N-sulfoglucosamine; IdoA, iduronic acid (Lin 2004).

The final HS structure depends in the activity of modification enzymes and differs greatly in various tissues, cells and physiological and pathological conditions. However, almost every cell has the capacity to express HS. Heparan sulfate and structurally related protein heparin interact with a wide variety of growth factors, morphogens, proteases and protease inhibitors, cytokine and ECM components. HS interactions mediate many biological functions from the formation of growth factor/ morphogen gradients, to the stabilization and activation of ligand-receptor-complexes, over acting as scaffolding proteins. The functional relevance of HS is reflected in the early lethality of mice at E8.5 lacking HS biosynthesis by deletion of glycosyl transferase *Ext1*. Ablation of the polymerization enzyme results in total absence of HS but increased chondroitine sulfate synthesis. *Ext1* homozygous mutants fail to gastrulate and generally lack organized mesoderm and extraembryonic tissues, resulting in smaller embryos compared to normal littermates (Lin, Wei et al. 2000).

The Drosophila *Ext1* homologue, tout-velu, regulates Hedgehog diffusion and signalling, which play an important role in tissue patterning.

Mutation of the *EXT1* and *EXT2* gene in humans result in a pathological condition, termed hereditary multiple exostosis (HME). *EXT* patients carrying mutations in one of the *EXT* genes develop multiple benign bone tumours and often have a short stature. *EXT1* heterozygous humans develop exostoses in their bones at an early age, correlating with reduced HS production. Further, HS on the tumour-cell surface have been shown to be important in many aspects of tumour phenotype and development, including cellular transformation, tumour growth, invasion and metastasis. *In vivo* studies in mice indicate that changes in the fine structure of tumour-cell-surface HSs have profound effects on tumour-cell growth kinetics and metastasis formation (reviewed in (Sasisekharan, Shriver et al. 2002)). Human heparanase, a matrix-degrading enzyme is rarely found in human tissues but its expression is often increased in tumours promoting invasion, angiogenesis and spontaneous metastasis. Heparanse-mediated cleavage of the HS chain releases 10-20 residue sugar long fragments that influence activity and availability of HS-binding growth factors that regulate cell behaviour of tumour cells and host cells in the tumour environment (reviewed in Sanderson et al., 2005). Inhibition of heparanase results in reduction of tumour growth and impaired angiogenesis, correlating with diminished VEGF-A interaction to VEGFR2 on the tumour endothelium (Joyce, Freeman et al. 2005). Taken together, genetic studies highlight the importance of HS biosynthesis and expression in human diseases such as

cancer and hereditary multiple exostosis.

The location of HS at the cellular-matrix interface makes them important modulators of cell signalling events, and thereby regulating how cells perceive their environment. The formation of growth factor gradients is essential during embryonic development as shown by target inactivation of global and cell-type specific deletion in HS-biosynthesis and altered HS modification.

As described previously, loss of HS-binding domain in VEGF and PDGF-B leads to abnormal vessel morphology and patterning defects as well as reduced PC recruitment, respectively. The vascular defects are caused by loss of spatial growth factor distribution due to lack of growth factor retention properties. Following the studies of Lindblom and colleagues, demonstrating that HS-binding of PDGF-BB is essential for proper pericyte recruitment and association to the vessel, Abramsson et al. investigated the functional relevance of N-sulfation in HS-mediated PDFG-BB binding and its effect on pericyte recruitment (Abramsson, Kurup et al. 2007). Studying PC recruitment in the developing hindbrain of mouse mutants for *Ndst1*, *Hsepi*, and *Pdgfb*$^{ret/ret}$ revealed an astonishing degree of correlation between *in vitro* binding of PDGF-BB to HS and *in vivo* PC recruitment/attachment. Moreover, the data demonstrate that *N*- and *O*-sulfation of HS are required for efficient PDGF-BB binding, whereas saccharide fine structure is of lesser importance. Cell culture assays provided corroborating direct evidence for reduced retention of PDGF-BB on cells deficient in HS and indicated that HS may contribute to PC recruitment by augmenting PDGFRb signalling and directed cell migration toward PDGF-BB. Therefore, interaction of PDGF-BB with sulfated HS regions is essential for PC recruitment in vascular development.

In agreement with these findings, endothelial PDGF-BB retention is indispensable for proper integration of PC in the vessel wall of tumour vessels (Abramsson, Lindblom et al. 2003). In tumours transplanted into PDGF-B retention motif–deficient (*Pdgf-b*$^{ret/ret}$) mice, PC were fewer and were partially detached from the vessel wall, coinciding with increased tumour vessel diameter and hemorrhaging. PDGF-B expression from the tumour cells enhances PC recruitment in both wildtype and *Pdgf-b*$^{ret/ret}$ mice but failed to correct the pericyte detachment in *Pdgf-b*$^{ret/ret}$ mice.

Fuster and colleagues addressed the function of endothelial heparan sulfate during angiogenesis by deleting *Ndst1* from endothelial cells. Physiological angiogenesis during cutaneous wound repair was unaffected, as was growth and reproductive capacity of the mice.

However, loss of endothelial *Ndst1* resulted in smaller tumours and reduced microvascular density and branching *in vivo* due to reduced growth factor binding and apoptosis. *Ndst1* deficient ECs exhibited reduced binding of FGF-2 and $VEGF_{164}$ to cells and to purified heparan sulfate, suggesting an cell-autonomous effect of endothelial HS (Fuster, Wang et al. 2007).

Likewise, embryonic stem (ES) cells lacking *Ndst1* and *-2* were unable to bind VEGF-A_{164} and failed to differentiate and form vessels that could not be rescued by addition of HS or heparin (Jakobsson, Kreuger et al. 2006). *Vegfr2* deficient ES cells also fail to form vascular structures, however mixing *Ndst1/2-/-* and *Vegfr2-/-* ES cells resulted in normal vessel formation and differentiation, suggesting that endothelial derived HS is dispensable for vascular development in embryonic bodies.

Therefore, VEGF signalling in ECs is fully supported by HS expressed in trans by adjacent perivascular smooth muscle cells, at least in this culture system. Transactivation of VEGFR2 leads to prolonged and enhanced signal transduction due to HS-dependent trapping of the active VEGFR2 signalling complex (Jakobsson, Kreuger et al. 2006).

This study highlights the crosstalk between endothelial and MC and a mechanism of transactivation by HS. The aspect of the spatial constellation of HS production between signal sending and signal receiving cell will become important in the third project of my thesis. I will follow up on this aspect later in thesis.

In summary, HS is required for embryogenesis and plays important roles during normal and pathological angiogenesis by shaping growth factor gradients, activation of receptor complexes and mediating many signalling pathways involved in vascular development.

4.16 Extracellular matrix/ mircoenvironment surrounding blood vessels

Maturation of vessel is accompanied by the recruitment of MC and the deposition of extracellular matrix (ECM) components. Both stromal cells and the ECM surrounding the endothelium provide crucial interaction to form stable quiescent vessels. The ECM, a scaffold of proteins secreted and organized by endothelial and MC, provides structural support, serves as a substrate for EC migration, and regulates pro-and anti-angiogenic factors (reviewed in(Red-Horse, Crawford et al. 2007)). ECM molecules directly influence EC morphogenesis by changing cytoskeletal arrangements and by mediating adhesion, migration and proliferation of ECs but ECM components also regulate endothelial functions indirectly by presenting and shaping growth factor gradients. Hence, the ECM affects many fundamental aspects of EC biology through mechanical support and signalling pathways.

The basement membrane (BM) underlying the basal side of ECs is a specialized form of the ECM, 50-100nm in thickness. Originally described as a distinct ultra structure in the electron micrographs, BMs are now defined as much by their molecular composition as by their intimate association with the cell surface (Sasaki, Fassler et al. 2004). In mature blood vessels BMs form a continuous sleeve around endothelial tubes, consisting of a tight meshwork mainly comprised of laminin, collagen, fibronectin and proteoglycans (Figure 4.17). Various isoforms of these matrix molecules have been identified and combine to form structurally and functionally distinct BMs.

Recent data suggest that extracellular scaffolding molecules control the signalling pathways necessary for blood vessels to form and stabilize, and disruption of these signals catalyzes vascular regression (reviewed in (Davis and Senger 2008)). Davis and Senger propose a concept in which collagen matrices stimulate vessel formation whereas exposure to laminin inhibits this process. Collagen-integrin interaction in ECs stimulates intracellular vacuole formation and regulates capillary lumen and tube formation. Lumen formation is mediated by Cdc42 and Rac1 GTPases and requires Pak2, Pak4 and Par3 and PKCγ activity (Bayless and Davis 2002);(Koh, Mahan et al. 2008). The role for laminin matrices in this process is less clear. Absence of any laminin matrices in embryoid bodies *in vivo* resulted in ES cell differentiation and vessel formation however vessels exhibited increased lumen diameter (Jakobsson, Domogatskaya et al. 2007).

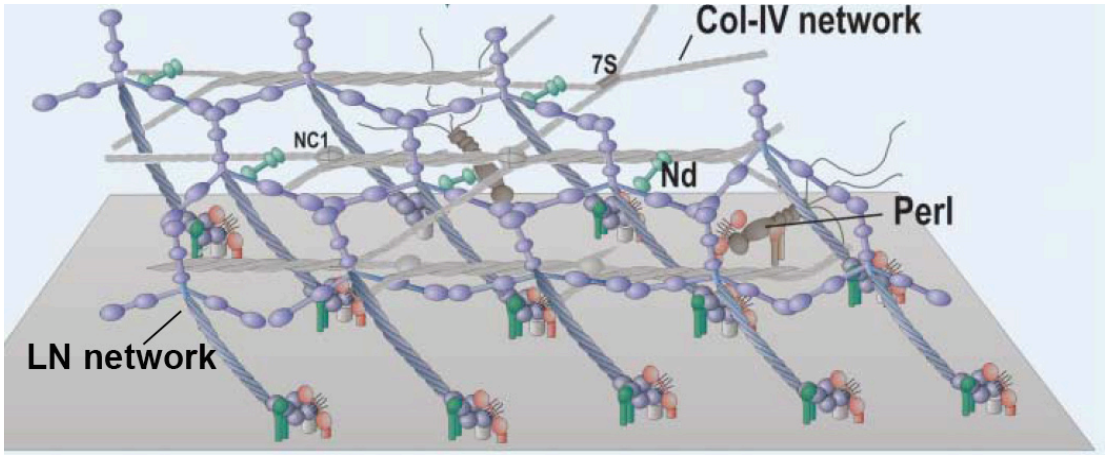

Figure 4.17 Basement membrane components forming a tight meshwork

Laminin polymerizes through its short arms creating a multivalent network. Type IV collagen (Col-IV network) forms a second network that is linked to the Laminin network (LN network) via nidogen (Nd). Perlecan (Perl) is incorporated in endothelial BM {Li, 2003 #681}.

Recent studies addressed the function of matrix metalloproteases (MMP) in regulating vascular morphogenesis and vessel regression. MMP degrade a variety of ECM molecules, cleave cell surface receptors and release apoptotoic ligands but also process bioactive molecules and thereby (in)activate a range of chemokines and growth factors. The ability of ECs and their supporting cellular elements to directly modify (ie, remodel) their immediate ECM environment is critically important for forming tubular networks, stabilizing these networks, and inducing regression of these networks. MMP mediated proteolysis appears likely to be critical during EC morphogenesis include the initiation of angiogenesis whereby BM breakdown occurs, invasion into collagen type I or fibrin matrices, and lumen formation (reviewed in (Davis and Senger 2005)).

MT1-MMP has been identified as a proteolytic modifier of PDGF-B/PDGFR-β signal transduction that cooperatively regulates vessel wall architecture *in vivo*.
In vSMCs, catalytically active MT1-MMP associates with PDGFR-β in membrane complexes that support the efficient induction of mitogenic signalling by PDGF-B. Conversely, *MT1-MMP*-deficient vSMCs display PDGF-B-selective defects in chemotaxis and proliferation and *MT1-MMP*-deficient brain tissues exhibit a marked reduction in MC density as well as abnormal vessel wall morphology similar to that reported in mice expressing *Pdgfb* or *Pdgfrb* hypomorphic alleles (Lehti, Allen et al. 2005).

Davis and colleagues found that PC stabilize tubes by inhibiting the natural

tendency of EC-lined tubes to regress by blocking MMP-1 and -10 dependent pathways of vascular regression. Periyctes perform this function by delivering the proteinase inhibitor TIMP-3, and thereby suppressing MMP-1 and -10 dependent regression.

MMPs also function in the release of ECM-bound VEGF by converting VEGF165 isoforms in VEGF121-like fragments resulting in a decrease of local VEGF concentration (i.e. VEGF withdraw) and thereby stimulating vessel regression (Lee, Jilani et al. 2005); reviewed in (Davis and Senger 2008).

One of the most fundamental functions provided by ECM involves support of EC proliferation and survival. Both proliferation and survival are highly dependent on adhesion to ECM through cell-surface integrins. In particular, activation of the p44/p42 (ERK1/ERK2) mitogen-activated protein kinase (MAPK) signal transduction pathway in ECs is critical for EC proliferation and angiogenesis (reviewed in (Davis and Senger 2005)).

4.17 Laminin

Little is known about which cell type expresses which BM component and whether the expression pattern changes during vessel development in embryogenesis and adult angiogenesis. However, a major finding in the last years is that laminins are the primary determinants of BM assembly and that other BM components such as collagen type IV variants, perlecan, nidogens, and collagen type XVIII are accessory components. The endothelial cell BMs have been demonstrated to be unique in regards of their laminin isoform composition.

Laminins are a family of large glycoprotein heterotrimers, composed of an alpha, a beta and a gamma chain that assemble to form a cross-shaped molecule. To date, 5 distinct alpha (α), 4 beta (β) and 3 gamma (γ) laminin chains have been identified that can combine to form up to 15 different isoforms. Laminin α, β and γ chains share homologous structures that include globular domains (domains IV and VI), rodlike domains containing EGF-like repeats known as laminin-like EGF or LE repeats (domain III and V), and domains forming the α-helical coiled-coil of the long arm of the molecule (domain I and II). In addition, all laminin alpha chains contain a large COOH-terminal globular (G) domain with five internal repeat motifs (known LG domains) that possess binding sites for several cell membrane-associated molecules

such as integrin, a-dystroglycan and nidogen, see Figure 4.18 (Hallmann, Horn et al. 2005).

The laminin alpha chains are considered to be the functionally important portion of the heterotrimers, as they exhibit tissue-specific distribution patterns and contain the major cell interaction sites. The diverse function of laminin chains has also been verified by inactivation and genetic ablation leading to distinct phenotypes.

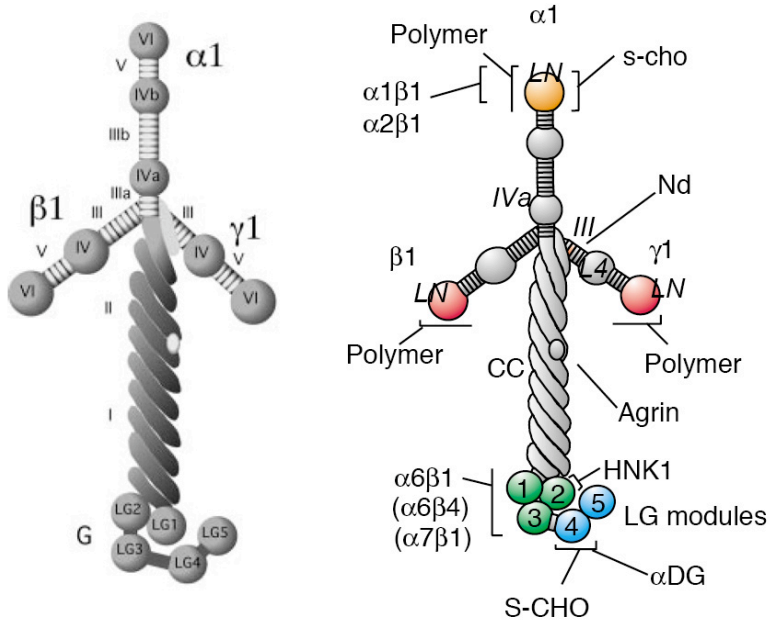

Figure 4.18 Laminin structure and domain composition

The prototype laminin 111 isoform is characterized by the presence of the laminin α1 chain, which combines with laminin β1 and γ1 chains. All laminin chains share structural similarities defined as domains, shown in Roman numerals. Note the NH_2-terminal short arms composed of laminin α, β, and γ chain sequences, and the COOH-terminal globular (G) domains composed solely of laminin α chain sequences. The central long arm of all the laminins is a coiled-coiled structure composed of all three chains. Globular domains contain binding sites for sulfated carbohydrates (S-CHO/s-cho; high and low affinity sites), integrins (e.g. a6b1), dystroglycan (aDG/adg), agrin and nidogen. The N-terminal end mediates laminin polymerization (adapted from (Hallmann, Horn et al. 2005); (Yurchenco and Wadsworth 2004)).

It is believed that the endothelium only expresses two laminin molecules, namely laminin 411 (α4, β1 and γ1) and laminin 511 (α5, β1 and γ1) and that their expression pattern varies depending on developmental stage, vessel type and activation state (reviewed by (Hallmann, Horn et al. 2005)).

Mice lacking *Laminin a5* die during late embryogenesis at E16.5, exhibiting exencephaly, syndactyly and placental dysmorphogenesis (Miner, Cunningham et al. 1998). The lethality of *Laminin a5* mice appears to relate to abnormalities of the placental as well as fetal vasculature. In these animals, reduced complexity in the branching patterns of these vascular beds was observed, and existing vessels had larger lumen diameters.

In contrast to *Laminin a5*, mice deficient for *Laminin a4* are viable. Thyboll and colleagues showed that *Laminin a4* knockout mice display haemorrhages during late embryonic development, and that the phenotype is rescued by postnatal laminin α5 expression, which occurs earlier than in wildtype mice (Thyboll, Kortesmaa et al. 2002). Previous studies showed that *Laminin a4* deficient mice exhibit enhanced blood vessel formation in pathological condition, such as tumour angiogenesis (Zhou, Doi et al. 2004). Using the cornea angiogenesis assay Thyboll and colleagues demonstrated aberrant branching of vessels with dilation and fluctuation in diameter, suggesting an inhibitory role of laminin α4 (at least in pathological angiogenesis).

Reduced expression of BM components including collagenIV, laminin β1 and γ1 chains, and nidogen 1 was found in BM surrounding *Laminin a4* null mice. Electron microscopic analysis revealed defects in BM assembly and density, suggesting that laminin α4 is required for the integrity of vessels and their proper maturation but not essential for blood vessel development *per se*.

Laminin α4 LG4–5 but not LG1–3 was shown to inhibit EC migration in an *in vitro* wound healing assay and to perturb tube formation in an *in vitro* model (Talts, Sasaki et al. 2000). Although the mode of action of laminin α4 LG4–5 is unclear, it has been proposed to involve interference with integrin α6β1- and α3β1-mediated interactions. DeHahn and colleagues suggested that laminin α4 mediates EC survival *in vitro*, by activating β1 integrins (DeHahn, Gonzales et al. 2004).

Interestingly, distinct functions for laminin α4 and α5 have also been reported in zebrafish (Pollard, Parsons et al. 2006). In contrast to laminin α5 that does not effect

notochord differentiation and intersegmental vessels (ISV) formation, laminin α4 in combination with laminin α1 fail to form the notochord and ISV in zebrafish.

Despite these and various other attempts very little is known about the precise function of the laminin α4 and – α5 although distinctive expression patterns and structural characteristics of laminin α4 and -α5 chains may provide some clues for possible functions. The laminin α4 chains is truncated and in comparison to laminin α5 much shorter, missing the N-terminal domain that has been associated with laminin self-assembly and cross-linking the laminin network to collagen.
In the absence of laminin, collagenIV is essentially excluded from the BM (Jakobsson, Domogatskaya et al. 2007). Laminins bridge between the cell surface and the collagen network via nidogens and perlecan forming a tight network.

Genetic inactivation of collagen IV and perlecan revealed that both BM components are essential for stability and integrity of BM in blood vessels but dispensable for the initiation of its assembly during early development (Poschl, Schlotzer-Schrehardt et al. 2004); (Costell, Gustafsson et al. 1999). These data indicate that laminin is sufficient for BM-like matrices during early embryonic development, but at later stages and under mechanical stress such as blood flow the specific composition of components including CollagenIV and perlecan defines integrity, stability and functionality.
The BM not only functions in vessel integrity but much likely controls cell polarity. Laminin and the small GTPase Rac1 are required for orientation of apical polarity in epithelial kidney cysts. Intracellular Rac1 activity regulates extracellular laminin assembly. Assembled laminin reciprocally acts back on the cell, initiating a transcellular signal that relays positional information to the site of apical pole formation. Disruption of the autocrine loop inverts apical polarity. Dominant-negative Rac1 alters the supramolecular assembly of endogenous laminin and causes a striking inversion of apical polarity (O'Brien, Jou et al. 2001).

4.18 Integrin

Vascular development is a multi-step process that involves cell-cell and cell-matrix adhesion. Each of the many ECM molecules mentioned above (e.g. laminin, collagen) has cell surface receptors, predominantly of the integrin family.

Integrins are a family of non-covalently associated heterodimeric transmembrane glycoprotein adhesion molecules. They comprise an α- and β-subunit, with numbers varying between species. In mammals, 18 α-and 8 β-subunits combine to form more than 24 different integrin heterodimers. Heterodimer composition confers ligand specificity, with most integrins recognizing several ECM proteins and, in turn, most matrix proteins binding to more than one integrin (reviewed in (Silva, D'Amico et al. 2008)). Genetic inactivation, receptor inhibition and expression studies have revealed that at least 10 integrins are expressed by EC and mediate angiogenic processes to one degree or another. The fibronectin receptors, α4β1, α5β1; the collagen receptors, α1β1, α2β1; the laminin receptors, α3β1, α6β1, and α6β4; and the osteopontin receptor, α9β1. In addition PC also express α7β1 (laminin receptor) and α8β1 (osteopontin receptor) integrins. The vitronectin receptors, αvβ3 and αvβ5, are expressed by ECs, and αvβ3 is also expressed on glial cells (reviewed in (Silva, D'Amico et al. 2008)). Their expression is not unique among ECs and it has become clear that their expression and activity is strongly regulated during sprouting angiogenesis. VEGF can modulate angiogenesis via increased expression and activation of α6β1 integrins, the specific blocking or siRNA knockdown of which inhibited capillary morphogenesis, adhesion and migration (Lee, Seng et al. 2006).

In the following, I will summarize the vascular phenotypes of integrin deficient mice that have been implicated in angiogenesis and proven to be relevant for my work.

Laminin receptors integrin α3 and α6 die during birth (Kreidberg, Donovan et al. 1996); (Georges-Labouesse, Messaddeq et al. 1996). Although, no vascular abnormalities have been reported, this does not exclude a possible function in adult and pathological angiogenesis. Integrin β4-/- mutants display reduced angiogenesis in response to bFGF in the Matrigel plug assay and to hypoxia in the retinal neovascularization model (Nikolopoulos, Blaikie et al. 2004). Signalling and tumour implantation studies revealed that integrin α6β4 promotes the onset of the invasive

phase of pathological angiogenesis (Nikolopoulos, Blaikie et al. 2004).

β1 intergins are essential during angiogenesis and expressed in both ECs and PC. Mice deficient in β1 integrin die at E5.5 before the onset of vascular development. Endothelial specific deletion of integrin β1 results in embryonic lethality at around E10, allowing the formation of a simple vasculature. Consistently with mice lacking endothelial integrin β1, embryoid bodies null in integrin β1 differentiate but display defects in angiogenic sprouting and vascular branching morphogenesis (Fassler and Meyer 1995); (Bloch, Forsberg et al. 1997).

β1 integrin expression on PC is thought to help stabilize the blood vessels. *In vivo*, mice deficient in pericytic integrin β1 die postnatally and display vascular abnormalities. Pericyte and vSMC proliferation is enhanced, whereas differentiation and their ability to support blood vessels are compromised. Integrin β1 deficient pericytes are poorly spread, adhesion to ECM molecules is delayed despite the presence of focal adhesions (Abraham, Kogata et al. 2008).

α7β1 integrin is mainly expressed by MC and loss of integrin α7 results in reduced vSMC number, assembly and differentiation leading to incomplete cerebral vascularization, and cerebral hemorrhage (Flintoff-Dye, Welser et al. 2005). A recent in vitro study suggested a cross talk between PDGF receptors and integrin α7β1, showing elevated α7β1 integrin expression levels and adhesion to laminin in the presence of PDGF (Chao, Martinez-Lemus et al. 2006).

The relevance of integrin α5 in angiogenesis is highlighted by genetic studies. Mice deficient in α5 fail to form a proper vascular network in yolk sac and the developing embryos (Yang, Rayburn et al. 1993). These defects result in embryonic lethality at E10 to 11 of gestation. Similar defects in vessel development are recapitulated in α5-null embryoid bodies, α5-null teratomas, and, to a greater extent, in the Fibronectin (FN) null embryos, indicating the importance of α5–FN interactions during vessel development (Taverna and Hynes 2001).

Integrin α5 expression is upregulated in tumours and blocking experiments resulted in reduced tumour growth. The anti-angiogenic properties of blocking reagents against α5 are currently tested in PhaseI clinical trials (reviewed in (Silva, D'Amico et al. 2008). Integrin α5 predominantly interacts with FN, however recent data highlight the capacity of integrin α5 to bind and signal via angiopoietin-1 and its receptor Tie-2, as well as VEGFR1 to mediate EC migration (reviewed by (Serini, Napione et al. 2008); (Orecchia, Lacal et al. 2003).

Similar properties have been described for integrin β3. Mice deficient in β3 integrin are viable and fertile and develop no apparent vascular defects during development, but exhibit increased tumour angiogenesis. The enhanced neovascularization in tumours correlates with elevated VEGFR2 levels. Serini and colleagues summarize recent finding in the tyrosine kinase receptor-integrin cross talk, highlighting the formation of VEGFR2-β3 integrin complex.

Complex formation requires the extracellular domain of VEGFR2, and receptor-2 activation by its ligand VEGF and the ensuing binding of PI3K and c-src.

Upon VEGF-A stimulation, VEGFR2 recruits and activates c-src, which, in turn, phosphorylates the cytosolic tail of β3 integrin. This c-src-dependent post-translational modification is required for the formation of the VEGFR2/αvβ3 complex and the conformational activation of the integrin. Recently, the transglutaminase factor XIII was shown to stabilize VEGFR2/αvβ3 integrin complex, leading to VEGF-A-independent receptor activation (reviewed by (Serini, Napione et al. 2008)).

The increased VEGFR2 expression observed in β3-/- mice could represent a molecular compensation that further emphasizes the importance of VEGFR2/αvβ3 integrin co-regulation in ECs. This hypothesis is supported by the recent finding that tumour angiogenesis is impaired in knock-in mice expressing a αvβ3 mutant unable to form a complex with VEGFR2 (reviewed by (Serini, Napione et al. 2008)).

As discussed in previous sections of my thesis, many other integrins including α5, α9β1 but also collagen receptors α1β1 and α2β1 interact with VEGF receptors and are, at least in part, able to bind VEGF ligands. Collagen I, the ligand of α1β1 and α2β1 integrins, exerts an inhibitory action on VEGFR2 by promoting the recruitment of the tyrosine phosphatase SHP2 to the receptor cytosolic tail. The higher VEGFR2 de-phosphorylation correlates with a higher degree of its internalization (reviewed by (Serini, Napione et al. 2008)).

Taken together, the recent findings convincingly demonstrate that integrins not only mediate cell-matrix adhesion and endothelial migration but also function actively in signalling events during sprouting angiogenesis.

4.19 Fibronectin

Fibronectin, is a major component of the vascular BM that mediates several functions, including the binding and assembly of ECM components, providing structural support for cell adhesion and controlling the availability of growth factors (summarized in (Leiss, Beckmann et al. 2008)). The functional relevance of FN is underscored by the dramatic consequence in mice that lack a constitutive FN gene. FN null embryos die at E8.5 due to severe mesodermal, vascular and neural tube defects (George, Georges-Labouesse et al. 1993). Detailed analysis of the cardiovascular system revealed that FN is essential for organization of heart and blood vessels, but is dispensable for cellular specification in the appropriate regions within the embryo (George, Baldwin et al. 1997).

FN is a large 220-250kDa modular protein, containing type I, II and III domains that mediate FN-binding and interactions (Figure 4.19). FN is secreted as a disulfide-bonded dimer; dimerization takes place at the C-terminus and seems to be required to assemble FN into a fibrilliar matrix).

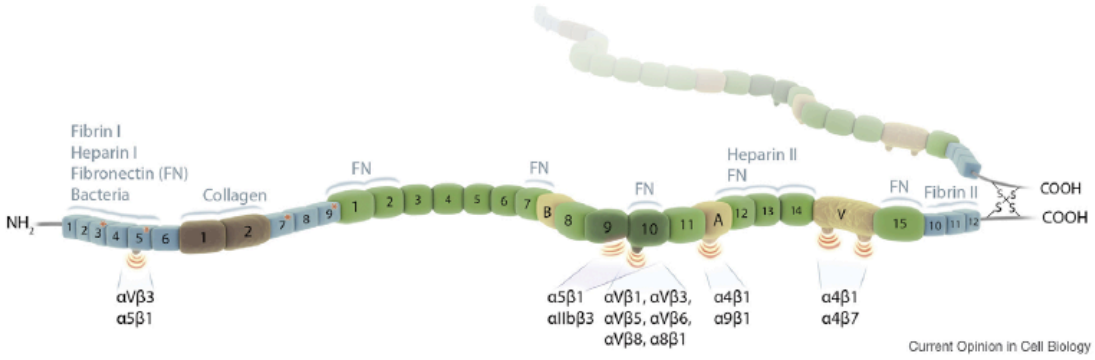

Figure 4.19 Molecular structure of Fibronectin

FN consists of three different modules (type I, blue; type II, brown; type III, green). The alternatively spliced extradomains B, A, and variable region (V) are shown in ochre. The dimer forms via two disulfide bonds at the C-terminus. Integrin binding sites are indicated. The N-terminal type I domains marked with a red asterisk harbour an IGD motif. Binding domains for FN, collagen, fibrin, heparin and bacteria are indicated. Note that the α5β1 as well as the αIIbβ3 integrins require the synergy region to bind to the RGD motif (Leiss, Beckmann et al. 2008).

Further, FN fibril assembly is a cell-driven process that crucially involves integrin interaction. The double knock out of the *integrin α5* and *av* gene results in a complete ablation of FN fibril formation (Yang, Bader et al. 1999). Cell adhesion to FN depends on the RGD motif (arginine –glycine- asparagine) that is located in the 10th type III domain and mediates binding to many integrins including α5β1 and αvβ3 (Figure 4.19Substitution of the RGD motif to an integrin-binding inactive RGE motif results in early embryonic lethality due to severe defects in the posterior mesoderm (Takahashi, Leiss et al. 2007). Surprisingly, FN assembly is not dependent on RGD-mediated integrin binding *in vivo*.

Fibronectin exists in two forms: cellular FN, which is present in tissues where it is assembled into a fibrillar matrix, and plasma FN, which is produced by hepatocytes and is secreted into the blood where it remains in a non-fibrillar, soluble form.

FN is alternatively spliced at three regions, which can be either completely (EIIIA and EIIIB, both type III repeats) or partially (the V region), included or excluded, generating up to 12 different variants in mammals and 20 in humans (reviewed in (Hynes 2007).

These FN isoforms are spatially and temporally differentially expressed, however their expression is re-activated and increased in development and disease. Surprisingly, mice lacking either the FN EIIIA or EIIIB fragments did not display vascular defects (Astrof, Crowley et al. 2004) but mice deficient in both segments exhibited multiple embryonic cardiovascular defects, including vascular hemorrhage, failure of remodelling embryonic and yolk sac vasculature, defective placental angiogenesis and heart defects (Astrof, Crowley et al. 2007). Deletion of both EIIIA and EIIIB exons did not affect synthesis or cell surface deposition of FN, indicating that embryonic lethality at E10.5 was due specifically to the absence of EIIIA and EIIIB exons from FN (Astrof, Crowley et al. 2007). The importance of FN isoforms has been demonstrated, however the precise function of extra domains EIIIA and EIIIB during developmental and pathological angiogenesis still remain to be elucidated.

FN controls the availability of growth factors, for example by regulating their activation from latent complexes as shown for TGF-β (Fontana, Chen et al. 2005). Wijelath and colleagues mapped two binding domains on FN that modulate the activity of the angiogenic factor, VEGF. Further analysis demonstrated that VEGF binds to the heparin-II domain of FN and that the cell-binding and VEGF-binding domains of FN, when physically linked, are necessary and sufficient to promote VEGF-induced EC proliferation, migration, and ERK activation (Wijelath, Murray et al. 2002; Wijelath,

Rahman et al. 2006). Mutation in heparin-II binding domain abolished VEGF-binding and reduced EC responses. However, presence of both integrin α5β1- and VEGF-binding domains significantly enhanced EC proliferation, migration and induced strong phosphorylation of the VEGF receptor and ERK, suggesting a synergistic function FN and VEGF.

4.20 Aim of my PhD

Extracellular matrix components modulate EC functions directly via integrin adhesion and indirectly by interacting with multiple signalling pathways, e.g. stabilizing receptor complexes, controlling growth factor (GF) availability or presentation to the EC.

The aim of my PhD was to elucidate the spatial expression and precise function of BM molecules during developmental angiogenesis. The projects undertaken investigate the role of fibronectin in vessel migration and laminin in vascular sprouting and patterning by studying the retinal vasculature.

In a third project I addressed the relevance of heparan sulfate proteoglycan in mural cell recruitment and explored the underlying mechanism.

5 Material and Methods

5.1 Animals

All mice analysed in thesis were housed in the Porta Cabin 2, Clare Hall and services were provided by Biological Resources, Cancer Research UK. Maintenance and breeding of mice are in accordance with legal and UK ethical standards.
Table 1 summarizes a list of mice used in my projects described. If not stated explicitly, mice were bred on C57Bl/6 background.

Briefly, to generate conditional transgenic mice lacking astrocytic Fibronectin (FN), FN floxed mice were crossed to GFAP Cre and Nestin Cre mice. To specifically analyse the functional role of RGD-binding motif in astrocytic FN, FN floxed GFAP Cre mice were bred to RGE/wildtype (RGE/wt) mice, containing a mutation in RGD sequence.
The *laminin a4* deficient mice were generated by targeted disruption of the first 2 exons of *Lama4* gene and replacement with PGK *Neo* cassette (Thyboll, Kortesmaa et al. 2002). Mice were kindly provided by Lydia Sorokin.
To investigate loss of pericytic heparan sulfate (HS) *Ext1* floxed mice were bred to *Pdgfrb* Cre mice, referred as $Ext1^{MCko}$. To obtain $Ext1^{MCko}$ embryos at specific embryonic stages, breedings were set up for timed mating and detection of a vaginal plug was considered as embryonic day 0.5 (E0.5).
To verify *Pdgfrb* Cre specificity, *Pdgfrb* Cre mice were crossed to reporter mice *ROSA26*eYFP and tissue was analysed at several embryonic stages.
Finally, to study the function of endothelial HS during embryogenic vascular development we breed *Ext1* floxed mice with *PDGFB*-iCreER transgenic mice. Cre mediated recombination and deletion of *Ext1* in endothelial cells (EC) expressing PDGF-B is dependent on tamoxifen induced translocation of $iCreER^{T2}$ to the nucleus of ECs. To activate Cre recombination, 4OH-tamoxifen (Sigma) was injected intraperitoneally in pregnant females in 2-3 constitutive days at embryonic stages E8.5-E12.5.
Eyes of FN splice variants (FNEIIIA, FNEIIIB, FNEIIIAB, FNEIIIBA), integrin alpha5 Tie2 (*Itga5ECko*), dy^{2J}/ dy^{2J}, integrin alpha 7 (*Itga7*), and integrin beta 3 (*Itgb3*) mice as well as embryos of *Pdgfrb* null and control mice were provided either PFA-fixed or

snap frozen for protein analysis. For further information regarding generation of mice and a detailed list on collaboration initiated during my PhD see Table 1.

All breedings, including experimental and stock breedings were set up by myself and I was in charge for maintenance of multiple colonies including *Ext1*, *Pdgfrb* Cre, *PDGFB*-iCreER^{T2}. Animal procedures were carried out in accordance with the UK Coordination Committee on Cancer Research UK guidelines and Home Office regulation. Experimental procedures on mice were performed by myself and/ or by animal technicians Sue Watling, Craig Thrussell and Claire Darnborough (Biological Resource Services).

mouse line	published by	in collaboration with
FN floxed	R. Faessler	R. Faessler
GFAP Cre	Bajenaru et al., 2002	D. Gutmann
Nestin Cre	Petersen et al., 2004	W. Zhong
RGE/ wt	Takahashi et al., 2007	R. Faessler
FNEIIIA	Tan et al., 2004	M. Vogelzang, R. Hynes
FNEIIIB	Fukuda et al., 2002	M. Vogelzang, R. Hynes
FNEIIIAB	Astrof et al., 2007	M. Vogelzang, R. Hynes
FNEIIIBA	Astrof et al., 2008	M. Vogelzang, R. Hynes
itga5 Tie2	A. v.d Flier, unpublished	A.v.d Flier, R.Hynes
itga7	Flintoff-Dye et al., 2005	D. Burkin
dy2J/dy2J	Besse et al., 2003	M. Hager & M. Durbeej
Lama4	Thybol et al., 2002	L. Sorokin
itgb3	Hodivala-Dilke et al., 1999	S.Robinson & K.Hodivala-Dilke
Pdgfrb Cre	Foo et al., 2005	R.Adams
PDGFB Cre ERT	Claxton et al., 2008	M. Fruttiger
Pdgfrb null	Soriano P., 1994	M.Nisancioglu
Ext1 floxed	Inatani et al., 2003	Y.Yamaguchi
ROSA26eYFP	Srinivas et al., 2001	R. Adams

Table 1 List of mouse lines used in this thesis

Administration of Tamoxifen to induce Cre mediated gene inactivation

4-hydroxy tamoxifen (4OH-tamoxifen, Sigma) was dissolved in 1ml of ethanol. A stock solution of 20mg/ ml was stored at 4°C. Corn oil was added to prepare a working solution of 4 mg/ml fresh for each experiment.

Cre induction was activated upon intraperiteonally injection of 75µl of working solution in pregnant *PDGFB*-iCreER^{T2} females at several embryonic stages.

5.2 Genotyping of mice

Ear and tails biopsis of mice as well as embryonic yolk sac samples of experimental mice were lysed over night (o/n) at 55°C using 200µl of direct lysis buffer (tail or yolk sac, respectively) (Viagen Biotech Inc.) containing 0.2mg/ ml proteinase K (Roche). After heat inactivation for 45 minutes (min) at 85°C samples were kept at -20°C.

Embryonic tail samples of *Ext1*^{MCko}, *Pdgfrb* null and control embryos were kept and lysed using 500µl tail lysis buffer (50mM Tris-HCl, pH8.0, 100mM EDTA, 100mM $NaCl_2$, 1%SDS) containing 15µl Proteinase K (20mg/ml stock solution, Roche) at 55°C o/n. Briefly, after NaCl precipitation (200µl of 5M NaCl), same volume of isopropanol was added to extract DNA. Centrifugation at 13,000rpm for 10min, 4°C resulted in a visible pellet that was resuspended in 100µl of distilled H_2O.

Polymerase chain reaction (PCR) was performed using HotStarTaq® *Plus* Mastermix (Qiagen), containing loading buffer, dNTPs and polymerase in the kit provided. To a final volume of 20µl, 1-2 µl of DNA samples and 1µl of 10µM primer were added to the PCR reaction. To detect sharper bands by gel electrophoresis 1µl of dimethyl sulfoxide (DMSO, Sigma) was added to PDGFB-iCreER^{T2} PCR reaction.

Details of primers used, their specific annealing temperature to amplify DNA and PCR product size are listed in Table 2. Conditions for PCR reaction are as follows.

Initial denaturation at 95°C for 5 min, 95°C for 1 min, annealing temperature (see Table 2) 30 sec, extension at 72°C for 1 min and a final elongation step at 72°C for 10 min were run on Mastercycler (Eppendorf).

The PCR reactions were separated on 1-2% agarose gel (Invitrogen) diluted in TBE buffer containing 0.2mg/ml ethidium bromide (Sigma).

10x TBE buffer was provided by Biological Resources, Cancer Research UK and contained 104g Tris base, 55g orthoboric acid, 10ml 0.2M EDTA and distilled H_2O in final volume of 1 litre. Bands of PCR products were visualized using UV light and compared to 1kb protein ladder (Invitrogen).

gene	primer sequence	annealing temperature	product size
FN	FW 5' GTACTGTCCCATATAAGCCTCTG 3' RV 5' CTGAGCATCTTGAGTGGATGGGA 3'	63°C 10 cycle 53°C 35 cycle	wt 230bp floxed 280bp
GFAP/ Nestin Cre	FW 5' GACACCAGACCAACTGGTAATGGTAGCGAC 3' RV 5' GCATCGAGCTGGGTAATAAGCGTTGGCAAT 3'	62°C 10 cycle 52°C 35 cycle	850bp
RGE	FW 5' CAAAGAAGACCCCAAGAGCA 3' RV 5' ACAAGCCCTGGCCTTTAGTT 3'	67°C 10 cycle 57°C 35 cycle	wt 340bp mut 480bp
Lama4	WT FW 5' CAGCAGGCATCACTGCATCTC 3' WT RV 5' CTGAGTCGCTAGTCTCCGATG 3' NEO FW 5' TGTCATCTCACCTTGCTCCTG 3' NEO RV 5' TCAAGAAGGCGATAGAAGGCG 3'	55°C 35 cycle	wt 280bp ko 520bp
Ext1	FW 5' AAGGATTCTCGCTGTGACAG 3' RV 5' CCAAAACTTGGATACGAGCC 3'	55°C 35 cycle	wt 389bp floxed 460bp
Pdgfrb Cre	FW 5' GGACATGTTCAGGGATCGCCAGGCG 3' RV 5' GCATAACCAGTGAAACAGCATTGCTG 3'	65°C 32 cycle	~200bp
PDGFB-iCreERT2	FW 5' GCCGCCGGGATCATCCTCG 3' RV 5' CCAGCCGCCGTCGAACTC 3'	57°C 35 c ycle	450bp
Rosa26 eYFP	FW 5' AAAGTCGCTCTGAGTTGTTAT 3' YFP RV 5' GCGAAGAGTTTGTCCTCAACC 3' wt RV 5' GGAGCGGGAGAAATGGATATG 3'	65°C 30cycle	YFP+ 350bp wt 650bp
Pdgfrb	FW 5' AAA AGT ACC AGT GAA ACC TCG CTG 3' wt RV 5' ACA ATT CCG TGC CGA GTG ACA G 3' mut RV 5' ATC AGC CTC GAC TGT GCC TTC TAG 3'	58°C 40 cycle	wt 114bp mut 320bp

Table 2 PCR primer and conditions used for genotyping

5.3 Immunofluorescence staining of whole-mount retinas

Pups were culled by decapitation and eyes were gently removed using curved forceps. If not stated otherwise, eyes were fixed with 4% paraformaldehyde (PFA, Sigma) in phosphate- buffered saline (PBS), pH 7.4 for 2 hours (h) at room temperature (RT) prior to dissection. Briefly, the cornea was incised with a needle and a microscissor was introduced through the incision. The cornea was removed by cutting circumferentially along the line of surgical limbus (defined as a gray zone that demarcates the transition between the cornea and sclera). The vitrous body was pulled out gently and the hyaloid vessels were separated. Finally, the pigment epithelium was detached and 4-5 small incisions were made to flatten the retina. In this state, retinas could be kept in PBS at 4°C.

For immunofluorescent (IF) staining with antibodies directed against VE-cadherin and claudin-5, pups were anaesthetized by injection of a combination of Hypnovel (Midazolam) and Ketaset intraperitoneally before transcardiac perfusion with PBS until

blood has drained from body. Eyes were removed, fixed in 4% PFA for 5-10 min at RT, and dissected in PBS to remove hyaloid vessels. Retinas were then flattened, excess PBS was removed and retinas were fixed in ice-cold methanol while flattened. Retinas were snap frozen on dry ice and kept at -20°C. Prior to staining retinas were rehydrated in a methanol/ PBT (PBS containing 0.1% Tween-20) gradient and finally washed in PBT for 10 min.

Generally, IF staining of retinas were performed by blocking retinas in PBS containing 1% bovine serum albumin (BSA, Sigma) and 0.5% Tween-20 for 1h at RT with gentle shaking. Retinas were then incubated with primary antibodies in appropriate dilution (Table) for 2h at RT or over night at 4°C. All primary antibodies listed in table were incubated in 0.5% BSA/ 0.25% Tween-20 in PBS except for isolectin B4, NG2 and endomucin which were incubated with PBlec (PBS, pH6.8 containing 1% Tween-20, 1mM $CaCl_2$, 1mM $MgCl_2$ and 0.1mM $MnCl_2$).

Primary antibody solution was removed and retinas washed 3 times in PBT for approximately 10 min followed by incubation with secondary antibodies in 0.5% BSA/ 0.25% Tween-20 for 2h at RT or over night at 4°C. A list of secondary antibodies used is presented in Table 3.

After final wash steps with PBT, retinas were post fixed using 4% PFA for 10 min and flat mounted on glass slides (Menzel) applying a drop of Mowiol (Calbiochem) containing anti-fading reagent DABCO (Sigma).

secondary antibody	conjugate	company
goat anti-rabbit	Alexa®488	Molecular Probes
goat anti-rabbit	Alexa®568	Molecular Probes
goat pAB anti-mouse IgM	FITC	Abcam
goat anti-mouse IgM	Alexa®568	Molecular Probes
goat anti-mouse IgG	Alexa®488	Molecular Probes
goat anti-mouse IgG	Alexa®568	Molecular Probes
ECL™ anti mouse IgG	HRP	GE Healthcare
ECL™ anti rabbit IgG	HRP	GE Healthcare
ECL™ anti-rat IgG	HRP	GE Healthcare
goat anti-rat	Alexa®488	Molecular Probes
goat anti-rat	Alexa®568	Molecular Probes
strepdavidin Alexa® Fluor	488	Molecular Probes
strepdavidin Alexa® Fluor	568	Molecular Probes
strepdavidin Alexa® Fluor	633	Molecular Probes

Table 3 List of secondary antibodies used

antibody	conjugated	raised in/ host	reactivity	company	dilution	Cat.No
biotin conjugate Isolectin B4				Sigma	1:10	L2140
isolectin IB_4	Alexa®488			Molecular Probes	1:1000	I21411
isolectin IB_5	Alexa®568			Molecular Probes	1:1000	I21412
PECAM-1 (CD31)		r	ms	BD Pharmingen	1:100	553370
endomucin		r	ms	D. Vettweber	1:20	
GFAP CloneG-A-5	Cy3			Sigma	1:75	C9205
biotinylated Pdgfra			ms	R&D Systems	1:40	BAF1062
NG2		rb		Chemicon	1:100	AB5320
SMA	FITC	ms		Sigma	1:100	F3777
SMA	Cy3	ms		Sigma	1:100	C6198
phalloidin	Alexa®568			Molecular Probes	1:40	A12380
BrdU	Alexa®488		ms	Molecular Probes	1:50	A21303
VE-cadherin (CD144)		r	ms	BD Pharmingen	1:50	555289
claudin-5		ms		ZYMED® Labortaories	1:100	35-2500
phosphoHistoneH3		rb		Upstate	1:100	06-570
Hoechst				Sigma	1:750	33258
paxillin		m		BD Pharmingen	1:100	610051
integrin alpha5 CD49e)		r	ms	BD Pharmingen	1:100	550540
integrin beta1 (CD29)		r	ms	BD Pharmingen	1:100	550531
integrin beta3	FITC	hamster	ms	BD Pharmingen	1:100	553346
laminin a4 (377)		rb	ms	L. Sorokin	1:200	
laminin a5 (405)		rb	ms	L. Sorokin	1:500	
fibronectin		rb	ms	Chemicon	1:100	AB2033
Heparan Sulfate 10E4		ms		Biodesign®	1:200	M56573M
pSMAD2		rb	h, ms, r	Chemicon	1:1000	AB3849
pSMAD3		rb	h, ms, r	Epitomics	1:1000	1880-1
SMAD2/3		rb	h, ms, r	Cell Signaling	1:1000	3102
SMAD4					1:1000	
connexin43		ms		Sigma	1:1000	C8093
b-tubulin		ms	mammalian	Covance	1:3000	MMS-435P
VEGFR2		rb	ms, h	Cell Signaling	1:1000	2479

antibody	conjugated	raised in/ host	reactivity	company	dilution	Cat.No
pVEGFR2		rb	ms, h	Cell Signaling	1:1000	2478
VEGFR2 pY951		rb	h, ms	Biosource	1:1000	44-1040
phospho tyrosine		ms		Cell Signaling	1:1000	9411
collagenIV		rb	ms	AbD Serotec	1:100	2150-1470
LYVE-1		rb		RELIA Tech	1:1000	102-PA50AG
phospho-Akt (Ser473)		rb	h, ms, r	Cell Signaling	1:1000	4060
Akt		rb		Cell Signaling	1:1000	9272
caspase 3 active		rb	h, ms	R&D systems	1:750	AF835
Pdgfrb		r	ms	Bioscience	1:75	14-1402-81
TUNEL assay				Promega		G7130

Table 4: List of primary antibody

h- human; ms- mouse; r-rat; rb-rabbit

5.4 BrdU administration and detection by IF staining

Bromodeoxyuridine (BrdU, Sigma) was dissolved in a final concentration of 10mg/ ml in PBS and stored at -20°C. Laminin a4 null and control pups were weight and injected 5µl/ g weight intraperiteonally at day 5 postnatally (P5). After 2 hours, pups were culled, eyes harvested and fixed in 4% PFA over night. Fixation was removed and eyes were dehydrated in an increasing methanol/ PBT gradient and were stored at -20°C. Prior dissection of retinas, eyes were rehydrated in methanol/ PBT and finally washed in PBT. Retinas were incubated in with 10µg/ml Proteinase K (Invitrogen) in PBT for 30 min, RT. Digestion was stopped by treatment of retinas with 2mg/ml glycine dissolved in PBT for 10 min, washed twice in PBT and post-fixed in 4% PFA, containing 0.1% glutaraldehyde in PBT for 20 min. Prior DNase treatment, retinas were washed in DNase I buffer (50mM Tris-HCl, 10mM MgCl2, pH 7.5) 3 times for 20 min, RT. Retinas were then treated with 0.1unit/µl DNase I diluted in DNase I buffer for 2 hours at 37°C and heat-inactivated by incubating samples for 10 minutes at 70°C with preheated 50 mM Tris-HCl, pH 7.5 and then cooled on ice for 3 min. After washing with PBT, retinas were blocked in 1% BSA/ 0.5% Tween-20 for 1h at RT. BrdU Alexa® Fluor 488 was incubated in 0.5%BSA/ 0.25% Tween-20 for 2h at RT and washed before incubation with isolectin B4 Alexa® Fluor 568 (1:500 in PBlec) for 2h at RT. Staining was completed by final washing with PBT, post-fixation in 4% PFA for 10 min and flattening of retinas in Mowiol.

5.5 Intraocular injection of peptides in C57Bl/6 pups

Fibronectin peptides inhibiting VEGF-A binding ($FnIII_{13-14}$) and control peptides were generated by the Peptide Synthesis Laboratory, Cancer Research UK. Peptide sequences are as follows

$FnIII_{13-14}$	AKKQRFRHRNRKGYR	IC_{50} 0.08µM
Fn control	KDRKRSELRRIASQVK	IC_{50} 250µM

Peptides were dissolve in distilled H_2O and prepared freshly for each experiment. Inhibitory concentration were calculated according IC_{50} and a total volume of maximal 500µl of $FnIII_{13-14}$ and control peptides were injected once intraocularly in C57Bl/6 pups at postnatal day 4. Eyes were collected 15-24 hours later. To carry out this procedure, mice were deeply anaesthetized by isoflurane inhalation. Injections were performed in the right

eye using 10µl gastight Hamilton syringes equipped with 33 gauge needles attached to a micromanipulator.

Eyes were either fixed in 4% PFA for IF staining or snap frozen on dry ice for protein analysis.

5.6 In situ hybridization of whole-mount retinas

5.6.1 Generation of in situ riboprobes

Vegfa and *Pdgfb* plasmid DNA was generated previously by (Gerhardt, Golding et al. 2003) and *Lama4* and *Lama5* plasmid DNA was kindly provided by Lydia Sorokin.

Competent XL-Blue subcloning–grade competent cells (Stratagene) were transformed with the plasmid according to manufacturer's instruction and cultured on LB agar containing the appropriate antibiotic, ampicillin o/n at 37°C. Clones were picked and cultured in LB medium containing ampicillin o/n at 37°C. Plasmid DNA was isolated using Qiagen Maxi Prep kit.

10-15 µg of plasmids containing template for riboprobe generation were linearized using the appropriate restriction enzyme and buffer according to NEB at 37°C for several hours (Table 5). Complete linearization was confirmed by gel electrophoresis. Plasmids were purified using Qiagen PCR clean up Kit to remove buffer and enzyme.

Gene	restriction enzyme	Vector	RNA polymerase
Pdgfb	XbaI	pBluscript SK+	T7
Vegfa	SalI	pGEM-T Easy	T7
Lama4	HindIII	pGEM3Z	T7
Lama5	BamHI	pGEM3Z	T7

Table 5 Enzymes used to generate antisense riboprobes for ISH

In vitro transcription was performed by adding 1µg linearized DNA, transcription buffer, DIG-labelled RNA Labelling Mix (Roche), 25U/µl RNase inhibitor (Promega) and 2U/µl of RNA polymerase (Stratagene) in nucleasefree water to a total volume of 20µl. Incubated

reaction in 37°C for 2 hours. To test probe quality, 0.5µl of reaction mix was run on a 1% agarose gel. At the end of the transcription, 2µl RNAse-free DNase I (Ambion) was added to the reaction and incubated for 30 min at 37°C. To precipitate the riboprobe, 2.5µl 4M lithium chloride and 75µl cold ethanol were added to the reaction, mixed well and incubated at -80°C for 30 min. Precipitated RNA was pelleted by centrifugation at 13,200 rpm at 4°C and stored at -20°C. RNA concentration was measured using a NanoDrop ND-1000 spectrophotometer.

5.6.2 In situ hybridization

Hybridization mix

50% deionized formamide (Sigma), 1.3X SSC, 5mM EDTA (2-[2(Bis(carboxymethyl) amino)ethyl-(carboxymethyl)amino]acetic acid), 50Mg/ml yeast RNA (Sigma), 0.2% Tween-20, 0.5% CHAPS (3-[(3-Cholamidopropyl)dimethylammonio]-1-propane sulfonate; Sigma) and 50mg/ml heparin (Sigma) prepared in nuclease-free water.

TBST

137mM NaCl, 2.7mM KCl, 25mM Tris-HCl, pH7.5, 0.1% Tween-20 and 2mM levamisole hydrochloride (Sigma) in Milli-Q water (ultrapure laboratory grade water that has been filtered and purified through reverse osmosis).

MABT

0.1M Maleic acid, pH 7.5, 0.15M NaCl and 1% Tween-20 in Millipore water.
MABT was made fresh on the day of use.

NTMT

100mM NaCl, 100mM Tris-Cl, pH9.5, 50mM MgCl2, 0.1% Tween 20 and 2mM levamisole in Milli-Q water.

Retinas and buffer used during the initial procedure until hybridisation were treated and kept in RNase free environment. Eyes were harvested from P5 *laminin a4* deficient and control pups and fixed in 4% PFA for 20 min at RT. Vitrous body and hylaoid vessels were removed before fixation in 4% PFA o/n at 4°C. Pigment epithelium of retinas were

dissected, 4-5 incision were made and retinas were fixed with cold methanol while flatten. Retinas were stored in methanol at -20°C until used.

Retinas were transferred from methanol in a decreasing gradient of methanol/PBT until finally washed in PBT. Pigmented retinas were bleached in 6% hydrogen peroxide in PBT for 1h, RT and washed again in PBT (3x 5 min). Retinas were treated with 10µg/ml proteinase K (Invitrogen) for 30-40 min, RT and digestion was terminated by addition of 2mg/ml glycine in PBT for 10 min. Samples are very fragile at this state and were carefully washed with PBT, 2x 5min before fixation in 4% PFA containing 0.1% glutaraldehyde for 20 min (25% stock solution of glutaraldehyde in PBT were kept at -20°C). Retinas were washed in PBT, rinsed in 1:1 PBT/hybridization mix and then in hybridization mix for 1 hour at 65°C. Retinas were then incubated with approximately 0.2µg/ml DIG-labelled RNA probe diluted in hybridization mix overnight at 65°C with gentle and intermittent shaking.

Next day, hybridization mix was removed and stored at -20°C for future use. Retinas were rinsed and subsequently washed twice with pre-warmed hybridization mix at 65°C for 30 min. This was followed by a wash step with pre-warmed 1:1 hybridization mix/TBST at 65°C for 20 min and another 4 washes in TBST, 30 min RT. Samples were then rinsed twice in MABT and blocked in 10% heat-treated sheep serum in MABT for 1h, RT. Finally, retinas were incubated over night at 4°C in MABT containing 10% sheep serum and anti-digoxigenin-alkaline phosphatase (AP), Fab fragments (Roche) diluted 1:1000.

Before detection and colour development, samples were washed in MABT throughout the day at RT and MABT solution was changed regularly until finally washed in MABT o/n at 4°C.

Retinas were washed in NTMT (2x 10 min) before incubation in NBT (Nitro-Blue Tetrazolium Chloride; Roche)/BCIP (5-Bromo-4-Chloro-3'-Indolyphosphate p-Toluidine Salt; Roche) diluted 2.5µl/ ml NTMT at RT. Colour development was stopped by washing with PBT and post fixation in 4% PFA. Finally, retinas were counterstained with isolectin B4 and/ or GFAP as described in section 5.3 .

5.7 PI3 kinase activity assay

Assays on PI3K isolated from retinas was performed by Mariona Graupera. Briefly, total protein lysate of P5 retinas was immunoprecipitated using phosphotyrosine peptide (p-peptide) matrix YPVPMLG (where YP is phosphotyrosine—the YPVPMLG peptide contains the consensus binding sequence for the SH2 domain of the class IA PI3K

regulatory subunits). Kinase assays were performed using phosphatidylinositol-4,5-bisphosphate (PtdIns(4,5)P2; Lipid Products, Redhill, Surrey, United Kingdom) as a substrate. Radioactivity in the phosphatidylinositol-3,4,5-trisphosphate (PtdIns(3,4,5)P3) spot was measured by a Molecular PhosphorImager FX (Bio-Rad, Hercules, CA) and expressed as arbitrary units. The activity present in the control IgG immunoprecipitates was subtracted from that found in IRS immunoprecipitates.

5.8 Immunofluorescent staining of embryos and embryonic tissues

Pregnant females were euthanised by CO_2 asphyxialation and/ or cervical dislocation at various gestational stages. Embryos were harvested and the yolk sac was removed. Embryos were fixed in 4% PFA for several hours at RT or o/n at 4°C before transferred to PBS. To visualize the embryonic vasculature, whole embryos were stained with endomucin, 1:20 in PBlec. Prior to antibody incubation, embryos were dehydrated in an increasing proportion of methanol/ PBT (25% methanol/ PBT- 50%- 75%- 100% methanol) and rehydrated in decreasing methanol/ PBT gradients until finally washed for 10 min in PBT. Permeabilization of embryos was achieved by incubation of embryos with PBlec for 1h at RT followed by endomucin/ NG2 incubation in PBlec o/n at 4°C. Embryos were washed extensively with PBT, 20 min at RT for at least 3-times and primary antibodies were detected using Alexa Fluor 488 or 568 (Molecular Probes) conjugated secondary antibody.

For detailed analysis of vessel morphology and vascular patterning of embryonic skin, back (vasculature along the spinal cord) and hindbrain the tissue of interest was dissected and cleaned from surrounding tissue prior staining. Stainings were performed as described in section 5.3 of this thesis and (Gerhardt, Golding et al. 2003).

Various organs have been analysed macroscopically and microscopically, including heart, placenta, brain and kidneys of $Ext1^{MCko}$ embryos. Therefore, the organ was removed from the remaining body and cleared of surrounding tissue prior to documenting the morphology with a stereomicroscope (Zeiss). For high magnification imaging and visualization of coronary blood vessels of E13.5 heart, the entire organ was stained using PECAM-1, 1:200

in 0.5% BSA/ 0.25% Tween-20 o/n at 4°C. After washing with PBT, primary antibody was detected using goat anti-rat Alexa® Fluor 488, 1:100 in 0.5% BSA/ 0.25% Tween-20 for 2h, RT.
Blood vessels of the placental labyrinth of E17.5 placenta were detected in the same way as described for coronary vessels of embryonic heart.

High resolution analysis of embryonic skin, brain and kidney were performed on paraffin sections as well as vibrotome sections.
In order to obtain vibrotome section of *Ext1*^{MCko} and control embryos, and sagittal as well as transverse section of embryonic brain (E19.5) the tissue was embedded in 3% agarose gel and cut in 100µm section using Vibrotome, Leica VT1000S. Staining of section was performed as described in 5.3 .

5.9 Immunohistochemic (IHC) analysis of embryonic tissue sections

After dissection and fixation of embryos and/ or embryonic tissues e.g. kidneys in 4% PFA o/n, embryos were embedded in paraffin and cut in section of 5µm size. Briefly, paraffin section were de-waxed using xylene and dehydrated in 100% ethanol, 70% ethanol and finally in H_2O before washing in PBS. Antigen retrieval was carried out by microwaving slides in sodium citrate buffer, pH 6.0 followed by incubation with 1.6% hydrogen peroxide. To block unspecific binding slides were incubated in PBS containing 10% normal goat serum (Sigma), 1% BSA for 30 min at RT. Primary antibodies were incubated for 1h in 1% BSA/PBS, except for NG2 and endomucin slides were incubated in PBlec. After washing in PBS, 3 times at RT slides were incubated with secondary antibodies. Generally, primary antibodies were detected by incubation of biotinylated secondary antibodies in 1%BSA/ PBS for 1h, RT before applying Avidin Biotin Complex Vectastain Elite Peroxidase-based kit (Vector Laboratories) with 3,3'diaminobenzidine tetrahydochloride (DAB, Vector laboratories) according to manufacturer's instructions.

For immunofluorescent staining and double labelling of slides, eg LYVE-1 and endomucin secondary antibodies conjugated with Alexa Fluor ® 488 and 568 (Molecular Probes) were applied for 1h at RT.

Sections were counterstained with haematoxylin and mounted in Permount (Sigma).

These procedures were done by Emma Nye, staff of the Experimental Pathology Laboratory in Cancer Research UK.

5.10 Real Time PCR

5.10.1 RNA isolation of tissues

Eyes were harvested from pups, immediately transferred to RNAlater (Qiagen) and kept at 4°C until dissection. Likewise, embryos were harvested and stored in RNAlater, 10 times the volume of RNAlater per tissue. Dissection was performed in RNAlater, liquid was removed, tissues snap frozen on dry ice and stored at -80°C until use.

To isolate RNA, 2 retinas/ pup or embryonic tissue samples (not exceeding 20mg) were lysed in Buffer RLT (RNeasy Mini Kit, Qiagen) containing 10µl/ml b-mercaptoethanol (Sigma). By pipetting and vortexting of samples, tissue was disrupted and finally homogenized by using QiaShredder (Qiagen). Total RNA was isolated using the RNeasy Mini Kit, according to the manufacturer's protocol. An on-column DNAse I (Qiagen) digestion was carried out to remove genomic DNA. RNA was eluted from RNeasy column by addition of 40µl RNase free water. Concentration was determined using a NanoDrop ND-1000 spectrophotometer and stored at -80°C.

5.10.2 Generation of complementary DNA (cDNA)

Next, cDNA was generated from isolated RNA by reverse transcription using Super Script III (Invitrogen). According to manufacturer's protocol, 1µg RNA was applied to oligod$T_{(20)}$ primer, dNTP mix and polymerase. Final RNase H (1U/µl) treatment was performed at 37°C for 20 min to remove excessive RNA templates that could interfere with PCR reaction. Long-term storage of cDNA was avoided and kept at -20°C until use.

5.10.3 Quantitative real-time PCR

Quantitative real-time PCR (qPCR) was performed to address differential gene expression between two experimental groups. TaqMan Gene expression assays (Applied Biosystems) were applied to assess differences in gene expression of *laminin a4* deficient mice and control retinas as well as to determine gene induction in treated and untreated control cells. Each assay consists of two unlabeled PCR primers, amplifying the sequence of interest (final concentration 900nM each) and a FAM™ dye labeled TaqMan® MGB (minor groove binder) probe for detecting the sequence of interest (final concentration 250nM), see

Table 6. TaqMan Endogenous Controls, b- actin are VIC® dye-labeled TaqMan MGB probes and added to each PCR reaction.

In the PCR step, PCR products are synthesized from 3µl cDNA samples (generated from 1µg RNA) using the TaqMan PCR master mix (Applied Biosystems) and performed on the Applied Biosystems 7900HT sequence detection system.

PCR reactions were carried out in duplicates or triplicates; The gene of interest was normalized to endogenous control, delta CT values were calculated and data compared by relative quantification.

gene	species	product number
Dll4	ms	Mm00444619_m1
Dll4	hu	Hs00184092_m1
Flt-1 (Vegfr1)	ms	Mm00438980_m1
Hey1	ms	Mm00468865_m1
Hey2	ms	Mm00469280_m1
itgb1	hu	Hs00236976_m1
itgb3	hu	Hs00173978_m1
itga3	hu	Hs00233722_m1
Kdr (Vegfr2)	ms	Mm00440099_m1
Nrarp	ms	Mm00482529_s1
Pdgfb	ms	Mm00440678_m1
Slc2a	ms	Mm00441473_m1
Vegfa	ms	Mm00437304_m1
b-atin	ms	4352341E
b-actin	hu	4326315E

Table 6 TaqMan® probes used in qPCR

5.11 Reverse – transcriptase PCR (RT-PCR)

RNA was isolated from *Laminin a4* null and control retinas and subsequently, cDNA was generated as illustrated in 5.10.2.

To determine differences in gene expression between *Lama4* genotypes we applied semi-quantitative PCR using ReactionReady^{TM} developed by Superarray. Internal Normalizer mouse glyceraldehyde-3-phosphate dehydrogenase (GAPD) was added to standard PCR (Hot Start "Sweet" PCR master mix, 2X) containing first strand cDNA template (1µl) and primers specific for gene of interest (Table 7) to a final volume of 25µl.

PCR reaction was performed at 95°C, 15 min; 30cycles of (95°C, 30 sec; 55°C, 30 sec; and 72°C, 30 sec); 72°C, 5 min; PCR product was run on 1% agarose gel containing ethidiume bromide (Sigma) and bands were visualized by UV ligt. When analyzing data, the expression level of the gene of interest is calculated as the target-to-GAPD signal intensity ratio.

gene	species	product number	band size (bp)
Lama4	ms	PPM35489A	83
Lama5	ms	PPM25090A	157
GAPD	ms	PA-021-24	436

Table 7 List of RT-PCR primers

5.12 SDS gel electrophoresis and Western Blotting

Eyes were harvested from pups and immediately dissected in PBS. Any excessive liquid was removed, retinas snap-frozen on dry ice and stored at -80°C. When eyes were sent from collaborators, the entire eye was snap-frozen and shipped on dry ice. Upon arrival, retinas were dissected and lysed in RIPA buffer.

RIPA buffer

50mM Tris-HCl, pH 7.5, 150mM NaCl, 1mM EDTA, 1% Nonidet P-40, 0.25% Na-deoxycholate and Complete® protease inhibitor cocktail (1 tablet/ 10ml, Roche) and

phosphotase inhibitor cocktail (1:100, Sigma)

Retinas were homogenized in RIPA buffer by pipetting up and down and finally lysed by sonication for 2-3 seconds on ice. Followed by centrifugation at 13,000 rpm for 10 min at 4°C the clear supernatant was transferred in a new tube and protein quantity was determined by bicinchoninic acid assay (BCA assay, Pierce). Basically, protein concentration was measured at 562nm in a spectrophotometer (SpectraMax Plus) and compared to a standard curve of known concentrations of bovine albumine serum (BSA, Pierce).

Equal amounts of protein containing 4x loading buffer (NuPAGE® LDS, Invitrogen) and reducing agent β-mercaptoethanol (final concentration 2.5%) were heated at 70°C for 10 min and then loaded on 4-12% NuPAGE® Novex Bis-Tris gel. The NuPAGE® electrophoresis system (Invitrogen) applied consist of SDS-PAGE, pre-cast polyacrylamide mini gels, running buffer and transfer buffer. Separation of protein was observed by pre-stained protein ladder (Amersham) loaded in the gel. After electrophoresis, gel was transferred onto polyvinylidene difluoride membranes (Amersham) that were pre-wetted in methanol. Successful transfer was achieved at 30V for 1h.

Next, membrane was rinsed in TBS and unspecific binding blocked by incubation in 5% milk powder in TBS-T (TBS containing 0.1% Tween-20) for 1h at RT.

10x TBS

24.2g Tris base, 80g NaCl in 1 litre H20, pH 7.6

Primary antibodies were incubated in 2% BSA/ TBS-T containing 0.02% sodium azide at 4°C over night. Primary antibody solution were removed and kept at 4°C for future use. After washing the membrane with TBS-T (3x 5 min), secondary antibodies were incubated in 2% milk powder/ TBS-T for 2h at RT. Secondary antibodies (Table 3) were HRP conjugated and detected by chemiluminescence ECL Western Blotting detection reagent (Amersham). Immunoreactive bands were visualized by incubating the membrane with ECL reagents and exposition to autoradiography film (Amersham). Exposed films were developed using automatic X-ray processor, JPI.

Several times the membrane was re-blotted with primary antibodies raised in the same

species. Therefore, stripping of membrane was achieved by incubation of the membrane in 100 mM 2-mercaptoethanol, 2% SD, 62.5 mM Tris-Cl pH 6.7 heated at 50°C for 30 min. Followed by washing in TBS-T (3x 10min), the membrane was blocked and incubated with primary antibodies as described above.

Embryos were harvested at E13.5 and yolk sac was removed. Embryonic skin sections of back and brain were dissected and snap frozen on dry ice. If not used immediately, samples were stored at -80°C.

Pdgfrb null and control embryos were harvested and snap frozen by collaborator Maya Nisancioglu. After shipping on dry ice, tissues were dissected as described (see 5.8).

Homogenization of tissue samples was achieved by lysation in RIPA buffer containing protease and phosphotase inhibitor followed by disruption using Disperser T18 (IKA® Fisher). Centrifugation at 13,000rpm for 10 min at 4°C pelleted insoluble material and supernatant was transferred for protein analysis. Protein quantity was measured by BCA assay as described in 5.12 . Equal amounts of protein were loaded on SDS PAGE gel and transferred to membrane. For details see 5.12 .

5.13 Immunoprecipitation of embryonic protein lysate

Embryos were harvested and yolk sac was removed and kept for genotyping. Entire embryos were lysed in RIPA buffer containing a mixture of phosphotase and protease inhibitor. After homogenizing embryos, protein lysates were incubated with 1.5µg/ ml primary antibody VEGFR2 (Cell Signalling) for 2 hours at 4°C. Protein G- sepharose beads (SAFC) were washed in RIPA buffer before 40µl 1:1 slurry was added to the protein lysate and incubated for 45min at 4°C while rotating. This was followed by short centrifugation at 3000rpm for 30 sec to separate supernatant form beads and 4 washes in lysis buffer. Pellet was resuspended in 40µl 4x loading buffer containing SDS and heated to 95°C for 5 min. Beads were spun down by short puls centrifugation and supernatant loaded onto a gel. Followed by SDS gel electrophoresis and blotting, membrane was incubated with phospho tyrosine and/ or pVEGFR2 antibodies. A detailed description on SDS electrophoresis and Western Blotting can be found in section 5.12 .

5.13.1 Densitometric quantification

Developed chemiluminescent films were scanned, tiff images were then analysed by Image J, applying uncalibrated OD (gray value). Bands sizes were measured and normalized to the appropriate control gene.

5.14 Confocal microscopy

Confocal laser scanning microscopy was performed using a Zeiss LSM 510 Meta microscope. Objectives used were: 63x water immersion NA1.2 CAPOCHROMAT, 40x water immersion NA1.2, C-APOCHROMAT, 25x water immersion NA0.8 Plan-NEOFLUAR and 2.5x NA0.075 Plan-NEOFLUAR.

Images were processed using Volocity 4.3.1, Improvision and Adobe Photoshop CS2.

5.15 Quantification of retinal parameters

5.15.1 Vessel density

A visual field (20x20 µm) was determined at the sprouting vascular front and branchpoints were counted.

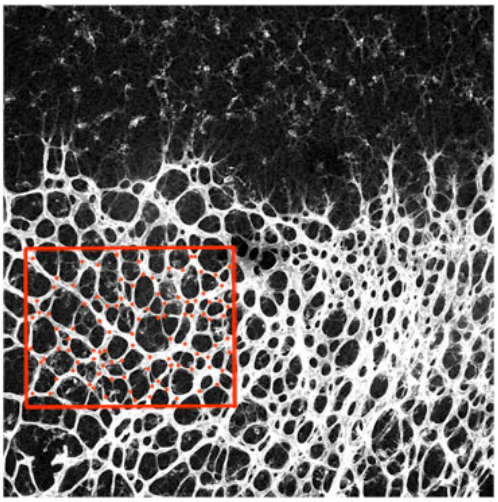

Figure 5.1 Quantification of vessel density

5.15.2 Migratory length/ speed of retinal vessels

Migration of vessels was analysed by measuring the total length of the retinal vasculature from the optic nerve towards the retinal periphery.

Migratory length of vessels upon treatment with blocking peptides was accessed by measuring the total length of retinal vessels (injected and uninjected eyes). The daily distance of migration was calculated by dividing the length of uninjected control eyes by 5 (5 days). This distance was multiplied by 4 (4 days without treatment) resulting in the distance of vessels have migrated in each group (control injected, peptide injected and uninjected eyes). By subtracting the distance vessels have migrated within first 4 days without treatment from the total migratory length of each group we determined the distance vessels have migrated from day 4 to day 5 when injected.

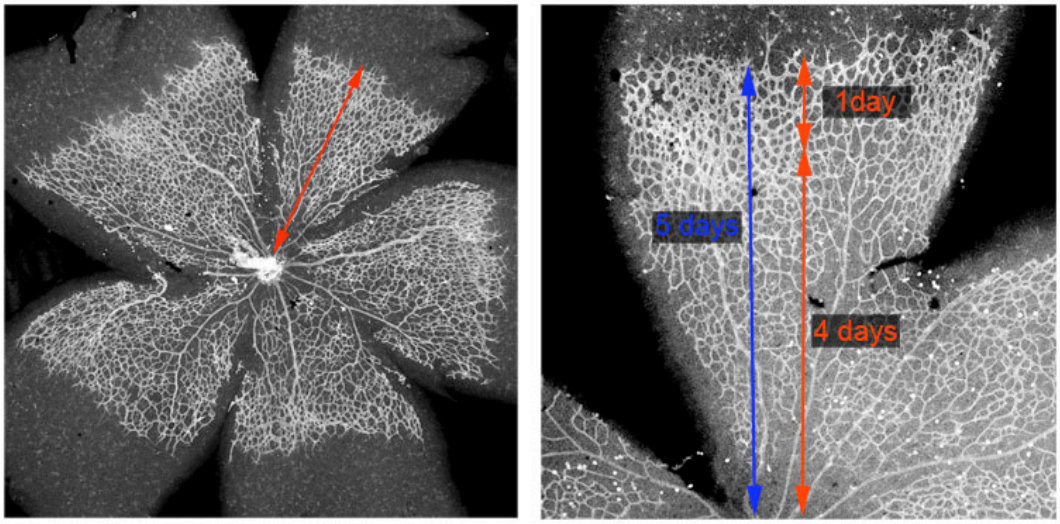

Figure 5.2 Determining migrational length of retinal vessels

5.15.3 Number of filopodia extension

To ascertain number of filopodia, vessel length at the leading tip cells were measured and filopodia were counted. For each quantification at least 4 confocal images /retina were taken and at least 4 mice/ genotype were analysed. Statistical significance was verified using t-test, Graph Pad Prism® Version 5.0a.

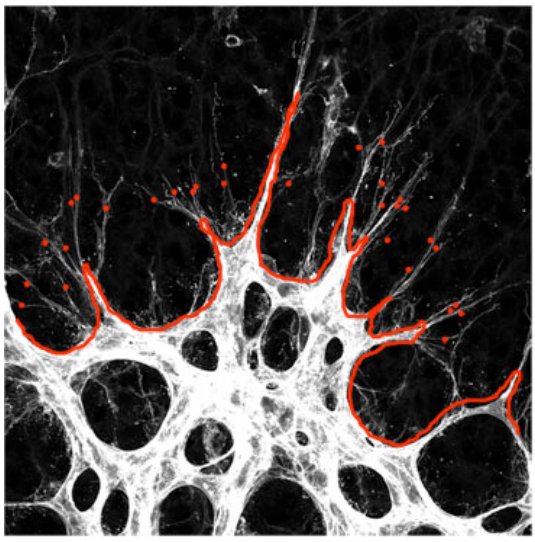

Figure 5.3 Quantification of filopodia number

5.15.4 Quantification of proliferation

Confocal microscopy images were taken with 40x objective and BrdU positive cells that are counterstained with isolectin were counted. n=3, mice per genotype;

BrdU positive endothelial nuclei were calculated per visual field. Statistical significance was determined by unpaired t-test, Graph Pad Prism® Version 5.0a.

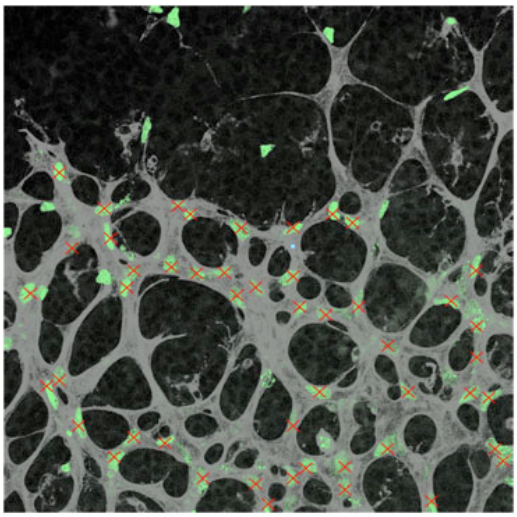

Figure 5.4 Quantification of endothelial cell proliferation

5.15.5 Quantification of vessel density, vessel diameter and regression of vessels in embryonic vasculature

Regression was determined by measuring the length of CollagenIV positive but endomucin negative profiles using the line measurement tool of Volocity 4.3.1, Improvision software. Quantification and graphic illustration represents a comparison of the sum of regression profile length per image analysed.

Total vessel length per image was quantified measuring the skeletal length of endomucin positive vessels.

Vessel diameter was quantified measuring the width of vessel profiles using the line measurement tool of Volocity, Improvision (n>20, images per genotype). Statistical significance was verified using t-test, Graph Pad Prism® Version 5.0a.

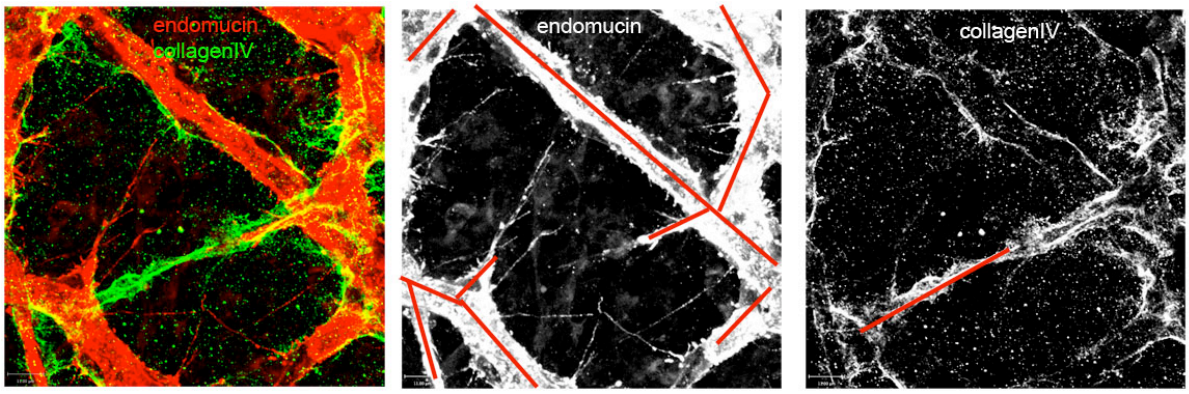

Figure 5.5 Quantification of vessel regression

5.16 Electron Microscopy of retinal tip cells and embryonic skin samples

Isolated eyes were fixed in 4% PFA for 5-10 min at RT before dissecting retinas. The sprouting vascular front was identified by light microscopic reflection of vessels and cut out from the remaining retina. Samples were then fixed in 2% PFA + 1.5% glutaraldehyde prepared in 0.1M phosphate buffer (PB) for 2–3 hours. Finally retinas were washed and stored in PBS at 4°C

Likewise, embryos were harvested at E13.5 and fixed in 4% PFA for 30 min before dissecting of embryonic skin samples. This was followed by fixation in 2% PFA + 1.5% glutaraldehyde prepared in 0.1M phosphate buffer overnight at 4°C before storing in PBS.

The following procedures were done by Ken Blight, staff from the Electron Microscopy

Unit, Cancer Research UK.

Tissue was post-fixed in reduced Osmium Tetroxide in 0.1M Sorensens buffer at RT for 1 hour, washed and fixed in 1% Tannic acid for 45mins at RT. Samples were then rinsed in 1% sodium sulphate before washing in double distilled water (ddH_2O), twice for 5minutes. After dehydration of samples through a graded series of ethanol (70%, 80%, 90% and 100%) 20mins each, tissue samples were washed in intermediate solvent [propylene oxide] for 20mins, RT. Overnight infiltration with 50:50 Epon/propylene oxide at RT was followed by three infiltration steps with Epon for 2 hours. Subsequently, the tissue was embedded in fresh resin and polymerized overnight at 60°C before cutting ultra-thin sections of approximately 75nm thickness on a Leica Ultracut S Ultratome and were collect on 200 mesh copper grids.

Finally, samples were stained with a saturated solution of uranyl acetate in methanol for approximately 6 minutes at RT, washed in methanol and stained with Reynold's lead citrate for 4mins at RT. Sections were analysed using an JEOL 1010 transmission electron microscope (TEM).

If not stated otherwise, solutions were made up in Sorensens buffer.

Sorensens Buffer System

Solution X:

0.2M Disodium Hydrogen Orthophosphate, Na_2HPO_4 29.82g in 1050ml ddH_2O

Solution Y:

0.2M Sodium Dihydrogen Phosphate, $Na_2HPO_4.2H_2O$ 15.6g in 500ml ddH_2O

Double Buffer:

0.2M Phosphate Buffer, 202.5ml Solution X, 47.5ml Solution Y

Reduced Osmium

5ml 0.2M Phosphate (Double Buffer), 2.5ml 4% Osmium Tetroxide in ddH_2O, 1ml of 15% Potassium Ferricyanide, 1.5ml ddH_2O

Araldite Resin

20ml Araldite CY212, 20ml Dodecenyl Succinic Anhidride (DDSA), 1ml Benzyl Dimethyl Amine, 0.25ml Dibutyl phthalate

5.17 Cultivation of endothelial cell lines

If not indicated otherwise, all reagents and media were provided by cell line and media production service, Cancer Research UK. Cells lines and isolated primary cells were cultured at 37°C in 5%CO_2.

5.17.1 Culturing of bEND5 cells

The endothelial cell line utilized during this thesis was established from brain endothelial cells of BALB/c mice and is referred to as bEND5 (ECACC). Immortalisation has been carried out by infection of primary cells with retrovirus coding for the Polyoma virus middle T-antigen. Cells were cultured in Dulbecco's modification of Eagles medium (DMEM) containing 10% fetal calf serum (FCS), 1% Penicillin/ Streptomycin (Pen/ Strep) and 1% glutamine.

Cells were passaged by incubation of trypsine/ versene (try/ver) for several minutes until cells floated of the cell culture flask. Cells were then pelleted by centrifugation at 1200rpm for 5 min and transferred to new flask; cells were split 1:3.

For long term storage in liquid nitrogen containers, bEND5 cells were collected by centrifugation and resuspended in DMEM containing 20% FCS and 10% DMSO.

Coating of dishes with laminin matrices

The laminin proteins used throughout my experiments were provided by Karl Trygvasson and are referred as LN411 (laminin $\alpha4\beta1\gamma1$) and LN511 (laminin $\alpha5\beta1\gamma1$). Both laminins are dissolved in PBS and were sterilized by filtration (0.2µm filter). Cell culture dishes and plates were incubated with a final concentration of 10µg/ml at 4°C over night. Laminin solution was removed before cells were cultured.

Immunofluorescence staining of bEND5 cells

Cells were cultured confluent or non-confluent on either coverslips or MatTek dishes and were passaged 24-48 hours before IF staining. Medium was aspirated and cells were rinsed in PBS before fixation with 4% PFA for 20 min at RT. Unspecific binding was blocked by incubation in 1%BSA/ 0.5% Tween-20 for 1h, RT before incubation of primary antibody in

0.5%BSA/ 0.25% Tween-20 for 1h, RT. After washing with PBT (3x 5min) cells were incubated with secondary antibody diluted 1:100 in 0.5%BSA/ 0.25% Tween-20 for 1h, RT. Finally cells were washed again and post fixed with 4% PFA for 10 min at RT.

Neutralizing of VEGFR2 in endothelial cells

bEND5 cells were cultured on LN411, LN511 and uncoated 12-well plates containing 30ng/ ml VEGF 165 (R&D systems) in DMEM medium supplemented with 10% FCS, Pen/Strep and glutamine. To block VEGFR2 signalling, mouse specific neutralizing antibody DC101 (ImClone) was added at a final concentration of 30µg/ml. After 24 hours, cells were harvested and prepared for protein or gene expression analysis; n>3

To determine VEGFR2 signalling, cells were lysed in RIPA buffer containing protease and phopshotase inhibitor cocktails. Equal amounts of protein samples were run on SDS PAGE gel followed by Western Blot to detect phospho VEGFR2 and total VEGFR2 levels upon DC101 neutralization. For details on this procedure see 5.12 .

To analyse differences in gene expression upon blocking of VEGFR2, cells were lysed in RLT buffer and RNA was extracted. After cDNA was generated samples were exploit to quantitative PCR (qPCR). A detailed description can be found in 5.10 .

Inhibition of Notch signalling by pharmacological inhibitor (DAPT)

Gamma secretase activity was inhibited pharmacologically using DAPT (N-[N-(3,5-Difluorophenacetyl-L-alanyl)]-S-phenylglycine t-Butyl Ester (Merck, Cat. No. 565770). DAPT was dissolved in DMSO and aliquotes were stored at -20°C.

DAPT was added to confluent bEND5 cells cultured on LN411 or uncoated dishes at a final concentration of 50µM. DMSO was used as a control substance. After 24 hours of incubation, cells were collected and RNA was isolated to determine differences in gene expression; n>3

siRNA transfection of human endothelial cells

Human umbilical vein endothelial cells (HUVECs) were cultured using EGM medium supplemented with Bullet Kit (Lonza) and passages P2-P5 were used for experimental procedures. Culture flasks were incubated with 0.5mg/ ml human plasma fibronectin (Chemicon) in PBS for at least 30 min at 37°C.

Short interfering RNA (siRNA) tranfection was applied to knock down integrin activity and assess its function in LN411 induced gene expression.

To silence integrin gene expression ON-TAGET*plus SMART*pool developed by Dharmacon was applied to HUVEC cells. The ON-TAGET*plus SMART*pool consists of a mixture of 4 siRNAs targeting one gene and guarantees most efficient knockdown. Table 8 summarizes the siRNAs used and the negative control targeting at least 4 mismatches to any mouse gene (ON-TAGET*plus* non-targeting control).

siRNA was dissolved in RNase free water to a stock concentration of 20µM and stored at -20°C. Transfection was performed according to Manufacturer's guidelines using Cell Line Nucleofector® Kit-V (Amaxa). In summary, $2.5x10^5$ HUVEC cells were mixed with 2µg of siRNA (100nM final concentration), 100µl of Nucleofector Solution V and transferred to amaxa cuvette applying AMAXA devise, program V-001. Cells were cultured on LN411, LN511 or uncoated plates for 72h before RNA extraction. To assess transfection efficiency GFP conjugated control plasmid was transfected to HUVEC cells and GFP expression was observed by fluorescent microscopy.

Likewise, Nucleofector® mediated transfection was performed with 2µg ILK plasmids (Table 8) that have been provided by Vassiliki Kostourou.

Gene expression upon siRNA and ILK transfection was determined by qPCR as described in 5.10 .

gene	product number
itgb1	004506
itgb3	004124
itga3	004571
non-targeting control	D-001810-01-05
ILK GFP	Vassiliki Kostourou
ILK PBS	Vassiliki Kostourou
ILK E395K	Vassiliki Kostourou

Table 8 List of OnTarget siRNA and Ilk plasmids used

Culturing of integrin b3 deficient endothelial cells

Integrin b3 -/- and wildtype control immortalized endothelial cell lines were established by Stephen Robinson (unpublished data). Briefly, endothelial cells were isolated from lungs of integrin β3 -/- and control mice crossed to C57Bl/6 /129 genetic background. Immortalized endothelial cell lines were generated by Polyoma virus middle T antigen expression introduced by ecotropic retrovirus transduction according to May (May, Mueller et al. 2005) et al., 2005. Cells were cultured in E4 low glucose, Ham's F12 containing 20% FCS, 0.1 mg/ml heparin (Sigma) and endothelial growth supplements (Sigma).

5.18 Retroviral Cre infection of primary smooth muscle cells

5.18.1 Mural cell isolation of mouse aorta according to (Ray, Leach et al. 2001)

Ext1 floxed mice were euthanized by CO_2 asphyxialation and aorta was dissected from its origin at left ventricle to the iliac bifurcation. Aorta was flushed with PBS and cleaned from tissue as well as adventitia until aorta appeared as a smooth tube. Aorta was cut into pieces of 1-2mm size and digested in 100µl filter sterilized enzyme solution containing 7.5mg collagenase A (Roche) in 5.5ml DMEM, 10% FCS, 1% Pen/ Strep and 1% glutamine. After 6 hours of incubation at 37°C in 5%CO_2, 3ml of culture medium were added and centrifugated at 300x *g* for 5 minutes. Medium was aspirated and replaced by 5ml of fresh medium followed by an additional centrifugation step before cells were resuspended in

700µl medium and transfered in 48-well plate. Cells were cultured and undisturbed for 5 days.

Mural cells were identified by IF staining for MC marker smooth muscle actin (SMA) and PDGFR-β.

5.18.2 Retroviral Phoenix cell line transfection

Phoenix cells were plated 24 hours before transfection at a density of $2x10^6$ cells per 6cm dish to reach subconfluency. Cells were cultured in DMEM supplemented with 10% FCS, 1% Pen/ Strep and 1% glutamine.

For the transfection plasmid DNA (pBabe CRE hygro, pBabe CRE puro, pBabe neo CRE IRES-EGFP) was prepared in HBS (2x HBS: 8g NaCl, 6.5g HEPES, 10ml Na_2HPO_4). About 5 minutes before transfection 25µM chloroquine was added to Phoenix cells to inhibit lysosomal DNases. Transfection mix containing 5-10µg DNA, 61µl 2M $CaCl_2$ and sterile water to a final volume of 500µl was added to 6cm dishes of Phoenix cells and distributed evenly. Medium was detoxified next day by addition of fresh medium. Supernatant was collected 48 hours post-transfection of Phoenix cell and centrifugated at 1500rpm for 5 min to pellet cell debris. Finally, 1ml of viral supernatant and 3µl of polybrene (5mg/ml) were added to primary mural cells isolated from *Ext1* floxed aortas. Medium was changed 24 h later and MC were analysed 24-48 hours post infection of viral supernatant.

Infection of *Ext1* floxed mural cells was analysed by fluorescence microscopy and detection of GFP-, RFP- Cre.

6 Astrocytic Fibronectin regulates retinal endothelial tip cell migration through integrin activation and VEGF-A retention

6.1 Results

6.1.1 Fibronectin localization in retinal vasculature

Fibronectin (FN) is a major component of the extracellular matrix (ECM) and functions in cell adhesion, spreading and cell migration. Its expression is widespread during embryonic development and is upregulated in various pathological conditions such as cancer and wound healing (Hynes 2007). In addition, FN promotes cell migration and is prominently deposited in areas of active cell migration in embryos. To address the function of FN during developmental angiogenesis and in particular during blood vessel sprouting and migration we analysed FN expression in the retinal vasculature.

Visualization of FN by immunofluorescence (IF, red) staining revealed strong FN localization on astrocytes ahead of the growing vessels at postnatal day 5 (P5) in the mouse retina (white arrows, Figure 6.1 a, b). Co-labelling with PDGFRα, a marker used to detect astrocytes (d) and staining with isolectin B4 (green) to visualize endothelial cells (EC) support the specificity of astrocytic FN (Figure 6.1 b-d).

These findings are in line with Uemura et al., 2006 showing FN expression by *in situ* hybridization on astrocytes ahead of the growing vasculature (Uemura, Kusuhara et al. 2006). Astrocytes enter the retina and spread just ahead of the newly formed vessels, initiating vessel growth. Jiang and colleagues demonstrated that fibronectin but not laminin is expressed in the astrocytic zone. Increased mRNA expression revealed that astrocytes synthesis FN. *In vitro* experiments using conditioned medium approaches showed that astrocytes stimulate endothelial cell FN expression, suggesting that FN expression is an essential component in the initiation of retinal vasculogenesis (Jiang, Liou et al. 1994).

In addition, RT-PCR of FACS sorted retinal endothelial and astrocytic cell fraction revealed FN expression in both cell types (Uemura, Kusuhara et al. 2006). Fibronectin assembly appears fibrilliar and is distributed over the entire network of central nervous system (CNS) derived astrocytes (b). Interestingly, FN expression is significantly reduced on astrocytes when vascular sprouts grow over the astrocytic network (arrowheads, a, b). Possibly, FN is transiently deposited by astrocytes

providing a provisional matrix and functioning in guiding sprouting endothelial tip cells. That would suggest that astrocytic FN is only transiently required and FN protein might be degraded once vessels have grown over the astrocytic matrix. Furthermore, the strong localization of FN around endothelial BM of retinal vessels suggest that astrocytic FN is re-distributed and taken up by ECs while growing over the astrocytic FN matrix. Alternatively, most of the BM FN deposition may represent *de novo* production by ECs and pericytes.

High magnification imaging revealed that extended filopodia protrusion lack FN but closely align to the FN-rich astrocytic network (e). In marked contrast to the FN distribution, we find collagenIV (green, f-g), a major basement membrane component localized along retinal vessels forming a continuous layer surrounding endothelial cells of growing vessels (f). Tip cells of the growing angiogenic sprout lack a continuous collagenIV matrix and collagenIV is completely absent from filopodia protrusions and the astrocytic BM (g).

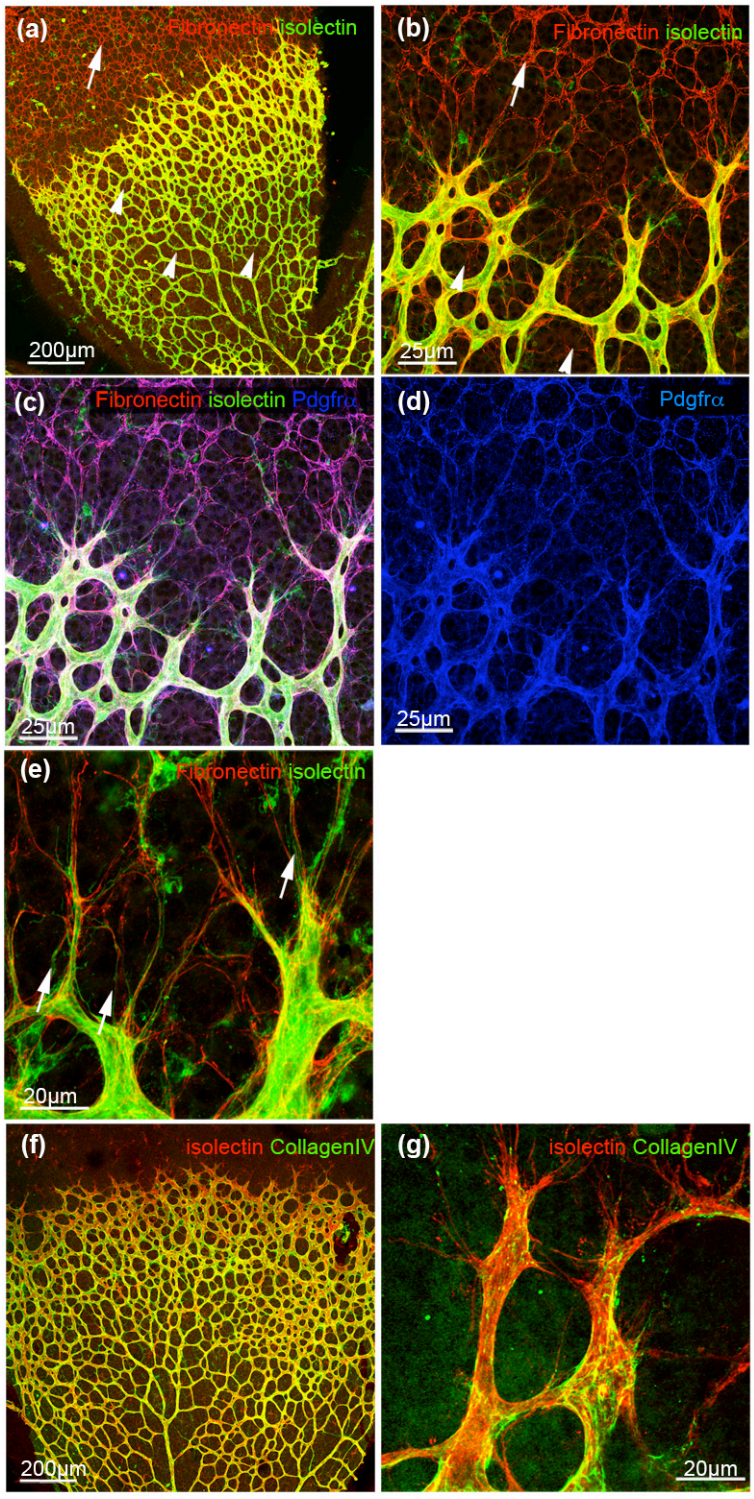

Figure 6.1 Localization of extracellular matrix component Fibronectin and CollagenIV in the retinal vasculature

Fibronectin (FN, red) staining revealed strong deposition ahead of the growing vasculature (white arrows, a, b) whereas astrocytic FN expression is reduced in the mature vascular plexus (arrowheads, a, b). Blood vessels were visualized with isolectin (green) and co-labeling with Pdgfrα (blue) confirmed astrocytic deposition of FN (c, d). High magnification imaging showed alignment of filopodia to astrocytic matrix, however arrowheads indicate absence of FN on extended filopodia (arrows, e). In contrast to FN, collagenIV (green, f) is distributed in the abluminal basement membrane of retinal vessels (red, f) and absent from endothelial tip cells and filopodia (g).

To study the function of astrocytic FN we took advantage of the Cre-lox system and specifically deleted fibronectin from astrocytes expressing glial fibrillary acidic protein (GFAP), an intermediate filament expressed by mature astrocytes in the retina. For details on the Cre-lox mediated gene targeting please see section **5.1** . After crossing FN floxed mice (provided by R. Faessler) with mice expressing Cre recombinase under the GFAP promoter (Bajenaru, Zhu et al. 2002), referred to as FN^{ACko} we observed a strong reduction of FN expression in astrocytes (Figure 6.2). Immunofluorescence staining with fibronectin (red) revealed astrocytic FN deposition ahead of the growing vasculature in control retinas (a) whereas astrocytic FN is completely absent (b) or significantly reduced (c) in FN^{ACko} retinas. Retinas in which GFAP Cre mediated recombination has effectively deleted FN from most astrocytes display absent/reduced FN ahead of the vessels (e) and also show severe reduction of FN localization around blood vessels (b, e) suggesting that astrocytic FN contributes to the endothelial BM. However, deletion of astrocytic FN is often incomplete resulting in variable degrees of mosaic loss of astrocytic FN staining in-between FN^{ACko} littermates. Recombination of only one allele in heterozygous FN flox/+ GFAP Cre mice leads to reduced astrocytic FN staining, illustrating a quantitative correlation between allelic contribution and FN protein deposition (Figure 6.2 c, f).

High magnification images revealed robust fibrilliar FN assembly in control mice (j). However, arrowheads highlight patches of efficient deletion of FN, while white arrows indicate astrocytes still expressing FN in FN^{ACko} (k, l). This mosaic pattern allows us to analyse astrocytic FN function in a dose dependent manner, comparing regions of Cre recombination and therefore FN inactivation and regions of reduced FN expression. We particularly applied that mosaicism when analysing the vascular defects at the sprouting front however, the following quantifications do not take the mosaic FN expression into account.

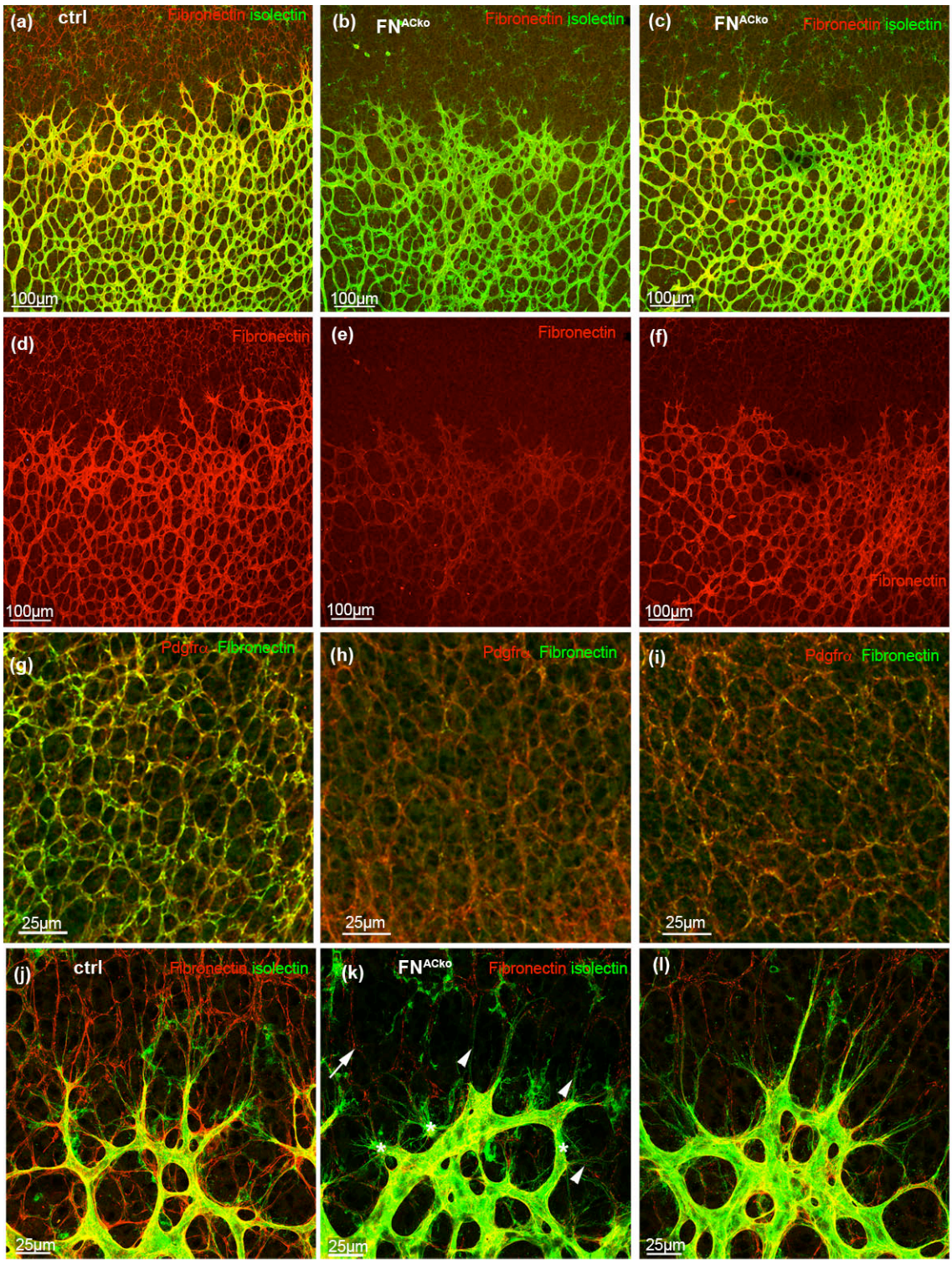

Figure 6.2 Loss of astrocytic fibronectin results in increased vascular density at the sprouting front

Cre mediated deletion of astrocyte-derived fibronectin (FN^{ACko}) leads to reduced FN expression in mutant mice (b, c, h, i) compared to control retinas (a, g) as shown by FN staining (red, d-f). Co-labeling of astrocytes with Pdgfrα (red) and FN (green) reveals normal network development but reduced FN deposition in FN^{ACko} (g- i). Images k, l illustrate residual FN expression (red, arrow) in FN^{ACko} resulting in mosaicism while arrowheads point to regions with complete loss of FN. Deficiency of astrocytic FN matrix leads to aberrant filopodia extension (asterisk, k).

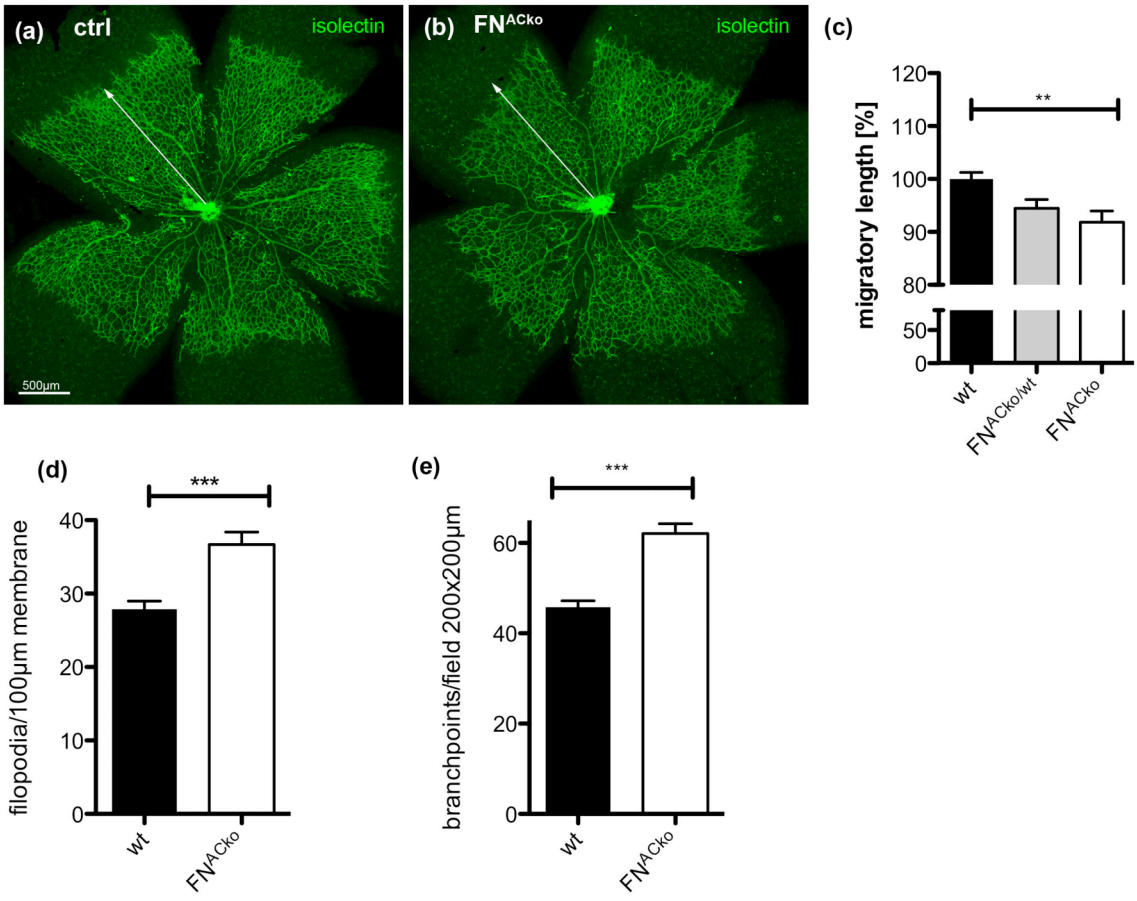

Figure 6.3 Loss of astrocytic fibronectin results in reduced migration of vessels and increased vascular density at the sprouting front

Overview images of the retinal vasculature visualized by isolectin staining (green, a-b) revealed reduced migration towards the retinal periphery in mice deficient of astrocytic FN. Vessel migration was quantified by measuring total length as illustrated by the white arrow (a, b). Graph (c) displays reduced radial expansion of superficial vessels at P5 in control ($n > 5$), heterozygous ($FN^{ACko/wt}$, $n > 3$) and FN^{ACko} mice ($n > 5$). **, $p < 0.01$ 1-Way ANOVA.Values represent mean ± S.E.M.
Deficiency of astrocytic FN matrix leads to aberrant filopodia extension and graph (d) summarizes the number of filopodia protrusion per vessel length at the migrating vascular front of P5 mice, $n \geq 20$. ***, $p < 0.0001$. Values represent mean ± S.E.M. Graph (e) illustrates the number of branchpoints per image field of P5 FN^{ACko} and control mice, $n \geq 10$. ***, $p < 0.0001$. Values represent mean ± S.E.M.

When comparing the migratory length of vessels towards the retinal periphery we observed that blood vessels of mice lacking astrocytic FN (Figure 6.3 b) have migrated significantly less than control littermates (a). The distance of vessel migration (c) in retinas of FN^{ACko} as well as $FN^{ACko/wt}$ as compared to wildtype (wt) littermates was delayed by 9% in FN^{ACko}, 1354 ± 31.58 vs. 1474 ± 18.50 μm, $p<0.01$, and reduced by 5.5% in $FN^{ACko/wt}$ 1393 ± 24.68 vs. 1474 ± 18.50 μm, $p<0.01$). We speculate that the delay in migration would be more drastic if the conditional deletion of FN were complete and uniform throughout the astrocyte population. Indeed, the most pronounced reduction in vessel outgrowth was regularly found in areas with strongest reduction in FN expression.

To investigate the possibility that the delay in migration is caused by defective network formation of astrocytes in the absence of FN, astrocytes were analysed using the marker PDGFRα. However, network formation and morphology of the astrocytes ahead of the vessels as well as astrocytes in the mature plexus were unaffected upon loss of FN (Figure 6.2 g-i), suggesting that loss of astrocytic FN selectively affects the forming vasculature.

GFAP has been described as a marker of mature astrocytes. GFAP expression is strongest after remodelling of the immature astrocytic network once retinal vessels have grown over the provisional network. It is possible therefore that late onset of the GFAP promoter driving Cre expression resulted in residual astrocytic FN, masking a more fundamental role in vascular patterning. To address whether the delay of vessel migration is enhanced when FN is deleted in early stages of retinal development we used a Cre line expressing Cre recombinase under the nestin promoter. Nestin is an intermediate filament transiently expressed by dividing and migrating cells of the CNS during early stages of development and is later replaced by cell-type specific intermediate filaments such as GFAP (Beech, Cleary et al. 2004). In order to delete FN from early stage and immature astrocytes we crossed FN floxed mice and Nestin Cre mice (Lin, Sandusky et al. 2003) and analyzed the distance vessels have migrated at P5. We could confirm that vessel migration was further reduced by 12% (Figure 6.4 a-c). Immunostaining with FN revealed a substantial loss of FN in the astrocytic network and in the vascular compartment (c-f), indicating that recombination of FN in astrocytes expressing Nestin takes place. To study that the increased delay in vessel migration of FN Nestin Cre mice indeed caused by an increased loss of astrocytic FN compared to FN^{ACko}, I propose to quantitatively analyse FN mRNA expression.

When comparing the sprouting vascular front of FN^{ACko} (Figure 6.2 k, l) and wildtype littermates (j) we observed increased number of filopodia and comparably short filopodia burst on endothelial tip cells (asterisk, k). The loss of astrocytic FN appears to affect the filopodia alignment and orientation towards the astrocytes. Further quantification of the growing vascular front in retinas lacking astrocytic FN revealed increased numbers or activity of endothelial tip cells, as determined by counting the number of filopodia (Figure 6.3 d) at the vascular front (filopodia number increased by 131%, 36.7 ± 1.7 vs. 27.9 ± 1.1, $p<0.0001$). To examine whether the loss of astrocytic FN affects vascular density we compared number of branch points in of FN^{ACko} and wildtype control littermates (Figure 6.3 e) and found a significant increase by 35% (62.1 ± 2.2 vs. 45.8 ± 1.4, $p<0.0001$). In addition to the denser vascular plexus at the sprouting front, we detected slightly dilated vessels (Figure 6.2 k, l) particularly in regions where astrocytic FN is absent. Initial analysis of FN^{ACko} and quantification of filopodia number and vessel density has been carried out by Andrea Lundkvist.

Similar defects seen in FN^{ACko} were observed when analysing the vascular front of mice lacking astrocytic FN in Nestin Cre mice. Although FN expression (green) is not completely absent in FN/ Nestin Cre positive retinas (d, f) we observed a reduction of FN assembly and deposition in astrocytes ahead of retinal vessels (c-f). The reduction of astrocytic FN resulted in morphological defects. Blood vessels of the sprouting front are dilated and the plexus appears denser than seen in control littermates (c, e). In addition, high magnification revealed increased numbers of filopodia (g, h) in FN/ Nestin Cre mice compared to control littermates.

In summary, loss of astrocytic FN leads to delayed migration of retinal vessels and an increased number of filopodia and subsequently a denser plexus in the sprouting vascular front that could be a result of increased proliferation due to instable vessels. The loss of astrocytic FN possibly affects basement membrane composition and assembly around mature blood vessels leading to aberrant sprouting and EC proliferation. Another possible explanation of vessel hyperplasia could be a failure of filopodia to align and stretch along the astrocytic network lacking FN resulting in non-adherent ECs causing delayed migration and therefore dilated vessels. Possibly, the increased number of filopodia extension could be a compensatory effect upon the loss of filopodia- astrocytic matrix adhesion. Or the increase in filopodia could reflect an increased number of endothelial tip cells as a result of enhanced proliferation.

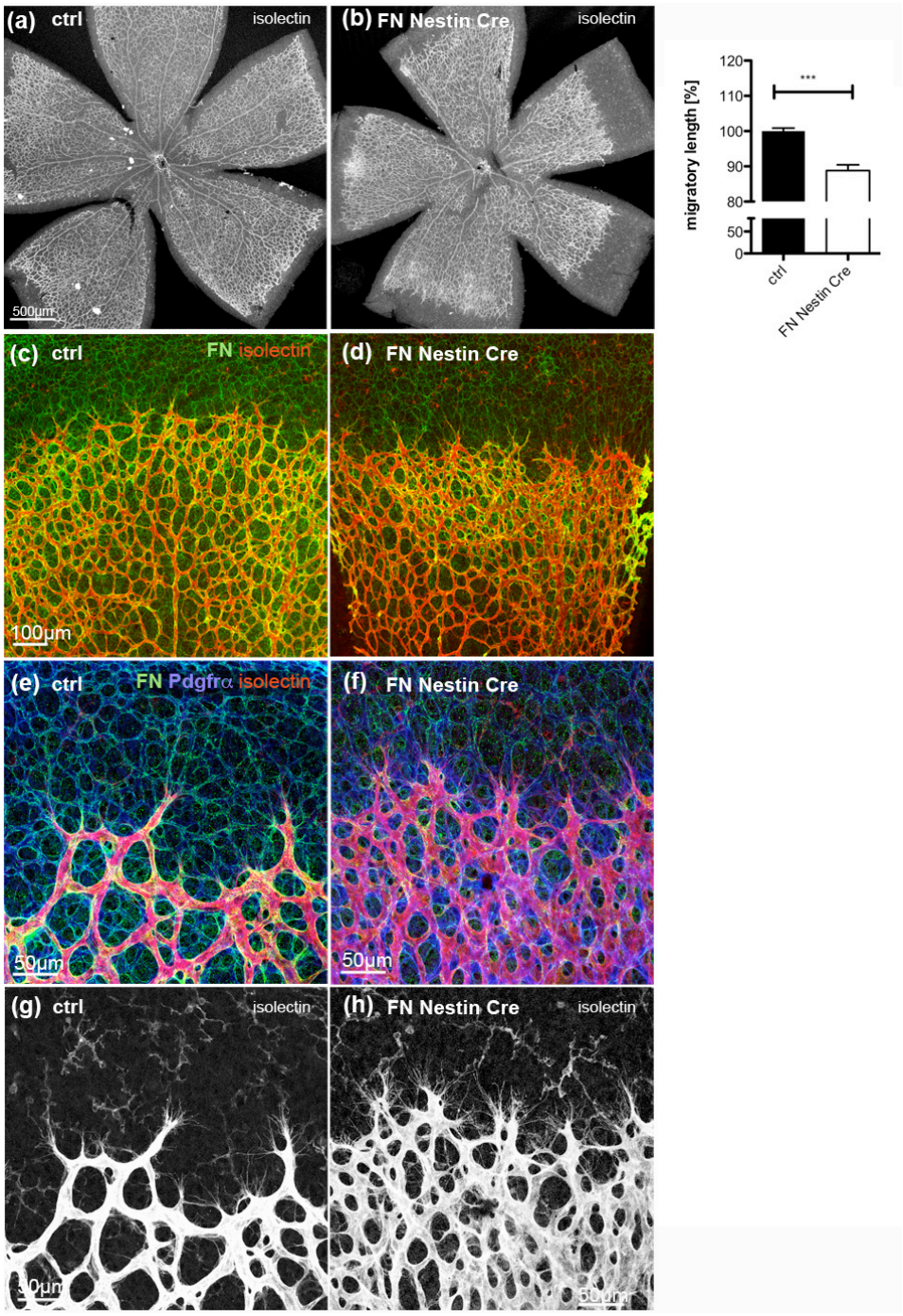

Figure 6.4 Nestin Cre mediated loss of fibronectin results in reduced vessel migration

Overview images of the retinal vasculature visualized by isolectin staining (a, b) revealed reduced radial expansion towards the retinal periphery in mice deficient of astrocytic FN (FN Nestin Cre). Graph c illustrates reduced migration in P5 FN Nestin Cre mice (n = 3) compared to control retinas (n =7). ***, $p < 0.0001$. Values represent mean ± S.E.M.

Fibronectin staining (green, c-f) shows reduced assembly and expression of FN in astrocytes (blue, e, f) and reduced deposition of FN in basement membrane of retinal blood (red, c-f) upon Nestin Cre recombination (d, f). Loss of astrocytic FN results in increased vessel density and excessive filopodia extension of vessels at the sprouting vascular front (g, h).

6.1.2 Migratory delay of retinal vessels in several FN splice variants

We hypothesized that the delayed migration of vessels lacking an astrocytic FN matrix could be caused by misguidance and/or a defective adhesion of vessels to the astrocytic plexus. Confocal microscopy revealed a close interaction of leading endothelial tip cells with the underlying matrix deposited by the astrocytic network providing a guiding network for growing vessels. As shown, FN is almost exclusively provided by the astrocytes ahead of the vessels and its deposition is strongly down regulated in the mature astrocytic plexus, while FN is mainly localized around blood vessels in the mature plexus (Figure 6.1**Error! Reference source not found.** a).

Fibronectin is high-molecular weight glycoprotein and its function in adhesion, migration, and cell survival has been extensively described. Its complexity is also reflected in its structural diversity, cell-type specific alternative splicing results in several FN isoforms. In collaboration with Richard Hynes, we analysed the retinal vasculature of FN spliced variants missing extra domain EIIIA or EIIIB as well as double splice mutants EIIIAB and EIIIBA. Although the presence of FN splice variants EIIIA and EIIIB correlates with embryonic vascular development and vascular remodelling, and their expression is strongly upregulated during pathological angiogenesis such as tumour development, mice lacking either domain are viable and vascular development and retinal angiogenesis appear normal (Astrof, Crowley et al. 2004). In contrast, EIIIA/EIIIB double null mice are embryonic lethal and exhibit severe cardiovascular defects, including hemorrhages and extraembryonic defects (Astrof, Crowley et al. 2007). Therefore, we analysed the retinal vasculature of mice null for EIIIB or EIIIA, and of compound mutants null for EIIIB and heterozygous for EIIIA, or null for EIIIA and heterozygous EIIIB, referred as EIIIBA or EIIIAB respectively. In all cases, we observed that a vascular plexus has formed, vessel density appeared normal and vessels have migrated towards the retinal periphery (Figure 6.5). However, when we determined the distances vessels have migrated we noticed a significant delay in FN splice variants *FN EIIIB, FN EIIIAB* and *FN EIIIBA,* but not *FN EIIIA* (c). Figure 6.5 is a summary of the analysis of multiple litters of FN splice mutants. The migratory length was compared to control littermates, set to 100%.

We observed the most prominent delay of vessel migration in FN splice mutant *FN EIIIB,* whereas mice deficient of splice variant *FN EIIIA* have no migrational defects. Fibronectin splice mutants *FN EIIIAB* and *FN EIIIBA* displayed a mild delay. To our

surprise, retinal vessels of mice null for *FN EIIIB* and heterozygous for *FN EIIIA* migrated further than vessels of single splice variant lacking *FN EIIIB*. A possible explanation for this observation could be that loss of both splice domains results in conformational changes of FN. As a consequence, FN-binding properties might be altered, enabling and/or enhancing the binding of additional integrins that positively influence migration. Alternatively, the additional loss of one allele *FN EIIIA* in *FN EIIIB* null mice may result in compensatory effects and allowing vessels to migrate on a discrete ECM substrate.

Next we analysed the vasculature of each FN splice variant in more detail.

Studying the sprouting vascular front of FN EIIIA single mutants we found no differences in vascular density, number or alignment of filopodia to the astrocytic network (Figure 6.6 a-b).

Similarly, no striking defects were observed when analysing *FN EIIIB* single mutants. We found that FN is expressed in *FN EIIIB-/-* to the same extend as control littermates and has assembled in fibrilliar structures (c-d). Immunofluorescence staining with PDGFRα, a marker for astrocytes and combined staining with FN illustrates deposition and assembly of FN on the entire astrocytic network. Co-labelling with isolectin to visualize the ECs revealed that leading tip cells follow the underlying astrocytic plexus and extended filopodia align closely to astrocytes. Interestingly, *FN EIIIBA* and *FN EIIIAB* double mutant mice developed an abnormal vascular pattern (Figure 6.6 h-j). In particular, we found that EC tip cells appeared blunt ended and seem to have lost the interaction and guidance of the astrocytic network (red arrows). When comparing the retinal vasculature to control littermates we observed that vessels are not restricted to a two-dimensional network as seen in control mice. Instead blood vessels have grown off their track and migrated over each other resulting in an abnormal patterning of the vascular sprouting front, indicated by red arrowheads (i, j). This could be a result of the slight reduction in FN deposition in the astrocytic network ahead of the growing vasculature as seen in *FN EIIIAB* -/- compared to control retinas (k-o).

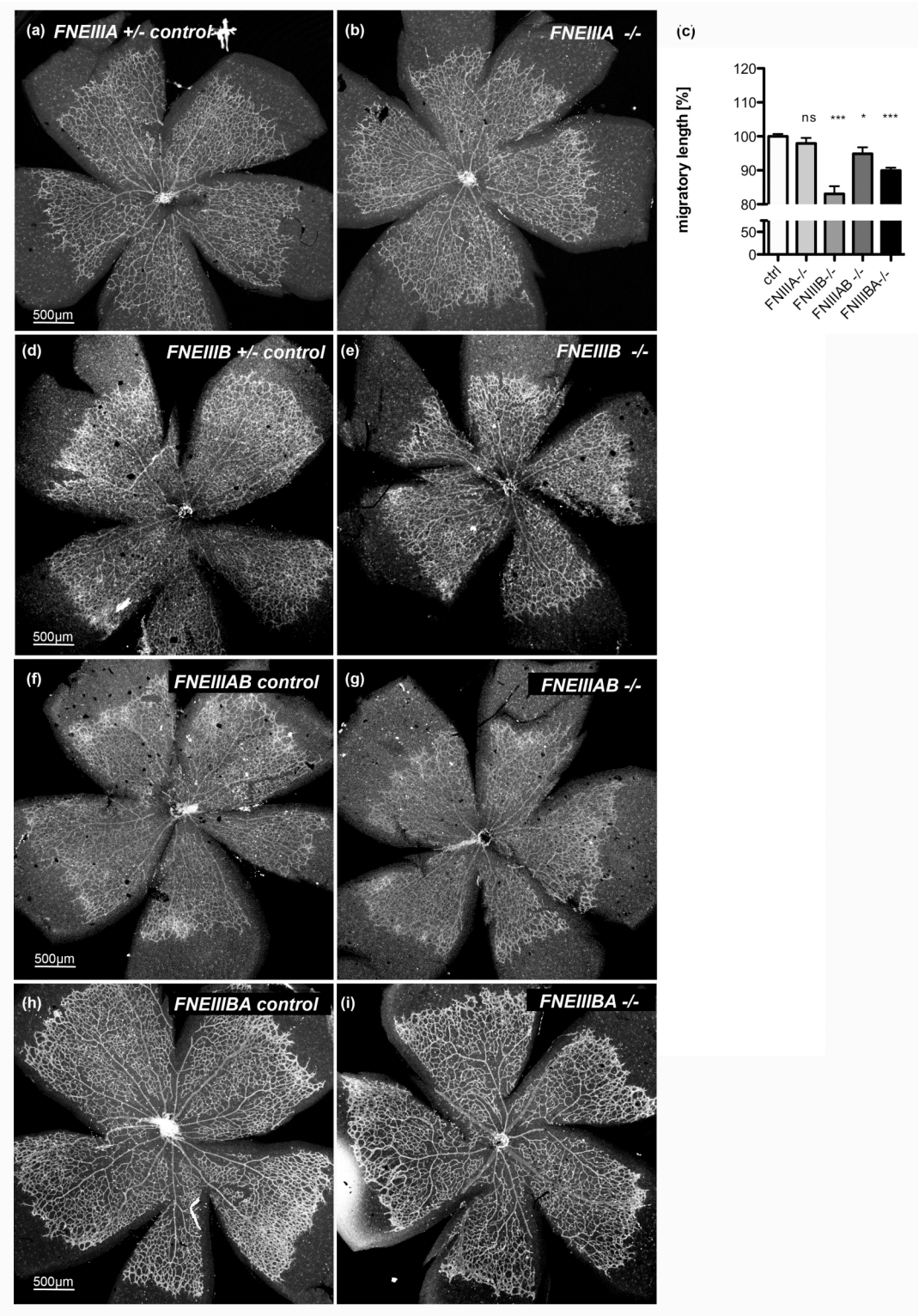

Figure 6.5 Fibronectin splice variant FNEIIIB and double splice variants FNEIIIAB and FNEIIIBA function in vessel migration during retinal angiogenesis

Isolectin staining to detect the retinal vasculature revealed reduced radial migration to the retinal periphery in FN splice variants FNEIIIB (d, e), FNEIIIAB (f, g) and FNIIIBA (h, i) but not FN isoform FNIIIA (a, b). Graph c represents a summary of distance vessels have migrated in comparison to control retinas. ***, $p < 0.0001$, *, $p < 0.05$. Values represent mean ± S.E.M.
FNEIIIA +/- and FNEIIIA -/- n=7; FNEIIIB +/- n=6, FNEIIIB -/- n=12; FNEIIIAB +/- n=3, FNEIIIAB -/- n=4; FNEIIIBA +/- n=16, FNEIIIBA -/- n=13

Therefore, we suggest that individually, the FN splice variant *EIIIA* has no significant function during vascular development in retina as reported previously by (Astrof, Crowley et al. 2004), while *FN EIIIB* may play a role in migration of retinal vessels. Interestingly, a possible effect of EIIIB on FN matrix assembly and proliferation was observed in *EIIIB-null* MEFs *in vitro* and recombinant *EIIIB*-positive FN incorporated somewhat more efficiently into ECM (Fukuda, Yoshida et al. 2002);(Guan, Trevithick et al. 1990), suggesting a possible role for EIIIB in FN matrix assembly. This could be a possible explanation for the migratory delay observed in *FN EIIIB* but not *FN EIIIA* null retinas.

Combined loss of both splice variances FN EIIIA and EIIIB results in embryonic lethality with vascular defects resembling the loss of full-length FN (Astrof, Crowley et al. 2007). In line with these findings, mice either null for *EIIIA* and heterozygous for *EIIIB* or null for domain *EIIIB* and heterozygous for *EIIIA* exhibited a reduction of migratory speed as well as abnormal vascular patterning, indicating that the presence of at least one domain is required for normal vascular development.

6.1.3 FN binding domain RGD is not required for vessel migration

Fibronectin has been reported to interact with various extracellular matrix components such as collagen and heparan sulfate proteoglycans, but also with growth factors such as vascular endothelial growth factor (VEGF). However, most extensively studied are the interactions of fibronectin with cell-surface receptors, namely integrins (ITG). Fibronectin binds to integrin receptor $\alpha5\beta1$ via the RGD (Arg- Gly- Asp) -binding domain and thereby mediates cell attachment.

Using antibodies directed against integrin alpha 5 (ITG$\alpha5$) or integrin beta 1 (ITG$\beta1$) we observed that both integrins (Figure 6.7, green) are expressed by endothelial cells and localized at the abluminal endothelial cell surface facing the basement membrane (BM) of retinal vessels (red). High magnification imaging revealed a spotty localization of ITG$\alpha5$ (g-i) and ITG$\beta1$ (a-c) on filopodia of leading tip cells (arrows). In addition, ITG$\beta1$ was strongly expressed by pericytes and vascular smooth muscle cells, indicated by arrowheads (d-f).

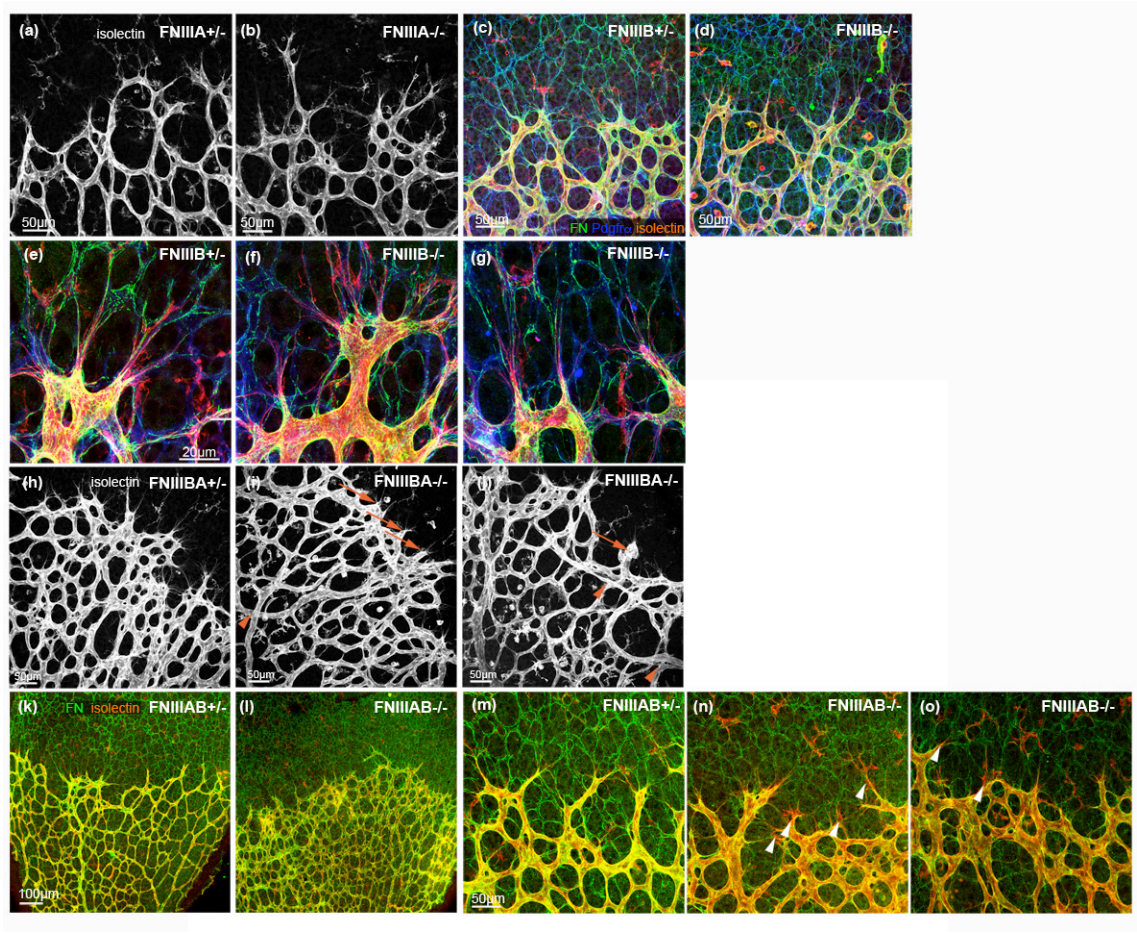

Figure 6.6 Fibronectin assembly and morphological analysis of retinal vasculature in fibronectin splice variants

FN splice variants *FNEIIIA* -/- display no defects in vessel sprouting and the vascular plexus forms normal (a, b). FN assembles in a fibrilliar network (green, c-g) in *FNEIIIB* -/- splice variants and co-localizes with the astrocytic network (blue). High resolution imaging reveals close alignment of filopodia to FN-rich matrix in *FNEIIIB*-/- (f, g) as seen in control *FNEIIIB* +/- (e). In contrast to the single spliced mutants, double splice variants *FNEIIIBA*-/- mice develop blunt ended endothelial tip cells (red arrows, i and h) that result abnormal vessel patterning (arrowheads). Tip cells penetrate into the vitrous body and don't align with the astrocytc matrix leading to vessels that grow over each whereas control vessels are restricted to a 2-dimensional plexus (h). Fibronectin staining (green) in *FNEIIIAB* splice mutants appears reduced in comparison to control *FNEIIIAB*-/- mice (k-o). This reduction might explain the mis-alignment of filopodia frequently observed in *FNEIIIAB*-/- (n, o) illustrated by red filopodia burst at leading tip cells (arrowheads, m-o)

To gain insight whether the reduced migration in retinas lacking astrocytic FN is due to a failure of fibronectin – integrin binding we took advantage of a mouse line bearing a mutation in the RGD binding domain of fibronectin. The RGD-motif is replaced by an inactive RGE motif and thereby inhibits the binding of FN to integrin α5β1 and αvβ3. *FN-RGE* homozygous mice are embryonic lethal and embryos display severe vascular defects resembling the phenotype of alpha 5 integrin (*Itga5*)-deficient mice (Takahashi, Leiss et al. 2007). We crossed FN^{ACko} mice with heterozygous *RGE* mice to obtain FN^{ACko} */FN RGE* mice. These mice are viable as they produce wildtype FN from one floxed allele in all Cre negative cells in addition to FN RGE from the second allele. Retinal astrocytes however loose the wildtype allele upon Cre mediated recombination, thus producing only FN RGE lacking the ITGα5 -binding domain.
We then analysed the retinal vasculature and the migratory length of vessels as well as FN assembly. Co-labelling of astrocytes with PDGFRα and EC with isolectin as well as staining for FN revealed that the FN is reduced ahead of growing blood vessels but the remaining FN has assembled in fibrils (Figure 6.8 a-f). Therefore, we concluded that the astrocytic RGD- binding motif is not required for FN assembly. Takahashi and colleagues have demonstrated similar findings that the absence of a functional RGD motif in FN did not compromise assembly of an FN matrix in mutant embryos or on mutant cells (Takahashi, Leiss et al. 2007).

To study the migration of retinal vessels we measured the distance vessels have reached towards the retinal periphery (g, h). As summarized in graph (i), we could not observe a significant delay in vessel migration of *RGE/ wt* mice compared to control littermates. Still, we found a similar degree of migratory delay in RGE/FN^{ACko} mice as seen previously for $FN^{ACko/\,wt}$. The reduction of 5% in both genotypes obtaining one allele of FN reflected that the delay is independent of the RGE-motif.

Therefore, we propose that RGD-mediated integrin binding of astrocytic FN is not required for retinal vessel migration. However, close examination of endothelial tip cells and alignment of filopodia along the astrocytic network revealed an increased number of mis-aligned filopodia in RGE/FN^{ACko} (a-c) compared to control littermates (arrowheads, d-f). Preliminary quantification identified a significant mis-alignment of filopodia to astrocytic FN containing the inactive RGE in comparison to FN expressing RGD-binding motif, suggesting a role of integrin-FN interaction in filopodia alignment.

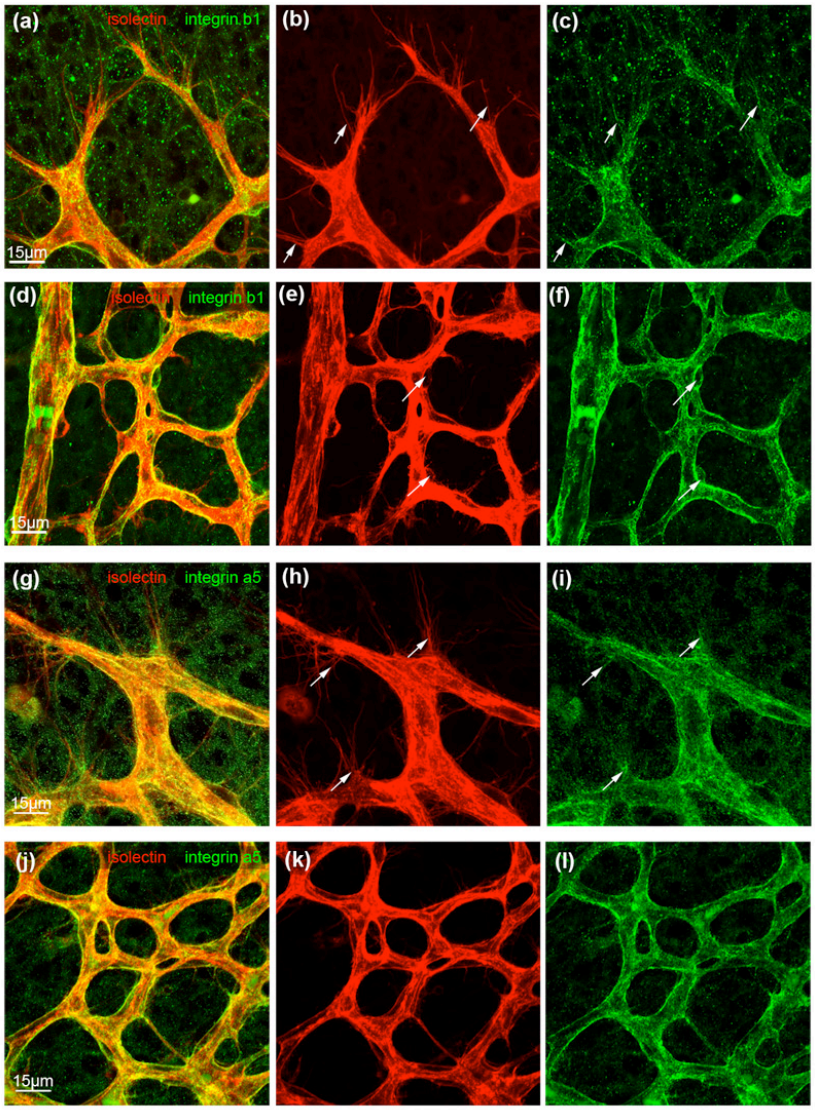

Figure 6.7 Localization of integrin α5 and β1 in retinal vasculature

Staining with integrin β1 (a-f) and integrin α5 (g-l, green) and isolectin (red) revealed co-localization of β1 and α5 integrin at the abluminal basement membrane of blood vessels and spotty localization at filopodia protrusion of endothelial tip cells (arrows, b-c, h-i). In addition, integrin β1 is deposited strongly at pericytes and vascular smooth muscle cells (arrows, e-f) but α5 chain is absent (j-l).

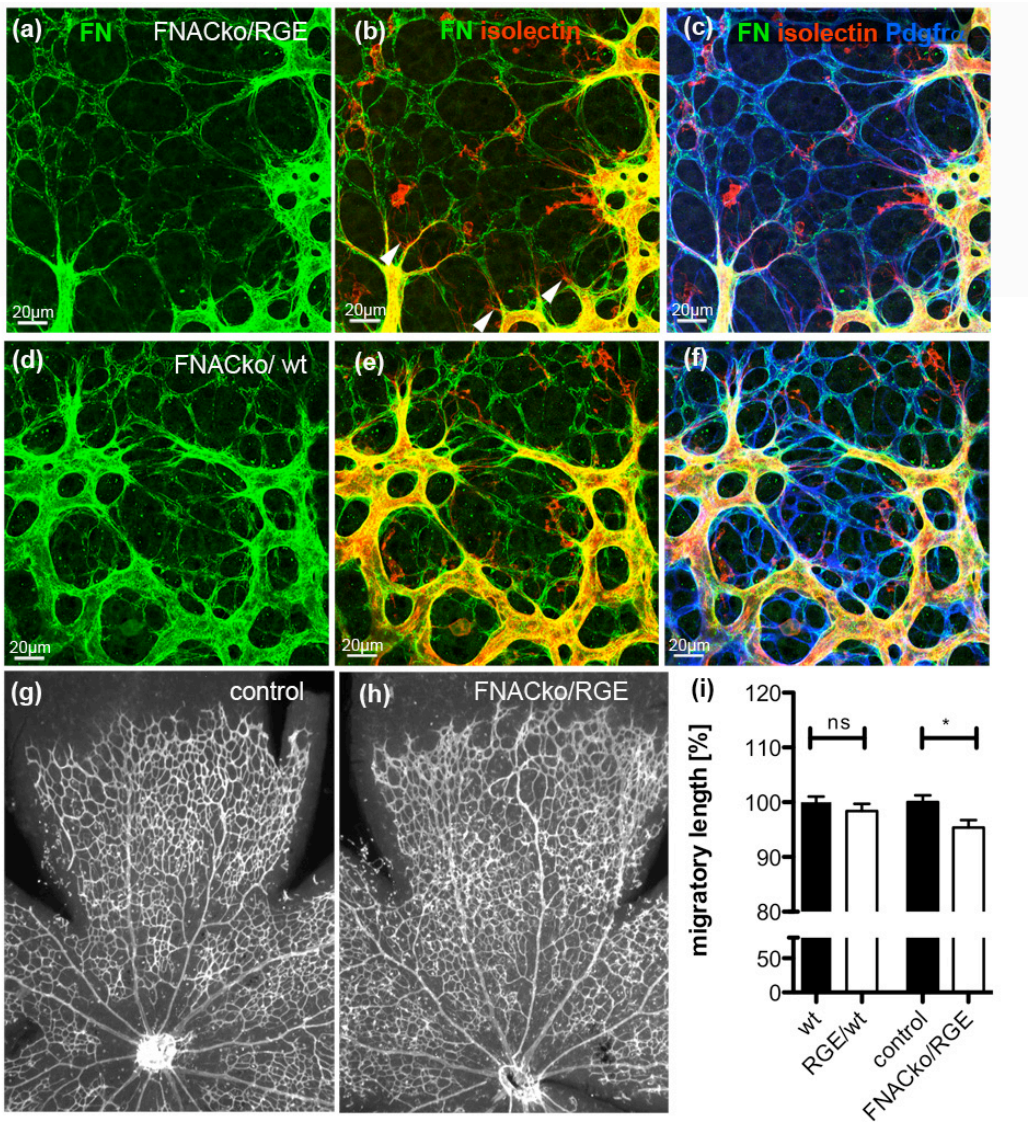

Figure 6.8 RGD-binding of astrocytic FN is dispensable for FN assembly and vessel migration

Mutation of integrin binding domain RGD in an inactive RGE motif in astrocytic FN does not affect FN assembly as shown by FN staining (green) and co-labeling of astrocytes with PDGFRa (blue, a-f). However, close examination of filopodia at leading tip cells displayed occasional mis-alignment of filopodia in mice lacking astrocytic FN RGD (arrowheads, a-c) when compared to control mice (d-f).
Overview images illustrate no defects in vessel morphology and radial expansion of vessels towards the periphery (g, h). Graph i displays vessel migration of RGE/wildtype mice and mice inhabiting inactive RGE motif in astrocytic FN.
Wt and RGE/wt n > 8; Control and FNACko/RGE n=5; *, $p < 0.05$. Values represent mean ± S.E.M.

6.1.4 Reduced migration of retinal vessels in mice deficient for endothelial integrin alpha 5

To investigate the hypothesis that vessel migration is independent of integrin-FN interaction we analysed the retinal vasculature of mice deficient in endothelial integrin alpha5, referred as *Itga5*^{ECko}. The mice have been generated in the laboratory of R. Hynes and retinal material was provided. Conditional excision of floxed *Itga5* exon 1 containing the ATG sequence was achieved in endothelial cells using the Tie2-Cre line. As shown in Fig.1.6 we detected endothelial ITGα5 staining juxtaposed to the abluminal BM of blood vessels.

Analysis of several stages of retinal vessel development, including postnatal day 3, 5 and 7 revealed a significant reduction of migration of *Itga5*^{ECko} compared to control littermates (Figure 6.8, a-c). Overview images of *Itga5*^{ECko} and control littermates (a, b) illustrate the distance vessels have migrated towards the retinal periphery.

When analysing the sprouting vascular front we observed similar defects as seen in *FN EIIIBA* double splice mutants. Blood vessels are not restricted to a two-dimensional network and grow partially over each other and filopodia penetrate into the vitreous body (arrowheads, f-g). However, staining with FN confirms the presence of an intact and complete network of FN fibrils (d-g, green). Therefore, we hypothesize that extended filopodia of *Itga5*^{ECko} do not closely align to the underlying astrocytic plexus and are not in close contact to the astrocytic FN matrix.

This observation would be in line with the finding that retinal vessels exhibit an increased number of mis-aligned filopodia when astrocytic FN lacks the RGD binding motif. And therefore, RGD-FN interaction functions in endothelial adhesion. However, *Itga5*^{ECko} display reduced vessel migration and these data are contradictory to our findings that FN-RGD-binding is not important for vessel migration. A possible explanation could be the finding that FN contains a novel motif for integrin binding and fibril formation whose activity is controlled by amino acid modification (Takahashi, Leiss et al. 2007) that compensates the loss of astrocytic FN RGD binding and therefore, does not affect vessel migration.

Alternatively, the diminished migration *Itga5*^{ECko} could be a result of alpha 5 integrin interaction with additional matrix component provided by astrocytes other than FN.

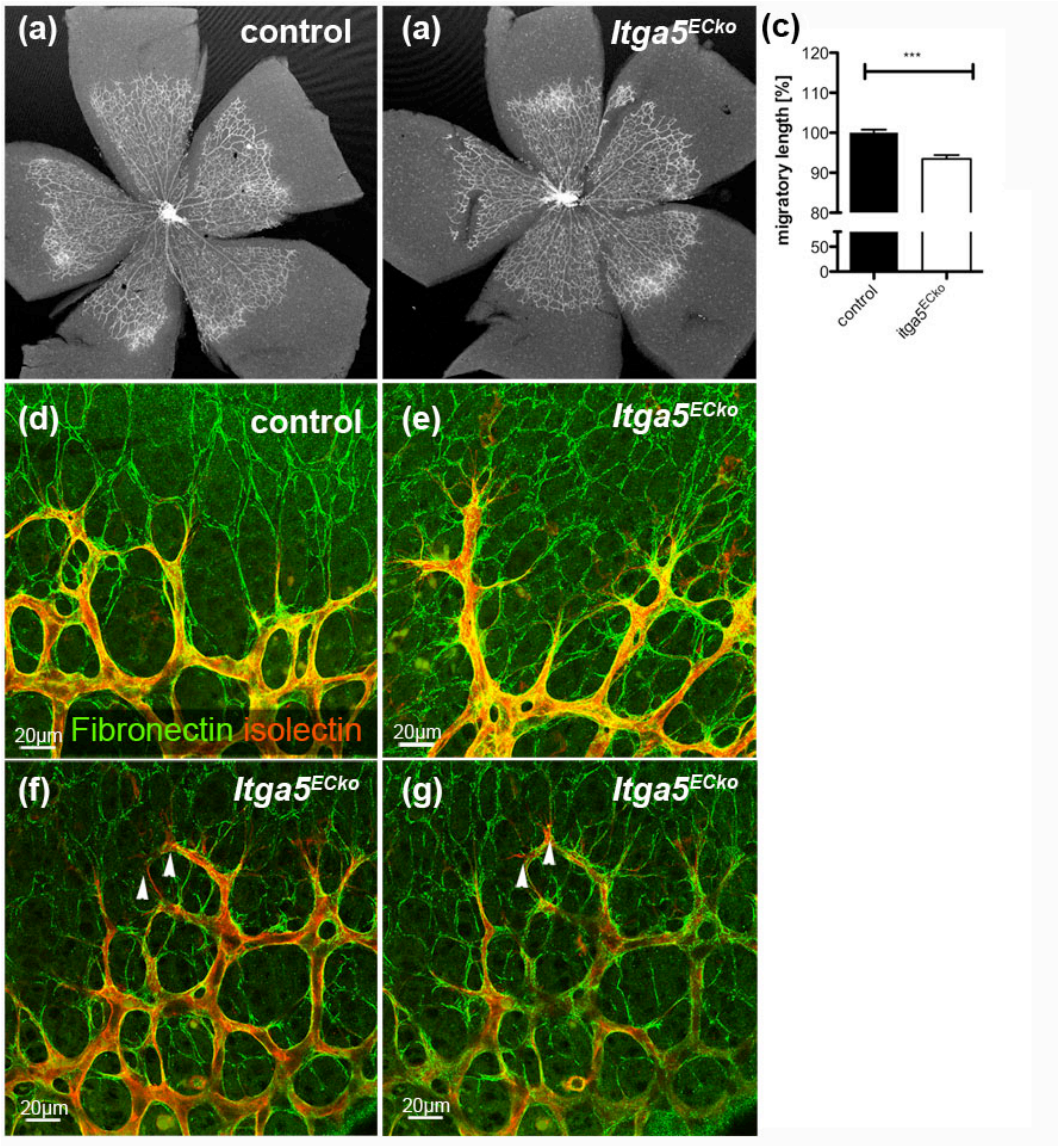

Figure 6.9 Loss of endothelial *integrin a5* expression results in delayed migration and mis-alignment of filopodia to astrocytic FN matrix

Overview images of retinal vasculature illustrate reduced migration of vessels in mice deficient of *integrin a5* (*Itga5*^{ECko} a, b). Graph c summarizes the radial expansion of superficial vessels of mice (P3-P6). Control mice n=10, *Itga5*^{ECko} n=9; ***, $p < 0.0001$. Values represent mean ± S.E.M.
FN staining (green, d-g) revealed that expression and FN assembly is not affected upon loss of endothelial integrin α5, however filopodia of *Itga5*^{ECko} mice fail to align to the astrocytic network and are not restricted to 2D plexus (arrowhead, f, g).

6.1.5 Decreased VEGFR2 signalling and PI3 kinase/ AKT activity in mice deficient for astrocytic Fibronectin

Recent studies reported the extracellular interaction of FN with VEGF and showed that binding of VEGF to the heparin-II domain of FN is necessary and sufficient to promote VEGF-induced endothelial cell proliferation, migration, and ERK activation (Wijelath, Rahman et al. 2006). In addition, mice expressing only the soluble isoform of VEGF ($VEGF_{121}$) missing the heparin-binding domain exhibit vascular defects, including misguidance of filopodia, ectopic filopodia extension (Ruhrberg, Gerhardt et al. 2002) and reduced migration (Gerhardt, Golding et al. 2003). Therefore, it has been suggested that filopodia sense a heparin- and extracellular matrix bound VEGF gradient expressed by astrocytes ahead of the growing vessels. Disruption of a VEGF gradient results in abnormal vessel morphology and patterning defects in the mouse retina.

To address whether the reduced migration in FN^{ACko} is a consequence of decreased VEGF signalling due to incomplete binding of VEGF to FN we analysed VEGFR2 activation by Western Blot. Total protein extracts of P5 retinas were analysed and total amount of VEGFR2 determined. Despite same levels of VEGFR2 protein expression the amount of phosphorylated VEGFR2 was strongly decreased in FN^{ACko} compared to control retinas (Figure 6.10 a), suggesting that FN is essential for a complete VEGF signalling.

Among the downstream effector of VEGF, is the class IA Phosphoinositide 3-kinases (PI3K), which has been recently shown to regulate endothelial cell migration (Graupera, Guillermet-Guibert et al. 2008). Class IA PI3K are heterodimeric lipid kinases consisting of a p110 catalytic subunit complexed to one of several regulatory subunits, collectively called p85. In response to stimulation by growth factors (i.e. VEGF), p110 subunits catalyze the production of phosphatidylinositol-3,4,5-trisphosphate (PIP3) at the membrane. This second messenger in turn activates the serine/threonine kinase AKT and downstream effectors (Vanhaesebroeck and Waterfield 1999). Interestingly, it has been shown that integrins and receptor tyrosine kinases (RTKs) such as VEGFR2 share a number of important signalling molecules, including Src, FAK, and PI3K (Eliceiri 2001).

We therefore assessed whether FN^{ACko} retinas exhibited defects in the PI3K pathway. Total class IA PI3K lipid kinase activity present in p85 immunoprecipitation was reduced by about 50% in FN^{ACko} retinas (Figure 6.10 c), indicating that FN contributes

to a full activation of the class IA PI3K in mouse retinas. In agreement with this, PI3K activity associated with a phospho tyrosine peptide matrix (which binds all p85 species; referred to as pY peptide) was also reduced by approximately 50% in FN^{ACko} retinas (Figure 6.10 c). Immunoprecipitation with p85 and pY to investigate PI3K activity in FN^{ACko} retinas has been carried out by Mariona Graupera.

We next assessed the impact of lack of astrocytic FN production on PI3K signalling. AKT is regulated via its phosphorylation on two highly conserved sites: the activation loop of threonine (Thr-308) in the kinase core and a hydrophobic phosphorylation site on the carboxyl terminus at serine (Ser-473) (Andjelkovic, Alessi et al. 1997).

Using antibodies detecting either AKT- pSer or AKT- pThr we found a reduction in AKT phosphorylation at Ser473 but not at phosphorylation site Thr308 (Figure 6.10 b). This could indicate differential involvement of activating kinases introducing the phosphorylation; while pSer is phosphorylated by mTORC2, pThr becomes activated by PDK-1. The level of total AKT is unaffected in FN^{ACko} compared to control littermates suggesting that the reduction in pSer473 signifies a specific reduction in AKT activity upon loss of astrocytic FN. Taken together, these results suggest that astrocytic FN plays an important role in stimulating endothelial migration by influencing endothelial VEGF-A signalling via the PI3K pathway.

A recent study by Graupera and colleagues highlighted p110α isoform selectivity in angiogenic sprouting and vascular remodelling. Genetic inactivation of p110α revealed a cell-autonomous function in endothelial tip cell migration; VEGF-A induced AKT phosphorylation was almost completely abrogated in ECs lacking p110α and migration speed as well as distance was drastically reduced in mice and primary ECs lacking p110α (Graupera, Guillermet-Guibert et al. 2008). Combined these data suggest that VEGF-A dependent migration requires PI3K activity and astrocytic FN functions in this process.

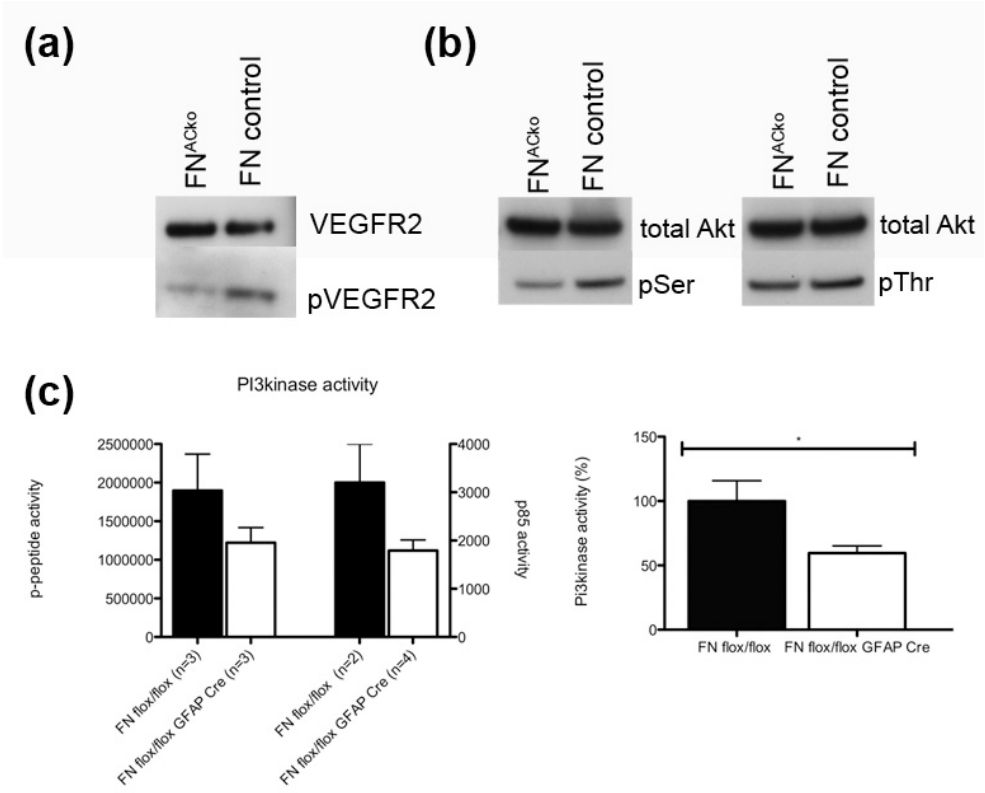

Figure 6.10 Loss of astrocytic FN impairs VEGFR2 mediated migration via PI3K pathway

Phosphorylation of VEGFR2 and VEGFR2 protein levels were examined in retinas of P5 mice lacking astrocytic FN (FN^{ACko}) and control mice by Western Blotting (a). Likewise, phosphorylation of Serine residue 473 (pSer) and Threonine residue 308 (pThr) of AKT were analysed in comparison to total levels of Akt (b). VEGFR2 phosphorylation was reduced by almost 50% and phosphorylation of Serine residue AKT is decreased while total levels of VEGFR2 and AKT are unaffected. Phosphorylation of Threonine is unchanged indicating differences in activating kinases of pSer and pThr.
PI3kinase activity was determined by pull down assays of p-peptides or targeting p85, regulatory subunit of PI3K. Graph c illustrates reduction PI3K activity in mice lacking astrocytic FN. Both approaches are not significantly different when analysed by student t-test, however when data were pooled of both assays by calculating percentage differences, PI3K activity was significantly decreased.
Control retinas for p-peptide n=3, FN^{ACko} n=3; control retinas for p85 pull down assay n=2, FN^{ACko} n=4; *, $p < 0.05$. Values represent mean ± S.E.M.

6.1.6 Inhibition of VEGF binding to FN

Based on the finding that loss of astrocytic FN leads to reduced migration and decreased VEGFR signalling we hypothesized that loss of astrocytic cell surface VEGF-retention to FN could represent the primary defects leading to impaired retinal angiogenesis.

To further investigate into the role of FN-VEGF binding and retention in retinal migration, we injected peptides inhibiting the binding of VEGF to FN ($FnIII_{13-14}$) intraocularly in postnatal C56Bl/6 pups. After 24h treatment eyes were harvested and stained to visualize retinal vessels (red) and FN matrix (green, Figure 6.11). We measured the total migratory length of retinal vessels injected with $FnIII_{13-14}$ peptides, control peptides and uninjected retinas. Graph (a) illustrates the total length of migration in relation to uninjected control eyes (100%) and we observed a 10% reduction in migration when comparing to uninjected and control peptide injected eyes. Firstly, this shows that the injection per se does not affect migration because retinal vessels in eyes injected with control peptides migrate the same distance as uninjected control retinas. Secondly, the 10% reduction in migration is very significant when taking in consideration that the peptides where only injected at postnatal day 4. On average, vessels migrate 200-250µm per day towards the retinal periphery. To estimate the acute effect of 24 hours peptide treatment, we reasoned that retinal vessels will have migrated normally before treatment on day 4 and therefore used the average day 4 level as the baseline to calculated the distance vessels have migrated after injection. This is represented in graph (b) showing that inhibition of FN-VEGF binding by injection of peptide $FnIII_{13-14}$ for 24 h drastically reduced vessel migration by almost 40% while control peptides had no affect.

In addition, overview images of the vascular front illustrate that a plexus has formed in retinas injected with $FnIII_{13-14}$ peptide (c, d). Again, assuming that the morphology and density of vascular plexus has developed the same in all groups before treatment on day 4, we analysed the sprouting front (~200µm) after injection (white dashed line). When study the sprouting vascular front, we observed subtle differences in vessels of retinas injected with $FnIII_{13-14}$ peptides. As shown in Figure 6.11 the vascular density of mice injected with inhibiting peptides (d, f) is rather sparse than seen in uninjected control littermates (c, e) and mice injected with control peptides.

Confocal microscopy revealed that the sprouting vessels are thin and poorly branched, stretching over long distances before making contact to neighbouring vessels in $FnIII_{13-14}$ injected retinas (white arrows, e).

Loss of VEGF binding to FN could affect migration in several ways. First, if FN should provide the major binding and thus retention mechanism of astrocytic VEGF-A, the overall protein distribution, and thus gradient formation of VEGF-A could be disturbed. Interestingly, vascular pattern defects, in particular the combination of reduced migration and branching frequency resemble the phenotype caused by reduced VEGF gradient formation in VEGF120 mice (Ruhrberg, Gerhardt et al. 2002); (Gerhardt, Golding et al. 2003). Secondly, FN binding could play a more local role in promoting a co-receptor function of integrin and VEGFR2 (Wijelath, Rahman et al. 2006). Heparan sulfate could still provide overall VEGF retention and thus gradient formation, but loss of co-receptor function and signalling complex formation between integrin and the VEGFR could severely affect signalling properties, leading to reduced migration. It is unfortunately very difficult to distinguish between the two possibilities as there are currently no good antibodies available to visualize the VEGF gradient in the developing retina.

To verify that VEGF-FN binding influences vessel migration, we analysed VEGFR2 signalling and AKT/PI3K activity in mice treated with $FnIII_{13-14}$ peptides. 15 hours post-injection of blocking peptide $FnIII_{13-14}$ and control peptide in P4 C56Bl/6 mice, eyes were harvested and protein extracted. We determined the total amount of VEGFR2 and found that protein expression levels are unaffected upon treatment with $FnIII_{13-14}$, however phosphorylation of VEGFR2 tends towards a decrease in retinas injected with $FnIII_{13-14}$ inhibiting the binding of VEGF to FN. Densitometric analysis indicated a 40% reduction (Figure 6.12 a, b) which numerically reflects the 40% reduced migration after peptide injection.

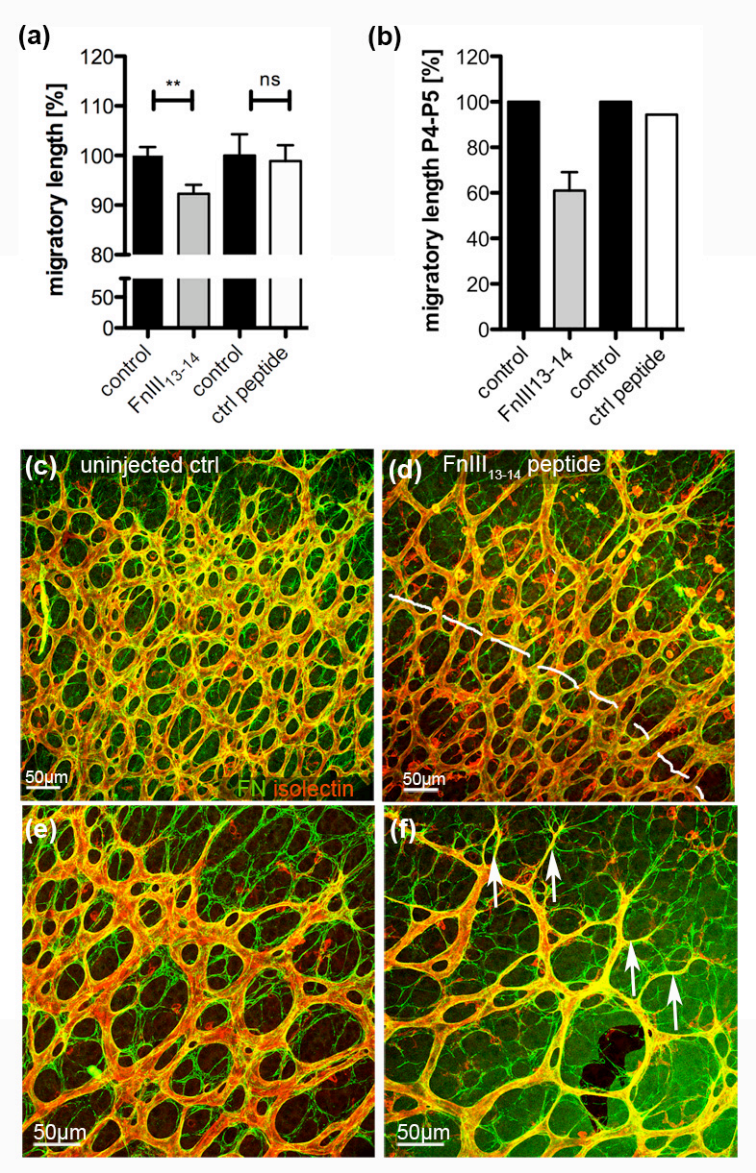

Figure 6.11 Inhibition of VEGF binding to FN leads to reduced vessel migration and affects sprouting of leading tip cells

Graph a illustrates distances vessels have migrated towards retinal periphery at P5 when treated with inhibiting peptide of FN-VEGF binding ($FnIII_{13-14}$) and control peptide for 24 hours compared to uninjected control eyes. By measuring the total length of radial expansion of vessels we determined a significant reduction upon injection of $FnIII_{13-14}$ while control peptides have no effects. When calculating the distance vessels have migrated during the 24h of peptide treatment (b, day P4-P5), we found an almost 40% decrease in vessel migration upon $FnIII_{13-14}$ injection.
Mice injected with $FnIII_{13-14}$ n=3, control peptide injected mice n=2; **, $p < 0.01$.
Values represent mean ± S.E.M.
Injection of peptides does not affect FN assembly as shown by IF staining with FN (green, c-f). Isolectin staining (red) revealed that the vascular plexus developed normally until P4 (dashed line, d) but upon injection of $FnIII_{13-14}$ peptides vascular plexus appears sparse (d) when compared to sprouting front of uninjected retinas (c). In addition, vessels are thin and un-branched (arrows, f) while control vessels connect to form a vascular plexus (e).

However, likely due to limited number of peptide injected retinas the decrease in VEGFR2 phosphorylation is not significant and needs further analyses.

To gain further insight into the underlying mechanism we studied the expression and phosphorylation of downstream signalling molecules AKT. Using an antibody directed against pSer-AKT and total AKT we detected a slight reduction in phosphorylated AKT in mice treated with $FnIII_{13\text{-}14}$ compared to control injected mice (c, d). These preliminary analysis and densitometric analysis revealed a 12% reduction in AKT activity (Figure 6.12 b, d). This numerical difference between VEGFR2 and AKT effects could be explained by a faster turnover and de-phosphorylation of AKT compared to VEGFR2 signalling. Combined these data suggest that inhibition of VEGF-FN binding and therefore, the likely disruption of a matrix bound VEGF gradient accounts for diminished vessel migration in the developing retina.

6.1.7 Delayed migration in FN splice variants and *Itga5^{ECko}* is independent of PI3K/AKT signalling

Finally, we asked whether the delayed migration of retinal vessels in FN splice mutants and *Itga5^{ECko}* is a result of diminished AKT/PI3K signalling. To address this question we examined AKT activity in relation to the total level of AKT. However, we could not detect any differences in phosphorylation levels of AKT (Figure 6.13). Although it has been described that Fn fragments containing both the α5β1 integrin-binding domain and the VEGF-binding domain significantly enhanced VEGF-induced EC migration and proliferation and induced strong phosphorylation of the VEGFR and ERK (Wijelath, Rahman et al. 2006) we cannot detect differences in PI3K signalling in mice lacking endothelial ITGα5.

Structurally, mutations in the extra domain EIIIA and EIIIB do not affect VEGF binding and therefore, we speculate that delayed migration of FN splice variants EIIIA/ EIIIB and double splice mutants is not caused by decreased VEGF binding and VEGFR activity. Since deposition of FN and assembly in a fibrilliar network appeared normal in the mutant retinas analyzed it is likely that the integrin binding site in the extra domain EIIIA is not essential for assembling a FN matrix and binding to integrin α5β1.

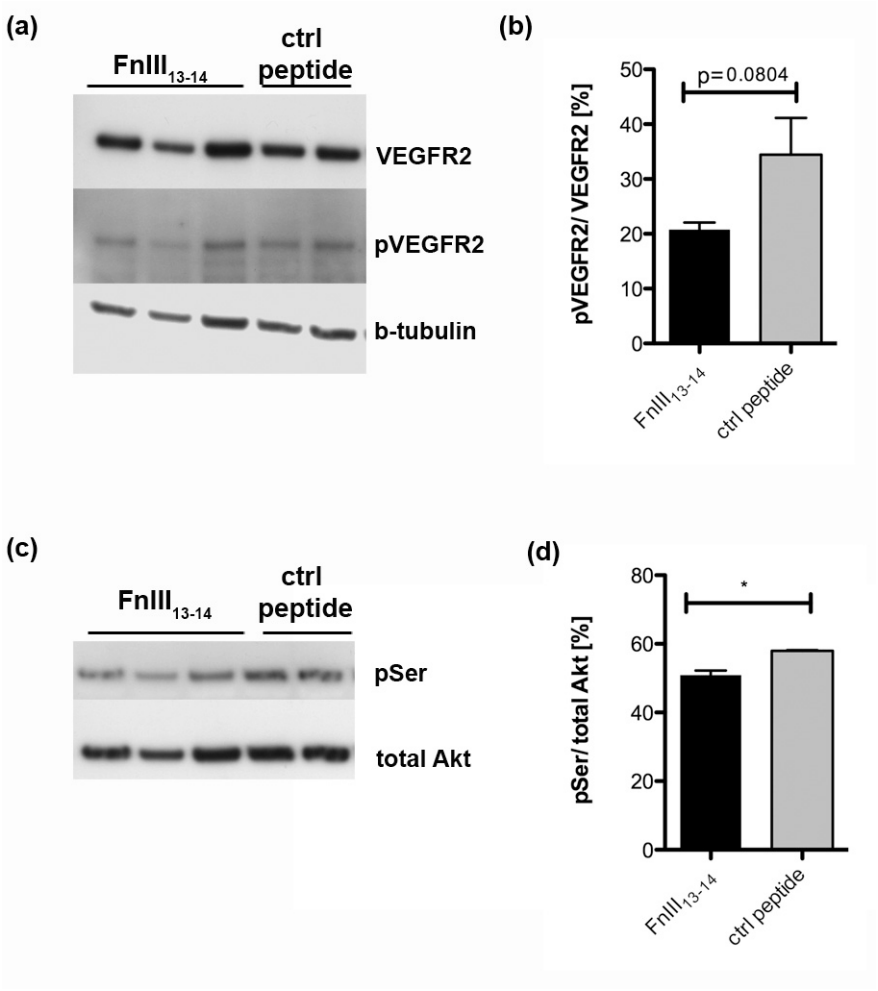

Figure 6.12 VEGFR2 signalling and PI3K activity is disturbed upon inhibition FN-VEGF interaction

Phosphorylation of VEGFR2 and VEGFR2 levels were accessed by total protein extraction and Western Blotting. VEGFR2 signalling upon intraocular injection of peptides inhibiting VEGF binding to FN and control peptides was analyzed 15 hours post injection (a). Densiometric analysis revealed a tendency towards reduced VEGFR2 phosphorylation compared to total VEGFR2 expression levels in $FnIII_{13-14}$ injected retinas (b).
PI3K activity was addressed by determining expression levels of Akt and its phosphorylation (pSer) by Western Blotting (c). Graph d summarizes the percentage of phosphorylated AKT in relation total amounts of AKT. *, $p < 0.05$. Values represent mean ± S.E.M. Mice injected with $FnIII_{13-14}$ n=3, control peptide injected mice n=2;

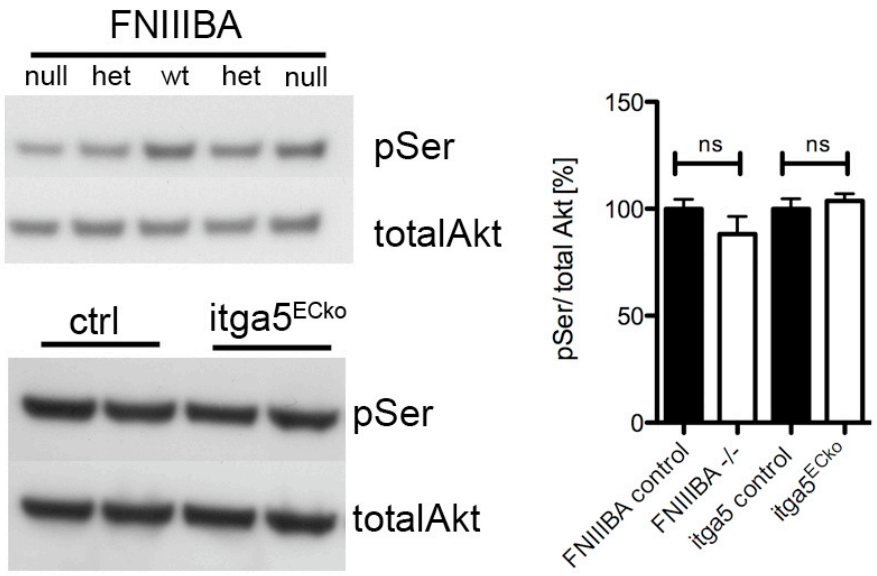

Figure 6.13 Migratory delay of FN splice variants is not caused by diminished PI3K activity

PI3K activity was addressed by analyzing expression levels of Akt and its phosphorylation (pSer) by Western Blotting. Protein was isolated of P5 retinas from FN splice mutants FNEIIIBA and mice deficient in endothelial integrin a5. Blots a and b illustrate the levels of total Akt and phosphorylation detected by pSer-AKT antibody were not significantly different.
Graph summarizes the percentage of phosphorylated AKT in relation total amounts of AKT. Values represent mean ± S.E.M. Litter 95H 1-7 FNEIIIBA wt n=1, FNEIIIBA+/- n=1, FNEIIIBA-/- n=1, *Itga5* control mice n=4, *Itga5*^{ECko} n=5

6.2 Discussion

The present study underlines a function of fibronectin in blood vessel migration by modulating VEGF availability. Directed EC migration and expansion of the retinal vascular plexus requires PI3K activity. Further, the study indicates that adhesion of leading ECs and filopodia protrusion rely on FN-integrin interaction.

6.2.1 Integrin-binding is dispensable for FN assembly and migration

In the retinal vasculature, astrocyte precursors enter the retina through the optic nerve and radiate towards the periphery. Blood vessels subsequently follow along the pre-existing astrocytic meshwork, therefore the astrocyte provide attractive cues and initiate vascularization. Hypoxia-induced expression and secretion of VEGF-A is mediated by astrocytes (Stone, Itin et al. 1995). The preceding newly formed vessels express high levels of VEGFR2, indicating that the secreted VEGF acts on the vessels in a paracrine fashion. Astrocytes further provide a provisional matrix that function as a preset track instructing retinal blood vessel growth. Extended filopodia at the leading endothelial tip cell closely align to the astrocytic network, suggesting controlled astrocytic-endothelial cell interaction. Already in 1994, Jiang and colleagues demonstrated FN expression by retinal astrocytes in the rat retina. Here we show that FN is deposited and assembled in a fibriliar network ahead of the growing vasculature. Counterstaining with an astrocytic marker revealed strong expression of immature astrocytes ahead of the growing vessels and reduced astrocytic FN deposition in BM of mature astrocytes in contact with the capillary vasculature. Loss of astrocytic FN results in delayed migration towards the retinal periphery.

The Cre-mediated recombination of astrocytic FN is not 100% efficient, and we observe most prominent vascular defects in areas deficient of FN, indicating that migrational delay and increased vascular density are indeed caused by loss of FN. During normal retinal development, we often observe extravasation of erythrocytes just behind the sprouting front of the growing vessels. This leakage possibly could result in the release of plasma fibronectin (pFN) at the growing vasculature. A recent study demonstrated that a major fraction of the cellular FN-matrix is plasma-derived and therefore, pFN is incorporated in the cellular FN fibrils (Moretti, Chauhan et al. 2007). Combined the variation in Cre-recombination between FN floxed littermates and the plasma leakage due to extravasation in the tissue might contribute to the FN matrix and may prevent

more severe vascular defects. Still, we observe a significant reduction in retinal vessel spreading radially towards the periphery when astrocytes are deficient in FN production. The migratory speed is independent of integrin-binding domain, RGD. Mice bearing an inactive RGE motif are embryonic lethal and display vascular defects reminiscent of mice lacking *integrin alpha 5*. However, FN-RGE mice are capable of assembling FN in fibrils (Takahashi, Leiss et al. 2007). We show that mice lacking astrocytic RGD-binding motif assemble FN and retinal vessels migrate a comparable distance to control mice. Therefore, integrin binding to FN-RGD is dispensable for vessel migration. In contrast, mice lacking endothelial ITGα5 display reduced expansion of retinal vessels to the periphery. Integrin a5β1 and all integrins of the αv family bind and interact with RGD domain of FN. One would hypothesize that endothelial ITGα5 adheres and binds to the astrocytic FN matrix via RGD and thereby mediate cell migration. However, our results indicate that ITGα5 is required for normal vessel migration but might interact with different binding motifs of FN. A recent study by Takahashi and colleagues discovered a new integrin-binding site in the N-terminus of FN. This finding could explain the migrational delays in endothelial specific *Itga5* mice. Further loss of endothelial ITGα5 does not affect FN assembly, likely because the remaining FN binding integrins, predominantly integrin αv compensates for the loss and assemble FN in fibrils (Yang, Rayburn et al. 1993).

Our findings also revealed that extra domain EIIIA or EIIIB individually are not required for FN assembly. Analyses of the retinal vasculature of alternatively spliced isoform lacking EIIIA did not exhibit vascular defects. Similar results have been described by Astrof et al., indicating that fibronectin domains EIIIA or EIIIB are dispensable for vascular development. However, mice lacking alternatively spliced domain *EIIIB* showed a reduction by 20% in retinal vessel migration suggestive that this particular domain plays a role in vessel migration. Detailed expression studies of the FN splice isoforms in the retina might help shedding light in the distinct function.

Mutants for both alternatively spliced domain are embryonic lethal and therefore, do not allow us to study their function in retinal angiogenesis. However, double mutants null for either domain *EIIIA* and heterozygous for *EIIIB* (*FNIIIAB*) or null for *EIIIB* and heterozygous for *EIIIA* (*FNIIIBA*) display a delay in expansion of vessels toward the retinal periphery. Further, theses splice mutants exhibit an abnormal vascular morphology at the sprouting front. Leading endothelial tip cells appear blunted and fail to align to the astrocytic networking resulting in patterning defects. Multiple cell-

binding sites are present in alternatively spliced regions, e.g. domain EIIIA contains sequences that are recognized by integrin α4β1, α4β7 and α9β1 (reviewed in (White, Baralle et al. 2008). These cell-binding properties might play a role in EC adhesion and migration of retinal vessels resulting in migrational delay and patterning defects observed.

Astrocyte-endothelial cell interactions are crucial for normal retinal vascular development. Disruption of these interactions by blocking R-cadherin, an adhesion molecule known to be involved in neuronal cell guidance, resulted in stunted retinal vasculature, which fails to recapitulate the astrocytic pattern and migrates into the normally avascular outer retina (Dorrell, Aguilar et al. 2002). When analyzing mice mutants for endothelial *Itga5* and FN double mutants *EIIIAB* and *EIIIBA* we occasionally observed filopodia that fail to align with the astrocytic network and penetrated into the vitreous body, indicating a loss of adhesion and possibly filopodia polarity. Defects in endothelial adhesion to the retinal astrocytes by integrin-Fibronectin interaction may account for the delayed migration as seen in $Itga5^{ECko}$ and several FN splice mutants.

6.2.2 Endothelial –Astrocyte interaction are crucial for vascular patterning

Normal growth and differentiation of retinal astrocytes provides essential cues for the retinal vascularization. Loss of PDGF-A results in a sparser astrocytic network, while expression of astrocytic PDGF-A leads to super-numerous astrocytes intertwining into a dense network of radially orientated bundles (Gerhardt, Golding et al. 2003).

Alteration of the astrocytic network is directly reflected in hypo- and hyperplasia of the retinal vascular patterning, emphasizing the close relationship of astrocytes and endothelial cells.

These fundamental cellular interactions of endothelial cells and astrocytes have been studied extensively in the brain, highlighting a functional complex between astrocytes and ECs. The blood-brain-barrier (BBB) constitutes of capillary endothelial cells, surrounded by pericytes and a basal lamina, as well as astrocytic perivascular endfeet. The specialized foot-processes of perivascular astrocytes are closely apposed to the outer surface of brain microvessels, and have specialized functions in inducing and regulating the BBB (Abbott, Ronnback et al. 2006). This close cell-cell association, the localization of ECM in the astrocytic endfeet and the induction/ regulation of growth factors by astrocytes highlight the importance of astrocytes in the development of

microvessels in the CNS, very similar to the cellular composition in the retinal vasculature. The deletion of integrin αv highlighted the complex interaction and essential function of astrocytes during vessel development. Loss of integrin αv results in intracerebral hemorrhages due to the absence of αvβ8 integrin from astrocytic endfeet. This absence interfered with apposition of the glia with the invading vessels and led to vessel dilation and eventual rapture (McCarty, Monahan-Earley et al. 2002).

6.2.3 Fibronectin modulates VEGF-A availability and thereby receptor activity and signalling

Our study further indicates that astrocytic fibronectin may not only mediate EC adhesion but also functions in growth factor retention and presentation and thereby influences endothelial migration. Blocking the binding of VEGF to the heparin II binding domain in FN by intraocular injection resulted in reduced migration of retinal vessels. Disruption of VEGF-FN binding is accompanied by reduced VEGFR2 signalling and PI3K activity. We hypothesize that VEGF, synthesized and secreted by astrocytes, binds to astrocytic FN and that this interaction is required for VEGF presentation to the leading tip cells that migrate towards the VEGF gradient. VEGF/VEGFR2 signalling mediates endothelial cell function via intracellular autophosphorylation of VEGFR2 and subsequent activation of signalling pathways such as PI3kinase and MAPK. PI3K activity is required for VEGF-A dependent migration of ECs (Gille, Kowalski et al. 2001). Graupera and colleagues further identified the catalytic subunit p110α to function selectively in EC migration. Endothelial specific and ubiquitous ablation of p110α resulted in embryonic lethality due to severe defects in angiogenic sprouting and vascular remodelling (Graupera, Guillermet-Guibert et al. 2008). Replacement of one allele of p110α with a kinase dead-allele resulted in a significant delay in the outgrowth of the primary vascular plexus towards the retinal periphery, indicating reduced migration of endothelial tip cells similar to seen in mice lacking astrocytic FN. In addition, p110α knockout ECs *in vitro* showed 30% reduction in migratory speed and total distance migrated as a consequence of reduced AKT phosphorylation (Graupera, Guillermet-Guibert et al. 2008). The reduction in PI3K activity analysed by pY peptide is 50 % in the heterozygous p110α, similar to mice lacking astrocytic FN.

Our data demonstrate that loss of astrocytic FN results in reduced VEGFR2 phosphorylation and PI3K activity, indicated by reduced phosphorylation levels of AKT

and pull down assays using pY-peptides and p85. Diminished VEGF/VEGFR2 signalling in the absence of astrocytic FN may be explained by reduced VEGF-FN interaction and therefore delayed migration. These findings may suggest that PI3K quantitatively regulates migration and the observed reduction in PI3K activity is sufficient to explain the reduced migration in mice deficient of astrocytic FN.

This hypothesis is further supported by studies of Wijelath and colleagues showing that VEGF binds to the heparin-II domain of FN and that the cell-binding and VEGF-binding domains of FN, when physically linked, are necessary and sufficient to promote VEGF-induced endothelial cell function (Wijelath, Rahman et al. 2006). Mitsi and colleagues identified two classes of VEGF binding sites on fibronectin. One was constitutively available whereas the availability of the other was modulated by the conformational state of fibronectin (Mitsi, Hong et al. 2006). Combined phenotypical analyses and biochemical studies revealed delayed migration of retinal vessels and reduced VEGFR2 and PI3K activity upon blocking VEGF-binding to FN and ablation of astrocytic FN. We further hypothesize that retention of VEGF to FN is important for normal retinal patterning. We observed increased filopodia extension, dilated vessels and an increase in vascular density predominantly at the sprouting vascular front, in the absence of astrocytic FN. These vascular defects are reminiscent of the morphology of vessels in mice expressing solely the diffusible VEGF isoform, VEGF120. $VEGF^{120/120}$ mice lack cell surface and ECM-bound VEGF isoform resulting in alter extracellular distribution of VEGF-A. Loss of a VEGF gradient led to impaired directed extension of tip cell filopodia and reduced branch formation. Instead of being recruited into additional branches, nascent endothelial cells were preferentially integrated within existing vessels to increase lumen caliber, resulting in dilated vessels (Ruhrberg, Gerhardt et al. 2002). Therefore, increased vessel diameter is not necessarily a result of increased EC proliferation, but can also result from ECs failing to form new branches.

Mouse mutants only expressing VEGF120 lacked a distinctive astrocytic association of extracellular VEGF; instead VEGF120 is distributed more diffusely in the retina resulting in loss of filopodia polarity and reduced cell migration (Gerhardt, Golding et al. 2003).

It is not clear whether $VEGF^{120/120}$ mice also express altered VEGFR2 and PI3K levels that could account for the reduced migratory phenotype. Ruhrberg and colleagues showed that the increased vessel diameter in $VEGF^{120/120}$ mice is independent of EC proliferation but due to reduced migration and additional integration of ECs in existing vessels. It still needs to be addressed whether this is the case for the dilation observed in

retinal vessels of mice lacking astrocytic FN. Reduced migration could be a result of misalignment, reduced adhesion and the failure of filopodia to extend and stretch along the astrocytic network when lacking FN. Alternatively, the increased caliber could be caused by increased or more widespread EC proliferation. Loss of VEGF retention could cause both reduced migration and more widespread proliferation due to VEGF diffusion.

Dayanir et al. demonstrated that activation of VEGFR2 results in activation of PI3K and that activation of PI3K/S6kinase pathway, but not Ras/MAPK, is responsible for VEGFR2-mediated cell growth (Dayanir, Meyer et al. 2001).

Wijelath and colleagues highlighted a mechanism in which FN induced enhancement of VEGF activity arises from both the formation of an extracellular complex interacting with the cell surface receptors (integrin) and the resulting promotion of co-stimulatory signalling from integrin and VEGF receptor. FN fragments containing both the $\alpha 5\beta 1$ integrin-binding domain and the VEGF-binding domain significantly enhanced VEGF-induced EC migration and proliferation and induced strong VEGFR2 and ERK phosphorylation (Wijelath, Rahman et al. 2006).

The findings indicate that loss of astrocytic FN and loss of VEGF-FN interaction may negatively effect EC proliferation. Analyzing EC proliferation by incorporation of BrdU as well as studying MAPK and ERK activity will allow to address EC proliferation and to elucidate the cause of increased vessel caliber in mice lacking astrocytic FN.

6.2.4 Future perspectives

The data presented in this chapter indicate that the loss of astrocytic FN results in decreased VEGFR2 signalling. Although VEGF receptors are expressed ubiquitously in endothelial cells, recent data highlighted that expression levels and signalling properties vary quantitatively between endothelial cell populations. Their expression levels and activity is influenced by a) co-receptors such as HSPG and neuropilins (Ruhrberg, Gerhardt et al. 2002), b) Dll4/ Notch signalling (Siekmann and Lawson 2007) and c) other VEGF receptors, such as soluble VEGFR1 splice variant negatively modulates VEGFR2 activity by binding VEGF-A (Roberts, Kearney et al. 2004).

Further, activation of VEGFR2 is negatively regulated by the phosphotyrosine phosphotase Src-homology phosphatase-1 (SHP1) and SHP2, as well as the rapid internalization and degradation of VEGFR2 by lysosomes or alternatively by the proteosomal pathway (reviewed in (Olsson, Dimberg et al. 2006).

We propose that VEGF availability and possibly presentation to migrating endothelial tip cells is impaired in mice lacking astrocytic FN. Therefore, it would be interesting to visualize the spatial expression pattern of VEGF-A protein in the presence and absence of FN.

As a consequence of disturbed VEGF/ VEGFR2 interaction, VEGFR2 activity and downstream effector PI3K are reduced and thereby affecting vessel migration. Likewise to visualizing VEGF-A, it would be interesting to visualize VEGF/VEGFR2 complex formation at leading endothelial tip cells. Since both FN and VEGF-A bind and interact with HSPGs, and HSPGs modulate VEGFR2 activity one could would like to investigate the role of HS in this FN/ VEGF interaction.
Unpublished data in our lab indicate that the loss of astrocytic HS production leads to delayed migration of retinal vessels similarly to the loss of astrocytic FN.

Activation of VEGFR2 triggers multiple cell behaviours, such as migration, proliferation and EC survival. We observed an increase in vessel calibre that could be a result of enhanced endothelial cell proliferation. EC proliferation and EC survival requires VEGFR2 activation via MAPK/ ERK pathway (Cho, Lee et al. 2004); (Takahashi, Yamaguchi et al. 2001). Therefore, it would be of interest to study EC proliferation by incooperation of BrdU and by analysing phosphorylation of ERK protein as mentioned in 1.2.3.

Interestingly, loss of endothelial ITGα5 also results in reduced vessel migration. Integrin α5β1 is the major binding and interaction partner for Fibronectin; binding is mediated by the FN RGD motif. However, RGD-binding is dispensable for retinal vessel migration, suggesting an additional binding domain for ITGα5. Alternatively, ITGβ1 has been shown to interact with notch, promoting Notch sequestering and trafficking to the nucleus. Loss of endothelial ITGα5 might affect integrin/ Notch interaction and thereby modulating the cellular outcome. It would of interest to investigate Dll4/ Notch mRNA expression in mice deficient of endothelial *itga5* and to determine protein localization of Dll4, Notch and integrin α5β1 at the cell membrane.

6.2.5 Summary

In summary, our findings indicate that Fibronectin expressed by astrocytes positively stimulate endothelial cell migration *in vivo*. This function is mediated through a coordinated and synergist mechanism of VEGF-binding and presenting to leading endothelial tip cells and adhesion of ECs to the FN-rich astrocytic matrix by integrins (Figure 6.14).

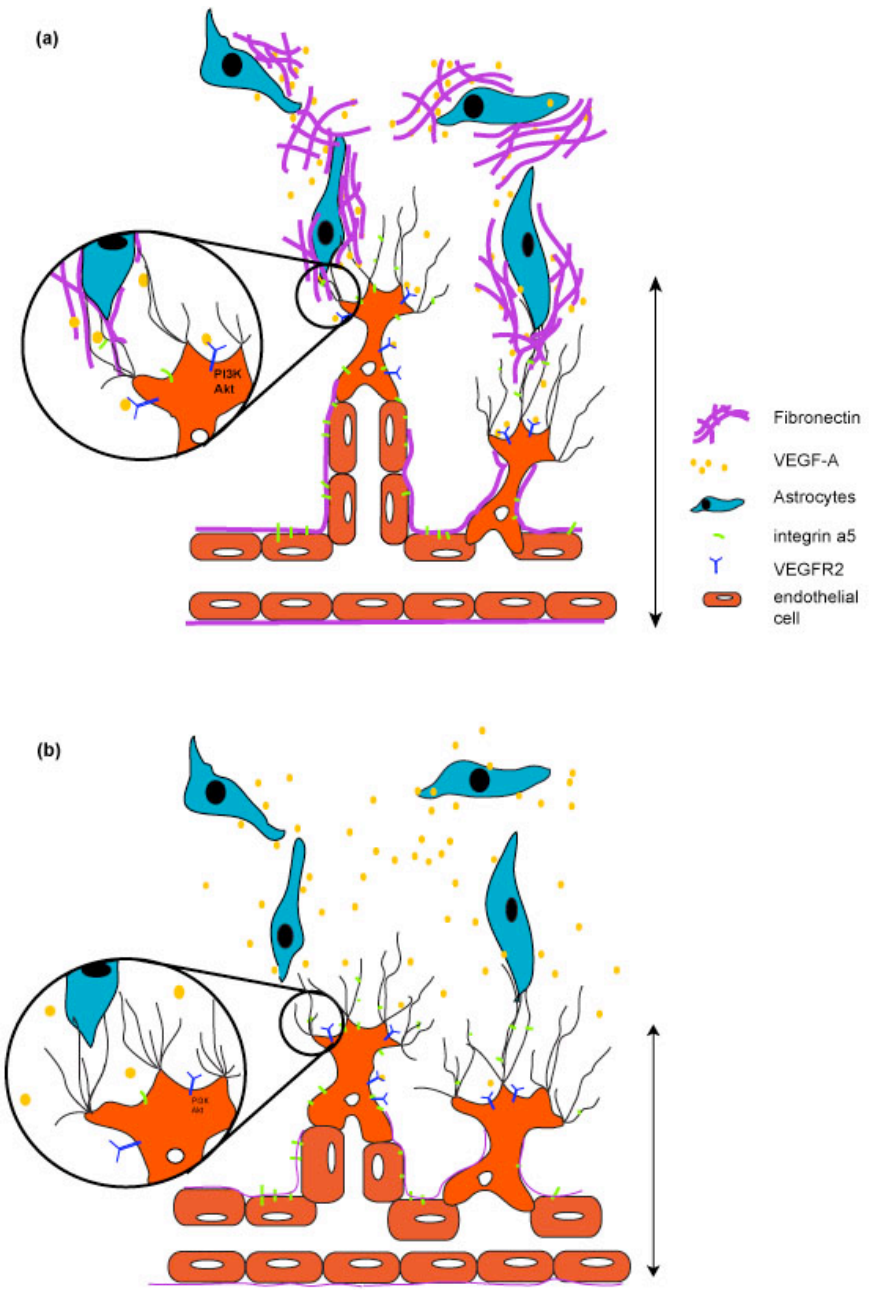

Figure 6.14 Proposed model of astrocytic VEGF-FN interaction regulating vessel migration

(a) FN is expressed by astrocytes ahead of the growing vasculature and assembled in a fibrilliar network providing instructive cues for vessel migration. Astrocytes produce and secrete VEGF-A in the extracellular milieu and are retained by the FN matrix. Endothelial tip cell filopodia express integrin receptors that guide filopodia alignment along the astrocytes and mediate adhesion to the FN matrix. VEGF-A binds to VEGFR2 expressed on leading EC, thereby triggering VEGF receptor signalling in tip cells and downstream effectors PI3K.
(b) Loss of astrocytic FN results in diffused VEGF-A gradient, reduced VEGF/ VEGFR2 signalling and decreased PI3K activity. As a consequence, migration of the vascular plexus is delayed. Endothelial tip cells extend increased number of filopodia and vessels appear dilated due to a still unknown mechanism, but possibly a result of ECs failing to spread and/ or increased proliferation.

7 Laminin α4 regulates angiogenic sprouting by modulating Dll4/Notch signalling

7.1 Results

7.1.1 Basement membrane formation in retinal angiogenic sprouts

In order to form a complex vascular network cells need attachment, migration and proliferation. Attachment of cells is mediated either directly by cell-cell contacts or indirectly via a network of extracellular matrix (ECM) components. Epithelia and endothelia organize ECM components at their basal or ablumenal side into a dense structure visible in electronmicrographs. This morphological appearance has led to the term basement membrane (BM). The endothelial BM consists of a tight meshwork of collagens, laminins, heparan sulfate proteoglycans (HSPG) and fibronectin. Little is known of the spatial and temporal expression pattern of the individual matrix components during vascular development, in particular during the initial sprouting process. We also still lack information on the maturation of the BM around the growing vascular sprout. Therefore, one important aim of my studies was to characterize composition, deposition and function of matrix molecules in retinal blood vessel sprouts.

We utilized transmission electron microscopy (TEM) to investigate whether the tip-cell and its leading filopodia, as well as the first stalk cells, show signs of beginning BM formation. After dissection of the retinal vascular front and identification of endothelial tip cells using reflective light microscopy semi-thin sectioning of retinal samples was performed. Figure 7.1a shows a cross-section of the mouse retina and illustrates the close interaction of retinal blood vessels with the underlying astrocytes, nerve fibers and ganglion cells. Retinal blood vessels are located at the inner most layer of the retina and to reach the vascular plexus *en face* sections through the underlying layers were made until we reached the area shown in (b). Characteristically, the endothelial tip cell extends fine filopodia that align tightly to the astrocytic network. Astrocytes (A) are numerous ahead of the vascular sprout, recognized by dark purple triangular nuclei. Once the correct region was identified, ultra-thin sectioning was performed. Confocal microscopy of angiogenic tip cells visualized by isolectin (c) showed the same morphology as seen in TEM. To illustrate the leading EC we highlight the cell in brown (Figure 7.1 d), asterisk point out filopodia protrusion and a lumen (L)

begins to form. Mitochondria (m) accumulate and locate close to the lumen in endothelial tip cells (d). Further magnification showed the close interaction of filopodia with surrounding astrocytes (e) and patchy matrix deposition as well as early BM formation could be detected (arrowheads, f-g). Figure g illustrates that endothelial tip cells of a vascular sprout deposit extracellular matrix in the extracellular space and form a BM (arrowheads).

Therefore, we conclude that first continuous BM formation can be seen along the cell body of the tip cell, while only patchy and discontinuous BM is found along filopodia extension. These findings are consistent with the current literature; It is generally believed that during vascular remodelling and sprouting, the quiescent EC layer becomes activated, EC breach the BM and migrate in the surrounding tissue (reviewed in (Hynes 2007)). In contrast, mature and non-proliverative vessels are surrounded by a complex meshwork, seen as continuous BM.

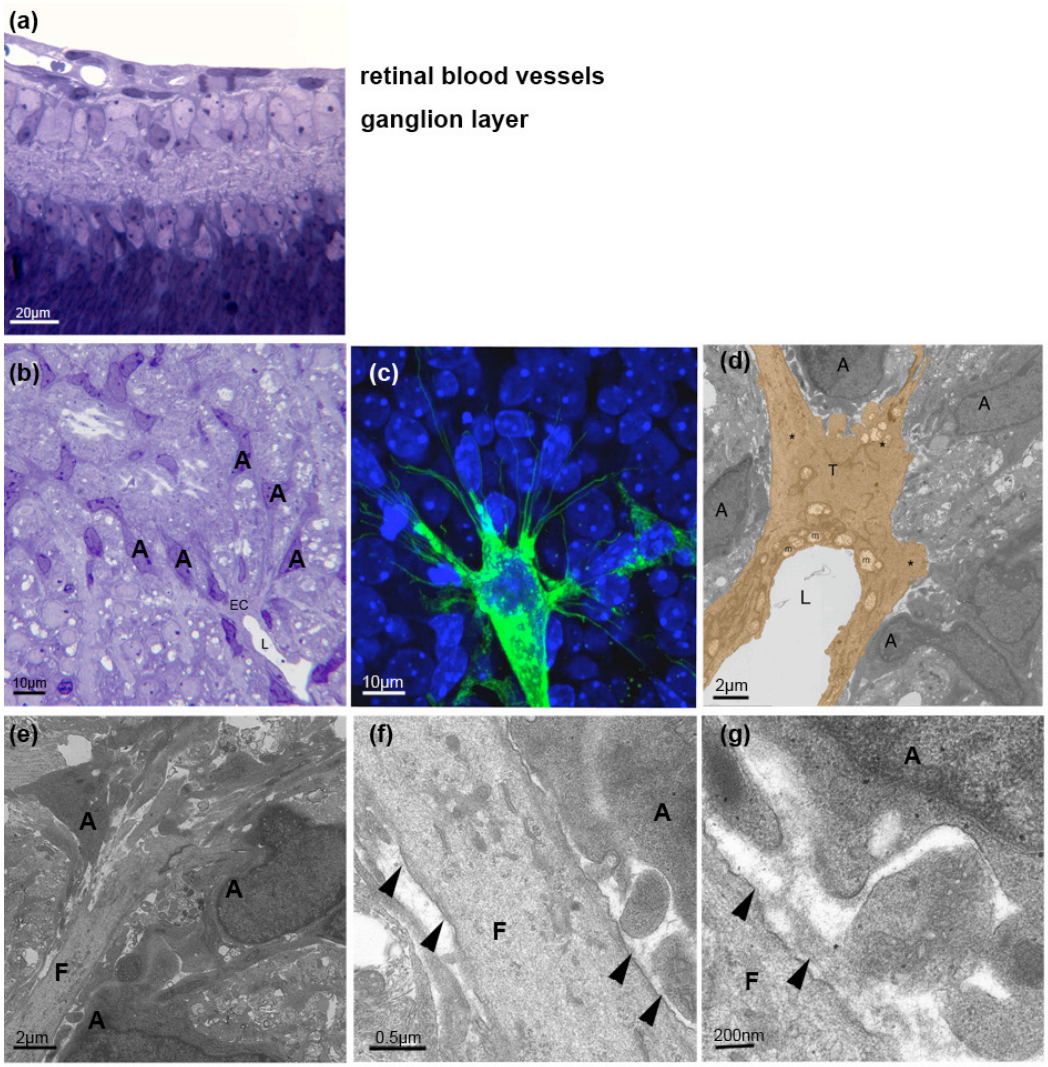

Figure 7.1 Basement membrane formation at sprouting endothelial tip cell

Semi-thin sagitall sections were prepared to identify region of interest (a) showing that superficial vessels of retina are localized at the outer most layer. By cutting *en face* through the various retinal layers, including ganglion layer astrocytic network and lumenized vessels were identified (b). Continuous ultra-thin sectioning of that area isolated endothelial tip cell (brown, d) with filopodia aligning to astrocytes ahead of the growing vasculature. The morphology of tip cells detected by electron microscopy resembled the sprouting tip cells seen by isolectin staining (green) by immunofluorescence microscopy (c). High magnification imaging revealed filopodia extension close to astrocytes (e) and patchy, discontinuous basement membrane formation along endothelial cell filopodia protrusion (arrowheads, f-g).
A= astrocytes, EC= endothelilal cell, L= lumen, F= filopodia, T= tip cell, m= mitochondria, *= filopodia protrusion

7.1.2 Laminin α4 and α5 expression and localization *in vivo* and *in vitro*

The expression of ECM components differs to some degree among vessels but certainly differ depending on the state of the vessel, e.g. migrating vessel vs. quiescent vessel. We therefore aimed to address the specific expression and deposition of ECM molecule laminin during guided angiogenic sprouting in the retina.

Laminin (LN) is a heterotrimeric cross-shaped glycoprotein and a major component of BMs. Composed of an alpha-, a beta- and a gamma chain, laminins can combine to form up to 15 different isoforms. The vascular BM is dominated by laminin chains alpha 4 and alpha 5, which assemble with the beta 1 and gamma 1 chains into Laminin 411 and Laminin 511, respectively.

Laminin 411 (LN411) expression is thought to be ubiquitous by all endothelial cells regardless of their stage of development, from early embryonic development, E8.5 till adulthood (Iivanainen, Kortesmaa et al. 1997). In contrast, Laminin 511 (LN511) expression is more restricted, commencing later in development during vessel maturation. LN511 is detectable primarily in BMs of capillaries and some venules commencing 3–4 weeks after birth (Hallmann, Horn et al. 2005).

Studying the expression of laminin alpha 4 (*Lama4*) by *in situ* hybridization in the postnatal retinal vasculature we unexpectedly found that *Lama4* expression is restricted to the vascular front (Figure 7.2 a, overview). More over, *Lama4* is specifically expressed by leading tip-cells. Co-labeling with markers detecting either endothelial cells (green) or astrocytes (red) revealed that *Lama4* expression is restricted to retinal ECs (Figure 7.2 b-d).

In marked contrast, laminin alpha 5 (*Lama5*) expression is not restricted to endothelial cells in the retina. Overview images (e) show a network-like expression of *Lama5*. The pattern strongly resembles the retinal vascular plexus, however combined staining with isolectin and GFAP revealed an astrocyic expression of *Lama5*. High magnification images of the sprouting tip region (f-g) as well as the mature plexus (h-i) illustrate expression that does not co-localize with endothelial marker isolectin (arrow) but instead overlap with the astrocyte marker GFAP. We also observed laminin α5 deposition ahead of the vascular plexus confirming non-endothelial, astrocyte-specific expression.

This study revealed a distinctive expression pattern for *Lama4* and *a5* in the retinal vasculature. While *Lama4* expression is restricted to leading endothelial tip cells, *Lama5* is mainly deposited by the astrocytes.

To analyse the localization of laminin protein along the vascular sprout we used antibodies detecting either the laminin α4 or laminin α5 chain.

Despite the tip-cell specific expression of *Lama4* mRNA, laminin α4 protein is distributed along the abluminal basement membrane of all retinal vessels (red, Figure 7.3 b, e). This discrepancy between the restricted mRNA expression and widespread protein distribution suggests that the laminin α4 chain when assembled into mature laminin 411 heterotrimeric protein is stably integrated in the ablumenal endothelial BM.

High magnification imaging revealed that laminin α4 is not located at extending tip cell filopodia and only weakly assembled along nascent sprouts despite the strong tip cell mRNA expression (white arrowheads, Figure 7.3 c-e). Intriguingly, laminin α4 protein is distributed not only at the ablumenal (basal) endothelial membrane consistent with BM formation, but additionally co-localizes with endothelial junctions. Staining with VE-cadherin, the primary endothelial cadherin expressed at endothelial adherent junctions and co-labeling with laminin α4 confirmed co-localization of laminin α4 at junctions in retinal vessel (yellow arrow, f-k). However, not all interendothelial junctions show laminin α4 localization (white arrow). A functional role of a BM component at junctions has to our knowledge not been described.

Interestingly, IF staining with laminin α5 revealed a strong expression of laminin α5 on the immature astrocytic network ahead of the growing vasculature (l). The astrocytic expression occurs transiently, once vessels have grown over the laminin α5 rich matrix laminin α5 is visibly reduced in the mature astrocytic plexus (arrow, l). In the more mature vascular plexus closer to the optic nerve head, Laminin α5 is predominantly localized in the abluminal BM of vessels and almost completely absent from the astrocytic network (n).

Our analysis as well as previous expression studies showed that the expression of laminin chains α 4 and α5 is distinct in different blood vessels.

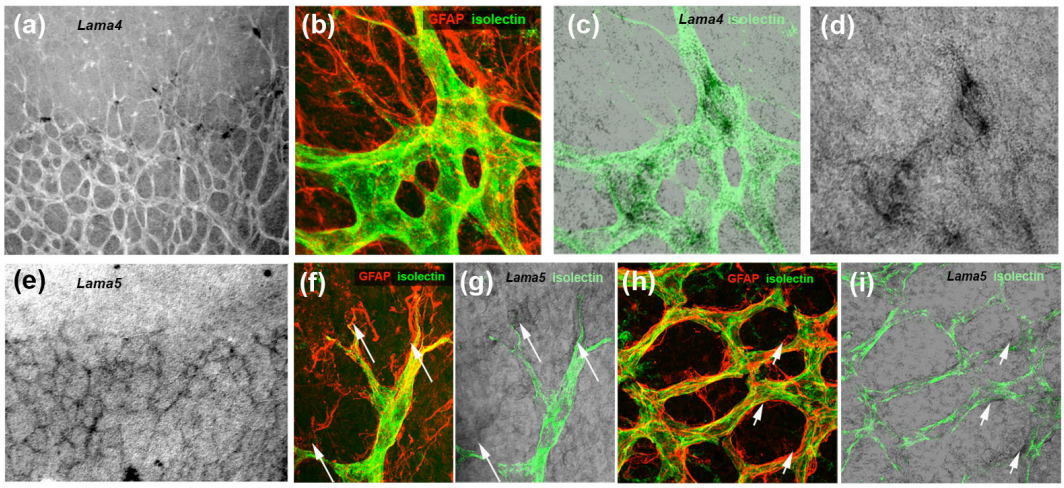

Figure 7.2 Differential *Lama4* and *Lama5* expression in the retinal vasculature

Lama4 and Lama5 ISH (black) of early mouse postnatal retinas (P5). Retinas were counterstained with Isolectin-B4 to visualize blood vessels (green) and GFAP to label the astrocytic network (red). *Lama4* is expressed is restricted to the migrating vascular front (a). High magnification microscopy revealed *Lama4* expression by ECs, but not astrocytes at the sprouting vascular front (b-d).
Lama5 expression could be detected throughout the developing vascular plexus (e), however counterstaining revealed astrocytic *Lama5* expression at the vascular front (f, g) and the capillary plexus (h, i).

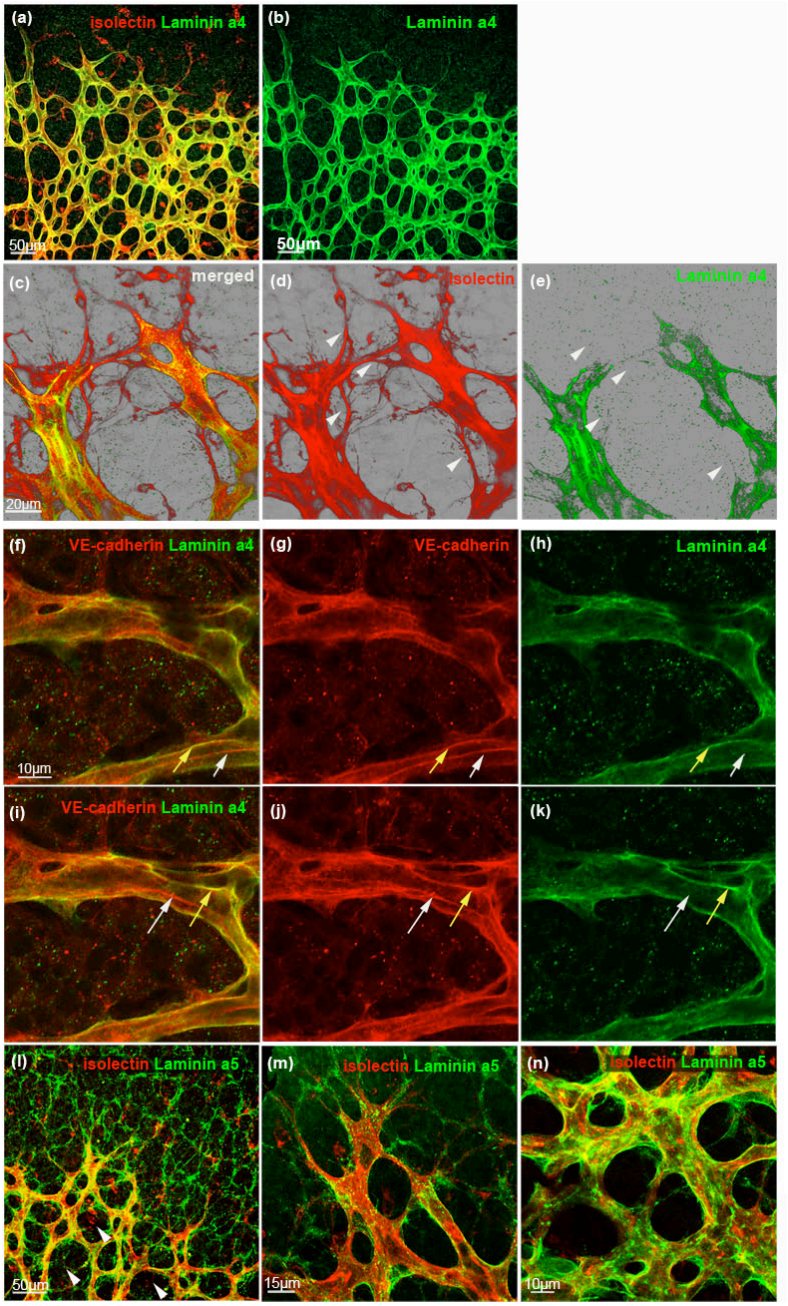

Figure 7.3 Laminin a4 is localized at endothelial cell junction while laminin a5 is deposited by astrocytic network and endothelial BM

Immunofluorescence staining with an antibody recognizing laminin α4 (green) and co-labeling with Isolectin-B4 (red) revealed abluminal localization of laminin α4 at endothelial BM in P5 mouse retina (a, b). Laminin α4 deposition is found in the developing vascular plexus (a) whereas laminin α4 is absent from newly formed sprouts at endothelial tip cells (arrowheads, c-e) and extended filopodia protrusion (c-e). Counterstaining with endothelial cell-cell junction molecule VE-Cadherin (red, f-k) revealed co-localization of laminin α4 (green) and endothelial junction (yellow arrows) in the capillary plexus while white arrows indicate junction with absent laminin α4 expression.
In marking contrast, laminin α5 (green) is deposited ahead of the growing vasculature (red) decorating the astrocytic network (l) and assembled in fibrilliar structures. In the mature vascular plexus, laminin α5 deposition is reduced (arrowhead, l) and can be found surrounding BM of retinal vessels (m, n).

Analysis with different cell lines derived from different tissues revealed that some ECs express predominantly *laminin a4* and others *laminin a*5 and that the expression pattern can be altered by the growth state or activation state of the cells (reviewed by (Hallmann, Horn et al. 2005). This is also reflected in the distinct expression pattern of laminin α4 and α5 within the same cell (Figure 7.4 a, b). Using brain endothelial cells (bEND5) we observed a wide distribution of laminin α5 (a), while laminin α4 is located at endothelial junction as seen *in vivo* (b) and in small patches at cell protrusions *in vitro* (b). One could imaging that endothelial cells cultured on uncoated dishes for 24 hours would express and secrete matrix components themselves however, IF staining with laminin antibodies a4 and a5 did not detect extracellular laminin localization, suggesting that no laminin matrix is formed by bend5 cells..

Although the deposition of laminin α5 is strongly reminiscent to the pattern formed by focal adhesion (FA) co-labelling with paxillin (Figure 7.4 c, green), a major focal adhesion molecule does not co-localize. In fact, laminin α5 and paxillin staining exclude each other suggesting that laminin α5 is deposited in other cell compartments than paxillin-positive FAs. Alternatively, one could speculate that paxillin staining shows the current FA in which laminin α5 is assembled and engaged whereas the spotty laminin α5 distribution marks historic FA.

One could also hypothesis that the antibody detects intracellular vesicular laminin a5 internalization. Further, co-labeling studies are required to determine laminin a5 intracellular localization in vitro.

In summary, we found a striking difference in laminin α4 and α5 expression in the retinal vasculature as well as in the localization of these chains in ECs *in vitro*.

7.1.3 Different laminin isoforms influence EC morphology

Laminins are crucial modulators for cell behaviour, e.g. laminin α4 regulates EC proliferation and protects the cell from apoptosis (DeHahn, Gonzales et al. 2004).

Fujita and colleagues reported the regression of glioblastoma tumours in mice following administration of LN411 inhibitors, while LN411 facilitates tumour progression and metastasis (Lu, Zhou et al. 2000). We therefore asked whether laminin α4 or α5 matrices can influence cell behaviour and are able to induce changes in EC morphology. When observing endothelial cell morphology of cells cultured on either LN411 (Figure 7.5 b, d) or LN511 (a, c) for 24 h we found that ECs on LN411 appear to loose their

contact inhibition to other cells when confluent and form less continuous adherent junction as seen when cultured on LN511. In contrast, endothelial cells cultured on LN511 display a confluent monolayer with firm junctions, indicated by VE-cadherin staining (red arrows, c) and exhibit an over all quiescent/mature state.

Therefore, we suggest that ECs cultured on LN411 take on a tip cell behaviour while cultured on LN511 they take on a stalk cell behaviour.

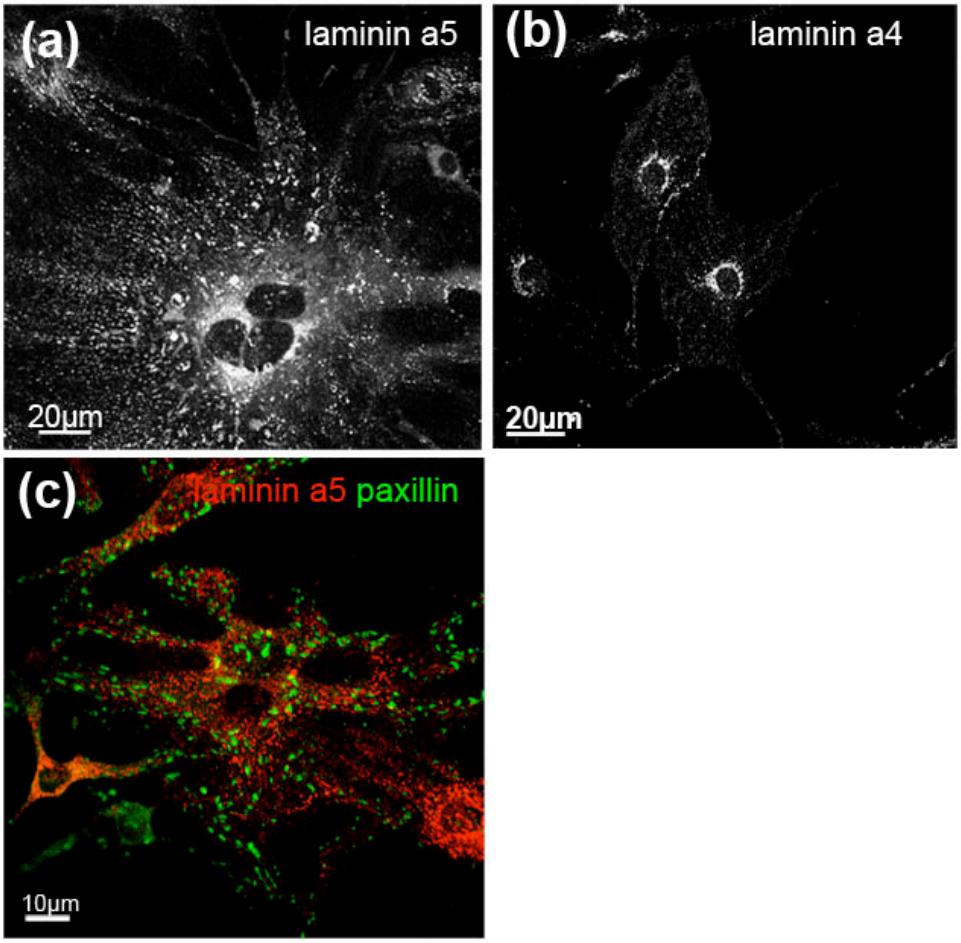

Figure 7.4 Laminin a4 and laminin a5 localize at different compartments in endothelial cells *in vitro*

Immunostaining of bEND5 endothelial cells *in vitro* with antibodies directed against laminin α4 and laminin α5 revealed a widespread distribution of laminin α5 (a) but restricted laminin α4 localization at endothelial cell junction (b). Counterstaining with paxillin (green, c) to identify focal adhesion contacts of laminin α5 elucidated exclusive expression of paxillin and no co-localization with laminin α5 (red, c).

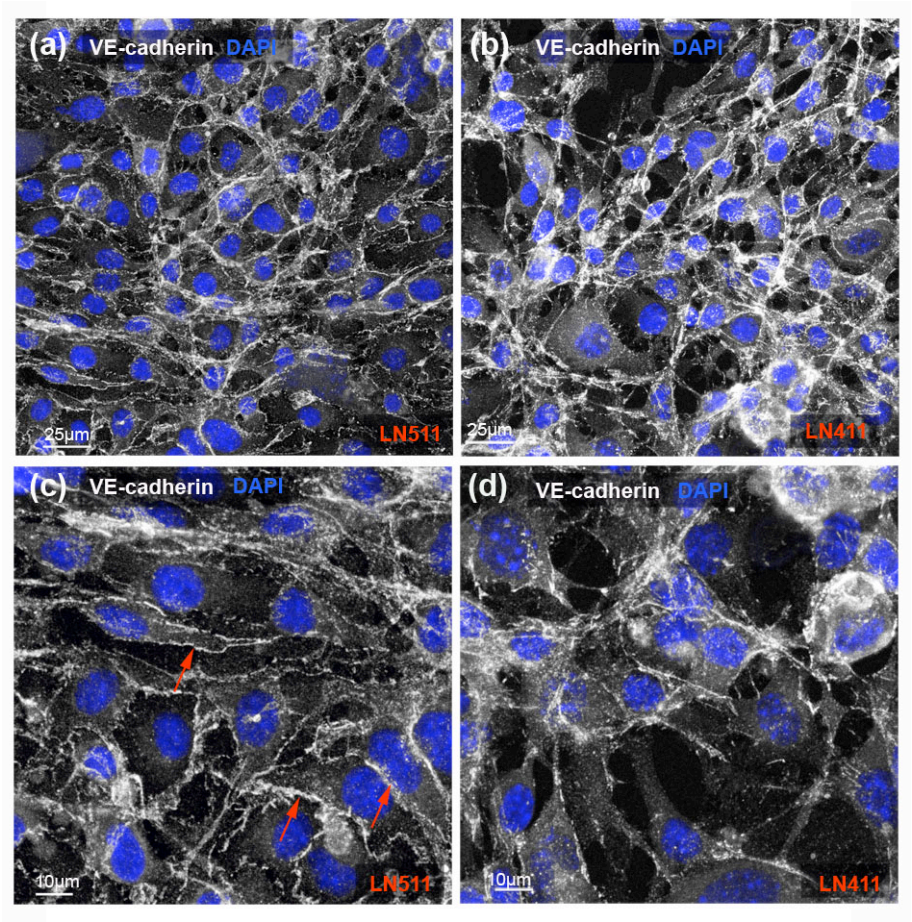

Figure 7.5 Laminin matrix influence endothelial cell morphology *in vitro*

bEND5 endothelial cells were cultured for 24h on Laminin α5β1γ1 (LN511) and LN411 matrices. Cells on LN511 (a, c) formed a confluent monolayer with firm continuous cell junction identified by VE-cadherin staining (red arrows, c). In contrast, cells coated on LN411 matrix develop a migratory phenotype and grow over each other, appearing to loose their contact inhibition (b, d).

7.1.4 Loss of *laminin a4* results in increased vascular density

Although previous studies described a role of laminin α4 in pathological angiogenesis, its function during vascular development received little attention.

To gain further insight we analysed the retinal vasculature of postnatal *laminin α4* knock out mice (*Lama4-/-*) in more detail.

We found a significant increase in vessel density and excessive branching in *Lama4* deficient mice. In particular the density of the sprouting vascular front was enhanced (Figure 7.6 a-b). By counting branchpoints per microscopic field we calculated a 60% increase in vascular density in *Lama4-/-* compared to heterozygous littermates (c).

7.1.4.1 Increased vascularization is independent of hypoxia

It has been reported that *Lama4-/-* mice develop oedema and are anaemic (Thyboll, Kortesmaa et al. 2002). Reduced oxygen delivery could potentially trigger increased (hypoxia-induced) vessel formation. To determine whether the increased density and aberrant sprouting of vessels in *Lama4 -/-* mice is caused by an upregulation of VEGF-A expression induced by hypoxia we analysed VEGF-A expression and localization in the retinal vasculature. However, the relative mRNA expression of *Vegfa* and *Slc2a*, another hypoxia induced gene in *Lama4* deficient mice did not show a significant increase (Figure 7.7 c). In addition, *in situ* hybridization revealed that the retinal pattern of astrocyte-derived *Vegfa* expression was unchanged in *Lama4 -/-* mice (a, b), together indicating that the observed increase in retinal vessel density is not a primary consequence of tissue hypoxia.

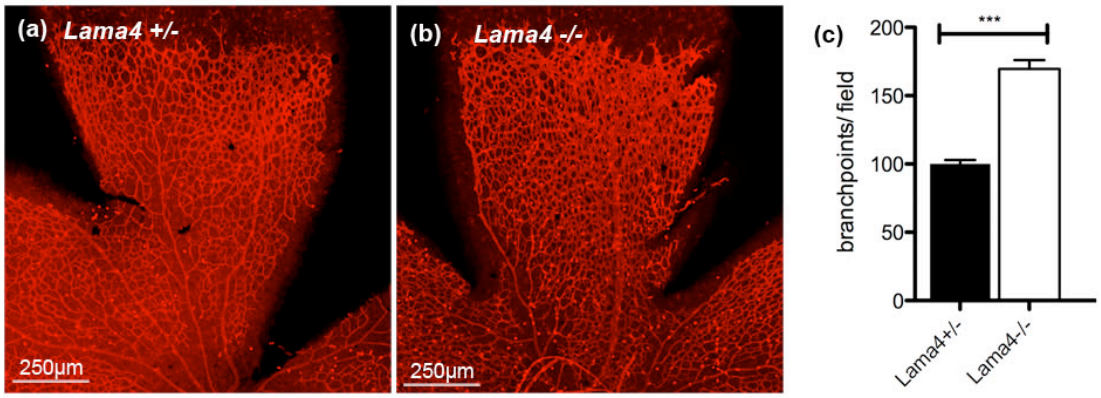

Figure 7.6 Loss of Lama4 leads to increased vascular density

Immunostaining with Isolectin B4 to visualize the retinal vasculature at P5 revealed an increased vascular density in mice deficient of *Lama4* (a, b). Graph c summarizes the number of branchpoints per image field of P5 *Lama4-/-* and heterozygous control mice, n ≥ 5. ***, p < 0.0001. Values represent mean ± S.E.M.

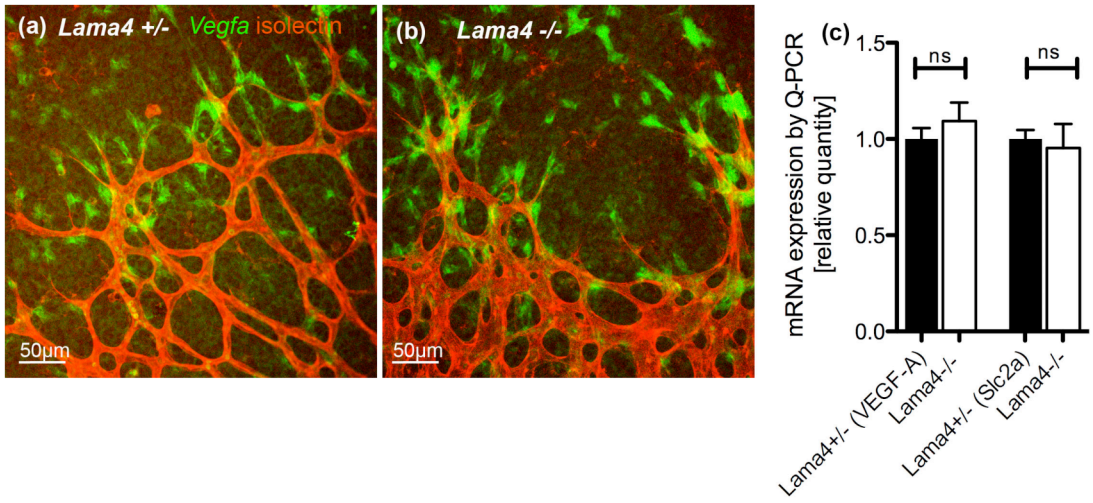

Figure 7.7 Increased vascularization in *Lama4* deficient mice is not caused by hypoxia or an upregulation of *Vegfa* expression

Vegfa ISH (green) and counterstaining with Isolectin-B4 (red) of *Lama4* and control retinas revealed normal *Vegfa* expression and distribution at P5 (a, b). qPCR of *Vegfa* and *Slc2a*, a hypoxia-regulated gene in retinas of P5 mice (c), *Lama4 -/-* and control mice n ≥ 3; Values are mean ± S.E.M.

7.1.4.2 Delayed retinal vessel migration in *Lama4* knock out mice

Measuring the total distance vessels have spread from the optic nerve towards the periphery (Figure 7.8 a, b; white arrow) we observed a mild decrease of vessel migration at day 5 postnatally (P5, c). Vessel migration is still delayed at P7 and vessel density of *Lama4* deficient mice is strongly increased when compared to control retinas (d, e). The delay in vessel migration in the retina possibly reflects the overall smaller body size by 10% and delayed development of *Lama4* -/- mice as reported by (Thyboll, Kortesmaa et al. 2002).

Although no differences in *Vegfa* expression were detected, we asked whether the increased vessel density and the delay in migration is a result of disturbed VEGFR2 signalling and subsequently, PI3K activity. To address that question we analysed retinal expression of VEGFR2 protein and phosphorylation levels of VEGFR2 as well as downstream target AKT. As shown in blot (f), no striking differences were observed in pVEGFR2/VEGFR2 levels and likewise, levels of total AKT and phosphorylated AKT (pSer) were equal in *Lama4-/-* and control littermates (f).

7.1.4.3 Detailed analyses of vessel composition and BM formation

Previous studies suggested that *Lama4* deficiency results in torturous vessels with defects in vessel maturation and integrity. Vessel maturation is accompanied by recruitment of pericytes (PC) and the formation of a shared BM between the endothelium and PCs. We observed normal PC recruitment in retinal vasculature of *Lama-/-* mice (Figure 7.9 a-d). Staining with NG2, a marker used to detect PC (red, b and d) revealed investment of PC and close association with retinal vessels in *Lama4-/-* to the same extent as seen in control retinas. Yet, we found an abnormal BM composition and reduction in CollagenIV expression, a major BM component. CollagenIV assembly appeared disturbed and immunofluorescence staining with CollagenIV (green) revealed a loose and fibrilliar collagen structure in *Lama4-/-* (Figure 7.10 d-f) while control littermates display a dense collagen network covering the entire vessel (Figure 7.10 a-c). We hypothesized that the linkage to collagenIV and the formation of a complex BM network fails in *Lama4-/-* mice.

It has been reported previously that the absence of laminin polymer assembly fails to sequester collagen in the same BM (Li, Harrison et al. 2002). Therefore, we

concluded that the reduction and abnormal deposition of ECM components reflects laminin α4 function in matrix assembly and BM integrity.

Thyboll and colleagues speculated that the vascular defects in *Lama4-/-* seen during postnatal development are rescued by compensatory upregulation of laminin α5 expression. We studied laminin α5 expression and deposition in *Lama4-/-* retinas and found laminin α5 deposition on the astrocytic network ahead of the growing vasculature as described earlier (Figure 7.11 a-c, e-g). Although laminin α5 expression appears reduced in *Lama4-/-* (g) compared to control littermates (c), it is present on the astrocytic network as well as in endothelial BM (e-g). Endpoint Reverse Transcriptase-PCR (RT-PCR) revealed loss of laminin a4 in Lama4-/- mice, however Lama4 heterozygous mice did not display reduced laminin a4 expression as one would predict due to genetic ablation of one Lama4 allele (d). This finding indicates that this method is not sensitive enough to distinguish gene expression levels and therefore, does not allow me to study laminin a5 compensation (d). In order to determine whether laminin a5 is upregulated and compensates for the loss of laminin a4 in Lama4 deficient mice, one would need to perform relative quantitative PCR.

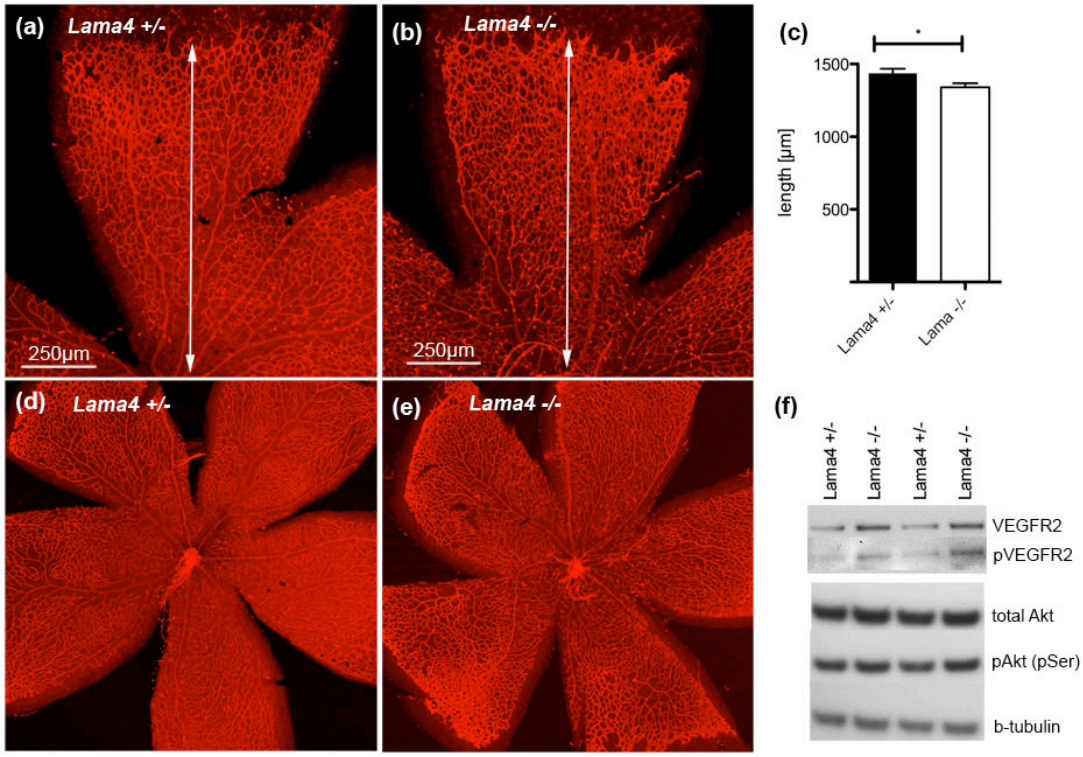

Figure 7.8 Reduced migration of retinal vessels in *Lama4* deficient mice

Vessel migration towards retinal periphery in *Lama4* deficient and control retinas at P5 (a, b) and P7 (d, e). Graph c summarizes radial expansion of superficial vessels in P5 retinas. *, $p < 0.05$, *Lama4 -/-* and control mice $n \geq 3$; Values are mean ± S.E.M.
VEGFR2 signalling and PI3K activity was determined by Western Blotting of *Lama4 -/-* and control retinas at P5 (f). No differences in phosphorylation of VEGFR2 could be observed, however total protein levels of VEGFR2 are increased in *Lama4 -/-* mice. PI3K activity was accessed by immunoblotting of total AKT and phosphorylation of serine residue 473 of AKT (f).

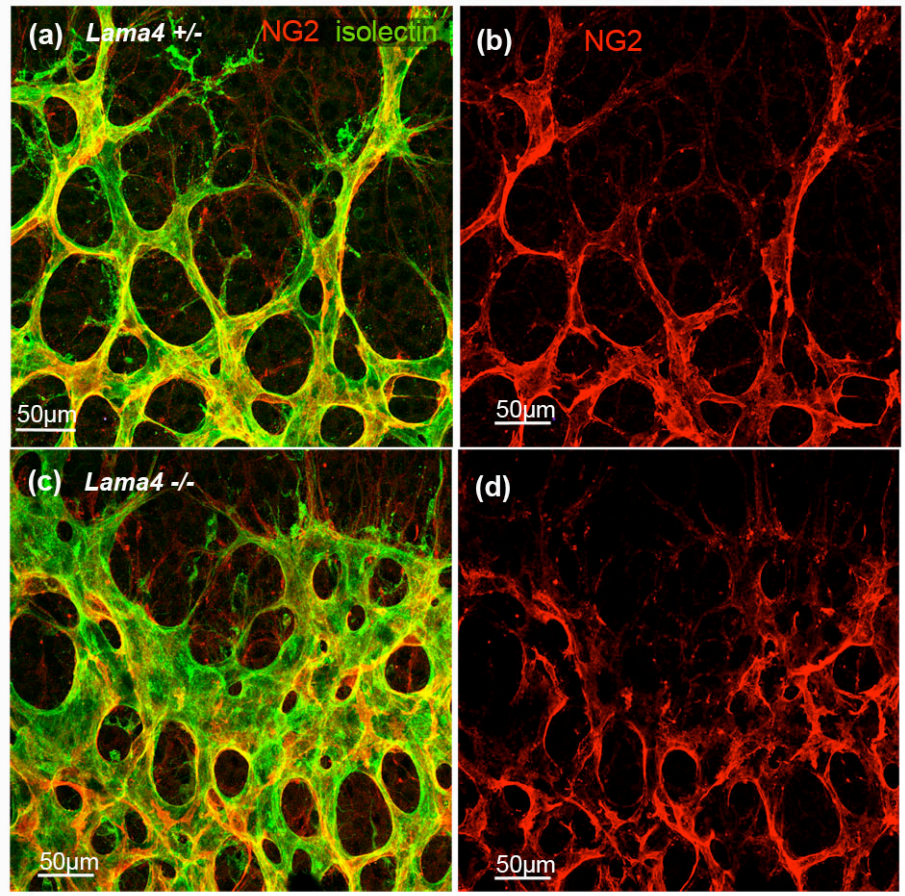

Figure 7.9 Pericyte recruitment is unaffected in *Lama4* deficient mice

Pericyte investment and association with retinal blood vessels (green) was analysed by immunostaining with NG2 (red, a-d). No defects could be observed and pericytes migrate to a similar extent in *Lama4* -/- mice (c, d) when compared to control retinas at P5 (a, b).

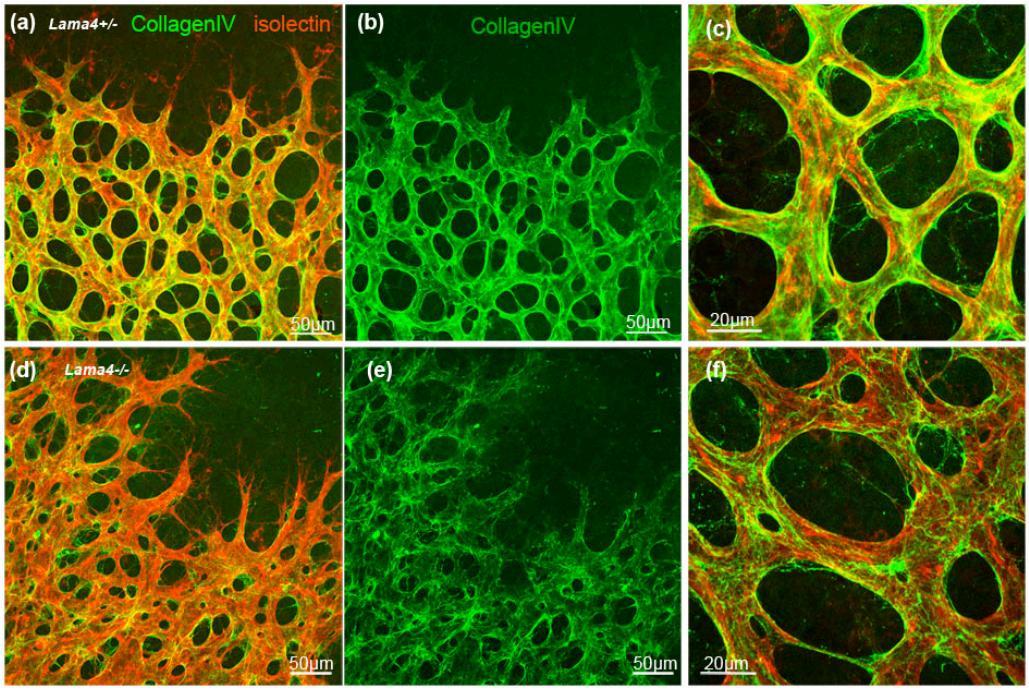

Figure 7.10 Reduced CollagenIV deposition and defective basement membrane assembly in *Lama4-/-*

Immunostaining with CollagenIV (green, a-f) revealed decreased CollagenIV deposition in *Lama4*-/- retinas (d-f). High magnification imaging identified abnormal assembly of CollagenIV in fibrilliar structures (e) while collagenIV appears as continuous BM sleeves in control vessels (b, c).

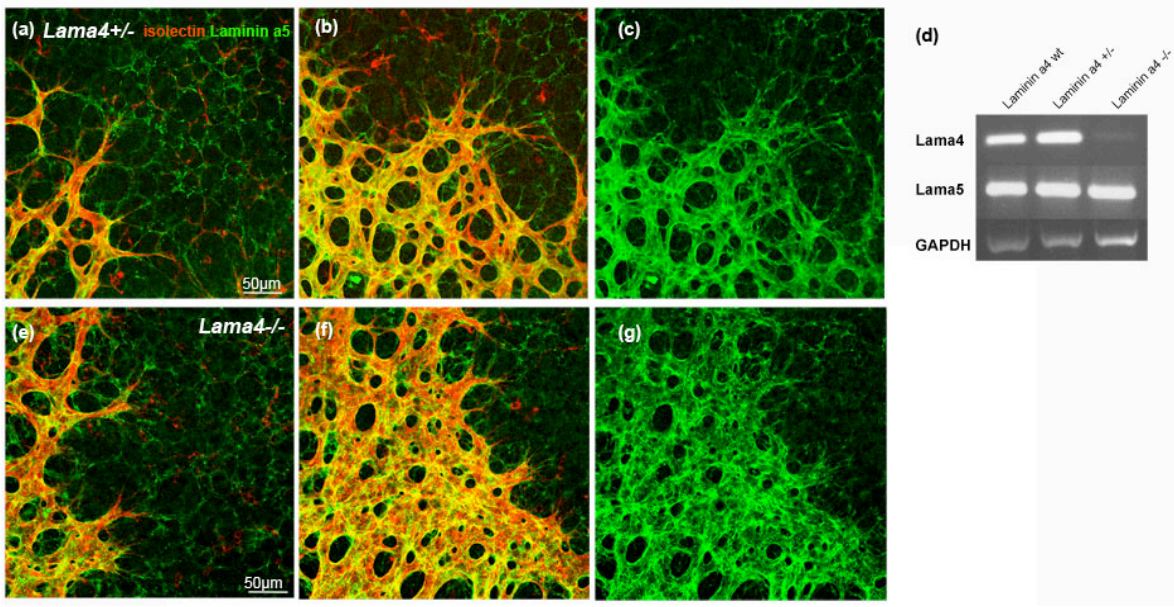

Figure 7.11 Laminin α5 does not compensate for the loss of *Lama4*

Immunostaining with laminin a5 (green, a-c, e-g) was performed to investigate laminin α5 localization and compensation upon loss of *Lama4*. Counterstaining with Isolectin B4 (red) showed laminin α5 deposition in the astrocytic network (a, d) and laminin α5 decorating abluminal BM of retinal vessels (b-c, f-g). RT-PCR (d) of total retinal RNA (P5) confirmed absence of *Laminin a4* in *Lama4* deficient retinas but no upregulation of *Laminin a5*.

7.1.4.4 Loss of *Laminin a4* results in increased proliferation

To address whether the increased vascular density observed in *Lama4-/-* mice is a result of enhanced proliferation, we injected BrdU for 2 hours into postnatal mice and quantified BrdU positive endothelial cells after co-labeling with isolectin. We observed a significantly increase number of BrdU positive ECs in *Lama4-/-* retinas (b) compared to control littermates (a), (Figure 7.13 a-c). Similar results were obtained when analysing proliferation by IF staining with phospho-Histone H3 (red, Figure 7.13 d, e). Positive staining was observed in the growing vascular front of *Lama4-/-* mice for proliferating endothelial nuclei in mitosis.

Therefore we concluded that the hypervascularization in *Lama4* deficient retinas is, at least in part, a consequence of enhanced EC proliferation, independent of hypoxia and VEGF-A mRNA expression.

7.1.4.5 Excessive tip cell formation and aberrant sprouting in *Lama4-/-* mice

When analysing the vasculature in greater detail, we found that the loss of *Lama4* results in elevated number of vascular sprouts and aberrant tip cell formation (Figure 7.12 a-b). By counting filopodia extension we identified a significant increase in filopodia protrusions (c). Also, filopodia extension was profoundly increased in the more mature, central vascular plexus of the retinal vasculature, as can be seen in many pathological conditions when maturation and quiescening of vessels is disturbed (Figure 7.12 d-f). By scanning through the entire plexus of the retinal vasculature we observed ectopic filopodia bursts reaching in deeper retinal layers. These additional filopodia extensions indicate excessive sprouting and enhanced tip cell formation in *Lama4-/-* mice.

Immunostaining with an antibody against phosphoHistone H3 (red, d, e) and counterstaining with Isolectin-B4 (green) identified proliferative ECs.

Furthermore, we show by *in situ* hybridization and relative quantitative PCR that *Pdgfb* expression, a selective tip cell marker (Hellstrom, Phng et al. 2007) is up to 2-fold increased and its expression is extended over the entire vascular front (Figure 7.12 g-i) compared to the restricted expression of leading tip cells in heterozygous littermates.

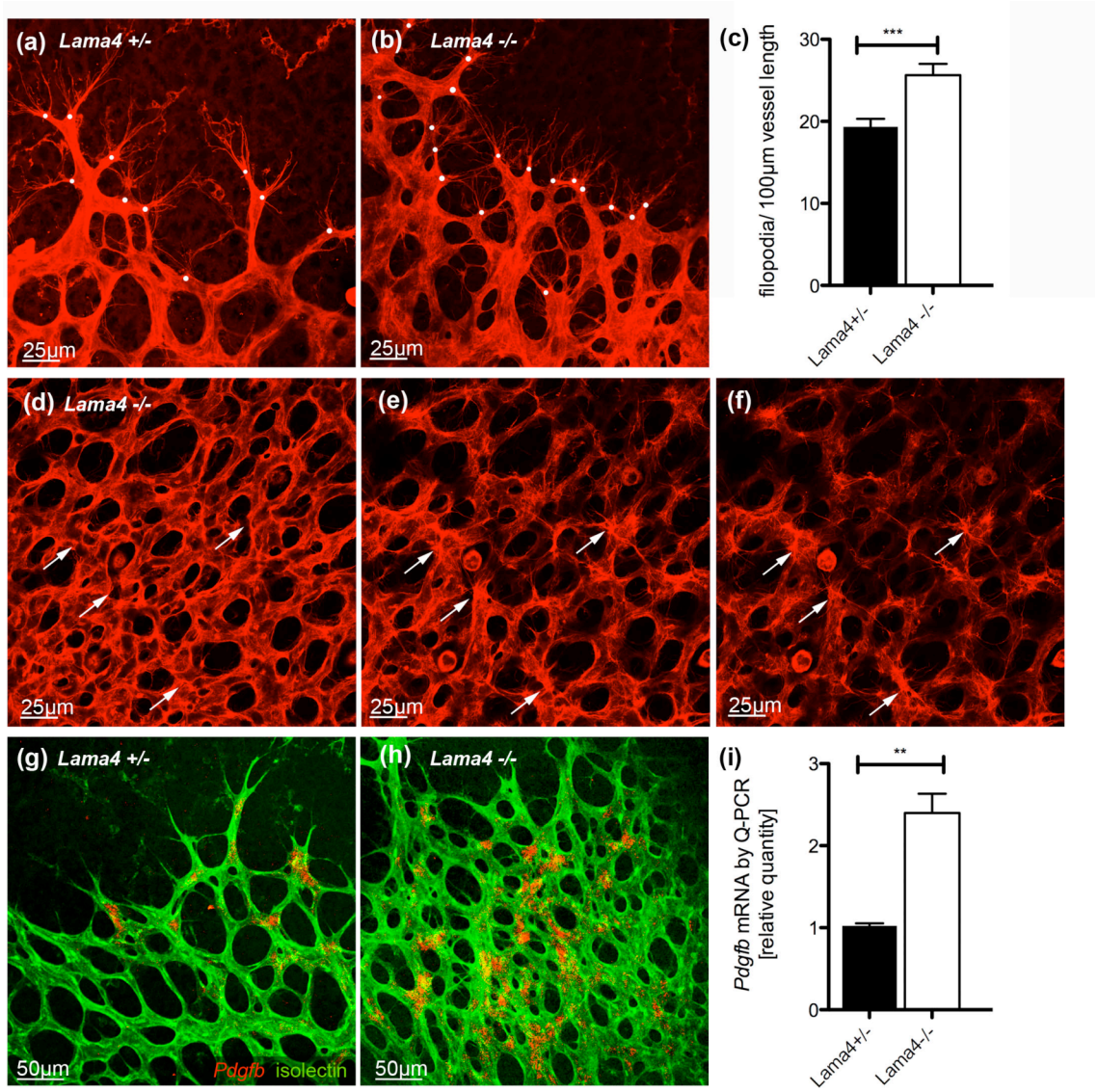

Figure 7.12 Increased tip cell formation and excessive sprouting in *Lama4-/-*

Confocal images of tip cells of P5 control and *Lama4*$^{-/-}$ retinas stained with Isolectin-B4 (red, a-b) revealed aberrant filopodia formation. By counting number of filopodia (white dots) extended per 100µm vessel length we found a significant increase in filopodia (c). ***, $p > 0.0001$. control and *Lama4*$^{-/-}$ mice $n \geq 3$; Values represent mean ± S.E.M.

Excessive filopodia formation was also detected in the mature capillary plexus of P5 *Lama4-/-* retinas (white arrows, d-f).

Pdgfb ISH (blue) of P5 retinas were counterstained with Isolectin-B4 (green) showing an increased area of *Pdgfb* expression in *Lama4-/-* retinas (g, h). Graph i illustrates the relative expression of *Pdgfb* in retinas of P5 animals. **, $p < 0.01$; control and *Lama4-/-* mice $n \geq 7$. Values represent mean ± S.E.M.

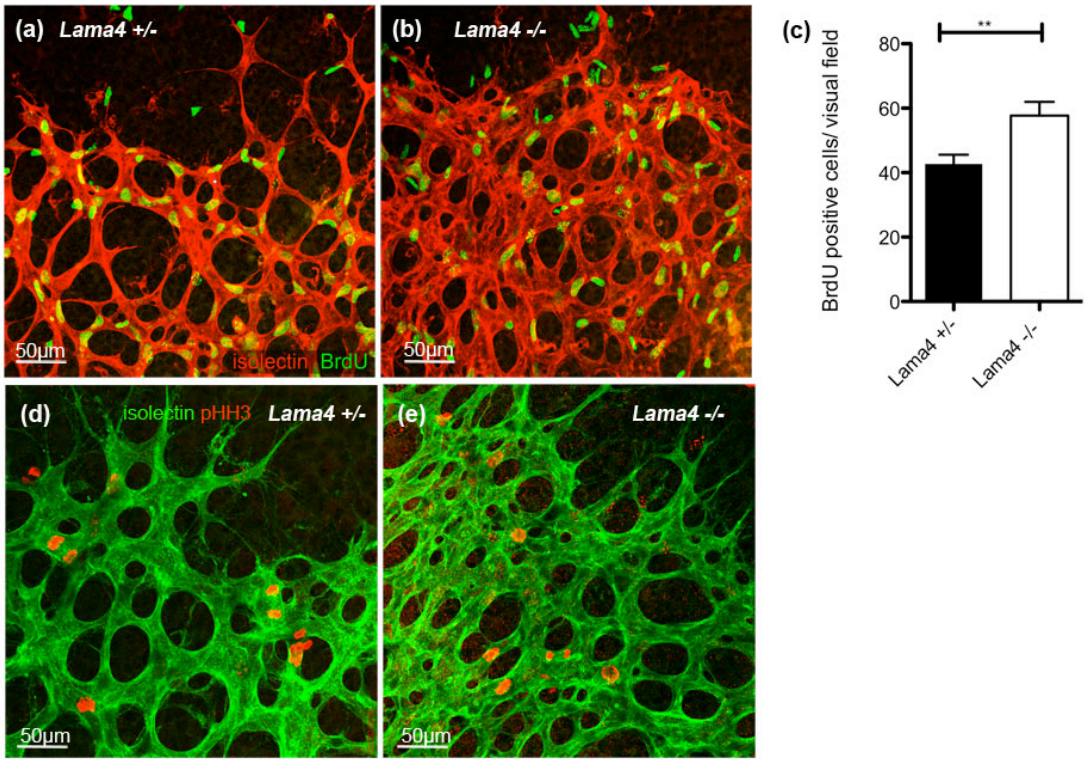

Figure 7.13 Loss of *Lama4* results in increased endothelial cell proliferation

P5 *Lama4-/-* and control mice were injected with BrdU intraperitoneally and retinas were analyzed for BrdU incorporation 2 h later. Retinas were stained with anti-BrdU antibody (green) and Isolectin-B4 (red, a-b). BrdU-positive ECs co-locabeled with isolectin were counted. Bars in graph c show number of proliferated endothelial cells per visual image. **, $p < 0.01$. control mice n=4, *Lama4-/-* n=3; Values represent mean ± S.E.M.

7.1.5 Loss of Lama4 alters Dll4/Notch gene expression

The phenotype of mice lacking *Lama4* strongly resembles the loss of Notch/ Dll4 signalling. When disturbing Notch signalling using pharmacological inhibitors (DAPT) or deleting the *Notch1* receptor or one allele of the ligand *Dll4* blood vessels undergo excessive sprouting as a consequence of increased tip cell formation (Hellstrom, Phng et al. 2007); (Suchting, Freitas et al. 2007); (Lobov, Renard et al. 2007).

To examine Dll4/ Notch signalling in *Lama4-/-* mice, we analysed the relative expression of mRNA levels of targets downstream of Dll4/ Notch signalling and found that expression of transcription factors such as *Hey1*, *Hey2* as well as the ligand *Dll4* are significantly downregulated (Figure 7.14 a). The regulation of genes downstream of the Notch/Dll4 signalling pathway has been studied extensively and previous studies have shown that expression *of the Notch regulated ankyring repeat protein (Nrarp)*, is decreased by up to 70% when treated with DAPT (Hellstrom, Phng et al. 2007); (Lobov, Renard et al. 2007); (Phng, Potente et al. 2009). Treatment of postnatal mice with the gamma-secretase inhibitor, DAPT results in increased retinal vasculature and downregulation of several Notch targets, such as *Hey1, Hey2* and *Nrarp* (Phng and Gerhardt 2009).

Interestingly, *Lama4-/-* mice also show a significant reduction of *Nrarp* mRNA expression (Figure 7.14 a).

7.1.6 *Dll4* mRNA expression is induced by laminin 411

Next we asked whether laminin α4 directly affects Dll4/Notch signalling in cultured endothelial cells. We cultured either human umbilical endothelial cells (HUVECs) or mouse brain endothelial cells (bEND5), on different matrices, including Laminin 411 (LN411), Laminin 511 (LN511), and uncoated control cell culture dishes. Already after 4h of incubation *Dll4* was induced in bEND5 ECs when cultured on LN411. Expression of *Dll4* was further increased over a period of 24h when bEND5 ECs were cultured on LN411 compared to uncoated dishes (Figure 7.14 b). In contrast to the effect of LN411, *Dll4* was not induced by LN511, but rather tend to result in reduction of *Dll4* expression, illustrating that these two endothelial BM components differentially influence expression of the endothelial Notch ligand Dll4. Similar results were obtained when human ECs (HUVECs) were cultured on distinctive laminin matrices or uncoated dishes.

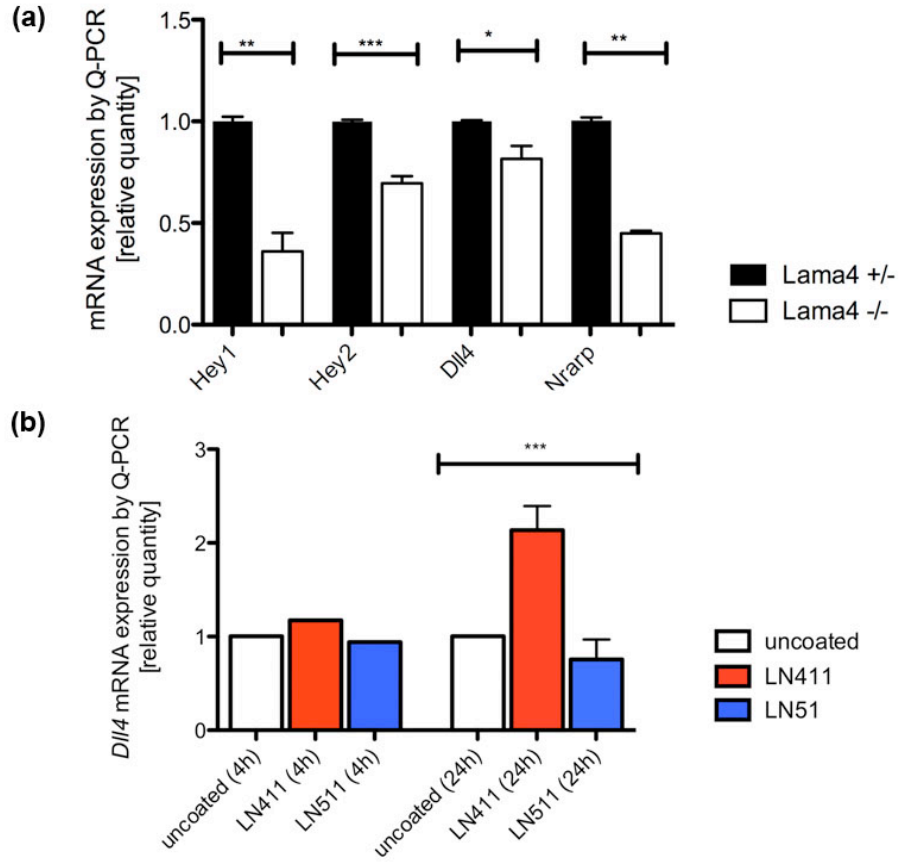

Figure 7.14 Laminin α4 modulates expression of *Dll4* and Notch downstream targets

Quantitative-PCR was performed to investigate differential gene expression in retinas of *Lama4* heterozygous control and *Lama4 -/-* mice (a). mRNA expression was analysed at P5. *, $p < 0.05$, **, $p < 0.01$, ***, $p < 0.0001$. *Lama4+/-* and *Lama4-/-* $n \geq 3$. Values represent mean ± S.E.M.
Endothelial cell line bEND5 was cultured on LN411, LN511 and uncoated matrices for 4 and 24 hours prior analysing *Dll4* mRNA expression by qPCR (b). $n \geq 5$. ***, $p < 0.0001$ ANOVA, 1way analysis. Values represent mean ± S.E.M.
Values represent mean ± S.E.M.

7.1.6.1 Laminin 411 induced *Dll4* expression is dependent on Notch signalling

To test whether Laminin 411 mediated *Dll4* induction requires Notch activity, we treated ECs cultured on LN411 with DAPT for up to 24h. Disturbing Notch signalling with DAPT abolished LN411- induced *Dll4* expression. *Dll4* expression was similarly reduced in ECs cultured on LN511 (not shown) and control uncoated dishes (Figure 7.15 a), suggesting that the induction of *Dll4* expression requires Notch signalling on all matrices.

7.1.6.2 Disturbing VEGFR2 signalling does not affect Laminin 411 induced *Dll4* expression

Previous studies illustrated an important role of VEGF/VEGFR2 signalling in inducing Dll4 expression (Lobov, Renard et al. 2007). To address whether LN411 induced *Dll4* expression correlates with increased *Vegfr2* mRNA expression and signalling, we studied VEGFR2 levels *in vitro*. When cells are cultured on LN411, *Vegfr2* is upregulated by 2 fold in comparison to ECs on uncoated dishes (Figure 7.15 b). To investigate whether Laminin 411 induces *Dll4* expression is dependent on VEGF-A/VEGFR2 signalling, we blocked VEGFR2 using neutralizing antibody DC101 and analysed *Dll4* expression of ECs cultured on LN411 or uncoated control dishes. Analysis of phosphorylated VEGFR2 levels confirmed effective inhibition of VEGFR2 activity by DC101 treatment (c).

We found a significant reduction of *Dll4* expression upon blocking VEGFR2 signalling in uncoated control ECs. Also in ECs cultured on LN411 blocking of VEGFR2 decreased LN411-induced *Dll4* expression. However, *Dll4* mRNA expression levels remained significantly greater compared to ECs on uncoated dishes (d), suggesting that Laminin α4 promotes *Dll4* expression at least in part independently of VEGF/VEGFR2 signalling.

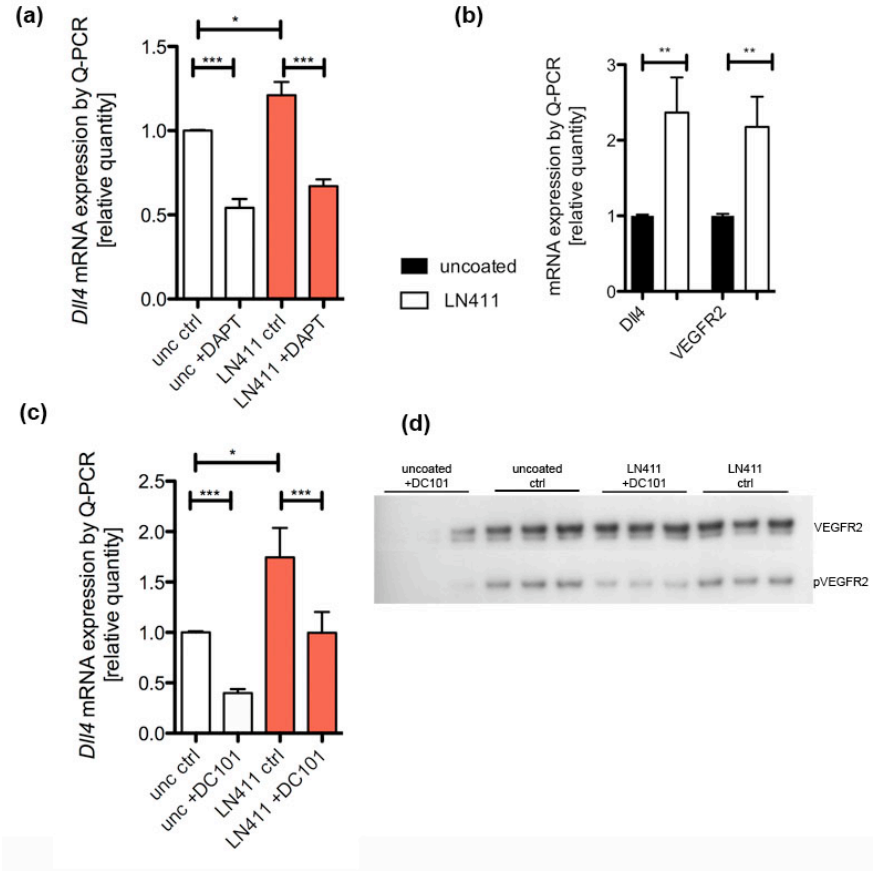

Figure 7.15 Laminin 411 modulates Dll4/ Notch signaling

Dll4 mRNA expression in bEND5 ECs was analysed after 24h inhibition of Notch signalling with pharmalogical inhibitor, γ-secretase. *Dll4* was decreased independently of matrix ECs were cultured on (a). $n \geq 3$, ***, $p < 0.0001$. Values represent mean ± S.E.M.

Dll4 and *VEGFR2* expression levels of bEND5 ECs were significantly increased when cultured on LN411 compared to uncoated dishes (b). Graph d illustrates mRNA expression levels by relative quantity. $n \geq 3$, **, $p < 0.01$. Values represent mean ± S.E.M.

Dll4 expression levels of bEND5 ECs were studied after treatment with VEGFR2 neutralizing antibody, DC101 for 24h (c). Blocking VEGFR2 signalling had a reducing effect on *Dll4* expression in uncoated and LN411 coated ECs. *, $p < 0.05$, ***, $p < 0.0001$. $n \geq 5$. Values represent mean ± S.E.M.

Inhibition of VEGFR2 signalling after DC101 treatment was examined by Western Blotting. ECs cultured with or without DC101 on LN411 or uncoated dishes were analysed after 24 hours. Wile VEGFR2 protein levels were similar in all samples, treatment with DC101 resulted in reduced phosphorylation of VEGFR2 (f).

7.1.7 Laminin-integrin interaction modulate *Dll4* expression

Previous work in neural stem cells suggested that integrin receptors for ECM molecules and growth factors present on the cell surface act together with the Notch pathway to control the neural stem cell responses to changes in the microenvironment (Campos, Decker et al. 2006). The authors propose physical interaction of Notch and integrin by sequestering Notch intracellular domain (NICD) and by modulating NICD trafficking in the cytoplasm to the nucleus by regulating internalization. Further studies outline that Notch activates integrins (Hodkinson, Elliott et al. 2007) and that constitutively active Notch-4 alters integrin conformation and thereby activation (Leong, Hu et al. 2002). Laminin α4 predominantly binds and interacts via integrin receptors comprising integrin α6β1, α3β1 and αvβ3 (Lian, Dai et al. 2006); (Belkin and Stepp 2000). Interestingly, transfection of HUVECs with Dll4-retroviral constructs leads to downregulation of integrin beta 3 (*Itgb3*) in microarray analysis (Harrington, Sainson et al. 2007). In addition, deletion of *Itgb3* results in vessel overgrowth mediated by elevated VEGFR2 levels (Reynolds, Reynolds et al. 2004) and causes enhanced pathological angiogenesis (Reynolds, Wyder et al. 2002).The phenotypical similarities of *Lama4 -/-* and *Itgb3-/-* described as well as the capacity of laminins to bind and interact with integrin β3 (Gonzalez, Gonzales et al. 2002) led us to the hypothesis that LN411 mediated induction of *Dll4* expression may require integrin signalling.

7.1.7.1 Integrin β3 localizes at endothelial cell junction

To characterize Itgβ3 expression and localization in greater detail we combined isolectin staining (red) of retinal blood vessels with an antibody detecting Itgβ3 (green, Figure 7.16 a-d). We found that Itgβ3 is represent in endothelial BMs and particularly co-localizes with endothelial cell junction (arrows, a-b). Interestingly, a similar expression pattern was seen for laminin α4 (Figure 7.3). But when comparing the expression pattern of Itgβ1 (Figure 6.7) and Itgβ3, we observed that Itgβ3 is absent in pericytes and vascular smooth muscle cells of arteries (arrowhead, c-d). Our findings are supported by a recent study from Naik and colleagues showing that Itgβ3 and junction molecule, JAM-A co-localize in EC junction of HUVEC cells (Naik, Mousa et al. 2003); (Naik and Naik 2006).

7.1.7.2 Reduced vascular sprouting in *itgb3* knock out retinas

Integrin β3 has been reported to function during angiogenesis but no vascular defect has been observed during retinal vessel development (Hodivala-Dilke, McHugh et al. 1999). We analysed the retinal vasculature of P5 pups using confocal microscopy. The following results are preliminary and require confirmation by additional numbers. Retinas of *Itgb3-/-* mice were provided by S. Robinson and K. Hodivala-Dilke, unfortunately the breeding did not provide us with control littermates. Therefore, the phenotype of *Itgb3-/-* was compared to P5 control retinas from a separate litter, which potential may result in subtle developmental differences.

Overview images of control (Figure 7.16 e) and *Itgb3-/-* retinas (f) revealed that a vascular plexus has formed and that no apparent defects are present. However, when observing the sprouting vascular front in more detail (g, h) we found that the plexus is sparse and the extension of leading tip cells is reduced in *Itgb3-/-* (red arrows, h) compared to control retinas. In addition, high magnification imaging revealed that *Itgb3-/-* tip cells are thin, long, and fail to fuse to neighbouring cells (k, l). It appears that filopodia of *Itgb3-/-* vessels are straight and elongated (red arrowheads, l) whereas control tip cells branch and connect to neighbouring vessels, indicated by spread and wide distributed filopodia burst (i, j). These phenotypical observations could be a result of diminished integrin-VEGFR2 signalling. It has been shown that αvβ3 integrin directly interacts with VEGFR2 and its engagement promotes phosphorylation and activation of VEGFR2 (Soldi, Mitola et al. 1999). In addition, this interaction appears to be synergistic, as VEGFR2 activation induces β3 integrin tyrosine phosphorylation that in turn, is crucial for VEGF-induced VEGFR2 phosphorylation (Mahabeleshwar, Feng et al. 2007). Given that *Itgb3* is expressed by leading tip cell in the retina, the reduced sprouting and filopodia extension observed in *Itgb3-/-* retinas could reflect a loss of effective VEGFR2 signalling and would indicate that hypervascularization of *Lama4-/-* is mediated independent of integrin β3 binding and interaction.

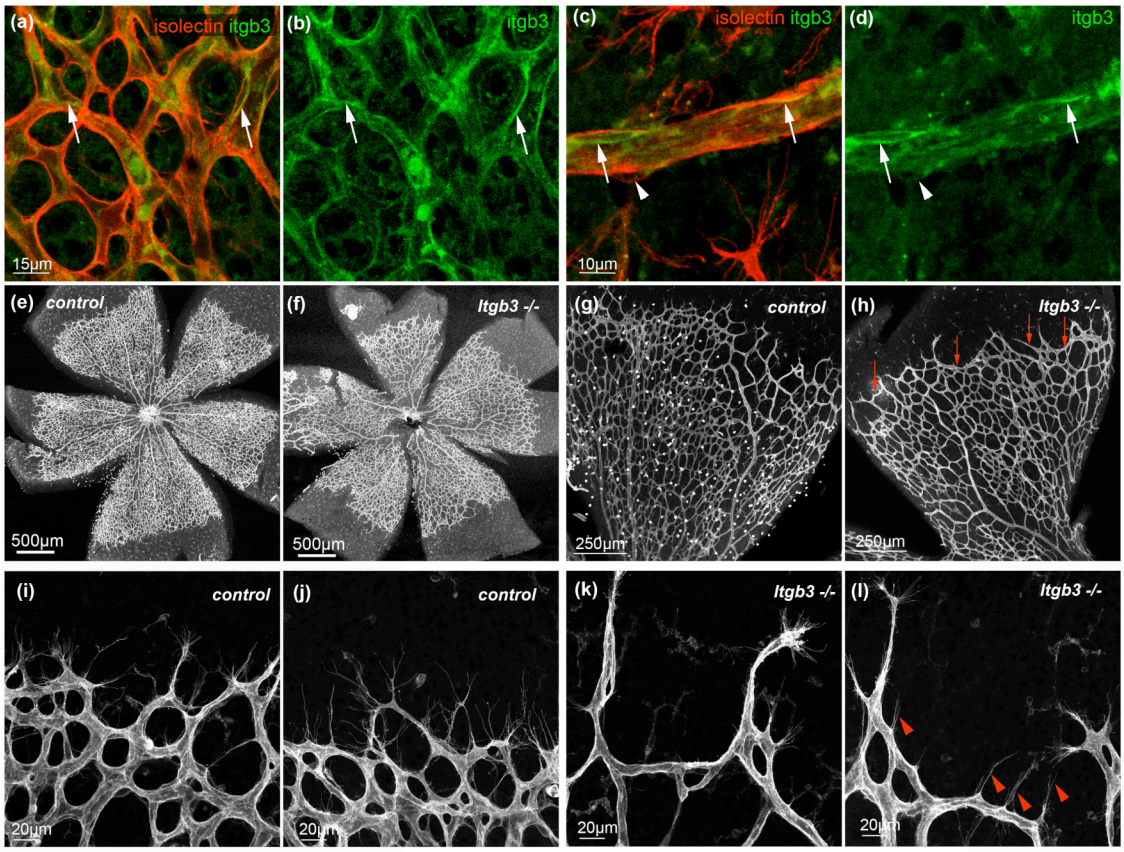

Figure 7.16 Integrin beta 3 localizes at endothelial junction and loss of *Itgb3* leads to reduced sprouting

Immunostaining with integrin beta 3 (green) and counterstaining of retinal vessels with Isolectin B4 (red, a-d) revealed junctional localization of itgb3 (arrows, b, d). Itgb3 staining was absent from pericytes (arrowhead, c).
Overview images of retinal vasculature of *ITGb*3 deficient and control mice, P5 (e-h) show that a vascular plexus has formed and vessels expanded radial over the entire retina. High resolution imaging of the migrating vascular front by Isolectin B4 staining revealed a reduced number of tip cells (red arrows, h). The extended tip cells of *Itgb3* -/- mice appear thin and fail to connect to neighbouring cells (k, l) when compared to control retinas (i, j). Red arrowheads indicated straight and unbranched filopodia protrusion (j).

7.1.7.3 Integrin β3 knockdown diminishes Laminin 411 induced *Dll4* expression

To test whether LN411 induced *Dll4* expression is mediated by integrin β3 signalling, we transfected HUVEC cells with *Itgb3* siRNA and analysed the *Dll4* mRNA expression in relation to *Itgb3* knock down.

Preliminary data, revealed that LN411-induced *Dll4* expression (Figure 7.17 a) is decreased when integrin β3 signalling is reduced (Figure 7.17 b). In contrast, ECs cultured on LN511(blue bar, a) that initially display a reduction of *Dll4* expression compared to ECs cultured on uncoated and LN411 coated dishes, result in an upregulation of *Dll4* upon *Itgb3* siRNA knock down (b). *Itgb3* knockdown in ECs plated on uncoated dishes does not have an effect on *Dll4* expression (a, b). All quantifications have been set in relation to EC treated with control siRNA in uncoated culture condition.

Despite a consistent induction of *Dll4* expression in HUVECs coated on LN411 (Figure 7.17 a, c), we found a highly variable degree of Dll4 expression in cells coated on LN511. One possibility resulting in the variation of LN511 mediated Dll4 expression is LN511 matrix formation *in vitro*. Laminin a5 is a particularly large glycoprotein, that is more adhesive due to its capability of self-polymerization and network formation when compared to the shorter, truncated laminin a4 isoform. Thus, inconsistency in matrix coating might result in gene expression discrepancies. Therefore, further experiments are required to establish a role of laminin a5 in the induction of *Dll4* expression.

An aggravating factor, as shown in Figure 7.17 b is the knock down efficiency of *Itgb3* siRNA is only around 20% reduction of *Itgb3* mRNA expression. This could explain the variations seen and the rather small effect of *Itgb3* siRNA treatment on LN411 induced *Dll4* expression. In summary, these data require additional experiments to be able to draw solid conclusion.

To investigate whether LN411-induced *Dll4* upregulation can be also mediated by other integrin subunits, we transfected HUVEC cells coated on either matrix with integrin beta 1 (*Itgb1*) and integrin alpha 3 (*Itga3*) siRNA. The following quantification and results were obtained from a single experiment and will need further confirmation.

Although we could detect a sufficient knockdown we did not observe any significant reduction of *Dll4* expression. (Figure 7.17 c-d) Thus, we hypothesise that integrin beta 3 specifically interacts with LN411 and LN511 but transmits diverse functions.

To gain further insights in ITGβ3- LN411 interaction we studied *Dll4* expression of *Itgb3-/-* EC and control wildtype EC. The cells were obtained from S. Robinson and K. Hodivala-Dilke.

Surprisingly, unlike bEND5 and HUVEC cells, control ECs derived by the Hodivala-Dilke lab did not significantly upregulate *Dll4* expression when cultured on LN411 (Figure 7.17 f). The reason for this difference is at present unclear. However, *Itgb3-/-* ECs *Dll4* mRNA expression was reduced by 80% independent of the coated matrix (f). Thus, knockdown or complete absence of *Itgb3* results in a reduced ability of ECs *in vitro* to promote *Dll4* expression.

7.1.8 *Lama4-/-* vessels display disorganized cellular junctions

Recent studies on Dll4/ Notch signalling during vascular development in mouse retina, in zebrafish intersegmental vessels and tumour angiogenesis led to a model that Dll4 expressed by the tip cell activates Notch on the neighbouring stalk cell to suppress tip cell formation in the stalk. The tip cell phenotype is the default response due VEGF-A stimulation, whereas Notch-signalling is cell autonomously required for stalk cell selection and quiescening of the growing sprout. Interfering with Dll4/ Notch has drastic effects on vascular development and genetic ablation of components of this pathway results in early embryonic lethality. Our study revealed that laminin α4 restricts tip cell formation and angiogenic sprouting by modulating Dll4/ Notch signalling. Although we clearly showed a role of ECM molecule laminin α4 in promoting *Dll4* expression, *Lama4-/-* mice are viable and develop a functional vascular system.

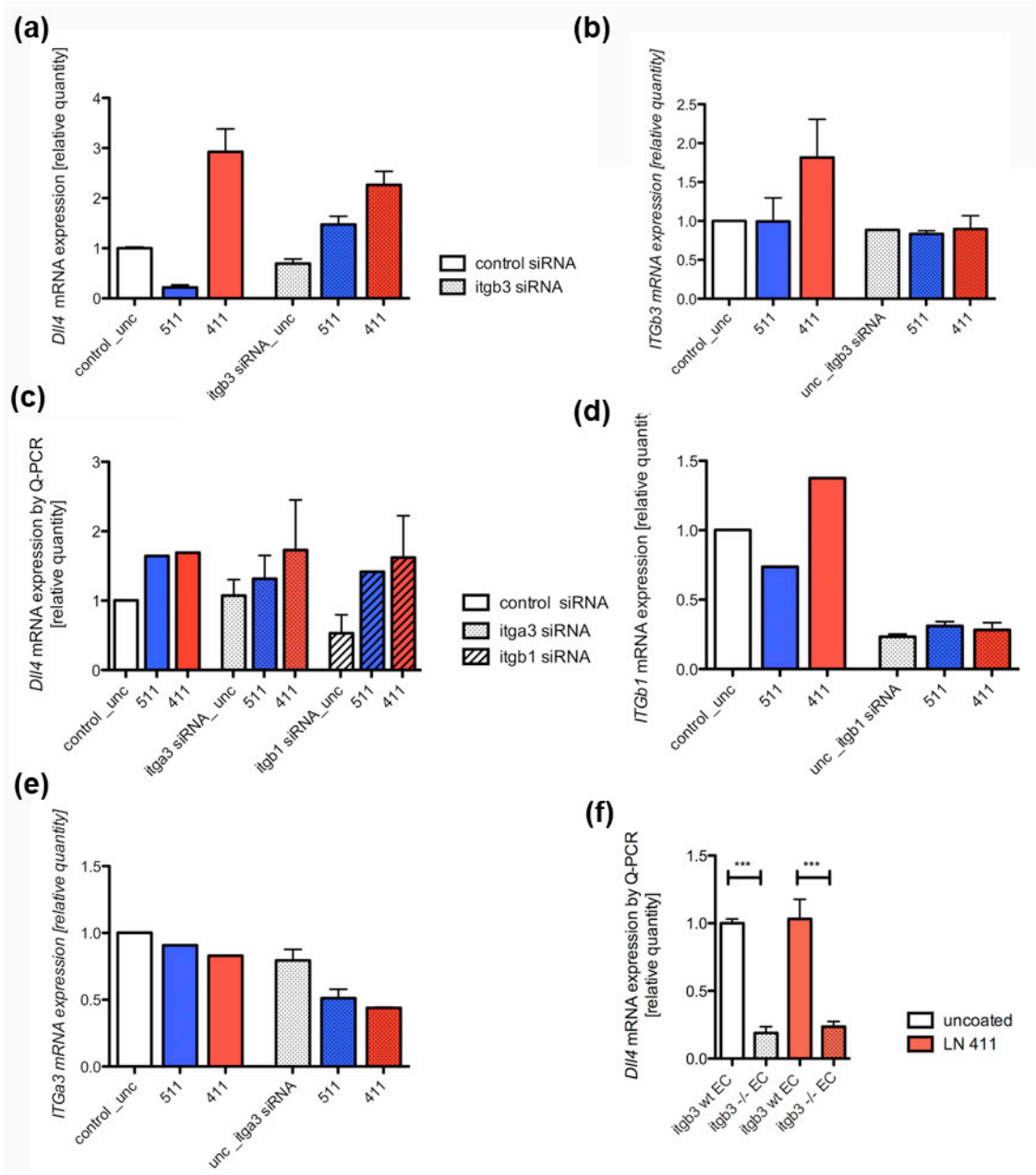

Figure 7.17 Function of integrins in LN411 induced *Dll4* expression

Dll4 mRNA expression was analysed of human ECs (HUVEC) cultured on LN411, LN511 or uncoated dishes after siRNA transfection with *Itgb3* (a), *Itga3* and *Itgb1* (c) for 72h. Efficiency of siRNA treatment and gene silencing was detected by qPCR of the appropriate gene, *Itgb3* (b), *Itgb1* (d) and *Itga3* (e) for cells treated with non-targeting control and OnTarget^{TM} siRNA. Transfection was performed in triplicates, qPCR in duplicates and *Itgb3* knockdown experiment was repeated twice.
Dll4 gene expression was analysed by qPCR of *Itgb3* deficient and control ECs coated on LN411 or uncoated dishes for 24h (f).

Therefore, we propose that laminin α4 is not absolutely essential for Dll4/ Notch signalling and vascular development rather 'helps' to restrict excessive sprouting and vessel formation by promoting *Dll4* expression and therefore more effectively pattern the growing sprout. We speculate that its junctional deposition may have a role in EC polarization and basolateral (basal-apical) EC orientation. Bayraktar and colleagues established a role for Par-1 in cell polarity and showed that Par-1 functions upstream of Notch and is critical for proper localization of the Notch ligand Delta (Bayraktar, Zygmunt et al. 2006). Unfortunately good antibodies and EC polarization marker, like Par-1 and Rab-5 are missing in mouse. Yet, visualization of EC adherent junction molecule VE-cadherin and tight junction molecule claudin-5 elucidated the morphology of EC-EC junction in *Lama4-/-* (Figure 7.18). Although VE-cadherin (a-f) and claudin-5 (g-l) can be localized in both, *Lama4-/-* (a-c, g-h) and control littermates, mice deficient for *Lama4* display a very chaotic pattern of EC junction at the growing vascular front. Control mice exhibit long, continuous junction along the leading vascular sprouts (d, h). In the capillary plexus of control retinas junction appear even more mature and firm (e, i). In contrast, EC junctions of *Lama4-/-* are jagged, disrupted and much shorter (arrows). Consistent with the observed increase in EC proliferation, we detected an enhanced number of EC-EC junction per circumference of *Lama4* deficient vessels (a). This holds true when analysing transverse section of retinal vessels by electron microscopy (data not shown). Preliminary analysis revealed excessive EC junction in the vascular plexus of *Lama4* -/- mice. Combined the increase in endothelial cells and EC-EC junction may account for the increase in vessel calibre. Thus, we hypothesize that lack of firm continuous junction is a consequence of the enhanced sprouting and tip cell formation in *Lama4* deficient mice. However, it is also possible that junctional abnormalities are a primary defect, which in turn impacts on Dll4/Notch signalling, together resulting in the hypersprouting phenotype.

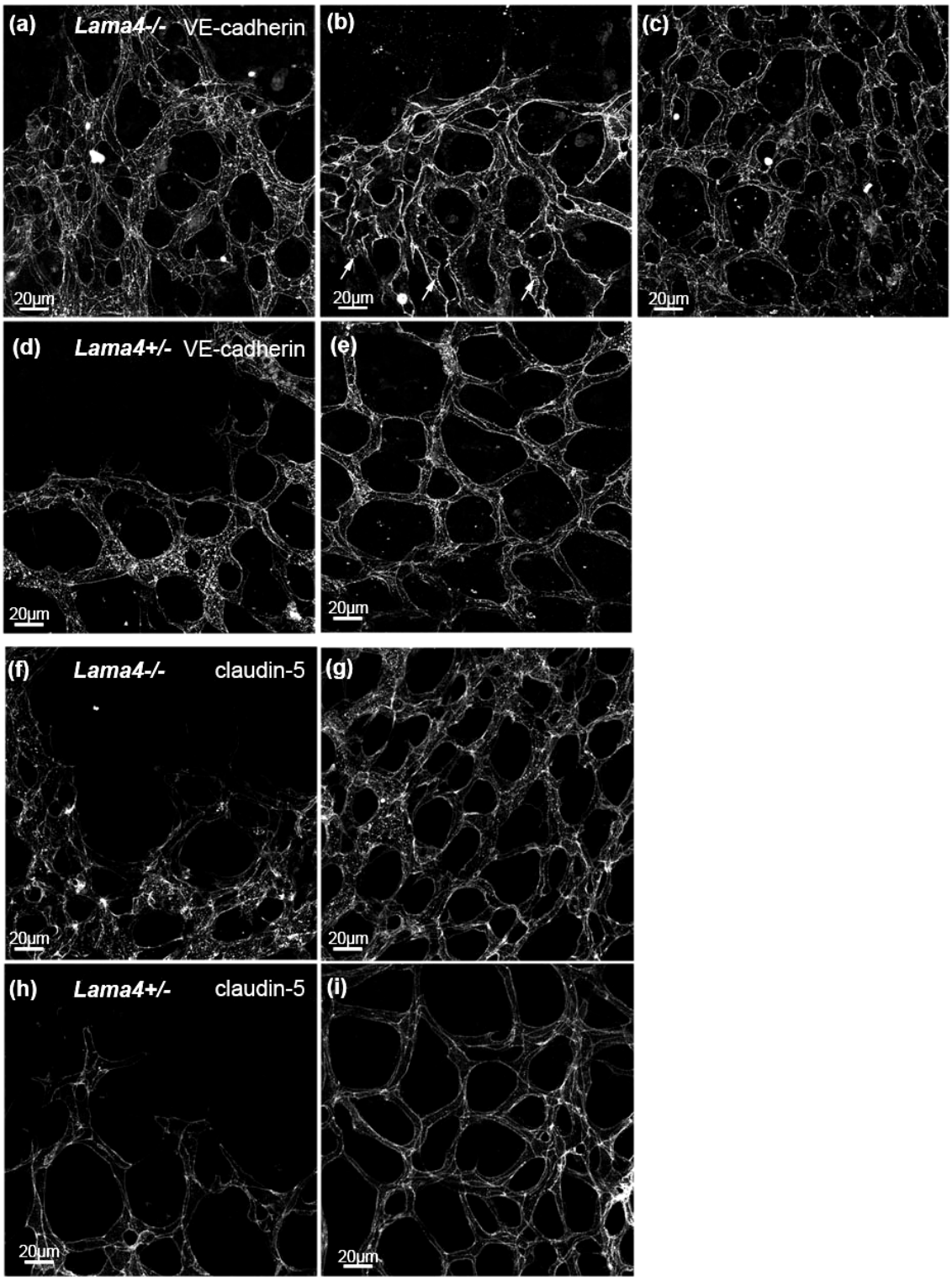

Figure 7.18 Immature EC-EC junction in *Lama4* deficient mice

Immunostaining of junction molecules VE-cadherin (a-e) and claudin-5 (f-i) at the migrating front and the mature vascular plexus in *Lama4* -/- and control P5 retinas. Staining revealed enhanced endothelial cell junctions in *Lama4* -/- (a-c) that appear immature, jagged shaped (arrows, b). In contrast, cell junctions are long and continuous in control vessels (d-e, h-i).

7.1.9 Laminin α2 and integrins β4 and -α7 are dispensable for retinal vascular development

Finally to study whether the similar defects could be observed in other laminin/integrin mutant mice, we analysed the retinal vasculature of laminin α2 (*dy^{2J}/ dy^{2J}*), integrin α7 and integrin β4 mice (data not shown). Deficiency in laminin α1, -γ1 and α5 chains as well as most integrin chains result in early embryonic lethality and does not allow us to study developmental angiogenesis.

IF staining with an antibody directed against laminin α2 showed deposition of laminin α2 in BM of retinal endothelial cells and therefore could have a function in the developing vasculature. Deficiency in laminin α2 chain leads to congenital muscular dystrophy and it has been shown that laminin α4 and integrin α6 are upregulated upon loss of *Lama2* (Sorokin, Maley et al. 2000). Investigation of the retinal vasculature showed no defects in the mature vascular plexus and no abnormal tip cell formation or defects in vessel sprouting (Figure 7.19), indicating that laminin α2 is dispensable for vessel formation in the retina.

Flintoff-Dye and colleagues demonstrated that the α7β1 integrin is important for the recruitment or survival of cerebral vascular smooth muscle cells and that this integrin plays an important role in vascular development and integrity (Flintoff-Dye, Welser et al. 2005). We studied vascular development in the retina of *Itga7* deficient mice. Staining with isolectin and NG2 however revealed no significant differences in vessel formation and pericyte recruitment (Figure 7.20). Given that PC recruitment in the CNS is impaired in *Itga7* deficient mice (Flintoff-Dye, Welser et al. 2005), it is surprising that we could not detect defects in PC investment in the retina. Retinal pericytes are recruited by longitudinal migration of PCs from the CNS. However, pericytes cover the capillary plexus (c, d) and have migrated to a similar extent towards the leading tip cells in *Itga7* -/- mice as seen in control retinas (a, b). These observations indicate that integrin α7β1 does not play a role in retinal PC investment and might be compensated by other integrins.

In summary, loss of laminin α2 or integrin α7β1 does not result in an increased vascular density as seen in *Lama4* deficient mice, suggesting that laminin α4 chain uniquely regulates vessel sprouting by modulating Dll4/Notch signalling.

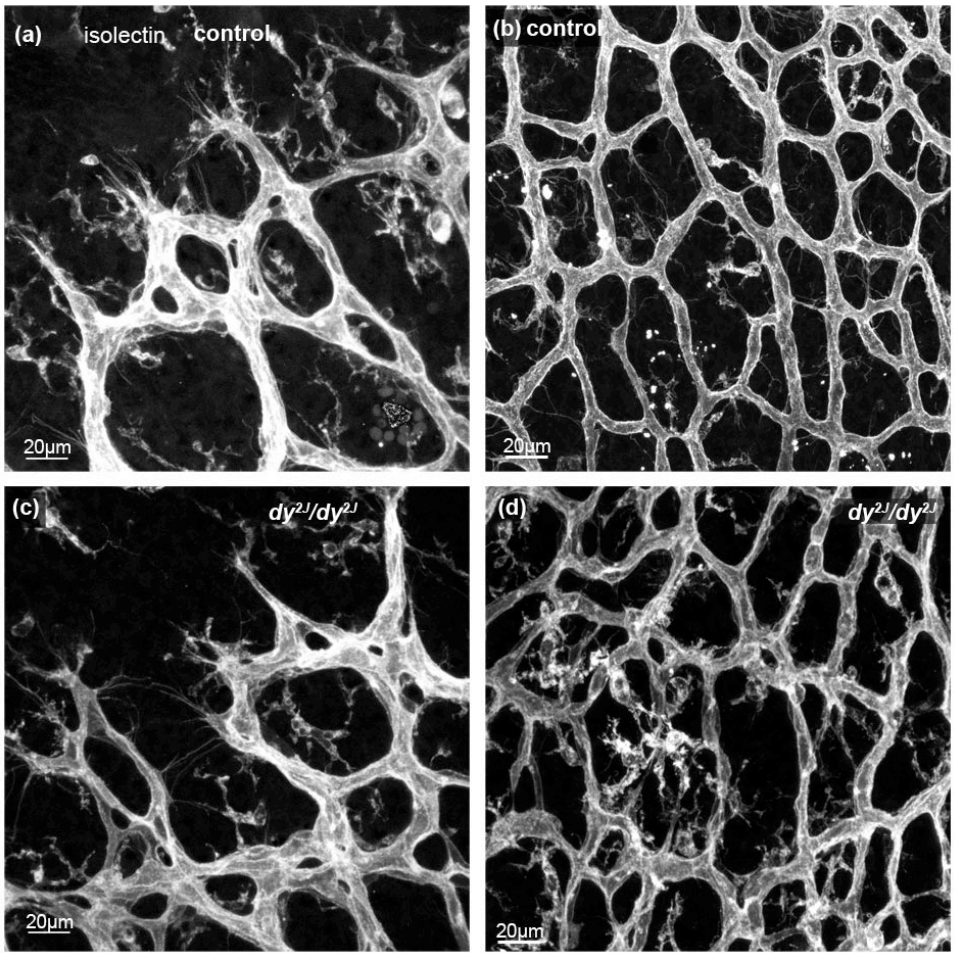

Figure 7.19 Loss of *Lama2* does not affect development of retinal vasculature

Isolectin B4 immunostaining of migrating front and capillary plexus of *Lama2* -/- (c, d) and control P5 retinas (a, b) revealed no defects in vessel formation and sprouting angiogenesis.

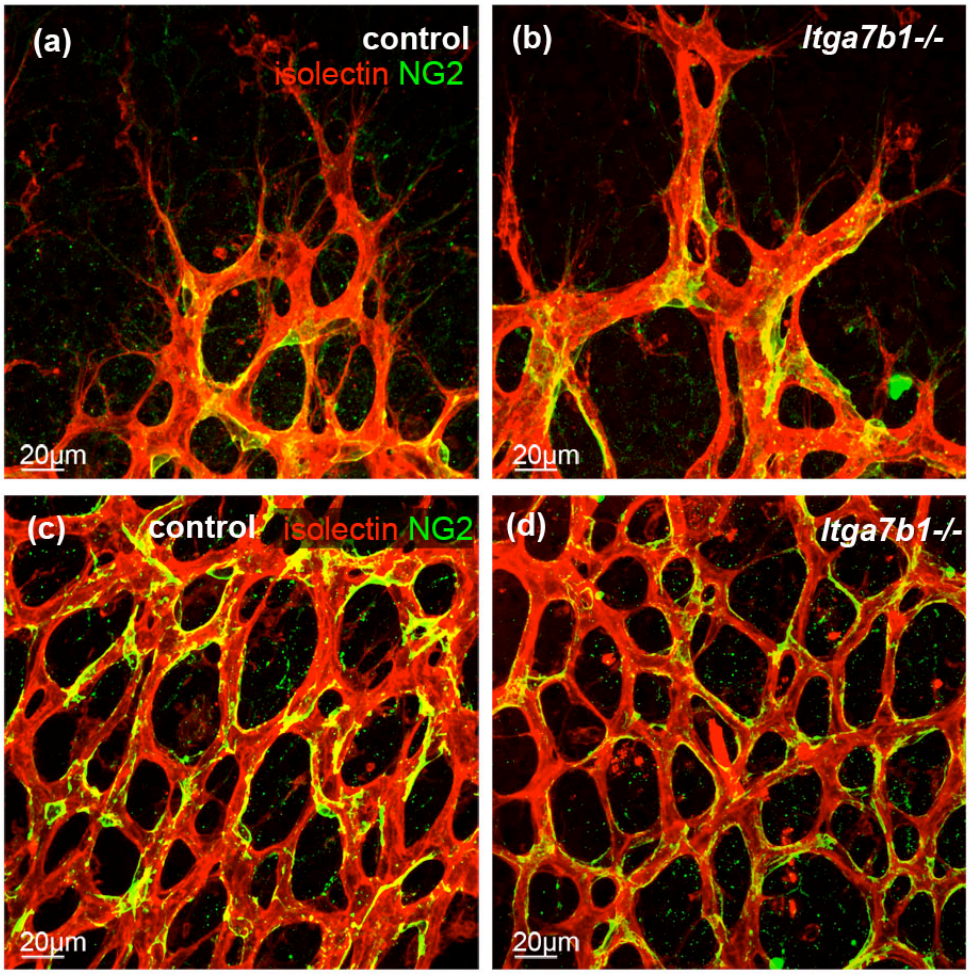

Figure 7.20 *Integrin a7* (*Itga7*) is dispensable for pericyte investment and vessel formation in the retina

Co-labeling of *ITGa7-/-* and control retinal blood vessel (red) with pericytes marker NG2 (green, a-d) showed close association of vessels with pericyes and almost complete coverage of vessels by pericytes in the capillary plexus (c, d).

7.2 Discussion

Our study identified a surprising and new function for the ECM molecule laminin α4 in restricting endothelial tip cell formation *in vivo* by modulating the expression of *Dll4* and thus activity of Notch signalling.

7.2.1 Expression pattern and loss of laminin a4 is phenotypically reminiscent to the vasculature when Dll4/ Notch signalling is disturbed

My expression studies revealed that *Lama4* mRNA is most prominently expressed by leading ECs at the sprouting vascular front and the mature protein is stably integrated in the BM of the growing retinal vasculature. Confocal microscopy showed a distinct expression pattern of laminin α4 at endothelial cell junction *in vitro* and *in vivo* whereas ECM components such as laminin α5, collagenIV and fibronectin are assembled in the BM and deposited at the abluminal basal site of the endothelium.

Detailed high-resolution microscopy showed that the loss of laminin α4 resulted in excessive tip cell formation indicated by ectopic and aberrant filopodia protrusion as well as increased and more widespread expression of the 'tip cell gene' *Pdgfb*. The increased vascular density is accompanied by enhanced EC proliferation as shown by incorporation of BrdU. These findings disagree with the current literature. DeHahn and colleagues demonstrated that the globular G domain of laminin α4 subunit plays a role in maintaining endothelial cell growth and proliferation and that an antibody directed against an integrin-binding region within the G domain of the α4 laminin subunit triggers the mitochondrial-dependent programmed cell death pathway in endothelial cells (DeHahn, Gonzales et al. 2004). The authors further speculate that antibodies against laminin α4 subunit inhibit angiogenesis *in vivo* and assembly of tubular arrays *in vitro* on Matrigel by promoting EC apoptosis.

Further, Lian et al. isolated an active site on the laminin α4 chain globular domain that binds to αvβ3 integrin and generated a corresponding peptide that is able to promote angiogenesis *in vivo* (Lian, Dai et al. 2006). However, neither of these studies identified the underlying mechanism of laminin α4 induced angiogenic responses.

In contrast to the studies mentioned, Davis and Senger propose a model in which collagen and laminin have opposing effects on vascular morphogenesis. Endothelial cells exposed to collagen matrices stimulate vessel formation, initiate sprouting and

migration by interacting with integrin and promoting Cdc42 and Rac1 activity. Conversely, laminin suppresses this morphogenic pathway by induction of Rac and PKA but suppression of Rho activity (Davis and Senger 2005; Davis and Senger 2008). These studies are in line with our finding that laminin α4 rather restricts excessive vessel formation and stabilizes the newly formed vessel *in vivo* than promoting angiogenesis. Still we need to take in consideration that the studies by Davis and Senger are carried out in collagen type-I and Laminin 111 (LN111) matrices. As we learnt from our own studies, different laminin isoforms can have opposing effects on ECs. Endothelial cells cultured on LN511 form a monolayer with firm endothelial junction while ECs coated in LN411 appear to lose their contact inhibition and exhibit a migratory phenotype.

When analyzing vessel migration in the retina of Laminin α4 deficient mice, we noticed a mild delay in the expansion of vessel towards the periphery. Unlike in mice deficient of astrocytic FN production, we could not detect reduced VEGFR2 signalling and activity as shown by immunoblotting. We also did not observe reduced levels of PI3K activity analyzed by phosphorylation of downstream target AKT. In fact, we would argue that we see a slight increase in VEGFR2 protein expression levels that possibly correlate with the increased density and vessel area. However, it still remains unclear whether there is a direct correlation between VEGFR2 levels and vessel quantity. Therefore, we argue that the mild delay in vessel migration reflects the developmental delay reported for *Lama4* null mice (Thyboll, Kortesmaa et al. 2002) rather than a function of laminin α4 in EC migration.

Defective pericyte (PC) recruitment results in hyperplasia and increased ECs proliferation (Hellström, Kalén et al. 1999). However when analysing PC coverage in *Lama4-/-* mice we observed a normal PC investment and close association of PC with the endothelium. Therefore, we concluded that increased EC proliferation and excessive sprouting is not due to disturbed EC-PC interaction.

Thyboll and colleagues showed that capillaries of the lower back muscle in laminin α4 deficient mice displayed a structurally abnormal BM and reduced expression of BM components, suggesting that laminin α4 is essential for vessel integrity. We also observed an abnormal deposition and assembly of BM components in the retinal vasculature. These findings are in line with a study by Jakobsson and colleagues, 2007, showing that embryoid bodies deficient in laminin chain γ1 differentiate and form vessels that recruit PC but almost fully lack collagenIV

deposition (Jakobsson, Domogatskaya et al. 2007). Nidogen-1 and -2 mediate the formation of a ternary complex with laminin and collagenIV, while heparan sulfate proteoglycans are integrated into the laminin-collagenIV network. These data indicate that in the absence of laminin α4, collagenIV is reduced and fails to integrate in the BM.

The phenotypical reminiscence of the retinal vasculature in *Lama4-/-* mice and mice defective in Dll4/Notch signalling led us to the hypothesis that laminin α4 may modulate this pathway.

At the present time, the precise molecular mechanism still remains unclear however, we propose that laminin a4 may (1) directly activate Dll4/Notch signalling, (2) regulate Dll4 expression by promoting integrin/ VEGFR2 signalling or (3) promote Dll4 protein localization at EC junction.

7.2.2 Alternative 1: Laminin a4 directly activates Notch

The transmembrane protein, Dll4 activates Notch in the neighbouring cell by direct cell-cell contact. During retinal vascular development, *Dll4* expression is dynamically regulated and most prominent in the ECs of actively growing capillaries at the leading front of the superficial vascular plexus. Coinciding with the cessation of angiogenic sprouting *Dll4* expression is lost in the maturing veins and capillary plexus (Hellstrom, Phng et al. 2007); (Lobov, Renard et al. 2007). This pattern of Dll4 expression strongly resembles *Lama4* mRNA expression, which is also most strongly present at endothelial tip cells. Laminin α4 deposition at endothelial junction led us to speculate that laminin may directly interact with Dll4 at EC-EC junction.

Our analysis revealed that mice deficient in *laminin a4* express reduced mRNA levels of Notch ligand *Dll4* as well as Notch downstream targets such as *Hey1, Hey2* and *Nrarp*. The altered gene expression profile in *Lama4-/-* retinas is comparable to mice deficient in one allele of *Dll4* or mice challenged with pharmacological inhibitor γ-secretase (Hellstrom, Phng et al. 2007); (Suchting, Freitas et al. 2007).

Conversely, ECs cultured on Laminin-411 induce *Dll4* expression in a Notch dependent manner.

Dll4 overexpression (*mDll4*) resulted in abundant deposition of ECM molecules and an upregulation of mRNA expression levels of laminin, collagenIV and fibronectin but a decrease in the expression of matrix degrading enzymes, MMPs (Trindade, Kumar et al. 2008), indicating that Notch signalling regulates ECM molecules.

Recent data implicated the co-expression of Notch and integrins and the activation of integrins by Notch signalling (Campos, Decker et al. 2006); (Hodkinson, Elliott et al. 2007); (Leong, Hu et al. 2002). According to Campos et al., β1-integrins may affect Notch signalling through physical interaction (sequestration) of the Notch intracellular domain fragment by the cytoplasmic tail of the β1-integrin and secondly, by affecting trafficking (internalization) of the Notch intracellular domain (NICD) via caveolin-mediated mechanisms (Campos, Decker et al. 2006). This event likely requires the β1-integrin binding to ECM component. The laminin α4 subunit binds and interacts with integrin α6β1, α3β1, αvβ3 (Gonzalez, Gonzales et al. 2002); (Lian, Dai et al. 2006), and therefore, laminin α4 could possibly regulate Dll4/Notch signalling via integrin interaction.

Alternatively, Laminin α4 directly activates Dll4 expression by binding Dll4 and/ or Notch. Although we have no evidence for or against this hypothesis, both laminin a4 and Dll4 contain EGF-like repeats which may mediate binding and interaction.

Dixelius and colleagues suggested that laminin may play a fundamental role in angiogenesis by directly affecting gene and protein expression profiles in ECs. Studying multiple *in vivo* and *in vitro* angiogenesis assays the authors reported that LN111 induced angiogenesis and promoted EC differentiation in the absence of the growth factor FGF-2. Further, vascular development was stimulated in a synergistic manner by FGF-2 and LN111 and the formation of tubular structures induced by LN111 was accompanied by increased expression of the Notch ligand Jagged-1 (Dixelius, Jakobsson et al. 2004). LN111 mediated angiogenesis does not alter endogenous laminin production and also does not affect ERK and AKT phosphorylation, indicating that LN111 does not converge with normal growth factor –induced signalling. Taken together with our findings, the data suggest that laminin induces expression of Notch ligands independently of additional growth factors such as VEGF and FGF.

7.2.3 Alternative 2: Laminin α4 regulates Dll4 expression by promoting integrin/ VEGFR2 signalling

Multiple studies find co-dependence or regulation of Dll4/ Notch signalling and VEGFR2 (Suchting, Freitas et al. 2007); (Lobov, Renard et al. 2007).

LN411 induced *Dll4* expression *in vitro* correlates with increased *Vegfr2* mRNA expression levels. Consistent with our observation, Lobov demonstrated that blocking

Dll4 expression by neutralizing antibodies decreased *Vegfr2* mRNA expression (Lobov, Renard et al. 2007).

The current model of tip cell formation and vascular sprouting suggests that VEGF/VEGFR2 signalling induces Dll4 expression in leading tip cells, activating Notch signalling in adjacent cells, which in turn results in down regulation of VEGFR2 and induction of stalk cell phenotype.

Our analyses revealed that LN411 promotes *Dll4* expression by a mechanism that is not entirely dependent on VEGF/VEGFR2 signalling. While baseline *Dll4* mRNA expression in EC is completely VEGF/VEGFR2 dependent, LN411 induced *Dll4* expression cannot be fully inhibited by neutralizing VEGFR2.

In addition, *Dll4* mRNA expression is not upregulated by VEGF-A. Concomitantly with initiating angiogenesis, VEGF-A upregulates Dll4 expression in the endothelium of an angiogenic sprout (Lobov, Renard et al. 2007). However, VEGF-A and hypoxia expression are unaffected in *Lama4*-/- mice and consistently, LN411 induced *Dll4* mRNA expression in ECs *in vitro* occurs independently of low oxygen levels and without addition of VEGF-A.

Further, β3 integrin forms a complex with VEGFR2 and promotes VEGFR2 phosphorylation (Soldi, Mitola et al. 1999); (Mahabeleshwar, Feng et al. 2007). Harrington and colleagues reported that Dll4 regulates the expression of endothelial integrin β3 *in vitro* (Harrington, Sainson et al. 2007).

The co-localization of Dll4, laminin and β3 at the cell membrane, and possibly at EC-EC contacts led to the hypothesis that laminin interacts with integrin β3 and thereby, modulates Dll4/Notch signalling. Preliminary data using integrin β3 siRNA knockdown indicate that LN411 induced *Dll4* expression is reduced upon blocking β3 integrin.

The expression of integrin β3 and Dll4 is directly regulated by Forkhead transcription factor*, Foxc2* (reviewed in (Kume 2008). Recent data imply that Foxc2 interacts with VEGF signalling to induce Dll4 expression (Hayashi and Kume 2008) and directly induces transcription of integrin β3 by activating their promoters via Foxc-binding elements (Hayashi, Sano et al. 2008). Therefore, one could speculate that Foxc2 is the transcriptional regulator of both, integrin β3 and Dll4, and mediates the angiogenic response.

7.2.4 Alternative 3: Laminin α4 promotes Dll4 protein localization by interacting at endothelial junction

Alternatively, we propose that laminin α4 may function in cell polarity and membrane-domain targeting, bringing Dll4 to the lateral cell membrane and thereby, regulating Dll4 availability and Notch activation in neighboring ECs.

Endothelial junctions contribute to the maintenance of apical-basal cell polarity (reviewed in (Dejana, Orsenigo et al. 2009); (Desai, Gao et al. 2009). Cell polarity is further established by the formation of a vascular lumen and the deposition/ assembly of ECM at the abluminal site of the endothelium. During zebrafish somitogenesis Notch and integrin α5-dependent cell polarization and FN assembly occurs concomitantly and interdependently during border morphogenesis (Julich, Geisler et al. 2005).

Many of epithelial cell processes, including cell motility and intracellular signalling rely on the polarized distribution of plasma membrane proteins. Recent studies revealed that apical localization of Notch depends on polarized exocytosis and transcytosis in *Drosophila* epithelial cells (Sasaki, Sasamura et al. 2007). Disruption of apical polarity failed to localize Notch and delta to the correct apical plasma membrane and adherent junctions. Bayraker and colleagues supported the finding showing that Par-1, a serine/ threonine protein kinase is required for the establishment of cell polarity in embryonic *Drosophila* epithelia. Par-1 also functions upstream of Notch and is critical for proper localization of the Notch ligand Delta and in addition promotes Notch-mediated lateral inhibition during embryonic neurogenesis (Bayraktar, Zygmunt et al. 2006).

We therefore hypothesized that ECM molecule laminin α4 might play a role in EC polarization and the correct localization of Dll4 to the membrane. Investigation of EC junctions by immunostaining with claudin-5 and VE-cadherin indicated that *Lama4* deficient vessels exhibit an increased number of EC junction that appear chaotic, immature and disorganized. Preliminary results from our ongoing analysis of *Lama4-/-* retinal vessels using electron microscopy support this notion (data not shown).

7.2.5 Future perspective

Preliminary data indicate that laminin α4 may bind to integrin β3 and thereby promoting integrin/ VEGFR2 crosstalk resulting in increased *Dll4* expression. However, this hypothesis is based on the assumption that laminin α4 and integrin β3 are expressed in the same cell, i.e. leading endothelial tip cells. Therefore, precise expression studies of integrin β3 will be of interest to investigate co-expression of

laminin α4 and integrin β3. Further, analyses of potential complex formation and/ or co-localization of Dll4, integrin β3 and laminin α4 at endothelial junction would be helpful to gain insight in a potential interplay between these molecules.
Detailed investigations of the role of integrin β3 in mediating Dll4 expression are necessary. *Itgb3* deficient endothelial cells will be helpful in this analysis. Can *Itgb3* deficient cells bind, interact and communicate on a laminin α4 matrix. Is *Dll4* mRNA expression still induced in these cells when plated on LN411? Is VEGFR2 required in this process? Although preliminary data do not support the hypothesis that loss of *Itgb3* results in excessive sprouting as seen in *Lama4* -/-, it will be interesting to analyse mRNA expression levels of *Dll4*, Notch downstream targets and *Vegfr2* in *Itgb3* null mice.

VEGFR2 functions up-and downstream of Dll4/ Notch signalling pathway. Activation of Notch modulates VEGF receptor expression levels; VEGFR2 mRNA levels are quantitatively downregulated while VEGFR1 expression is increased in endothelial cells with active Notch signalling (Suchting, Freitas et al. 2007); (Hellstrom, Phng et al. 2007). Therefore, it might be of interest to analyse the spatial expression and distribution of these receptors in *Lama4* -/- mice. Laminin α4 could have a role in locating VEGFRs to the cell surface and bring the receptor to the junction to form a VEGFR/ VE-cadherin complex and thereby, promote Dll4/ Notch signalling.

Laminin α4/ integrin interaction may also play a role in endothelial polarization. Loss of laminin assembly by Rac1 results inversion and replacement of apical pole position during cyst development in *Drosophila* (O'Brien, Jou et al. 2001). The mis-assembly correlates with reduced integrin expression, and lack of lumen formation due to lack of apical-basal polarization (O'Brien, Jou et al. 2001). Therefore, it would be interesting to study vessel and lumen formation of *Itgb3* and *Lama4* deficient endothelial cells in a 3D setting. One would also like to investigate the cell-autonomous function of laminin a4 in a 3D sprouting model described by Jakobsson and colleagues (Jakobsson, Kreuger et al. 2007). It would be of interest to analyse *Lama4* -/- embryoid bodies differentiating in vascular sprouts and to monitor cell migration, remodelling and sprouting events in high magnification. The lack of firm endothelial junction in *Lama4* -/- retinas could also reflect increased active migration which could be addressed in a 3D *in vitro* model.

Studying the dynamics of *Lama4* embryonic stem (ES) cells in chimeric embryoid bodies containing colour-coded wildtype and laminin α4 ECs will allow us to study the cellular behaviour and competition of *Lama4*-/- cell during sprouting.

Lastly, transduction of extracellular matrix signals through integrins requires intracellular interaction of the cytoplasmic tail of integrins with cellular proteins. Integrin-linked kinase (ILK) binds to β-subunit of integrins and mediates cell- adhesion, migration and signal transduction (Kaneko, Kitazato et al. 2004).
Therefore, it would be interesting to explore whether ILK has a function in mediating Laminin/ Integrin induced Dll4 expression.

7.2.6 Summary

Taken together, my study revealed for the first time that the ECM molecule laminin α4 functions in restricting excessive tip cell formation and enhanced sprouting by modulating Dll4/Notch signalling (summarized in Figure 7.21). Laminin α4 and Dll4 are upregulated in many tumours correlating with enhanced pathological angiogenesis and increased tumour growth and metastasis (Zhou, Doi et al. 2004); (Thurston, Noguera-Troise et al. 2007), suggesting that a deeper understanding of the co-dependence of LN411 and Dll4 may have substantial pathological relevance. Further analyses to fully understand the molecular mechanism are necessary. Nevertheless, our present results combined with recent findings in integrin-Notch interaction indicate that laminin potentially modulates Dll4/Notch signalling via integrins.

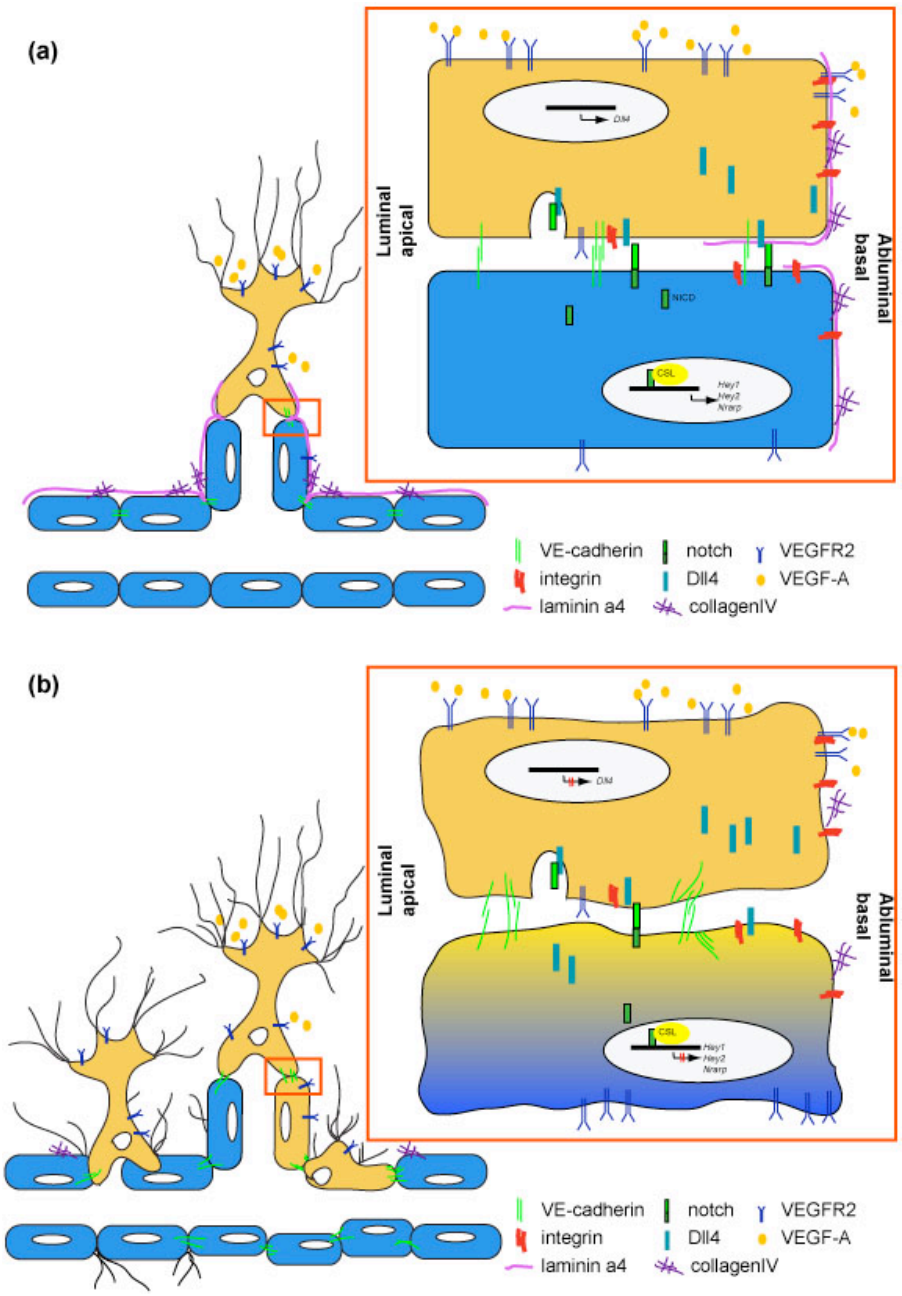

Figure 7.21 Proposed model of laminin α4 modulating Dll4/Notch signalling

(a) VEGF expressed ahead of the growing vasculature binds to endothelial tip cells and thereby, triggers VEGFR2 signalling. Dll4 expression in tip cells is upregulated by VEGF and activates Notch signalling by binding to Notch receptors in neighbouring ECs. Notch intracellular domain (NICD) is translocated to the nucleus and initiates the expression of Notch target genes (such as Hey1, Hey2 and Nrarp). The induction of Notch is acquired to restrict sprouting.
Laminin a4 and itgb3 are located at EC junction and laminin a4 is deposited at the abluminal side of the endothelium.
(b) Loss of laminin a4 results in excessive filopodia formation and increased sprouting. We propose that laminin a4 is required for EC polarization and its absence fails to locate Notch ligand Dll4 to the cell membrane. Hypersprouting correlates with a decrease of Dll4 mRNA expression and reduced expression of Notch targets due to reduced Dll4/ Notch signalling at EC-EC contacts.

8 Peripheral mural cell recruitment requires cell-autonomous heparan-sulfate

8.1 Introduction

The recruitment of pericytes (PC) is required to stabilize the newly formed angiogenic sprout and is essential to establish a functional vasculature. Loss of PC attachment and engagement to the blood vessel is associated with many vascular diseases and pathological condition such as diabetic retinopathy and cancer. In fact, the degree of PC dissociation in the tumour vasculature correlates with tumour metastasis.

Various pathways have been described to play a role in PC investment, proliferation and attachment of PCs to the endothelium, including TGF-β and PDGF-B signalling pathway. Based on phenotypical observations, Hellstrom et al. demonstrated the fundamental role of paracrine signalling of PDGF-B expressed by EC via its receptor PDGFR-β (expressed by mural cells) in mural cell (MC) recruitment. Deletion of *Pdgfb* or *Pdgfrb* leads to embryonic lethality due to vascular defects, with a significant reduction of MC and loose attachment of present MCs resulting in abnormal vessel morphology and leaky blood vessels (Hellstrom, Gerhardt et al. 2001).

The growth factor PDGF-B contains a highly conserved C-terminal sequence, so called retention motif, mediating the binding to heparan sulfate proteoglycan (HSPG) within the cell, anchored to the cell surface, or secreted in the extra cellular matrix. Mice deficient in the PDGF-B retention motif (*Pdgfb ret*/*ret*) display similar, but less severe vascular defects observed in the *Pdgfb*/ *Pdgfrb* null mice. However, the lack of HS bound PDGF-B leads to detachment of MCs Lindblom (Lindblom, Gerhardt et al. 2003) consistent with the idea that matrix components retain a PDGF-B gradient that is required for proper MC recruitment and adhesion to the vessel.

Multiple studies highlighted the importance of HSPG interacting with various growth factors, morphogens and matrix molecules. In order to specifically bind and interact with the large variety of molecules, the HS chain consists of a highly complex structure, involving N-and O-sulfation (Esko and Lindahl 2001).

Interestingly, we have been able to show that an altered HS biosynthesis by global reduction of N-sulfation on the HS chain leads to mural cell detachment, and delayed MC migration, but not proliferation. Appropriate N-sulfation is required to retain

PDGF-B and activate PDGFR-β in MCs *in vivo* (Abramsson, Kurup et al. 2007). Therefore, HSPG are important co-receptors and activators of signalling events.

Jakobsson and colleagues demonstrated *in vitro* that pericytic HS is sufficient to support vessel formation in embryoid bodies deficient in endothelial N-sulfated HS. These studies illustrated that HS presented *in trans* can fully support VEGF-A signalling (Jakobsson, Kreuger et al. 2006).

However, we lack information on the cell specific contribution of HS in normal vascular development and it has remained unclear whether pericytic HS is required for vessel formation and stabilization *in vivo*. This study address the relevance of pericytic HS in MC recruitment and attachment in order to stabilize newly formed vessels.

8.2 Results

8.2.1 Genetic approach for the deletion of HS in MCs

The *Ext1* gene encodes for the key glycosyltransferase that is essential for elongation of the dissacharide backbone chain of HS. The EXT1 protein forms homodimers or heterodimers with EXT2 and resides as single pass transmembrane protein in the Golgi apparatus. Deletion of *Ext1* leads to complete loss of HS. The original observation that loss-of function mutations cause multiple exostosis in humans led to the name Exostosis proteins (EXT1). In order to study the functional role of MC derived HS in angiogenesis, we deleted the floxed *Ext1* allele (Inatani, Irie et al. 2003) selectively in MC using transgenic *Pdgfrb Cre* mice (Foo, Turner et al. 2006). This genetic approach results in the excision of *Ext1* in MCs (for simplicity we will refer to *Pdgfrb Cre+/Ext1*$^{flox/flox}$ mice as *Ext1*^{MCko}).

We initially confirmed the selectivity of Cre mediated deletion in MC at embryonic stages by crossing the *Pdgfrb Cre* to the *ROSA26R eYFP* reporter line (Soriano et al., 1999). The *ROSA26 eYFP* mice carry a targeted insertion of an enhanced yellow fluorescent protein (EYFP), preceded by a loxP-flanked (floxed) strong transcriptional termination sequence (tpA), into the ubiquitously expressed ROSA26 gene locus. The ROSA26 allele terminates transcription prematurely, but when mice are crossed with Cre-expressing transgenic mice e.g. *Pdgfrb Cre*, the Cre-mediated excision of the floxed termination sequence leads to YFP expression. Thus, these doubly transgenic animals express e*YFP* only in the cells that have expressed *Pdgfrb Cre*, as well as in all of their daughter cells (Srinivas, Watanabe et al. 2001).

Analysis of the embryonic back and skin of an E13.5 embryo (Figure 8.1 a-b) as well as skin samples of the vasculature of an E17.5 embryo (c) reveals nuclear YFP staining in mural cells closely attached to blood vessels (dashed line). The YFP expression pattern (a-c) closely resembles MC staining, indicating specific and efficient Cre-mediated recombination. These data are in line with findings of Abraham and colleagues showing a highly specific deletion of itgβ1 in mural cells at embryonic stage E17.5 but not endothelial cells using the *Pdgrfb* Cre line (Abraham, Kogata et al. 2008).

In addition we studied *Pdgfrb Cre* specificity in E10.5 hindbrain samples (d-e). YFP expression is strongly observed in *ROSA26 eYFP/ Pdgfrb Cre* hindbrain samples (e). Co-labelling with isolectin (red, d) to visualize ECs revealed YFP expression exclusively in pericytes and not in the endothelium of the hindbrain vasculature.

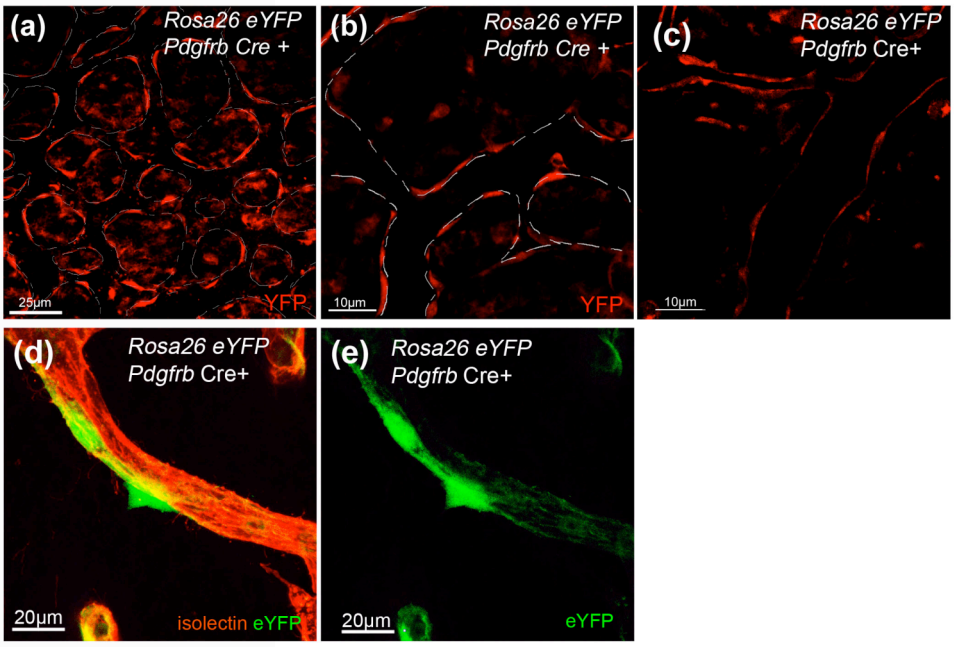

Figure 8.1 *Pdgfrb* Cre line specificity detected by *ROSA26 eYFP* expression in embryonic skin and hindbrain

Crossing of reporter line *ROSA26 eYFP* with *Pdgfr* Cre mice revealed pericyte specific eYFP (red) staining in embryonic skin samples at E13.5 (a, b) and E17.5 (c).
Co-labeling of embryonic hindbrains of *Pdgfrb* Cre *ROSA26 eYFP* at E10.5 with Isolectin B4 (red, d) revealed pericyte specific expression of eYFP (green, d, e).

To further evaluate the specific loss of HS in pericytes, we analysed HS expression in paraffin section of *Ext1*^{MCko} and control embryos.

HS staining (green) confirms substantial loss of HS in the MC compartment of major arteries and veins of *Ext1*^{MCko} embryos (Figure 8.2 a-b). The 10E4 antibody is widely used to detect HS and recognizes an epitope that is destroyed by N-desulfation (David, Bai et al. 1992). Co-labelling of HS (10E4) and MC using NG2-antibodies that selectively label MC in many tissues (Ozerdem, Grako et al. 2001) indicates that a small fraction of MCs does not recombine the floxed *Ext1* allele (d, arrow). Alternatively, slow HS turnover and more recent recruitment could explain residual HS as more cells of the outermost smooth muscle layer around arteries retain HS staining (b, d). High resolution analysis of vessels in the embryonic skin revealed NG2 positive cells lacking HS expression (e, f) whereas pericytes in control samples deposit both, HS and NG2 (g, h). Effective depletion of HS from most MCs allows us to address for the first time the functional importance of MC HS expression for vascular development.

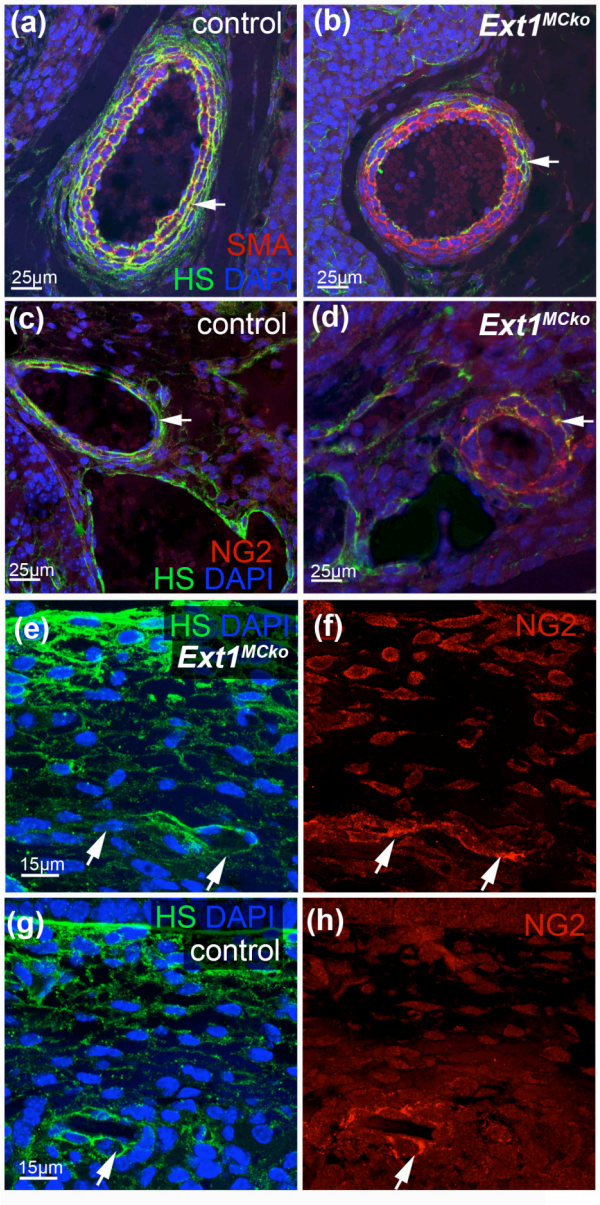

Figure 8.2 Reduced heparan sulfate (HS) expression in *Ext1*^{MCko} embryos

Sections of E13.5 embryos were stained with an antibody directed against the HS chain (green), NG2 (red) and DAPI. Vascular smooth muscle cells (vSMCs) of the dorsal aorta (a, b) have strongly reduced HS deposition with residual HS on the most outer layer of vSMCs in *Ext1*^{MCko} embryos (arrow, b).
Immunostaining revealed loss of HS in vSMC and pericytes of *Ext1*^{MCKO} (b, d) while HS is strongly expressed in control littermates (a, c) and localized at the abluminal surface of mural cells (MCs).
High magnification imaging of capillaries in the embryonic skin (e-h) showed co-localization of HS and NG2 in control sections (arrows, g-h) while NG2 positive cells in *Ext1*^{MCko} sections lack HS (arrows, e-f).

8.2.2 MC HS is not required for MC recruitment in the CNS

Ext1^{MCko} embryos harvested at E11.5 are macroscopically indistinguishable from control littermates. We labelled hindbrain samples with isolectin-B4 to visualize ECs (Figure 8.3 a-h) and NG2 antibody to detect MCs (Figure 8.3 b, f). Overview images of the developing vessel network in the hindbrain show no significant differences in vessel formation, patterning and vessel density (Figure 8.3 a, e).

Confocal microscopy analysis of *Ext1*^{MCko} hindbrains reveals that MCs are recruited to the blood vessels and closely associated with the endothelium, as seen in control littermates (Figure 8.3 b, f). Detailed analysis of MCs investment at the midline (k-l) and migration of MCs towards the periphery of hindbrains (i-l) shows no substantial differences. This lack of phenotype stands in marked contrast to findings in mice deficient in PDGFR-β signalling, such as *Pdgfrb*$^{-/-}$ (n), the PDGF-B retention motif knockout (Lindblom, Gerhardt et al. 2003), and the *Ndst1*$^{-/-}$ mice with a global reduction in *N*-Sulfated HS (Kurup, Abramsson et al. 2006; Abramsson, Kurup et al. 2007). Both the PDGF-B retention motif knockout and the *Ndst1*$^{-/-}$ mice show defective pericyte recruitment due to absent or reduced ability of PDGF-B to bind to HS (Kurup, Abramsson et al. 2006; Abramsson, Kurup et al. 2007).

To address whether the attached MCs in the *Ext1*^{MCko} indeed lack HS expression, we labelled the hindbrains with the 10E4 antibody (Figure 8.3, Figure 8.4). In control hindbrain samples, we detect HS in the endothelium as well as in MCs, particularly at the interface of ECs and MCs (Figure 8.3 f, h arrows and Figure 8.4). Interestingly, hardly any HS could be seen in the abluminal BM of pericytes in *Ext1*^{MCko} and control vessels. In contrast to control PCs, less HS decorates the membrane of MCs in the mutant and significantly less HS is found at the abluminal side of the endothelium of mutant vessels (arrows, Figure 8.4 a-d) suggesting that pericytic HS is indeed absent and normally contributes to the BM surrounding the vessel. These results indicate, however, that pericytic HS production is not required for MC recruitment, at least in the context of sprouting angiogenesis in the developing CNS.

Therefore we propose that endothelial HS production is essential for PC investment in the CNS. Loss of HS binding motif in PDGF-B retention knockout as well as reduced N-sulfation of HS show defective PC recruitment, highlighting the importance of HS in this process. To further test this hypothesis we are currently generating mice deficient in EC HS production. By crossing *Ext1* floxed mice with endothelial specific *PDGFB* Cre

ERT mouse line (Claxton et al., 2008) we generate mice that lack HS biosynthesis in cells expressing *Pdgfb*. To evaluate EC HS function during vascular development we induced Cre mediated deletion of *Ext1* by administration of 4OH tamoxifen at various embryonic stages. However, despite several attempts we did not achieve sufficient deletion of endothelial HS to study the effect on PC recruitment in the embryonic hindbrain (Figure 8.5). Heparan sulfate (green, d, h) can still be detected to a similar extent in mice treated with 4OH tamoxifen (h) as in control hindbrains. In addition, vessel morphology appears normal (a-h) and pericytes closely align to vessels (c, g).

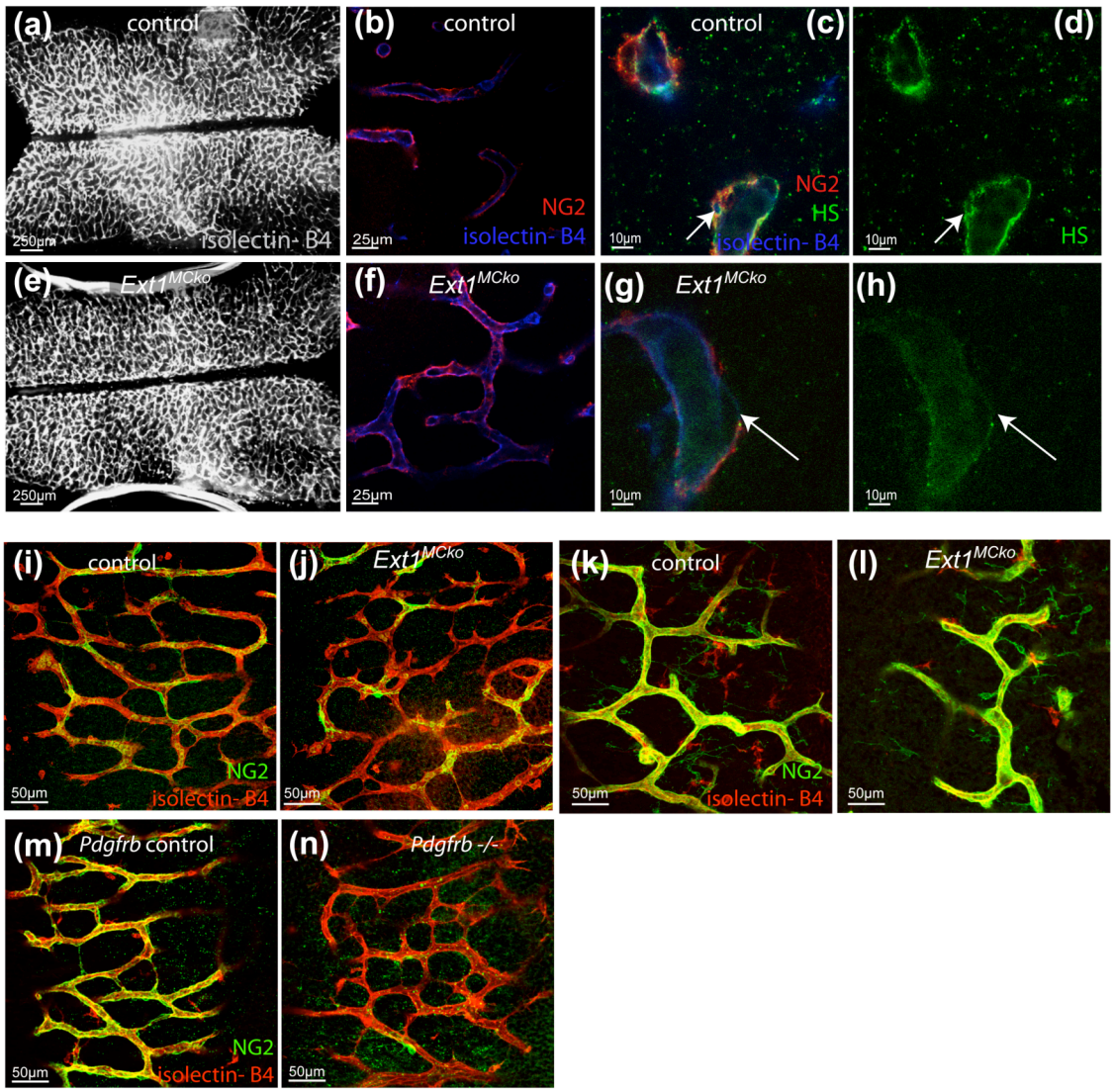

Figure 8.3 Blood vessel formation and MC recruitment in the CNS

Overview images of the vasculature from control (a) and *Ext1*^{MCko} (e) hindbrains. Wholemount hindbrains of E11.5 embryos were labelled with isolectin-B4 (blue) and NG2 (red) to detect ECs and MCs, respectively. High-resolution imaging revealed recruitment and attachment of MCs in *Ext1*^{MCko} (f) as well as control (b) embryos. Immunofluorescence staining with HS (green) confirmed the lack of pericytic HS (arrow, g, h), while HS expression is still detectable in MCs of control blood vessels (c, d).
Comparison of MC coverage in *Ext1*^{MCko} and control hindbrains at the periphery (i, j) and midline (k, l) showed no differences in MC recruitment and migration by co-labeling vessels (red) with pericyte marker NG2 (green). In contrast, *Pdgfrb* -/- hindbrains (n) lack MC coverage when compared to control littermates (m).

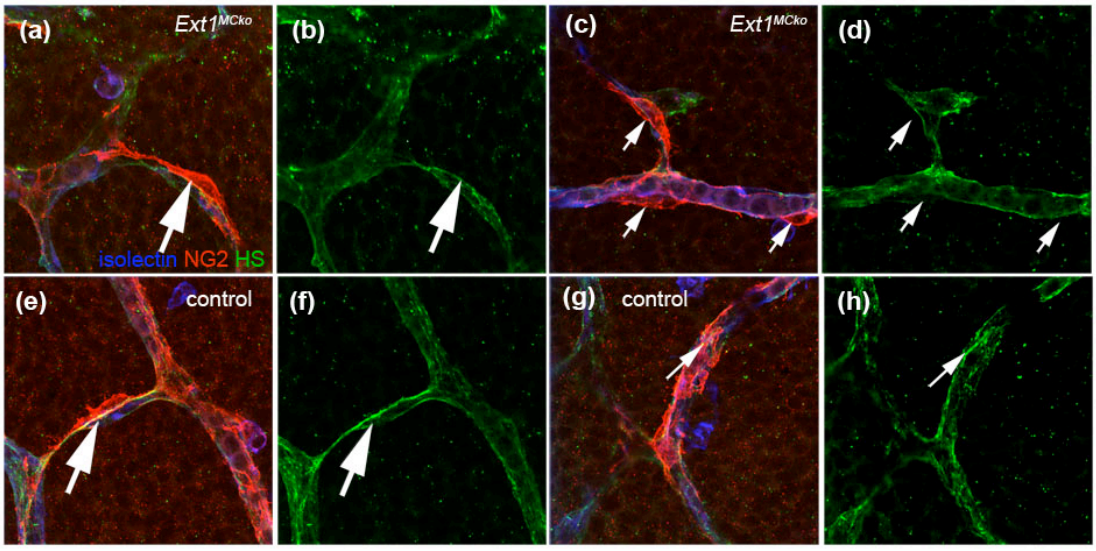

Figure 8.4 HS expression in hindbrain of *Ext1*^{MCko} embryos

Immunostaining of E10.5 *Ext1*^{MCko} and control hindbrains with HS (green), NG2 (red) and isolectin B4 (blue) showed reduced HS deposition in *Ext1*^{MCko} (a-d). Strong HS localization was detected at interface between ECs and MCs in control hindbrains (arrow, e-h) but reduced in *Ext1*^{MCko} hindbrains (arrow, c-d).

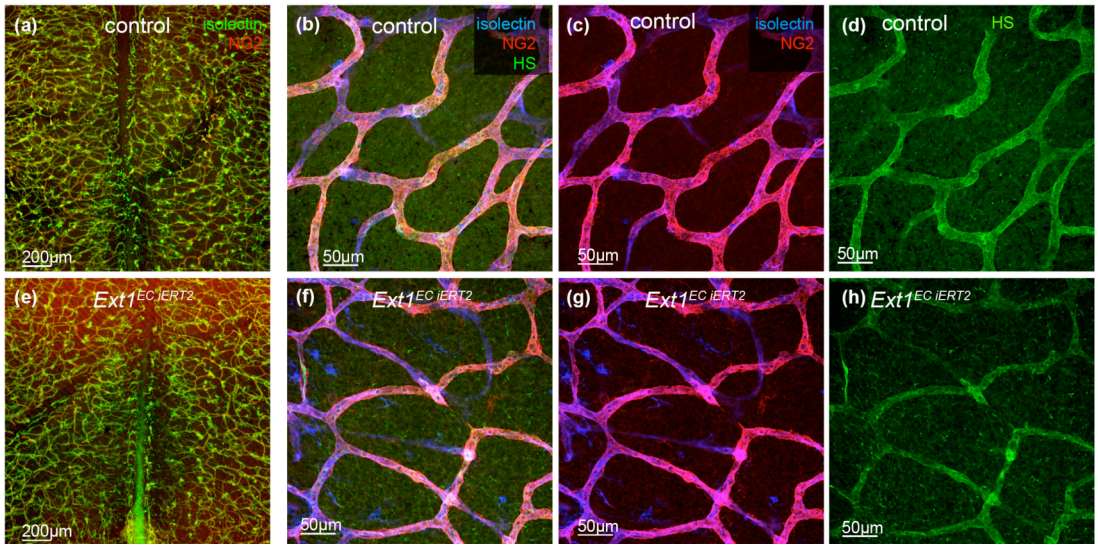

Figure 8.5 Tamoxifen induced deletion of endothelial HS in the embryonic hindbrain

Analysis of pericyte investment and blood vessel formation in E11.5 embryonic hindbrains of *Ext1*^{ECiERT2}. Pregnant female was injected intraperiteonally with 10mg/ml tamoxifen at E9.5 and E.10.5 before harvesting embryos.
Overview images display blood vessel network formation (a, e) by immunostaining with isolectin-B4 (green) and mural cell recruitment by co-labeling with NG2 (red, a, d). High magnification revealed HS deposition (green) in BM of blood vessels (blue) associated with pericytes (red, b-d and f-h). Expression of HS (green) correlates with close alignment of pericytes and normal vessel morphology in control (a-d) and *Ext1*^{ECiERT2} embryos (e-h).

8.2.3 Lack of MC HS results in abnormal vessel morphology and reduced vessel stability

8.2.3.1 Analysis of vessel morphology in embryonic skin

Despite apparently normal vascular patterning at E11.5, no viable mutants were born, indicating that the deletion of pericytic HS causes embryonic lethality at later stages. Further analysis revealed that lethality occurs between E13.5 and E19. At E13.5, *Ext1*^{MCko} embryos exhibit hemorrhages (Vascular defects in embryos lacking HS production b, white arrowhead) and edema (black arrow, b) in the skin. Histological transverse sections illustrate edema formation visible as increased interstitial space between the skin, spinal cord and muscle blocks (Vascular defects in embryos lacking HS production c-d; arrow). Loose connective tissue in the hypodermis of mutant embryos further confirms the presence of fluid accumulation (Vascular defects in embryos lacking HS production e, f). However, erythrocyte extravasation is only occasionally observed, implicating increased plasma leakage and/or poor lymphatic uptake as primary cause of edema formation.

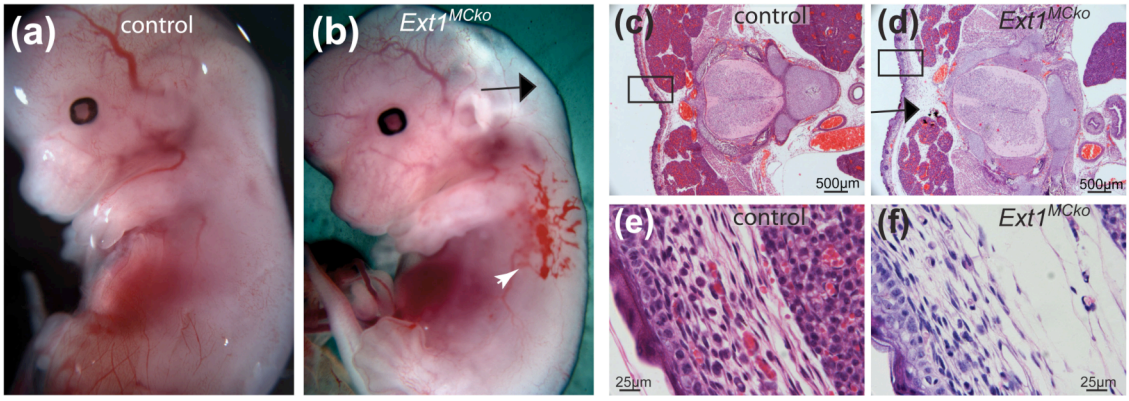

Figure 8.6 Vascular defects in embryos lacking HS production

Macroscopical analysis of E13.5 control (a) and *Ext1*^{MCko} embryos revealed edema (black arrow, b) and haemorrhages (white arrowhead, b) in the skin. Transverse sections demonstrate increased interstitial space (d, black arrow) and loose connective tissue in the epidermis of *Ext1*^{MCko} (f) compared to the control littermate (c, e).

Detailed wholemount analysis of these skin areas using endomucin labelling to detect endothelial cells (Brachtendorf, Kuhn et al. 2001) reveals striking abnormalities in superficial vessels around the spinal cord in mutant embryos (Figure 8.7 a-h). While control embryos display an organized and hierarchical vascular pattern (a), vessels in

mutant embryos appear random and chaotically branched with variable diameter (b). Higher magnification analysis emphasizes diameter variability (Figure 8.7 d) and shows frequent formation of glomeruloid structures resembling microaneurysms (arrow, Figure 8.7 d).

Confocal microscopy confirms the presence of a patent network of vessels in control embryos (Figure 8.7 e), whereas mutant tissue shows slender processes without filopodia resembling regressing vessels (arrowheads in Figure 8.7 f), and also numerous new sprouts alongside tortuous vessels of variable calibre (h). Quantification reveals a significant increase in the diameter variation between smallest and largest diameter vessels in mutant tissues (i). Diameter variations and co-existence of potential regression profiles and new sprouts suggest that vessels lacking pericytic HS are less stable.

8.2.3.2 Pericytic HS does not affect cardiovascular development and vessel perfusion

Given that perfusion is a stabilizing factor important for vessel maturation, we studied heart function, and major vessel perfusion. Invariably, all mutant and control embryos displayed effective heartbeat and evans blue or FITC dextran distributed quickly through the major central vessels following injection into the heart (not shown). Proper cardiac function beyond E14 requires coronary vessel formation, which is regulated by a series of HS dependent signalling pathways including hedgehog, TGF-β, FGF and VEGF reviewed in (Olivey, Compton et al. 2004). However, coronary vessel formation is unperturbed in $Ext1^{MCko}$ embryos at E13.5. Overview images of the heart stained with PECAM to visualize coronary vessels showed no difference in vessel formation, morphology and patterning of $Ext1^{MCko}$ and control embryos (Figure 8.8 a-d). Thus, central cardiovascular development and function appear not to require MC HS production. The observed vascular defects in the skin are therefore likely due to local defects associated with MC HS deficiency.

Confocal 3D-analysis illustrates that the vascular network in mutant skin samples spanned a greater depth (Figure 8.9 g, h), possibly due to increased sprouting or due to the tissue swelling and edema. Paraffin cross sections confirm the presence of multiple layers of vascular profiles in the hypodermis (Figure 8.9 a, b). Quantification of vessel density by measuring the skeletal length of all vessel profiles in confocal z-

stacks, reveal no significant difference between mutants and controls (Figure 8.9 g), suggesting that the same number of vessels expand over larger depth in the mutant tissue.

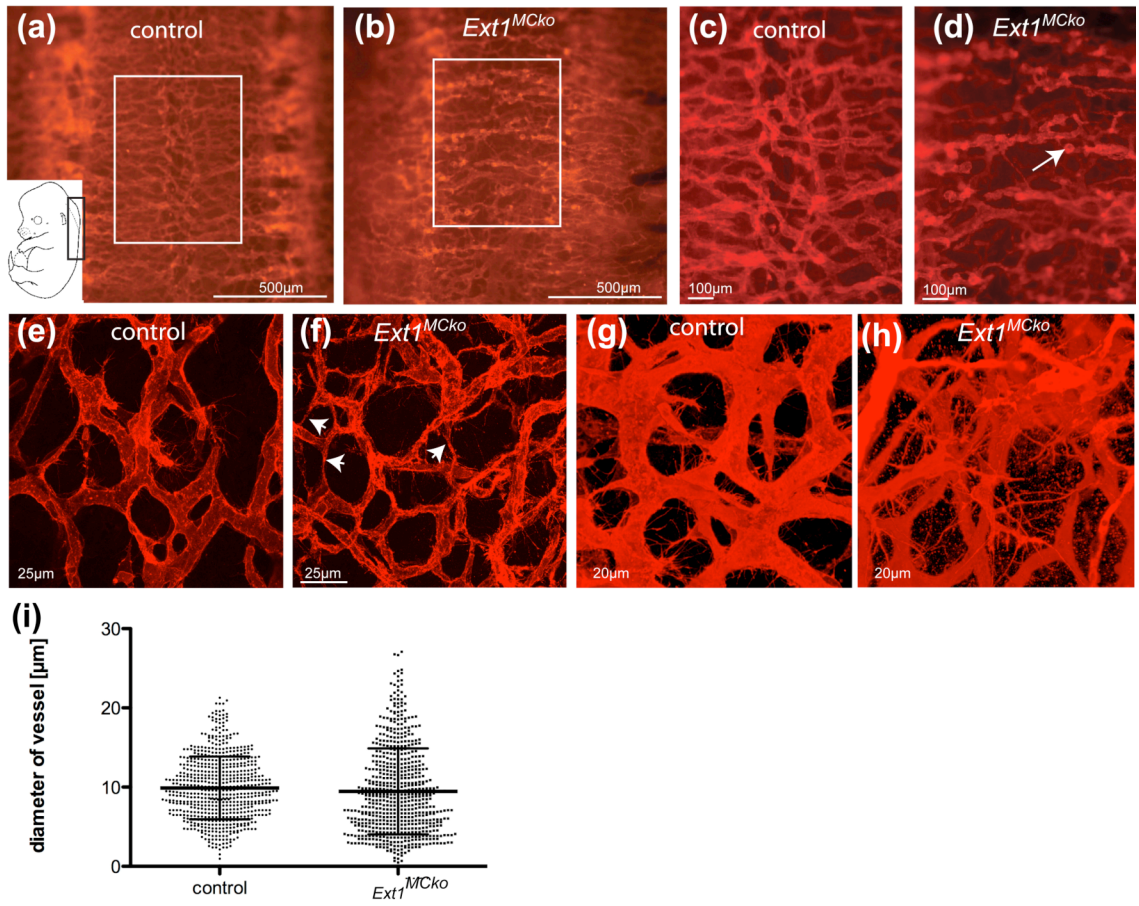

Figure 8.7 Abnormal vessel morphology and patterning defects in *Ext1*^{MCko}

Endomucin staining (a-h, red) of E13.5 mutant embryos revealed abnormal patterning of the superficial vessels at the back along the spinal cord (a, b); (c) and (d) present higher magnification images of the boxed area in (a) and (b). The skin vasculature of the control littermates is uniform in its size and diameter (e). In contrast, *Ext1*^{MCko} display irregular shaped, tortuous vessels with fluctuation in their diameter (arrowheads, f). *Ext1*^{MCko} exhibit excessive filopodia extension (h) indicating aberrant sprouting processes On the contrary, the skin vasculature in control embryos is restricted to a 2dimensional network (g). Graph i illustrates the measurement of 650 vessel profiles (n > 15 images/ embryo) reflecting the variability in vessel diameter in *Ext1*^{MCko} embryos. n =2, ***, F < 0.0001, F-test, variance of standard deviation.

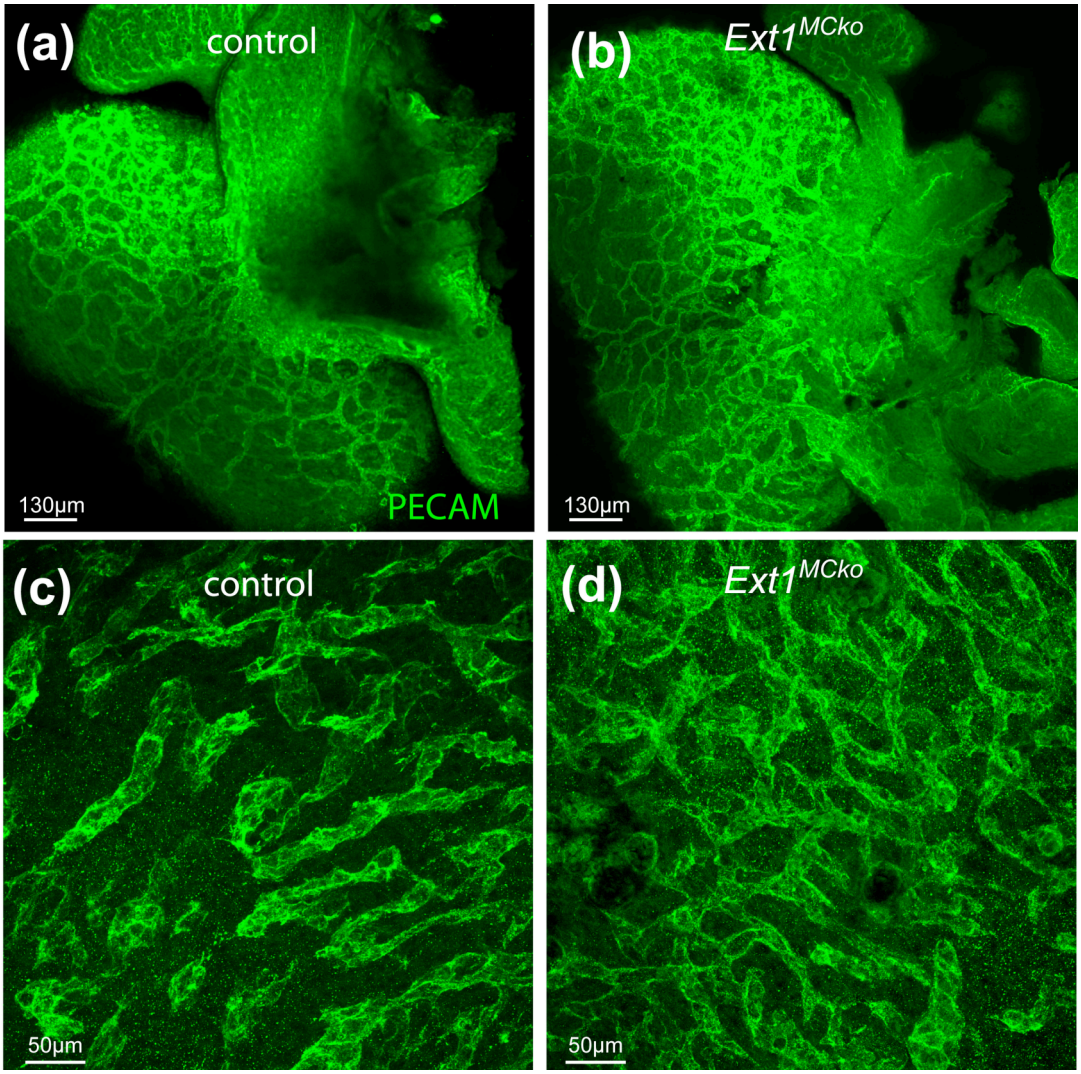

Figure 8.8 Loss of pericytic HS does not affect cardiovascular development

Visualization of coronary vessels in the developing embryonic heart at E13.5 with PECAM-1 (green, a-d) revealed uniform vessel formation. No morphological changes could be detected when comparing coronary vessels of *Ext1*^{MCko} (b, d) with control littermates (a, c).

8.2.3.3 Lymphatic vessel development occurs normally in mice lacking pericytic HS

Edema formation during embryonic development can result from either primary defects in blood vessels, or alternatively, from defects in lymphatic development. Mutations in major signalling pathways relevant for lymphangiogenesis and the separation of blood and lymphatic vessels lead to edema formation between E12.5 and 13.5, similar to pericyte HS mutants. LYVE-1 labelling (a marker for lymphatic endothelium (Banerji, Ni et al. 1999) sections illustrates an increase in lymphatic vessel profiles in the embryonic skin of $Ext1^{MCko}$ E13.5 embryos compared to control littermates (Figure 8.9 c, d). Double-labelling with endomucin show a clear separation of blood and lymphatic vessels. Formation of mayor lymphatic vessels and jugular lymph sacs also appear unaffected in $Ext1^{MCko}$ (Figure 8.9 e, f). These results indicate that lymphangiogenesis and segregation do not require HS production by MCs, and that the observed edema formation is likely caused by increased permeability in the blood vascular compartment.

8.2.3.4 Loss of MC HS results in increased vessel regression and defective vessel integrity

Detailed studies of the blood vessel morphology using endomucin wholemount labelling reveals a remarkable increase in filopodia extension, indicating increased sprouting activity (Figure 8.10 g, h). This increased sprouting, however, does not result in greater vascular density (Figure 8.10 g), suggesting that nascent vessels are less stable and prone to regress in the absence of MC HS production. To test this hypothesis, we studied the distribution of the basement membrane component collagen IV (CIV). CIV is a major component of the basement membrane (BM) surrounding the mature blood vessel but is absent from the tips of new sprouts. When blood vessels regress they leave behind empty BM sleeves containing CIV (Baluk, Lee et al. 2004). Comparing endomucin and CIV staining thus enables assessment of the relative amount of newly forming and regressing vessels.

Using this technique, we consistently observe increased CIV staining and numerous CIV positive structures devoid of endomucin staining, signifying vessel regression. Control embryos also display occasional regression profiles as part of normal vascular remodelling (Figure 8.10 a-c). Quantification of regression profiles in relation to the total skeletal length of vessels, however, reveals a significant increase in the length and number of CIV sleeves in mutant tissue (Figure 8.10 j). Higher magnification occasionally shows vascular sprouts with isolated endothelial cells not properly interconnected and apparently failing to form a patent stalk (Figure 8.10 g, boxed area in d). Together these results illustrate that the loss of MC HS leads to reduced stability of nascent vessels, promoting both increased regression and sprouting.

The precise mechanism of blood vessel regression *in vivo* is not fully understood. It is conceivable that increased sprouting and concomitant regression would correlate with an increase in endothelial cell turnover. We therefore performed TUNEL assay and caspase 3 staining to detect cell death, as well as phospho Histone H3 staining to analyse proliferation. Intriguingly, neither cell death nor proliferation are significantly changed in HS mutants during various stages of embryonic development (Figure 8.11 and Figure 8.12) suggesting that migration/rearrangement of existing cells contributes substantially to the remodelling process.

Increased regression of vessels can potentially be caused by the failure to form firm adherent cell-cell junction between endothelial cells. VE-cadherin, EC specific adherent

molecule functions in cell adhesion and controls permeability but also has been described to transfer intracellular signals that contribute to vascular stabilization. Ridini et al. reported a regulatory function of VE-cadherin in promoting HS dependent TGF-β signalling in ECs. The observation that *Ext1*^{MCko} vessels fail to form patent connections and partially lack EC connection (Figure 8.10 g-i) led to the hypothesis that VE-cadherin clustering and formation of EC-EC junction is disturbed in mice lacking pericytic HS. Unfortunately, immunofluorescent staining of wholemount embryonic skin samples did not succeed in detection of junctional VE-cadherin in control and mutant samples. In addition, analysing VE-cadherin protein expression in embryonic back skin samples of *Ext1*^{MCko} and control embryos revealed no significant differences in VE-cadherin (Figure 8.13) suggesting that production of pericytic HS is dispensable for VE-cadherin expression but still could play a role in clustering and formation of firm EC-EC junction.

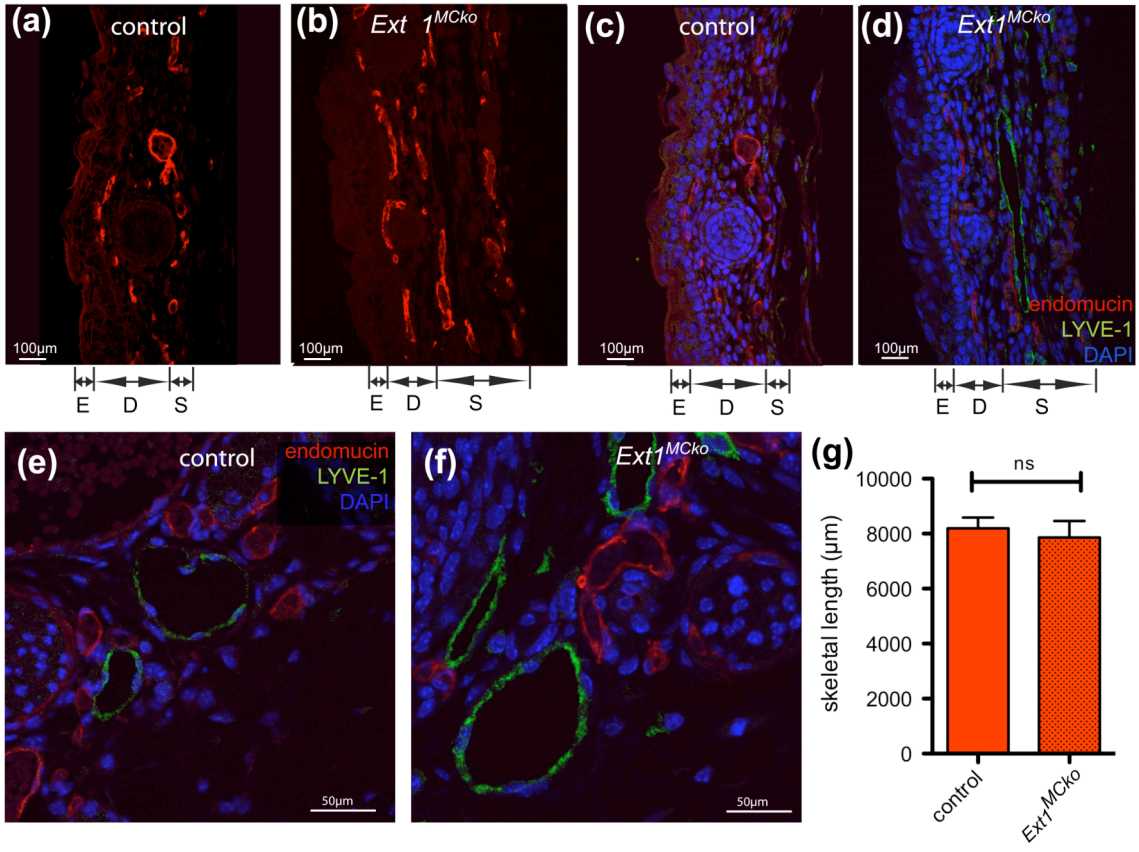

Figure 8.9 Lymphatic vascular defects in mice deficient of pericytic HS

Excessive sprouting and patterning defects of *Ext1*^{MCko} embryos are reflected in embryonic skin sections showing a widespread network of blood vessels (red, endomucin) through the entire depth of the skin (a, b).
Visualization of lymphatic vessels (LYVE-1, green) revealed an increase in lymphatic vessels in *Ext1*^{MCko} embryonic skin (d) compared to control littermates (c) however, co-labeling with endomucin (red) showed separation of lymphatic and blood vessels and no defects in lymphangiogenesis. (E=epidermis, D=dermis, S=subcutis).
Staining of embryonic sections with LYVE-1 (green) and endomucin (red) showed no differences in lymphatic vessel development and expression of early lymphatic marker LYVE-1 in major vessels at the paired jugular lymph sacs in *Ext1*^{MCKO} mice (f) compared to control (e). Despite vessels spreading through the entire depth, graph g summarizes the density of the vascular network by measuring the skeletal length of skin vessels. n > 15 images/ embryo and n = 2/ genotype

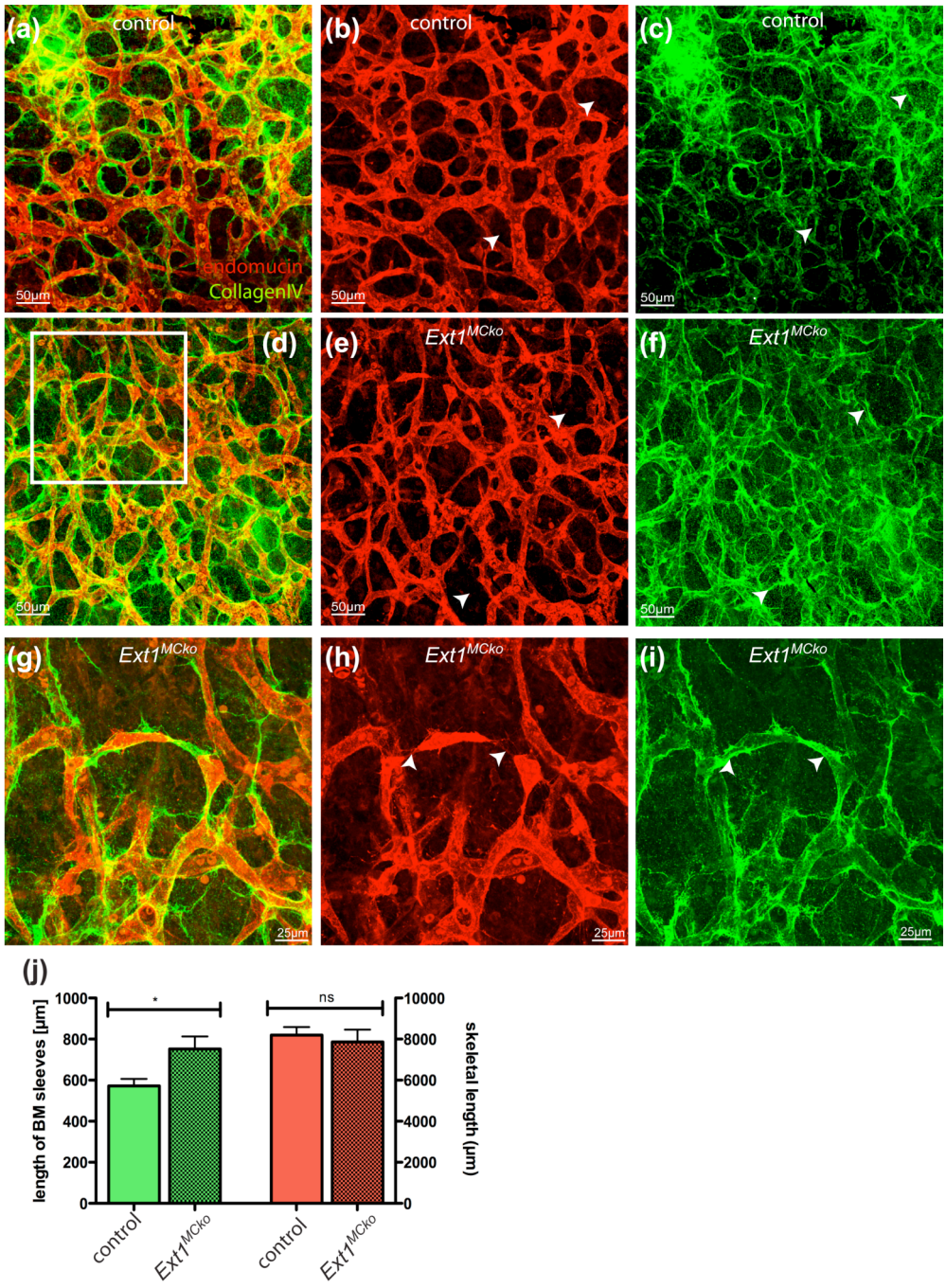

Figure 8.10 Loss of pericytic HS leads to increased regression of vessels in embryonic skin

Endomucin (red) and collagenIV (green) staining of embryonic skin revealed regressing blood vessel in *Ext1*^{MCko} embryos compared to control littermates (a-i). White arrowheads indicate regressing vessels lacking endothelial cell marker endomucin but positively stain for BM component CollagenIV. Higher magnification images (g-i) of the boxed area in (d) show disconnected endothelial cells that lack proper formation of lumen (arrowheads). Quantification for CollagenIV positive and endomucin negative vessels confirmed significant increase in regressing blood vessels of *Ext1*^{MCko} (j) while the density of the vascular network in the skin is unaffected (j, red bars). Quantifying the fluctuation in vessel diameter verified the significance in variance in *Ext1*^{MCko} compared to the control vessels (k).

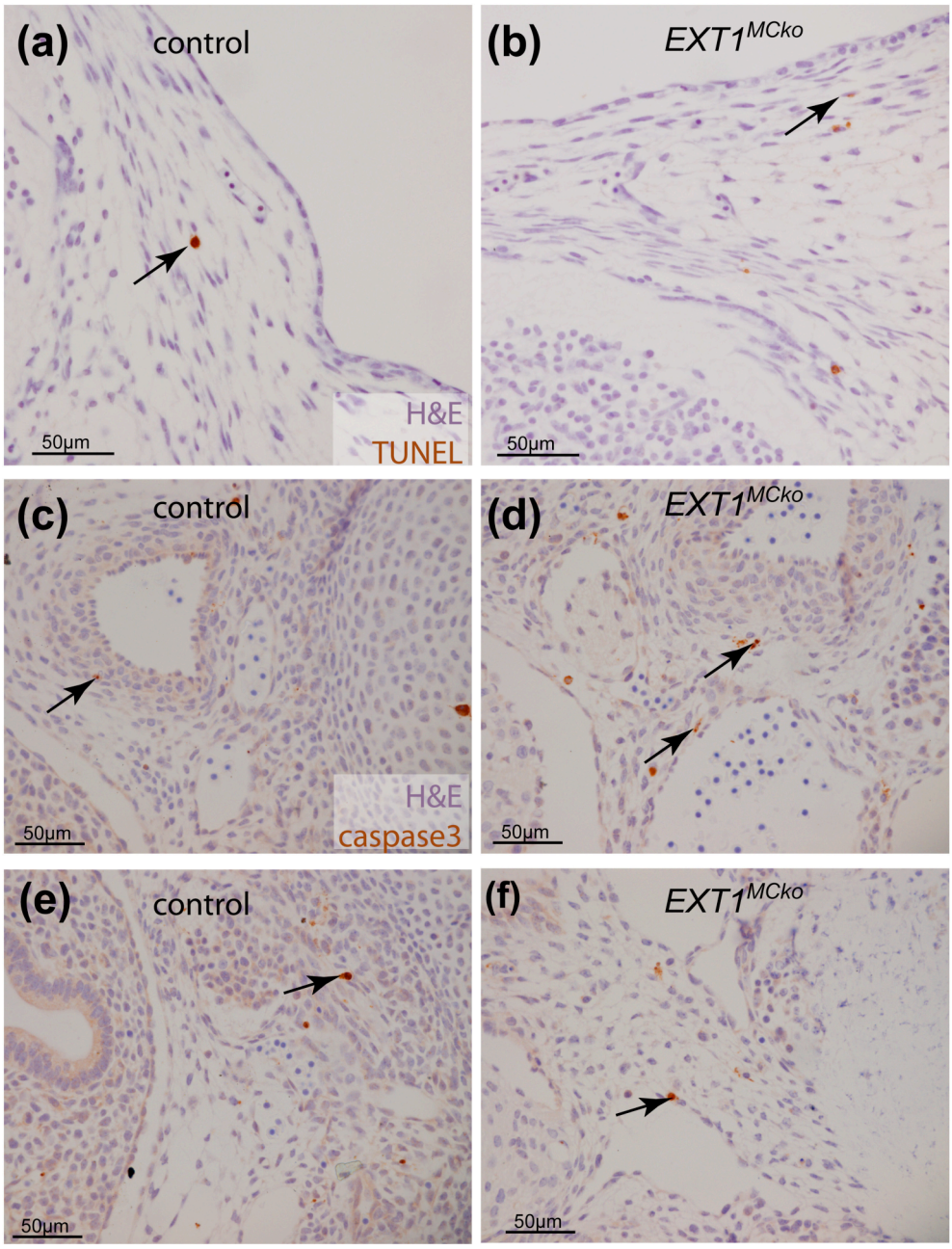

Figure 8.11 Vessel regression does not correlate with increased apoptosis

Immunohistochemistry staining of embryonic sections with TUNEL (a, b) and active caspase3 (c-f) illustrated no significant differences in apoptotic mural and endothelial cells (arrows) in *Ext1*^{MCko} as well as control embryos at E13.5.

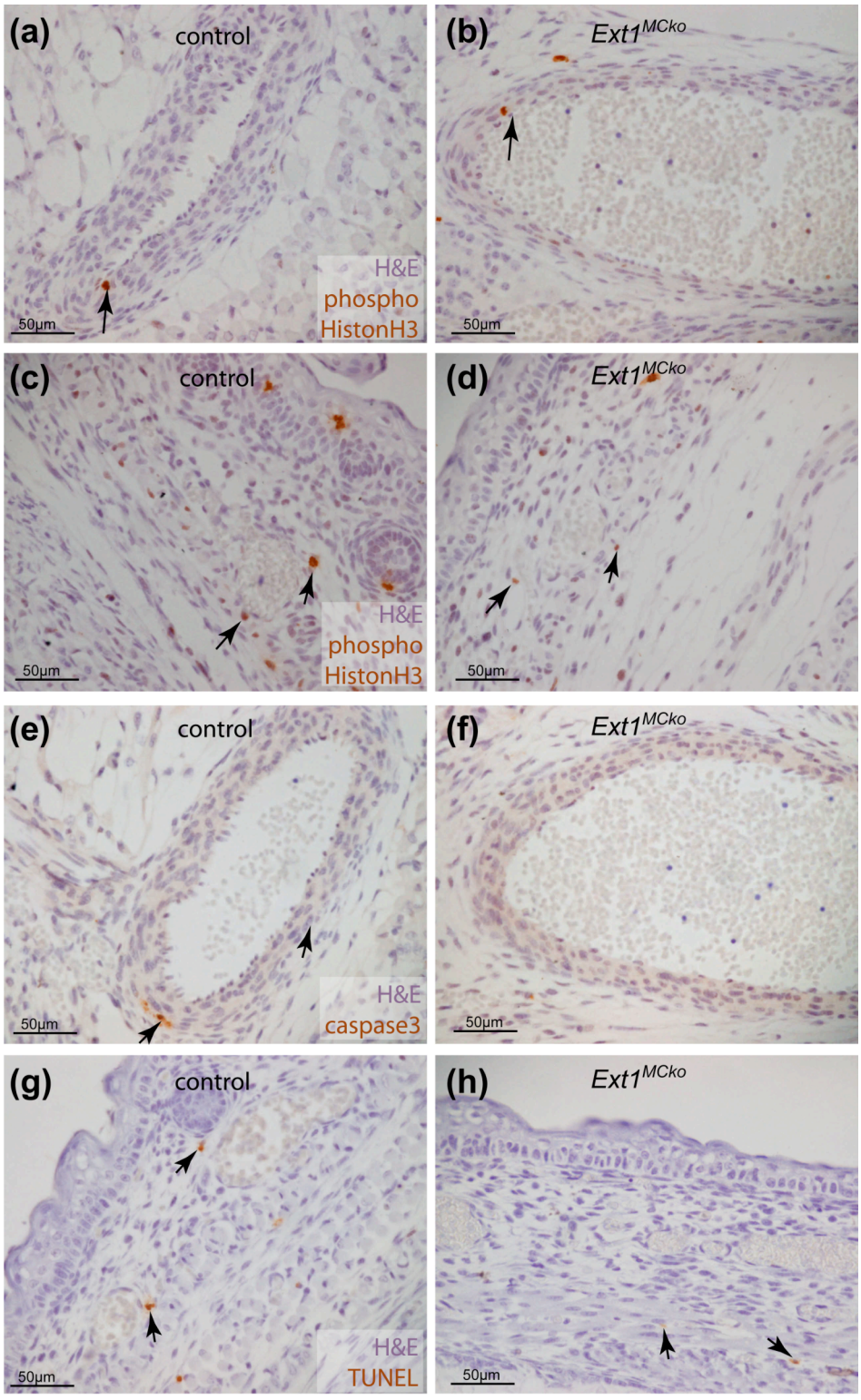

Figure 8.12 Regression of vessels is not a result of increased proliferation and apoptosis

Analysing proliferation of MCs by staining with phosphoHistone H3 (a-e) revealed no changes in *Ext1*^{MCko} and control vessels (a-b). No significant increase of apoptotic MC could be detected by caspase3 (e-f) and TUNEL staining (g-h) in E16.5 skin sections of mutant blood vessels (f, h) compared to control (e, g).

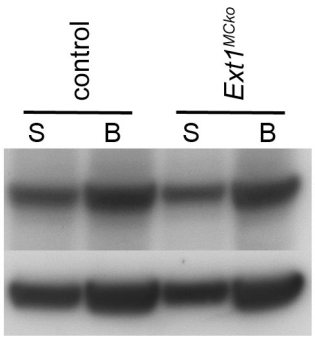

Figure 8.13 Vessel regression in Ext1MCko embryos is not caused by diminisehed expression of endothelial junction

Immunoblotting of embryonic brain (B) and skin (S) samples of E13.5 control and *Ext1*^{MCko} embryos revealed no significant changes in protein levels of EC-EC junctional molecule VE-cadherin.

8.2.3.5 Pericytic HS is dispensable for BM formation and placental vessel development

To evaluate vascular defects in *Ext1*^{MCko} further we harvested embryos at later developmental stages. The number of *Ext1*^{MCko} embryos obtained decreased with embryogenic development and mutant embryos display sever macroscopically defects. Mutant embryos appear grossly swollen with excessive deposition of fat on lymph nodes at the neck, indicating lymphatic defects proceed during late embryonic development. Furthermore, we observed bleedings along the spinal cord of the back of *Ext1*^{MCko} embryos concentrated at regions we found abnormal vascular patterning and vessel morphology at E13.5 embryos. In addition, brains isolated from *Ext1*^{MCko} and control embryos revealed bleedings in both cerebral hemispheres (Figure 8.14 a, b). However, high resolution analysis of transverse section and IF staining revealed no drastic defects in the morphology of CNS blood vessels (c, d). Co-labeling of vessels with HS showed a reduced expression of HS in the CNS. Nevertheless, HS deposition can still be found at BM enveloping PCs due to the endothelial expression and HS contribution to the BM. Despite the apparent loss of pericytic HS and the hemorraghing observed, PC closely associate to the vessel (e-h). In addition, auto fluorescence of erythrocytes within the vessel reveal functional vessels and normal blood flow, suggesting the bleeding occurred from a localized aneurism.

Also matrix deposition appeared normal in *Ext1*^{MCko} embryos (Figure 8.14 i-p). We co-labeled vessels with laminin α4 (i-l) and laminin α5 (m-o) to visualize ECM components and found no significant differences in matrix assembly and deposition suggesting that pericytic HS productions is not required for ECM deposition in CNS vessels.

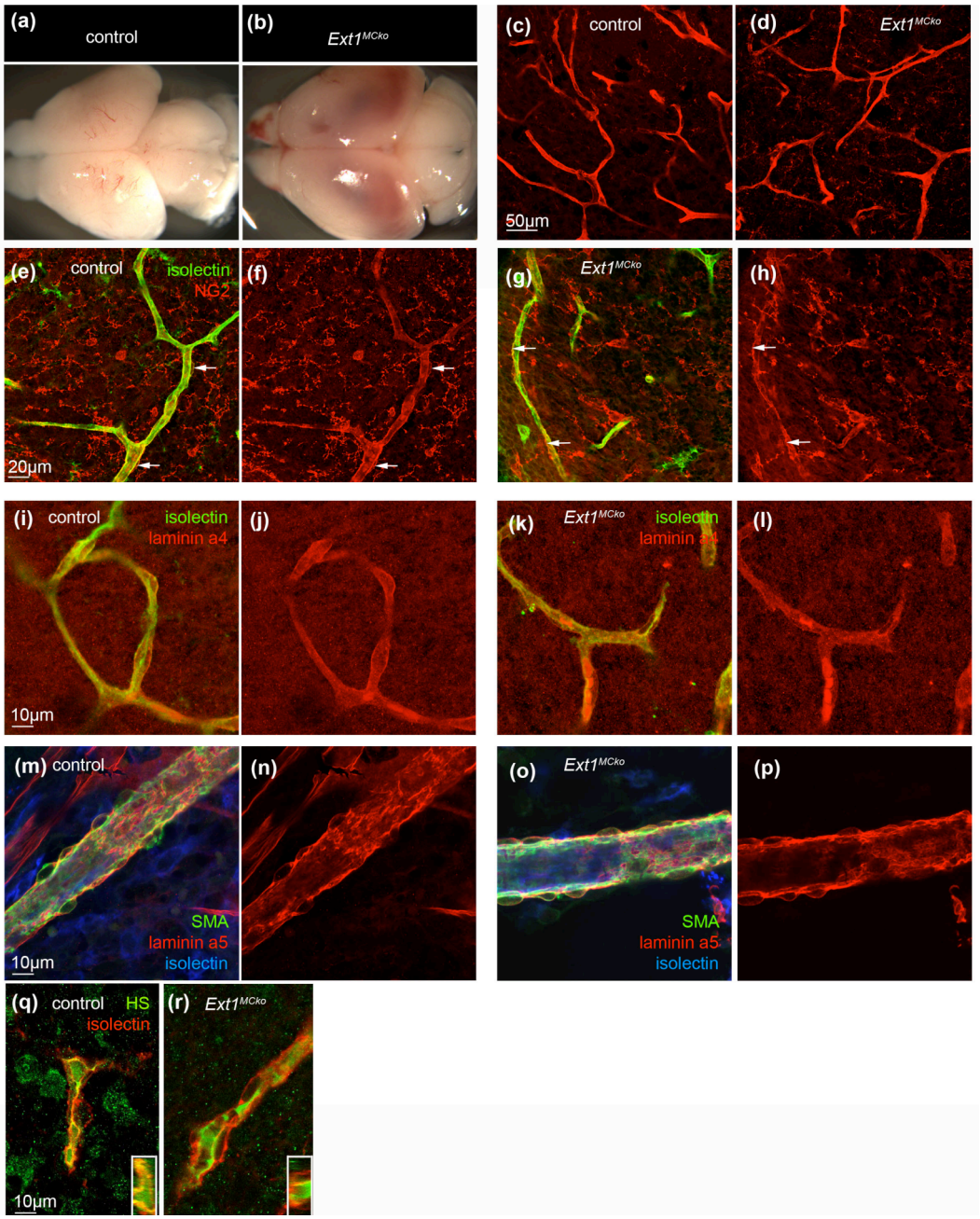

Figure 8.14 Pericytic HS is dispensable for pericyte recruitment in CNS and BM formation

Brains of E18.5 *Ext1*^{MCko} embryos exhibit sever bleedings and haemorrhaging (a, b). Sectioning and IF staining of the brain with endothelial marker isolectin B4 (red, c-d) revealed normal vessel morphology and vessel density in *Ext1*^{MCko} (d). Co-labeling of vessels (green, e-h) with NG2 to visualize pericytes (red) showed attachment of pericytes despite loss of MC HS (arrows, h). Likewise, staining with extracellular matrix components laminin a4 (red, i-l) and laminin a5 (red, m-p) displayed no defects in matrix assembly and deposition in vessels of *Ext1*^{MCko} embryos. Counterstaining of arteries in the brain with SMA (green, m-p) confirmed close attachment of vascular smooth muscle cells (vSMC) and formation of BM surrounding vSMCs. Staining with HS (green) revealed the presence of HS in control (q) and *Ext1*^{MCko} embryos (r). However, while control vessels express luminal and abluminal HS co-localized with isolectin (insert), *Ext1*^{MCko} vessels display luminal HS lacking HS at the interface of endothelial-pericyte interaction (insert).

8.2.3.6 Loss of pericytic HS affects renal development

Nevertheless, the hemorrhagic phenotype and the abnormal skin vessel morphology partially resembles the phenotype observed in *Pdgfb* or *Pdgfrb* deficient animals (Lindahl, Johansson et al. 1997). Lindahl and colleagues showed that PDGF-B/ PDGFR-β signalling controls mesangial cell development in the kidney glomeruli (Lindahl, Hellstrom et al. 1998). Furthermore, PDGF-B retention knockout mice exhibit defects in renal glomeruli formation as well as the excessive accumulation of ECM similar to *Pdgfb* null mice, indicating a function of HS binding in this process. Therefore, we analysed embryonic kidneys in mice lacking pericytic HS-production. PDGFR-β localizes to undifferentiated metanephric mesenchyme in the rat kidney and is later expressed in the cleft of the comma-shaped and S-shaped bodies and in more mature glomeruli in a mesangial distribution (Arar, Xu et al. 2000).

To test the hypothesis that pericytic HS is required for activation of PDGFR-β in mesanglial cells, specialized PC contributing to PDGF-B dependent capillary formation of glomeruli, we would analysed capillary formation in mice deficient for the production of pericytic HS.

Macroscopical examinations of kidneys of E19.5 mutant embryos revealed a reduction in size. More over, the surface of the kidney is nearly fully covered with tiny red dots (arrows, Figure 8.15 a), possibly indicating defects in proper glomerular capillary formation.

However, paraffin sections indicated that developing glomeruli appear normal (b-e) and high magnification revealed no defects in glomeruli and capillary loop formation (c, e) but vacuolated proximal tubules with cytoplasmic disruptions. HS labeling also illustrated a significant loss of HS in $Ext1^{MCko}$, suggesting that mesangial HS significantly contributes to glomeruli basement membrane formation (f, g). TUNEL staining (h-l) confirmed an increased number of apoptotic cells at the metanephric cortex of $Ext1^{MCko}$ kidneys and enhanced apoptotic bodies in proximal and distal collecting tubules, indicating a function for HS in renal cell survival.

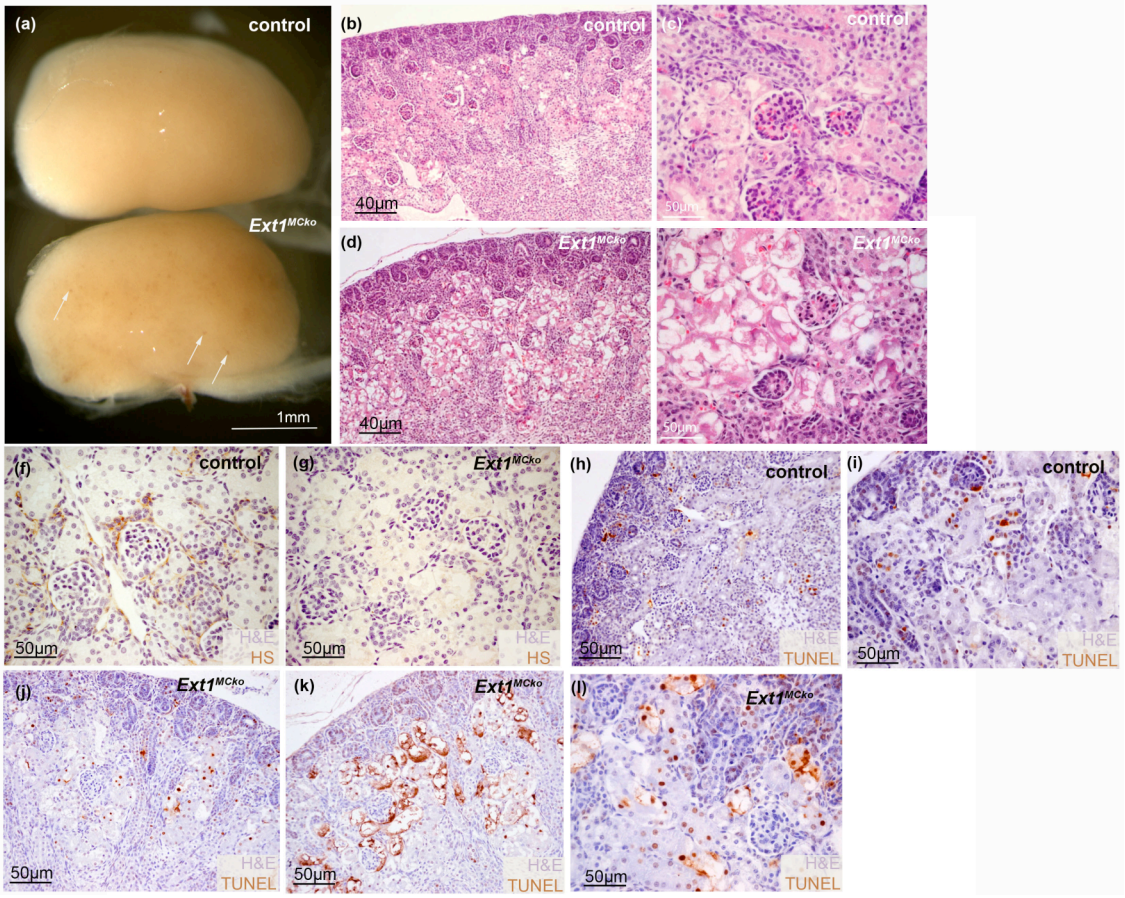

Figure 8.15 Lack of HS production affects metanephric cell differentiation and survival in *Ext1*^{MCko} kidneys

Macroscopical analysis of E18.5 kidneys of *Ext1*^{MCko} embryos revealed red dots (arrows, a) indicating hemorrhages. Sectioning and counterstaining of embryonic kidneys with H&E showed normal glomeruli formation in *Ext1*^{MCko} embryos but increased vacuolated proximal tubules (b-e). Co-labeling of paraffin section with HS revealed HS expression in control kidneys (f) that is absent in *Ext1*^{MCko} (g) indicating efficient Cre mediated deletion of HS in Pdgfrb positive cells in embryonic kidneys. TUNEL staining (h-l) revealed increased apoptotic cell bodies at the metanephric cortex and enhanced apoptotic bodies in proximal and distal collecting tubules in *Ext1*^{MCko} kidneys.

In situ hybridization analysis in the murine embryonic kidney revealed preferential expression of *Pdgfc* mRNA in the metanephric mesenchyme during epihthelial conversion (Li, Ponten et al. 2000). Loss of PDGF receptors alpha shows selective loss of mesenchymal cells adjacent to sites of PDGF-C expression. Arar et al. suggest that PDGF B-chain acts in a paracrine fashion to stimulate the migration and proliferation of mesangial cell precursors from undifferentiated metanephric mesenchyme to the mesangial area (Arar, Xu et al. 2000). A recent study confirmed the mitogenic signalling via PDGFR-β in metanephric mesenchymal cells and the PDGF-B induced PI3K activity in this process (Wagner, Ricono et al. 2007). In line with these data reported, HS production of metanephric mesenchymal cells appear to function in differentiation and cell survival however, deficiency of pericytic HS results in apoptotic cell bodies.

Embryonic lethality is probably connected to the various vascular defects observed resulting in microvascular dysfunction in $Ext1^{MCko}$ embryos. Despite a widespread function of PDGF-B signalling in PC recruitment, PDGFB/ PDGFR-β signalling has been demonstrated to specifically regulate cellular processes in various organs such as the placental vasculature. Placenta trophoblasts express PDGF-B and PDGFR-β (Goustin, Betsholtz et al. 1985) as well as HS (Chen, Liu et al. 2008). *Pdgfb* or *Pdgfrb* null mice show a reduction in trophoblast numbers (Ohlsson, Falck et al. 1999), suggesting that the proliferation of these cells is under autocrine control. To further investigate whether $Ext1^{MCko}$ develop placental defects we analysed the placental vasculature of E17.5 embryos. Macroscopically blood vessels of $Ext1^{MCko}$ appear normal (Figure 8.16 a-d) and visualization of microvessels by IF staining with PECAM-1 did not show signs of vascular defects and dilation of vessels (e, f) as seen in *Pdgfb* null mice. Therefore, we concluded that MC HS production does not contribute to the formation of the placental vasculature.

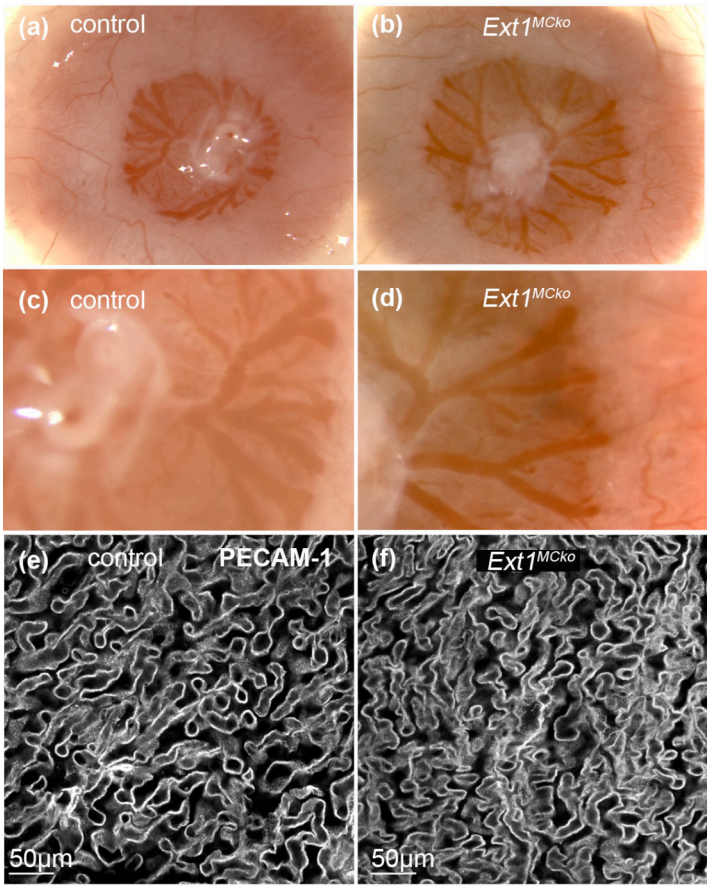

Figure 8.16 Pericytic HS is not required for vessel formation in placental labyrinth

Macroscopical examination of *Ext1*^{MCko} and control placenta at embryonic stage E17.5 revealed no defects in vessel formation, density and morphology (a-d). Sectioning of the placenta and visualization of vessels in the placental labyrinth with PECAM-1 (e, f) showed normal vessel development in *Ext1*^{MCko} embryos.

8.2.4 Loss of MC HS results in reduced MC coverage in the skin

Increased vessel permeability and regression can directly result from pericyte loss, both during development and in disease processes such as diabetic retinopathy (Hellström, Gerhardt et al. 2001); (Enge, Bjarnegard et al. 2002); (Hammes, Lin et al. 2002; Hammes, Lin et al. 2004). In order to address whether the regression of vessels and vascular dysmorphogenesis is caused by MC detachment/loss, we visualized MCs in skin samples using NG2.

In control embryos MC are closely attached to the endothelium, covering almost the entire vascular network (Figure 8.17 a-b). In $Ext1^{MCko}$ skin samples from identical regions, however, MC coverage is clearly reduced, with many vessels lacking properly attached MCs (Figure 8.17 c-f). In addition to MCs in contact with the endothelium (arrows, Figure 8.17 d, f), NG2 antibodies labelled isolated cells situated in between vessels (arrowheads). In control samples, such cells are few and far between, and most of these appear spindle-shaped. In contrast, isolated NG2 positive cells in mutant tissues are much more abundant and conspicuously round. Such isolated NG2 positive cells could represent MCs progenitor cells not yet recruited to the vessels, or MCs that have detached. Detached MCs in the CNS of PDGF-B retention mutants or *Ndst1*-/- mice usually appear spindle-shaped or extend multiple processes, but do not appear round. TUNEL analysis and Caspase 3 detection does not label these cells, indicating that the rounded appearance is not associated with cell death. Whether these cells represent MC progenitor cells that fail to be recruited remains to be determined.

We further noted that MCs surrounding the cardinal vein at E16.5 also appear disorganized and more rounded in $Ext1^{MCko}$ embryos, loosing the neat stratification observed in littermate controls (black arrows, Figure 8.17 g, h). Thus it is possible that MC that are not in direct cell-cell contact with endothelial cells require cell autonomous HS production for proper polarization, recruitment and organization.

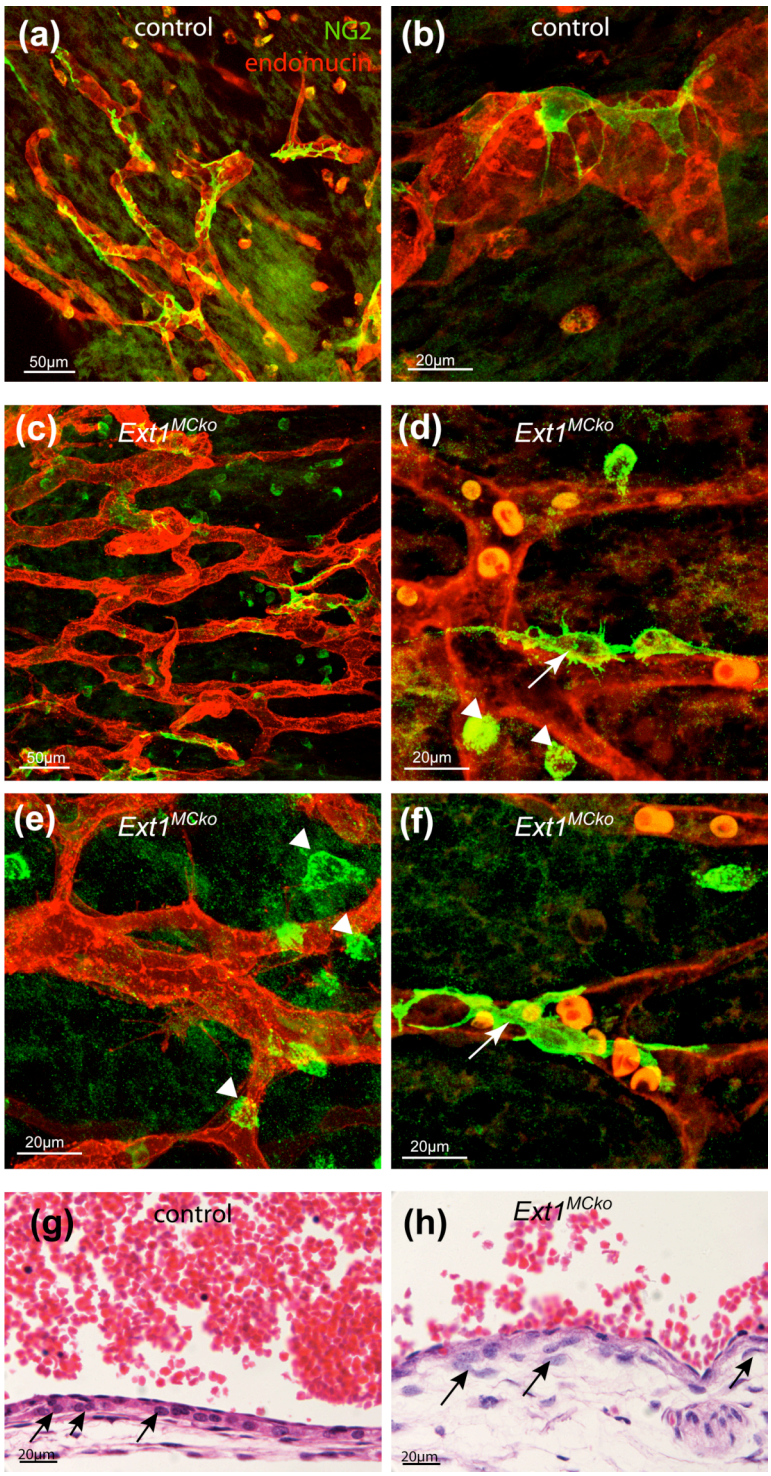

Figure 8.17 Recruitment and attachment of HS deficient MCs in embryonic skin

Mural cells of the skin vasculature were visualized with NG2 (green, a-f) in E13.5 control (a, b) and *Ext1*^{MCko} embryos (c-f). Blood vessels in the mutant display a reduced number of MC in the vascular plexus (c) compared to the control (a). White arrows indicate MCs that attach to the vessel and are in close contact to the endothelium (red; d, f) as seen similarly in the control (b). However, *Ext1*^{MCko} vessels are dominated by rounded NG2 positive cells in close proximity to the vessel (arrowhead; d, e) indicating progenitors cells that fail to differentiate. Embryonic transverse section (g, h) confirm presence of MC, however MC organization is chaotic (h, black arrows) compared to the tight alignment of MC in control cardinal vein (g).

To gain further insights in PC attachment and vessel morphology we analysed skin sections of *Ext1*^{MCko} using transmission electron microscopy. Applying this technique allows us to study EC morphology and EC-EC as well as EC-PC junction in great detail.

Blood vessels in the control skin of E13.5 embryos formed a monolayer of endothelial cells with close cell-cell contacts (black arrows, Figure 8.18 a-b). Pericytes and their protrusion align in close proximity to the endothelium and BM is formed. Analyses of the mutant vasculature revealed diverse vessel morphology. Sections of blood vessels could be seen that resemble those found in the vasculature of control littermates (c). However, some blood vessels formed a lumen enclosed by ECs and with PCs attached that appear apoptotic (Figure 8.18 d, PC). On the other hand, vessels can be observed that have a highly abnormal EC shape with long thin protrusion (Figure 8.18 e, arrowheads). These abnormalities may explain the defect in lumen and vessel diameter control that is associated with fluctuations in the thickness of the ECs. Also, defects in endothelial cell alignment may lead to leakiness of the vessels and hemorrhages occur as indicated by the erythrocytes in the tissue (asterisk, f).

To study cell-autonomous function of mural cells lacking HS production we aimed to isolate primary MCs. However, the early embryonic lethality does not allow me to extract MCs from whole *Ext1*^{MCko} embryos. Therefore, we isolated vascular smooth muscle cells (vSMC) from adult aorta of *Ext1 flox/ flox* mice and applied retroviral transfection of a Cre plasmid to mediate loxP site excision. Figure 8.19 shows primary vSMC from the aorta, identified by IF staining with MC markers smooth muscle actin (SMA) and PDGFR-β (Figure 8.19 a-c). Although the Cre-plasmid contained a fluorescent marker GFP that should be visible upon successful transfection, I failed to detect GFP positive MC cells. In addition, primary vSMCs did not proliferate and cell number was limited to successfully infect cells.

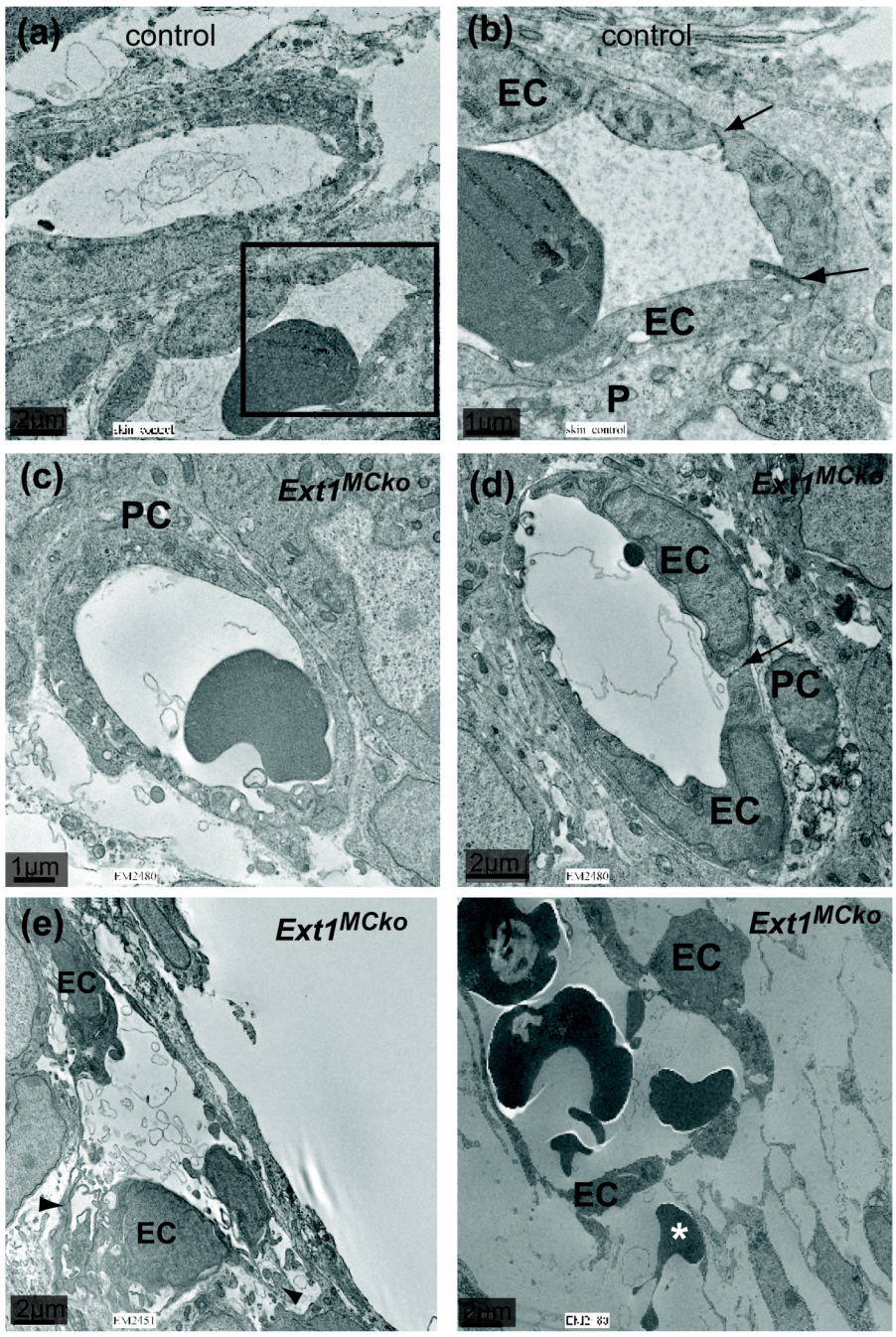

Figure 8.18 Electron microscopic analyses of vessel morphology in the skin

Vessel morphology and pericyte attachment was analysed in E13.5 *Ext1*^{MCko} and control embryos by electron microscopy. Vessels of the control skin vasculature form a monolayer of endothelial cells (EC) with tight cell -cell contacts (b, black arrows). Pericytes (P) align closely to the endothelium (a, b).
Images c-f represent vessel profiles observed in *Ext1*^{MCko} skin vasculature. Vessels resembling the morphology of control vessels were detected (c). However, we also noticed blood vessels with pericytes attached, which seem apoptotic (d, indicated by PC). Furthermore, we observed vessels with strikingly abnormal EC shape (e, f). Arrowheads point out long thin protrusion formed between the ECs. The asterisk illustrates an erythrocyte outside the blood vessel, indicating leaky vessels that might result in hemorrhages (f).

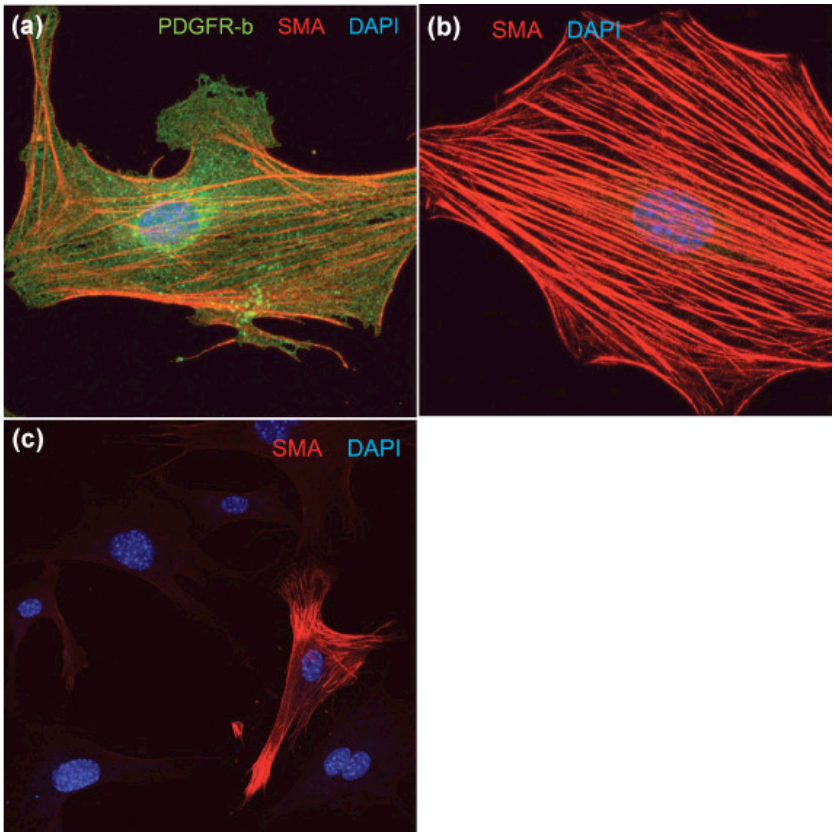

Figure 8.19 Characterization and morphological analysis of primary smooth muscle cells isolated from dorsal aorta

Vascular smooth muscle cells (vSMC) were isolated from the aorta of *Ext1* floxed mice. After culturing cells for 13 days, cells were analysed by immunostaining for SMC markers smooth muscle actin (SMA, red, a-c) and PDGFR-b (green, a). Counterstaining with DAPI revealed presence of non-SMC (c) deficient in SMA.

8.2.5 PDGF-B and TGF-β signalling defects in mice lacking MC HS

To gain a better understanding of potential signalling pathways affected by MC HS depletion, we analysed RNA and protein expression and activation of growth factor receptors as well as downstream signalling molecules of signalling pathways that have been described in previous studies to be dependent on HS-mediated binding and interaction.

After RNA isolation of embryonic skin samples of $Ext1^{MCko}$ and control embryos we performed quantitative real time PCR in order to access whether loss of MC HS production disturbs expression of relevant HS dependent growth factors and receptors. However, analysis of *Pdgfb, Vegfa* and their receptors *Pdgfrb, Vegfr2* did not reveal any differential gene expression and data obtained were extremely various between control and $Ext1^{MCko}$ mice. Possibly, the fluctuations reflect the variation in degree of the phenotype but also the fact that MC numbers are comparably small in embryonic skin samples. Ideally, laser capturing of MC followed by single cell qRT-PCR would shed light in differential gene expression of $Ext1^{MCko}$ and control samples.

To determine protein expression levels and phosphorylation events, we dissected samples of embryonic back skin for protein analysis.

Phosphorylation of PDGFR-β is profoundly reduced in various $Ext1^{MCko}$ skin, consistent with the observed reduction in MC coverage. Phospho-ERK1/2 and phospho-SHP-2, which relay signalling downstream of PDGFR–β are consistently reduced, while p-AKT signalling is unaffected (Figure 8.20 a). The graph summarizes the reduction of p-PDGFR-β in the skin but reveal no significant defects in p-PDGFR-β and its downstream targets in protein samples of the CNS. Thus, the biochemical data are consistent with the observed phenotype in the skin and with the lack of a MC phenotype in the CNS.

Jakobsson and colleagues previously showed *ex vivo* that MC HS is sufficient to induce vessel formation and to support VEGF signalling during sprouting angiogenesis in 3D-cultures of embryoid bodies (Jakobsson, Kreuger et al. 2006). We therefore hypothesized that VEGF signalling might be affected upon deletion of pericytic HS *in vivo,* possibly leading to the observed alteration in sprouting and regression. However, immunoprecipitation of VEGFR2 using total embryonic tissue followed by detection with a phospho-VEGFR2 antibody reveal no significant differences in VEGFR2

phosphorylation levels in *Ext1*^{MCko} compared to control littermates (Figure 8.20 c). Overall VEGFR2 levels are also comparable in several embryos (Figure 8.20 b), together illustrating that MC HS might not be required for VEGF signalling during vessel development *in vivo*. Matsumoto and colleagues showed differential patterns of VEGFR2 phosphorylation within developing blood vessels in mouse embryoid bodies (Matsumoto, Bohman et al. 2005). Interestingly, more developed patent vessels associated with mural cells displayed different patterns of VEGFR2 phosphorylation than endothelial cells lining immature blood vessels.

Therefore, we used a phospho-specific antibody that detects Y951 phosphorylation that has been shown to be phosphorylated upon contact with mural cells. However, we could not detect any differences in Y951 phosphorylation in *Ext1*^{MCko} embryos (Figure 8.20 d). Although VEGFR2 Y951 phosphorylation levels are similar in *Ext1*^{MCko} and control embryos, visual analysis of the blot (d) might suggest a decrease in total VEGFR2 protein expression levels in *Ext1*^{MCko} embryos. Decrease in overall VEGFR2- but equal Y951 phosphorylation levels therefore, might reflect an increase in activated Y951 VEGFR2 upon loss of MC HS.

Thus, one could imagine that pericytic HS functions as a co-receptor *in trans,* activating VEGFR2 signaling in endothelial cells that are in contact with MCs.

These speculations are based on preliminary data and further experiments are required to elucidate a role of MC HS in VEGFR2 phosphorylation. In addition, combined analyses of VEGFR2 expression levels (b), and phospho VEGFR2 expression levels in *Ext1*^{MCko} and control embryos would argue that pericytic HS does not function in VEGFR2 activation as expression is not consistently altered in samples analyzed.

Other HS-dependent signalling pathways involved in vascular development and MC recruitment include the TGF-β pathway, involving TGF-β, TGFIIR, Alk1/Alk5, the auxiliary receptor endoglin and the downstream effectors SMAD1, 2, 3 and SMAD5 (Belenkaya, Han et al. 2004); (Chen, Sivakumar et al. 2007); (Eickelberg, Centrella et al. 2002); (Rider 2006).

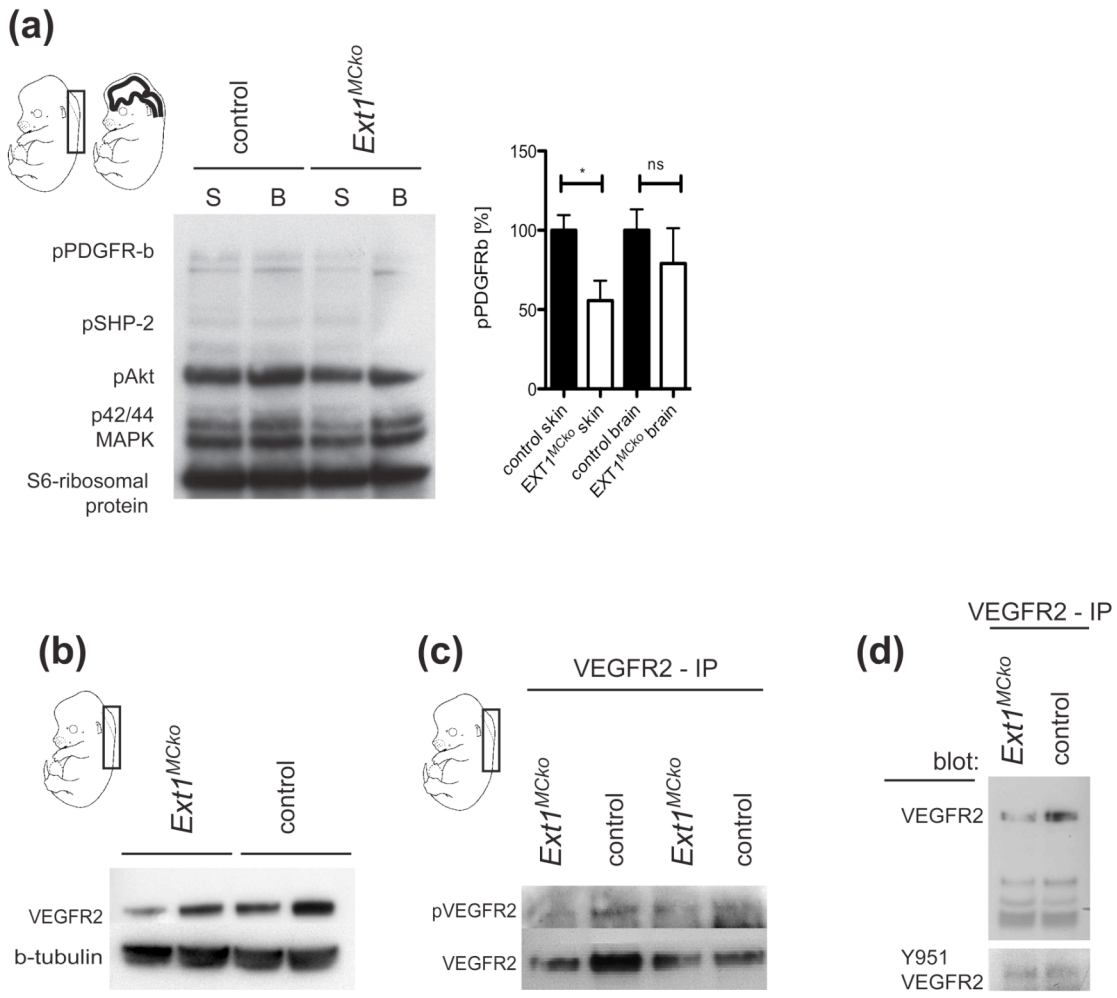

Figure 8.20 Molecular mechanism and signalling defects in mice lacking pericytic HS

Phospho-PDGFR-β protein expression levels as well as downstream signalling molecules p-ERK1/ 2 and p-SHP-2 were analysed by Western Blotting (a). *Ext1*^{MCko} littermates (a) display reduced levels of pPDGFR-β and pERK in skin samples, while p-AKT signalling is unaffected (a). Comparison of pPDGFR-β levels in skin and CNS of *Ext1*^{MCKO} confirmed that PDGFR-β signalling is unchanged in the CNS of *Ext1*^{MCKO} mice (a).
VEGFR2 expression levels (b) in the skin of MCs deficient in HS are similar in comparison to control littermates (*Ext1*^{MCko} and control). Immunoprecipitation of VEGFR2 in embryonic skin samples and subsequent detection of phosphorylated VEGFR2 (c) revealed no differences in pVEGFR2, indicating no defects in VEGFR2 signalling and activation.
Using an antibody directed against VEGFR2 phosphorylation, Y951 (d) we analysed a specific phosphorylation site that has been described to be activated upon MC attachment. No differences in expression levels were found in *Ext1*^{MCko} and control embryos.

TGF-β is involved in local induction of MC from progenitor cells of the mesenchymal cell lineage as well in differentiation and proliferation of ECs and MCs (Hirschi, Rohovsky et al. 1998; Hirschi, Burt et al. 2003) . Protein analysis of the embryonic skin vasculature reveals reduced SMAD2/3 (data not shown) expression as well as reduced phosphorylation of SMAD2, SMAD3 (Figure 8.21 a) and SMAD1 (data not shown). Similar to the tissue specific deficiency in phosphorylation of PDGFR-β, pSMAD3 levels are reduced in the skin, but not in the brain of *Ext1*^{MCko} embryos (Figure 8.21 b). Control littermates show comparable pSMAD3 levels in skin and brain.

To confirm these findings at the cellular level, we visualized phosphorylated SMAD3 in the dermal vasculature of embryos. Immunohistochemistry staining reveals that most endothelial as well as perivascular cells express pSMAD3 in control embryos (Figure 8.21 c, d). In contrast, endothelial cells lining the blood vessels (indicated by asterisk) of *Ext1*^{MCko} embryos frequently lacked pSMAD3 expression (arrows, Fig.3.21 e, f). Co-labelling with endomucin to visualize ECs confirmed the specificity of ECs lacking pSMAD3 expression indicating that MC HS plays a role in TGF-β signalling between MCs and the endothelium (Figure 8.21 g-j).

Loss of endothelial SMAD4 results in defective vascular integrity and impaired vascular smooth muscle cell development. The failure of patent vessel formation is accompanied by a decreased expression of gap junction molecule, connexin 43 (Lan, Liu et al. 2007). To analyse whether loss of pericytic HS results in decreased SMAD4 and connexin expression that could account for the reduced mural cell coverage in *Ext1*^{MCko} embryos we analysed SMAD4/ connexin 43 by Western Blot. Surprisingly, we did not observe differences in protein expression levels of either when comparing to control littermates (Figure 8.21 i). Thus, we conclude that SMAD2/3 signalling is specifically disturbed upon loss of HS production in mural cells.

Although TGF-β signalling appears specifically reduced in skin samples of *Ext1*^{MCko} it is not fully clear whether TGF-β signalling is decreased as a consequence of MC loss or whether diminished TGF-β signalling causes the failure of MC recruitment in the skin vasculature of *Ext1*^{MCko} To further characterize we compared TGF-β signalling to skin and brain samples from *Pdgfrb* -/- embryos lacking MC investment (Figure 8.21 a, b). As described previously pSMAD2/ pSMAD3 signalling is reduced in skin but not brain samples of *Ext1*^{MCko} correlating with MC loss. In contrast, *Pdgrfb* embryos show diminished signalling in brain but no significant decrease in pSMAD2 and pSMAD3 expression in the skin (a, b). Since PC investment in the CNS is dependent on PDGF-B

mediated PC migration we concluded that the loss of MC causes reduced TGF-β signalling rather than TGF-β signalling causes MC dissociation from the CNS.

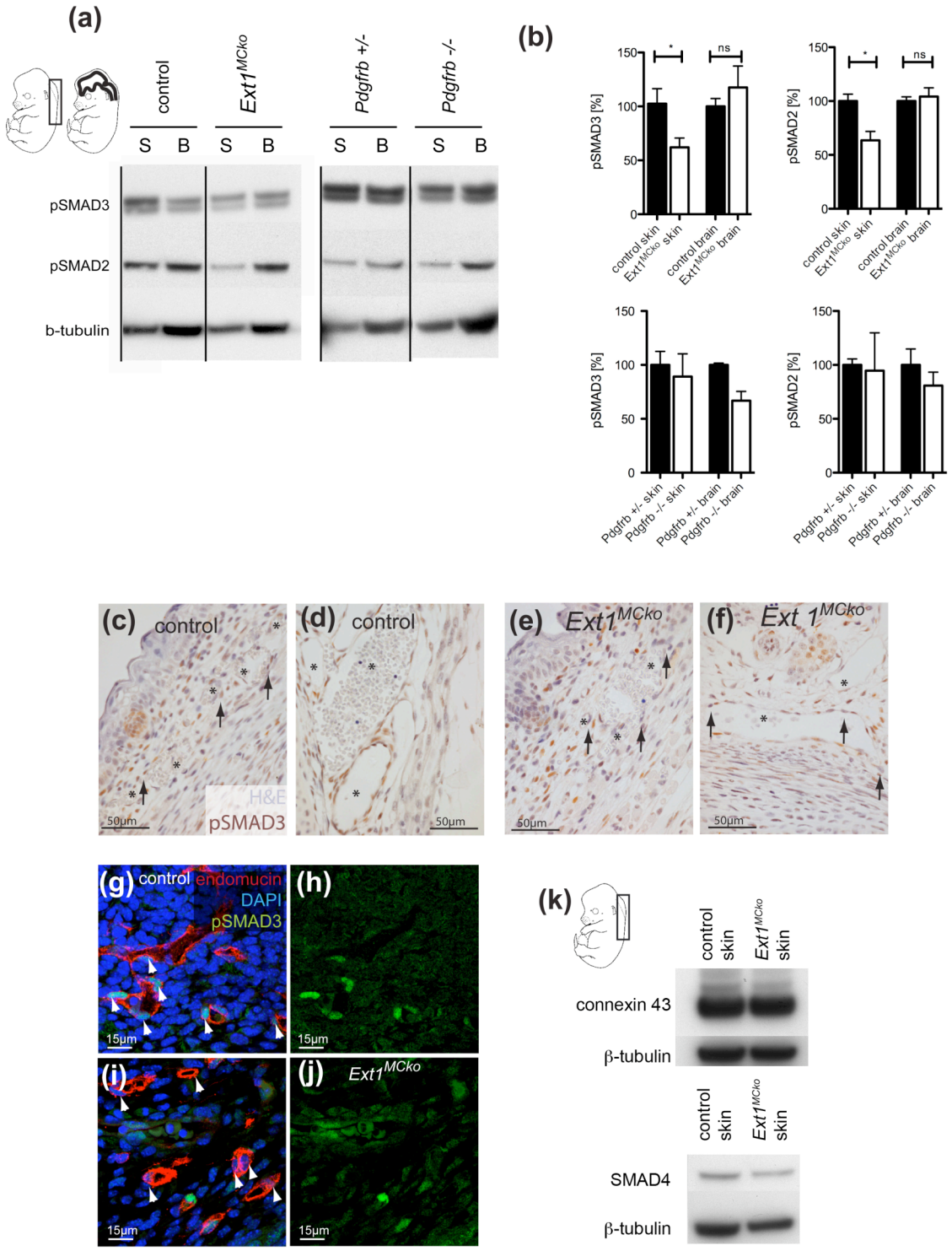

Figure 8.21 Loss of pericytic HS production results in reduced TGF-β signalling

Expression studies of pSMAD2 and pSMAD3 molecules by Western Blotting, downstream effectors of the TGF-β pathway revealed a significant down regulation in *Ext1*^{MCko} embryos (a). The reduction in pSMADs is restricted to *Ext1*^{MCko} skin samples

while pSMAD levels in the CNS of mice lacking HS in MCs are unchanged when compared to control littermates (a). To access whether reduced TGF-b signalling is a result of MC loss in the skin of *Ext1*^{MCko} embryos, we analysed TGF-b signalling in *Pdgfrb* null mice lacking MC investment (a). Graphs in (b) summarize densiometric analyses illustrating the expression levels of pSMAD2 and pSMAD3 normalized to β-tubulin, internal loading control. *, $p < 0.05$. *Ext1*^{MCko} and control embryos n = 4, *Pdgfr*β +/- and *Pdgfr*β -/- n=2. Values represent mean ± S.E.M.
Loss of TGF-b signalling could be confirmed by IHC staining with a pSMAD3 antibody on embryonic skin sections (c-j). While most endothelial cells of blood vessels in control mice are stained positively for pSMAD3 (arrows; c, d, g, h) endothelial cells in *Ext1*^{MCko} lost pSMAD3 expression (arrows; e, f, i, j). Counterstaining with endothelial marker endomucin (red) confirmed endothelial specific loss of pSMAD3 (green) in *EXT1*^{MCko} embryos (arrows; i, j). n>3
Investigation of SMAD4 and connexin43 expression levels, implicated in vessel integrity and SMC association are not significantly regulated in *Ext1*^{MCko} skin samples (k)

.

8.3 Discussion

The present study underscores the fundamental importance of HS in tissue biology. Selective deletion of all HS in MC is incompatible with embryonic survival due to an important role of MC HS during the late stages of vascular morphogenesis and stability.

ECs and pericytes share a basement membrane, and both cell types potentially contribute to the establishment thereof by production of various ECM proteins including HSPGs. The vascular basement membrane at the interface between endothelial cells and mural cells is rich in *N*-sulfated HS. Reduced *N*-sulfation impairs PDGF-B binding and PDGFR-β signalling, leading to delayed pericyte recruitment and increased detachment (Abramsson, Kurup et al. 2007); (Kurup, Abramsson et al. 2006). Complete loss of *N*-sulfated HS in vascular structures growing from embryoid bodies ex vivo illustrated that VEGFR signalling requires HS as co-receptor during vascular morphogenesis. In the absence of endothelial HS, MC derived *N*-sulfated HS is sufficient to support VEGFR signalling, illustrating that HS and VEGFR can interact *in trans* during this process (Jakobsson, Kreuger et al. 2006).

Our genetic approach to generate $Ext1^{MCko}$ embryos effectively depleted HS from MCs during vascular development. Major vascular defects associated with MC deficiencies occur in $Ext1^{MCko}$ embryos selectively outside of the CNS, most notably along the embryonic back skin at stages after E12.5. Edema and swelling, as well as haemorrhaging indicate profound vascular dysfunctions as a result of HS deficiency. Histological sections confirm edema formation in spite of abundant lymphatic vessel development. Central lymphatic development including segregation of jugular lymph sacs from the vein appear unaffected, suggesting that the edema is a result of increased vascular permeability and not of defective lymphangiogenesis.

Wholemount analysis of $Ext1^{MCko}$ skin samples at E13.5 and later illustrates increased vascular diameter irregularities and frequent regression profiles, as well as excessive sprouting. These abnormalities are similar to those caused by MC deficiencies in *Pdgfb* or *Pdgfrb* knockouts. MC attachment reduces vessel regression; vessels associated with MC undergo less regression upon hypoxia in retinas or VEGF withdraw in tumours. We observed increased regression profiles in the skin vasculature coinciding with reduced MC coverage.

Pericyte/MC detection by NG2 staining confirms a profound reduction in MC coverage in the affected vascular plexus areas. At the same time, conspicuously rounded NG2

positive cells are found in close proximity to many skin vessels. We speculate that the concomitant appearance of these cells and the apparent loss of pericytes may signify a defect in recruitment of local progenitor cells. LeJan and Kreuger observed a strikingly similar rounded pericyte phenotype in embryoid bodies deficient in *Ext1* (personal communication; manuscript submitted) suggesting the HS may be cell-autonomously required for local induction and/or polarization and spreading of MC progenitor cells. In line with this idea, we observed defective alignment of HS deficient MCs around the cardinal vein in $Ext1^{MCko}$ embryos.

Several studies have highlighted the roles for Syndecan-1, a transmembrane HSPG in cell spreading, actin bundling and cell migration (Chakravarti, Sapountzi et al. 2005). Also, epithelial cell polarization in organotypic cultures is mediated by Laminin and HSPG interaction. Isolated NG2 positive cells were also found in the skin of $Pdgfrb^{-/-}$ embryos (data not shown), again correlating with a severe loss of MC on vascular profiles. Protein lysates from $Ext1^{MCko}$ and control skin samples revealed a strong reduction in PDGFR-β activation, including loss of SHP2 and ERK1/2 activation. Similar to the results obtained in *Ndst1*-/- MEFs, AKT activation was not affected. Thus unlike brain pericytes, pericytes in the periphery require HS production for effective PDGFR-β signalling and recruitment to the vessel wall. The differential requirement of HS could be related to different modes of recruitment. Longitudinal recruitment of pericytes during angiogenic sprouting in the CNS relies on migration and proliferation of pericytes along the ablumenal endothelial surface (reviewed in (Armulik, Abramsson et al. 2005)). This process depends on HS mediated PDGF-B retention close to the endothelial surface (Abramsson, Kurup et al. 2007); (Kurup, Abramsson et al. 2006). Arguably, endothelial HS production and deposition in the endothelial BM would be ideally suited to control PDGF-B retention and function as co-receptor for pericytic PDGFR-β activation *in trans*. In contrast, MC progenitor cells that reside at a distance from the vessel may cell autonomously require HS on the cell surface for activation *in cis*. Recruitment of MC to vessels in the skin involves induction of new progenitor cells from mesenchymal lineages (reviewed in (von Tell, Armulik et al. 2006)). Thus, the spatial relationship between signal sending cell (the endothelium) and signal receiving cell (the MC), are very different during longitudinal recruitment in the CNS and local progenitor induction in the periphery (see **Error! Reference source not found.**). In the former case, migration will occur along a HS-rich basement membrane even when MCs themselves do not produce HS. In the latter, however, recruitment will require polarization towards the signal, and migration over variable distances and the attractive

signal may require transport or diffusion across several neighbouring cells. It is possible that this particular spatial constellation requires cell-autonomous HS production by MCs or their progenitors. An alterative explanation could be that CNS MCs require fundamentally different signals than peripheral MCs, possibly because they derive from distinct lineages. Indeed, lineage-tracing studies indicated that MCs in the brain derive from neural crest, whereas MC in the periphery are of mesodermal origin (Etchevers, Vincent et al. 2001). However it seems unlikely that PDGFR-β signalling differentially relies on HS in neural crest versus mesenchymal cell populations. Rather, the proximity to normal endothelial basement membrane, and the juxtacrine versus paracrine spatial configuration represent a more plausible explanation for the observed differences.

Ex vivo studies using endothelial and 10T1/2 cell co-cultures illustrated that, in addition to PDGF-B/PDGFR-β signalling, TGFβ signalling is involved in pericyte recruitment and differentiation (Sato, Tsuboi et al. 1990); (Hirschi, Rohovsky et al. 1998; Hirschi, Burt et al. 2003). Defective vascular development associated with reduced MC recruitment and impaired vessel stability is observed in mouse mutants of TGFRII, Alk1, Alk5, endoglin and SMAD1/5 (reviewed in (Goumans and Mummery 2000)). Similar defects are observed in patients suffering from hereditary telangiectasia, a genetic disease associated with loss-of function mutations in TGF-β pathway components (reviewed in (Fernandez, Sanz-Rodriguez et al. 2006)). TGF-β is expressed by both ECs and MCs and reciprocal signalling regulates MC induction from mesenchymal progenitors and various endothelial cell functions including expression of stabilizing matrix components, cell proliferation and differentiation. The observed profound reduction in SMAD1, 2 and 3 phosphorylation in western blots of skin samples, and in endothelial cells identified on skin sections, indicates that indeed endothelial TGF-β signalling is defective in the absence of MC HS. In contrast, brain samples from the same embryos show no defects in SMAD phosphorylation. Thus, the loss of HS impairs both TGF-β and PDGFR-β signalling selectively in the skin, but not in the brain.

In addition to the direct binding of TGF-β dimers to HS, recent work illustrated that HS can play an important role in linking the latent TGF-β binding protein LTBP1 to fibronectin, providing a mechanism for TGF-β storage in the ECM (Chen, Sivakumar et al. 2007). In drosophila wing patterning, a process regulated by gradients of the TGF-β family protein Dpp, HS proved essential for gradient formation by facilitating extracellular transport of Dpp across the epithelial cells (Han, Belenkaya et al. 2004).

Thus, HS could be important for the availability, potential gradient formation and activity of TGF-β during the induction and recruitment of MC from mesenchymal progenitors. In line with these observations, Forsten-Williams and colleagues further elaborate the control of growth factor networks by HSPG using experimental and computer simulation models (Forsten-Williams, Chu et al. 2008). Further TGF-β and HSPG modulate vSMC growth and migration. Tran and colleagues suggested that HSPG perlecan contributes to SMC growth control both *in vitro* and during intimal hyperplasia, possibly by sequestering heparin-binding mitogens such as FGF-2 (Tran, Tran-Lundmark et al. 2004).

Finally, the recent observation that TGF-β induces actin reorganization mediated by SMAD2 and -3 by activating Rho-GTPases (Vardouli, Vasilaki et al. 2008) could potentially explain the rounded appearance of NG2 positive cells residing in the mesenchyme, as well as changes in endothelial cell responses. Studies from the blood brain barrier (BBB) revealed that the expression of HSPG agrin correlates with cell polarization of astrocytes and is important for BBB integrity (reviewed in (Abbott, Ronnback et al. 2006)). One could speculate that HS also controls polarization and directed migration of MC progenitors towards the blood vessel.

8.3.1 Future perspective

The data presented in this chapter demonstrate a vital role for pericytic HS during embryonic development. The phenotyical analyses of mice lacking pericytic HS production are still incomplete. So far, no $Ext1^{MCko}$ mice are born though the cause of death remains unclear. Recent findings indicate a function for PDGF-B/PDGFR-β in epicardial development. Loss of PDGF-B ligand or its receptor results in muscular ventricular septal defects, maldevelopment of the atrioventricular cushions and valves, impaired coronary arteriogenesis, and hypoplasia of the myocardium and cardiac nerves (Van den Akker, Winkel et al. 2008). Although initial analyses of coronary vessels and macroscopical observation of the heart in mice lacking pericytic HS revealed no apparent defects, a detailed study of the ventrical and septa might be of interest.

Mice lacking pericytic HS accumulate rounded NG2 positive cells in the peripheral vasculature. Crossing *ROSA26 eYFP* mice with $Ext1^{MCko}$ mice would allows us to detect GFP positive pericytes that lack HS. Using embryonic cultures and live-imaging techniques, it would be interesting to monitor GFP expressing HS negative pericytes

and study their migration, directed movement and polarization *in vivo*. Applying this method, we would be able to follow the dynamics and study pericyte induction *in vivo*.

Isolating mural cells from the CNS and the peripheral skin would complete our studies. One could test differential signalling pathways that are involved in the skin but not in the CNS (e.g. TGF-β) and vice versa. Further, that would allow us to study cell-autonomous function *in vitro*, e.g. whether pericytic HS is required for TGF- β dependent proliferation or directed migration using gradient chambers. One could further analyse gene expression of MCs lacking HS. It would be of interest to investigate the function of pericytic HS in the induction of pericytes from progenitor cell and the induction of MC specific genes such as SM22α, SMA and desmin (Xie, Fang et al. 2008); (Han, Dong et al. 2009); (Ding, Darland et al. 2004).

After addressing the function of pericytic HS in MC recruitment during embryonic development, it would be interesting to understand the role of endothelial HS in this process. Since mice lacking PDGF-B retention motif and mice deficient in N-sulfation display defects in pericyte migration and association to the vessel, one would speculate that endothelial HS is required for MC recruitment in the CNS.

8.3.2 Summary

In conclusion, the present work provides evidence for a differential involvement of cell autonomous HS production in activating PDGFR-β and TGF-β signalling during pericyte recruitment in the CNS and in the periphery (Figure 8.22). Our results also suggest that the involvement of HS in receptor activation acting *in cis* or *in trans* may be context dependent and will arguably be affected by the distance between signal sending and receiving cell. For pericyte/mural cell biology, the current findings advance our understanding of selective cellular interactions during recruitment and of the importance of mural cell-derived heparan sulfate proteoglycans for functional vascular patterning.

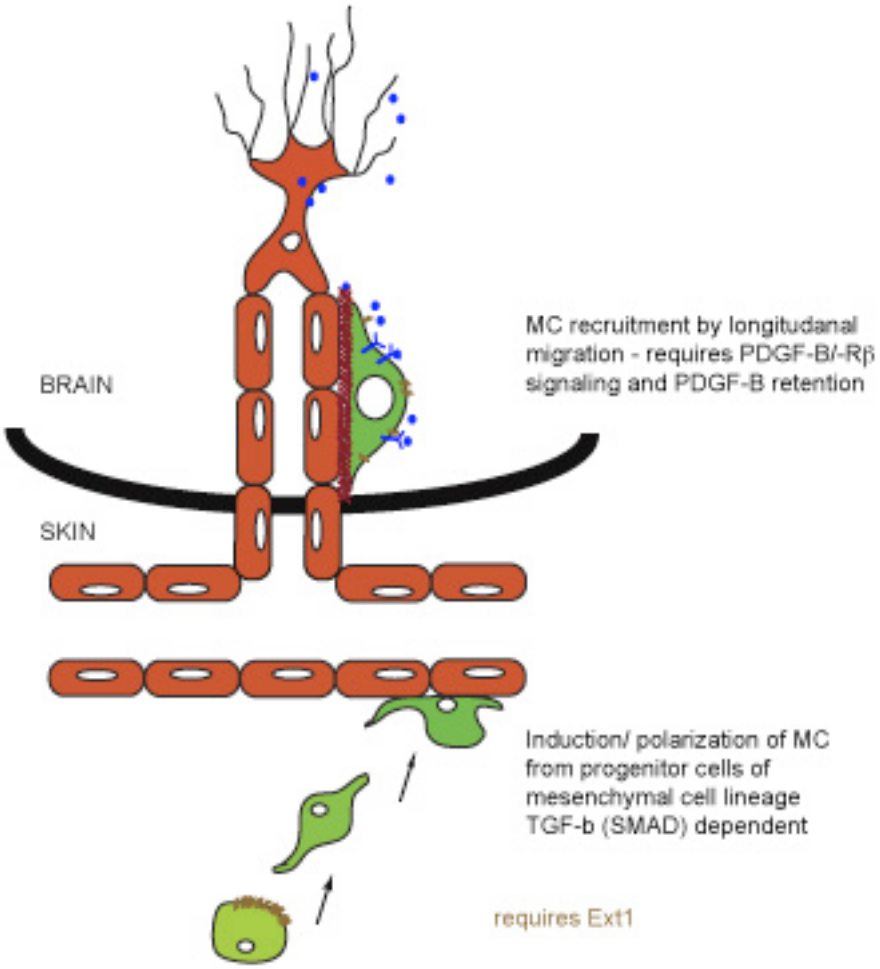

Figure 8.22 Proposed model of MC recruitment and induction in skin and brain
Production of pericytic HS is dispensable during MC recruitment in the CNS but is required for the local induction and possibly polarization and migration of MC progenitors in the peripheral vasculature.

9 Conclusion

The work presented in this thesis addressed the function of ECM molecules during developmental angiogenesis. I studied the expression and localization of several matrix components in the mouse retina. Further, I demonstrated how distinct matrix molecules shape and influence endothelial cell behaviour.

During the last decade, the scientific community studying the process of angiogenesis- the formation of new blood vessels- almost exclusively focused on finding pro-and anti-angiogenic inhibitors. The field experienced major insight in the function of vascular endothelial growth factor (VEGF) and its receptors during developmental and pathological angiogenesis. At the present time, multiple drugs with anti-angiogenic activity are in clinical trials. In 2004, the Food and Drug administration (FDA) approved Bevacizumab (Avastin), a monoclonal antibody against VEGF-A for the treatment of cancer and several anti-angiogenic drugs e.g. targeting VEGFR2 are approved and will follow (reviewed in (Folkman 2007)). However, most drugs did not display the anticipated and desired outcome in mice transplanted with tumours, possibly due to compensatory effects by other growth factors and resistance to the drug.

Further in this field, many laboratories including ours focused their research on understanding the role of Dll4/Notch signalling in regulating angiogenic sprouting. The signalling pathway is upregulated in many tumours and disruption of Dll4/ Notch signalling results in excessive sprouting and vessel formation. Endothelial cells that are exposed to an angiogenic stimulus, induce Dll4 expression and signal to the adjacent cells to restrict sprouting.

Virtually all these studies exclusively concentrated on cellular and molecular mechanisms between endothelial cells in the formation of new vascular sprouts but lack information on the extracellular microenvironment.

Already in the early 1980, Mina Bissell, a pioneer in the extracellular matrix field proposed that extracellular matrix molecules direct gene expression. Her radical idea that the surrounding of a cancer cell is just as important in shaping its behaviour as the genes inside it, has long been ignored.

The extracellular matrix often considered as a passive scaffold for cells, is now widely recognized as an important source of signals that regulate the changes in gene expression, cell division, survival, shape and movement that control tumour progression. Mina Bissell and her lab demonstrated over the last decades that normal cell behaviour can be induced when cancerous cells are placed in 3D microenvironment. Her studies indicate that the extracellular matrix and its receptors dictate the phenotype of mammary epithelial cells, and thus in this model system the tissue phenotype is dominant over the cellular genotype (Weaver, Petersen et al. 1997).

In accordance with the finings that ECM molecules direct cell behaviour, Maniotis and colleagues described matrix-embedded channels devoid of endothelial cells in human tumours, referred to as vasculogenic mimicry (Maniotis, Folberg et al. 1999). Tumour cells may therefore, generate vascular channels that facilitate tumour perfusion independent of tumour angiogenesis. Because the microcirculation of many tumours may be heterogeneous, including incorporated or co-opted vessels, angiogenic vessels, mosaic vessels, and vasculogenic mimicry of the tubular and patterned matrix types, therapeutic regimens that target angiogenesis alone may be ineffective against highly invasive tumours that contain patterned matrices (Folberg and Maniotis 2004).

Tumour blood vessel morphology is dramatically altered compared to the normal vasculature. Pre-existing vessels come in contact with tumour cells, releasing a series of factors altering the basement membranes and the intrinsic properties of endothelial cell lining. Defective and architectural abnormal tumour vessels feature reduced blood flow and hyperpermeability, leading to plasma protein leakage and the basis for perivascular tumour matrix alteration (Del Rosso, Fibbi et al. 2002); (Chiarug, Ruggiero et al. 2002). In turn, these matrix alterations likely influence tumour cells as well as endothelial and smooth muscle cells of the tumour vasculature by modulating cell morphology and invasive, migratory behaviour.

Cells can sense physical forces such as stretch through adhesions to the extracellular matrix. Several investigators have demonstrated that cell–ECM adhesions are critical in the transduction of mechanical stretch into biochemical signals, e.g. stretch induces proliferation in cells attached to different ECM proteins by activating integrins (Wilson, Sudhir et al. 1995); (Katsumi, Naoe et al. 2005). In addition, matrix stiffness, i.e. the degree to which the surrounding adhesive scaffold resists deformation plays a role in endothelial cell behaviour and biological outcome. Chen and colleagues propose that matrix stiffness

influences growth factor mediated endothelial cell responses. Endothelial cells require cell–cell contact and vascular endothelial cadherin engagement to transduce stretch into proliferative signals. Both, endothelial and smooth muscle cells exhibited an increase in proliferation in response to stretch but using distinct mechanisms (Liu, Nelson et al. 2007), suggesting that elasticity of matrix modulates cellular behaviour and needs to be taken into account when targeting EC proliferation by anti-angiogenic drugs such as Bevacizumab (Avastin) inhibiting EC proliferation.

Taken together, the extracellular matrix provides essential cues for physiological and pathological angiogenesis. My own studies highlight that distinct matrix molecules modulate endothelial behaviour in very different ways by regulating essential cellular mechanism.
Fibronectin influences endothelial cell migration by modulating the availability of growth factor, VEGF. Laminin a4 modulates Dll4/ Notch signalling and thereby, restricts excessive vascular sprouting. And heparan sulfate expressed by mural cells, cell-autonomously controls the local induction of mural cells to peripheral blood vessels.

- Life emerged, I suggest, not simple, but complex and whole, and has remained complex and whole ever since—not because of a mysterious élan vital, but thanks to the simple, profound transformation of dead molecules into an organization by which each molecule's formation is catalyzed by some other molecule in the organization. The secret of life, the wellspring of reproduction, is not to be found in the beauty of Watson-Crick pairing, but in the achievement of collective catalytic closure. So, in another sense, life—complex, whole, emergent—is simple after all, a natural outgrowth of the world in which we live. -

Stuart Kaufman

(At Home in the Universe, Oxford University Press, 1995, pp 47-48)

10 References

Abbott, N. J., L. Ronnback, et al. (2006). "Astrocyte-endothelial interactions at the blood-brain barrier." Nat Rev Neurosci **7**(1): 41-53.

Abraham, S., N. Kogata, et al. (2008). "Integrin beta1 subunit controls mural cell adhesion, spreading, and blood vessel wall stability." Circ Res **102**(5): 562-70.

Abramsson, A., S. Kurup, et al. (2007). "Defective N-sulfation of heparan sulfate proteoglycans limits PDGF-BB binding and pericyte recruitment in vascular development." Genes Dev **21**(3): 316-31.

Abramsson, A., P. Lindblom, et al. (2003). "Endothelial and nonendothelial sources of PDGF-B regulate pericyte recruitment and influence vascular pattern formation in tumors." J Clin Invest **112**(8): 1142-51.

Affolter, M. and E. Caussinus (2008). "Tracheal branching morphogenesis in Drosophila: new insights into cell behaviour and organ architecture." Development **135**(12): 2055-64.

Aird, W. C. (2009). "Molecular heterogeneity of tumor endothelium." Cell Tissue Res **335**(1): 271-81.

Albig, A. R., D. J. Becenti, et al. (2008). "Microfibril-associate glycoprotein-2 (MAGP-2) promotes angiogenic cell sprouting by blocking notch signaling in endothelial cells." Microvasc Res **76**(1): 7-14.

Andjelkovic, M., D. R. Alessi, et al. (1997). "Role of translocation in the activation and function of protein kinase B." J Biol Chem **272**(50): 31515-24.

Andrae, J., R. Gallini, et al. (2008). "Role of platelet-derived growth factors in physiology and medicine." Genes Dev **22**(10): 1276-312.

Arar, M., Y. C. Xu, et al. (2000). "Platelet-derived growth factor receptor beta regulates migration and DNA synthesis in metanephric mesenchymal cells." J Biol Chem **275**(13): 9527-33.

Armulik, A., A. Abramsson, et al. (2005). "Endothelial/pericyte interactions." Circ Res **97**(6): 512-23.

Ashikari-Hada, S., H. Habuchi, et al. (2005). "Heparin regulates vascular endothelial growth factor165-dependent mitogenic activity, tube formation, and its receptor phosphorylation of human endothelial cells. Comparison of the effects of heparin and modified heparins." J Biol Chem **280**(36): 31508-15.

Astrof, S., D. Crowley, et al. (2004). "Direct test of potential roles of EIIIA and EIIIB alternatively spliced segments of fibronectin in physiological and tumor angiogenesis." Mol Cell Biol **24**(19): 8662-70.

Astrof, S., D. Crowley, et al. (2007). "Multiple cardiovascular defects caused by the absence of alternatively spliced segments of fibronectin." Dev Biol **311**(1): 11-24.

Bajenaru, M. L., Y. Zhu, et al. (2002). "Astrocyte-specific inactivation of the neurofibromatosis 1 gene (NF1) is insufficient for astrocytoma formation." Mol Cell Biol **22**(14): 5100-13.

Bakker, W., E. C. Eringa, et al. (2009). "Endothelial dysfunction and diabetes: roles of hyperglycemia, impaired insulin signaling and obesity." Cell Tissue Res **335**(1): 165-89.

Ball, S. G., C. A. Shuttleworth, et al. (2007). "Mesenchymal stem cells and neovascularization: role of platelet-derived growth factor receptors." J Cell Mol Med **11**(5): 1012-30.

Baluk, P., C. G. Lee, et al. (2004). "Regulated angiogenesis and vascular regression in mice overexpressing vascular endothelial growth factor in airways." Am J Pathol **165**(4): 1071-85.
Banerji, S., J. Ni, et al. (1999). "LYVE-1, a new homologue of the CD44 glycoprotein, is a lymph-specific receptor for hyaluronan." J Cell Biol **144**(4): 789-801.
Bayless, K. J. and G. E. Davis (2002). "The Cdc42 and Rac1 GTPases are required for capillary lumen formation in three-dimensional extracellular matrices." J Cell Sci **115**(Pt 6): 1123-36.
Bayless, K. J. and G. E. Davis (2004). "Microtubule depolymerization rapidly collapses capillary tube networks in vitro and angiogenic vessels in vivo through the small GTPase Rho." J Biol Chem **279**(12): 11686-95.
Bayless, K. J., R. Salazar, et al. (2000). "RGD-dependent vacuolation and lumen formation observed during endothelial cell morphogenesis in three-dimensional fibrin matrices involves the alpha(v)beta(3) and alpha(5)beta(1) integrins." Am J Pathol **156**(5): 1673-83.
Bayraktar, J., D. Zygmunt, et al. (2006). "Par-1 kinase establishes cell polarity and functions in Notch signaling in the Drosophila embryo." J Cell Sci **119**(Pt 4): 711-21.
Bazzoni, G. and E. Dejana (2004). "Endothelial cell-to-cell junctions: molecular organization and role in vascular homeostasis." Physiol Rev **84**(3): 869-901.
Beech, R. D., M. A. Cleary, et al. (2004). "Nestin promoter/enhancer directs transgene expression to precursors of adult generated periglomerular neurons." J Comp Neurol **475**(1): 128-41.
Belenkaya, T. Y., C. Han, et al. (2004). "Drosophila Dpp morphogen movement is independent of dynamin-mediated endocytosis but regulated by the glypican members of heparan sulfate proteoglycans." Cell **119**(2): 231-44.
Belkin, A. M. and M. A. Stepp (2000). "Integrins as receptors for laminins." Microsc Res Tech **51**(3): 280-301.
Benedito, R., A. Trindade, et al. (2008). "Loss of Notch signalling induced by Dll4 causes arterial calibre reduction by increasing endothelial cell response to angiogenic stimuli." BMC Dev Biol **8**: 117.
Bertolino, P., M. Deckers, et al. (2005). "Transforming growth factor-beta signal transduction in angiogenesis and vascular disorders." Chest **128**(6 Suppl): 585S-590S.
Bjarnegard, M., M. Enge, et al. (2004). "Endothelium-specific ablation of PDGFB leads to pericyte loss and glomerular, cardiac and placental abnormalities." Development **131**(8): 1847-57.
Bloch, W., E. Forsberg, et al. (1997). "Beta 1 integrin is essential for teratoma growth and angiogenesis." J Cell Biol **139**(1): 265-78.
Blum, Y., H. G. Belting, et al. (2008). "Complex cell rearrangements during intersegmental vessel sprouting and vessel fusion in the zebrafish embryo." Dev Biol **316**(2): 312-22.
Brachtendorf, G., A. Kuhn, et al. (2001). "Early expression of endomucin on endothelium of the mouse embryo and on putative hematopoietic clusters in the dorsal aorta." Dev Dyn **222**(3): 410-9.
Campochiaro, P. A. (2004). "Ocular neovascularisation and excessive vascular permeability." Expert Opin Biol Ther **4**(9): 1395-402.
Campos, L. S., L. Decker, et al. (2006). "Notch, epidermal growth factor receptor, and beta1-integrin pathways are coordinated in neural stem cells." J Biol Chem **281**(8): 5300-9.
Carmeliet, P. (2000). "Mechanisms of angiogenesis and arteriogenesis." Nat Med **6**(4): 389-95.

Carmeliet, P. (2005). "Angiogenesis in life, disease and medicine." Nature **438**(7070): 932-6.
Carmeliet, P., V. Ferreira, et al. (1996). "Abnormal blood vessel development and lethality in embryos lacking a single VEGF allele." Nature **380**(6573): 435-9.
Carmeliet, P. and R. K. Jain (2000). "Angiogenesis in cancer and other diseases." Nature **407**(6801): 249-57.
Carmeliet, P., M. G. Lampugnani, et al. (1999). "Targeted deficiency or cytosolic truncation of the VE-cadherin gene in mice impairs VEGF-mediated endothelial survival and angiogenesis." Cell **98**(2): 147-57.
Carvalho, R. L., F. Itoh, et al. (2007). "Compensatory signalling induced in the yolk sac vasculature by deletion of TGFbeta receptors in mice." J Cell Sci **120**(Pt 24): 4269-77.
Cattelino, A., S. Liebner, et al. (2003). "The conditional inactivation of the beta-catenin gene in endothelial cells causes a defective vascular pattern and increased vascular fragility." J Cell Biol **162**(6): 1111-22.
Chakravarti, R., V. Sapountzi, et al. (2005). "Functional role of syndecan-1 cytoplasmic V region in lamellipodial spreading, actin bundling, and cell migration." Mol Biol Cell **16**(8): 3678-91.
Chao, J. T., L. A. Martinez-Lemus, et al. (2006). "Modulation of alpha7-integrin-mediated adhesion and expression by platelet-derived growth factor in vascular smooth muscle cells." Am J Physiol Cell Physiol **290**(4): C972-80.
Chen, C. P., S. H. Liu, et al. (2008). "Heparan sulfate proteoglycans in the basement membranes of the human placenta and decidua." Placenta **29**(4): 309-16.
Chen, Q., P. Sivakumar, et al. (2007). "Potential role for heparan sulfate proteoglycans in regulation of transforming growth factor-beta (TGF-beta) by modulating assembly of latent TGF-beta-binding protein-1." J Biol Chem **282**(36): 26418-30.
Chiarug, V., M. Ruggiero, et al. (2002). "Angiogenesis and the unique nature of tumor matrix." Mol Biotechnol **21**(1): 85-90.
Cho, C. H., C. S. Lee, et al. (2004). "Localization of VEGFR-2 and PLD2 in endothelial caveolae is involved in VEGF-induced phosphorylation of MEK and ERK." Am J Physiol Heart Circ Physiol **286**(5): H1881-8.
Claxton, S. and M. Fruttiger (2004). "Periodic Delta-like 4 expression in developing retinal arteries." Gene Expr Patterns **5**(1): 123-7.
Cook, B. D., G. Ferrari, et al. (2008). "TGF-beta1 induces rearrangement of FLK-1-VE-cadherin-beta-catenin complex at the adherens junction through VEGF-mediated signaling." J Cell Biochem **105**(6): 1367-73.
Corley, K. M., C. J. Taylor, et al. (2005). "Hypoxia-inducible factor 1alpha modulates adhesion, migration, and FAK phosphorylation in vascular smooth muscle cells." J Cell Biochem **96**(5): 971-85.
Costell, M., E. Gustafsson, et al. (1999). "Perlecan maintains the integrity of cartilage and some basement membranes." J Cell Biol **147**(5): 1109-22.
D'Souza, B., A. Miyamoto, et al. (2008). "The many facets of Notch ligands." Oncogene **27**(38): 5148-67.
David, G., X. M. Bai, et al. (1992). "Developmental changes in heparan sulfate expression: in situ detection with mAbs." J Cell Biol **119**(4): 961-75.
Davis, G. E. and D. R. Senger (2005). "Endothelial extracellular matrix: biosynthesis, remodeling, and functions during vascular morphogenesis and neovessel stabilization." Circ Res **97**(11): 1093-107.
Davis, G. E. and D. R. Senger (2008). "Extracellular matrix mediates a molecular balance between vascular morphogenesis and regression." Curr Opin Hematol **15**(3): 197-203.

Dayanir, V., R. D. Meyer, et al. (2001). "Identification of tyrosine residues in vascular endothelial growth factor receptor-2/FLK-1 involved in activation of phosphatidylinositol 3-kinase and cell proliferation." J Biol Chem **276**(21): 17686-92.

DeHahn, K. C., M. Gonzales, et al. (2004). "The alpha4 laminin subunit regulates endothelial cell survival." Exp Cell Res **294**(1): 281-9.

Dejana, E., F. Orsenigo, et al. (2009). "Organization and signaling of endothelial cell-to-cell junctions in various regions of the blood and lymphatic vascular trees." Cell Tissue Res **335**(1): 17-25.

Del Rosso, M., G. Fibbi, et al. (2002). "Multiple pathways of cell invasion are regulated by multiple families of serine proteases." Clin Exp Metastasis **19**(3): 193-207.

Desai, R. A., L. Gao, et al. (2009). "Cell polarity triggered by cell-cell adhesion via E-cadherin." J Cell Sci **122**(Pt 7): 905-11.

Ding, R., D. C. Darland, et al. (2004). "Endothelial-mesenchymal interactions in vitro reveal molecular mechanisms of smooth muscle/pericyte differentiation." Stem Cells Dev **13**(5): 509-20.

Dixelius, J., L. Jakobsson, et al. (2004). "Laminin-1 promotes angiogenesis in synergy with fibroblast growth factor by distinct regulation of the gene and protein expression profile in endothelial cells." J Biol Chem **279**(22): 23766-72.

Doi, H., T. Iso, et al. (2006). "Jagged1-selective notch signaling induces smooth muscle differentiation via a RBP-Jkappa-dependent pathway." J Biol Chem **281**(39): 28555-64.

Dorrell, M. I., E. Aguilar, et al. (2002). "Retinal vascular development is mediated by endothelial filopodia, a preexisting astrocytic template and specific R-cadherin adhesion." Invest Ophthalmol Vis Sci **43**(11): 3500-10.

Dufraine, J., Y. Funahashi, et al. (2008). "Notch signaling regulates tumor angiogenesis by diverse mechanisms." Oncogene **27**(38): 5132-7.

Ebnet, K., M. Aurrand-Lions, et al. (2003). "The junctional adhesion molecule (JAM) family members JAM-2 and JAM-3 associate with the cell polarity protein PAR-3: a possible role for JAMs in endothelial cell polarity." J Cell Sci **116**(Pt 19): 3879-91.

Eickelberg, O., M. Centrella, et al. (2002). "Betaglycan inhibits TGF-beta signaling by preventing type I-type II receptor complex formation. Glycosaminoglycan modifications alter betaglycan function." J Biol Chem **277**(1): 823-9.

Eliceiri, B. P. (2001). "Integrin and growth factor receptor crosstalk." Circ Res **89**(12): 1104-10.

Enge, M., M. Bjarnegard, et al. (2002). "Endothelium-specific platelet-derived growth factor-B ablation mimics diabetic retinopathy." Embo J **21**(16): 4307-16.

Enge, M., M. Bjarnegård, et al. (2002). "Embryonic cardiovascular and kidney defects resulting from endothelium-specific ablation of PDGF-B in mice." Manuscript.

Esko, J. D. and U. Lindahl (2001). "Molecular diversity of heparan sulfate." J Clin Invest **108**(2): 169-73.

Etchevers, H. C., C. Vincent, et al. (2001). "The cephalic neural crest provides pericytes and smooth muscle cells to all blood vessels of the face and forebrain." Development **128**(7): 1059-68.

Fassler, R. and M. Meyer (1995). "Consequences of lack of beta 1 integrin gene expression in mice." Genes Dev **9**(15): 1896-908.

Feinberg, M. W., M. Watanabe, et al. (2004). "Transforming growth factor-beta1 inhibition of vascular smooth muscle cell activation is mediated via Smad3." J Biol Chem **279**(16): 16388-93.

Fernandez, L. A., F. Sanz-Rodriguez, et al. (2006). "Hereditary hemorrhagic telangiectasia, a vascular dysplasia affecting the TGF-beta signaling pathway." Clin Med Res **4**(1): 66-78.
Ferrara, N. and R. S. Kerbel (2005). "Angiogenesis as a therapeutic target." Nature **438**(7070): 967-74.
Flintoff-Dye, N. L., J. Welser, et al. (2005). "Role for the alpha7beta1 integrin in vascular development and integrity." Dev Dyn **234**(1): 11-21.
Folberg, R. and A. J. Maniotis (2004). "Vasculogenic mimicry." Apmis **112**(7-8): 508-25.
Folkman, J. (2007). "Angiogenesis: an organizing principle for drug discovery?" Nat Rev Drug Discov **6**(4): 273-86.
Folkman, J., E. Merler, et al. (1971). "Isolation of a tumor factor responsible for angiogenesis." J Exp Med **133**(2): 275-88.
Fong, G. H. (2008). "Mechanisms of adaptive angiogenesis to tissue hypoxia." Angiogenesis **11**(2): 121-40.
Fontana, L., Y. Chen, et al. (2005). "Fibronectin is required for integrin alphavbeta6-mediated activation of latent TGF-beta complexes containing LTBP-1." Faseb J **19**(13): 1798-808.
Foo, S. S., C. J. Turner, et al. (2006). "Ephrin-B2 controls cell motility and adhesion during blood-vessel-wall assembly." Cell **124**(1): 161-73.
Forsten-Williams, K., C. L. Chu, et al. (2008). "Control of growth factor networks by heparan sulfate proteoglycans." Ann Biomed Eng **36**(12): 2134-48.
Forsythe, J. A., B. H. Jiang, et al. (1996). "Activation of vascular endothelial growth factor gene transcription by hypoxia-inducible factor 1." Mol Cell Biol **16**(9): 4604-13.
Fujio, Y. and K. Walsh (1999). "Akt mediates cytoprotection of endothelial cells by vascular endothelial growth factor in an anchorage-dependent manner." J Biol Chem **274**(23): 16349-54.
Fukuda, T., N. Yoshida, et al. (2002). "Mice lacking the EDB segment of fibronectin develop normally but exhibit reduced cell growth and fibronectin matrix assembly in vitro." Cancer Res **62**(19): 5603-10.
Fuster, M. M., L. Wang, et al. (2007). "Genetic alteration of endothelial heparan sulfate selectively inhibits tumor angiogenesis." J Cell Biol **177**(3): 539-49.
Gariano, R. F. and T. W. Gardner (2005). "Retinal angiogenesis in development and disease." Nature **438**(7070): 960-6.
Geering, B., P. R. Cutillas, et al. (2007). "Regulation of class IA PI3Ks: is there a role for monomeric PI3K subunits?" Biochem Soc Trans **35**(Pt 2): 199-203.
George, E. L., H. S. Baldwin, et al. (1997). "Fibronectins are essential for heart and blood vessel morphogenesis but are dispensable for initial specification of precursor cells." Blood **90**(8): 3073-81.
George, E. L., E. N. Georges-Labouesse, et al. (1993). "Defects in mesoderm, neural tube and vascular development in mouse embryos lacking fibronectin." Development **119**(4): 1079-91.
Georges-Labouesse, E., N. Messaddeq, et al. (1996). "Absence of integrin alpha 6 leads to epidermolysis bullosa and neonatal death in mice." Nat Genet **13**(3): 370-3.
Gerber, H. P., K. J. Hillan, et al. (1999). "VEGF is required for growth and survival in neonatal mice." Development **126**(6): 1149-59.
Gerhardt, H., M. Golding, et al. (2003). "VEGF guides angiogenic sprouting utilizing endothelial tip cell filopodia." J Cell Biol **161**(6): 1163-77.
Gerhardt, H. and H. Semb (2008). "Pericytes: gatekeepers in tumour cell metastasis?" J Mol Med **86**(2): 135-144.

Gerhardt, H., H. Wolburg, et al. (2000). "N-cadherin mediates pericytic-endothelial interaction during brain angiogenesis in the chicken." Dev Dyn **218**(3): 472-9.

Gibson, M. A., D. I. Leavesley, et al. (1999). "Microfibril-associated glycoprotein-2 specifically interacts with a range of bovine and human cell types via alphaVbeta3 integrin." J Biol Chem **274**(19): 13060-5.

Gille, H., J. Kowalski, et al. (2001). "Analysis of biological effects and signaling properties of Flt-1 (VEGFR-1) and KDR (VEGFR-2). A reassessment using novel receptor-specific vascular endothelial growth factor mutants." J Biol Chem **276**(5): 3222-30.

Gonzalez, A. M., M. Gonzales, et al. (2002). "Complex interactions between the laminin alpha 4 subunit and integrins regulate endothelial cell behavior in vitro and angiogenesis in vivo." Proc Natl Acad Sci U S A **99**(25): 16075-80.

Goumans, M. J., Z. Liu, et al. (2009). "TGF-beta signaling in vascular biology and dysfunction." Cell Res **19**(1): 116-27.

Goumans, M. J. and C. Mummery (2000). "Functional analysis of the TGFbeta receptor/Smad pathway through gene ablation in mice." Int J Dev Biol **44**(3): 253-65.

Goustin, A. S., C. Betsholtz, et al. (1985). "Coexpression of the sis and myc proto-oncogenes in developing human placenta suggests autocrine control of trophoblast growth." Cell **41**(1): 301-12.

Graupera, M., J. Guillermet-Guibert, et al. (2008). "Angiogenesis selectively requires the p110alpha isoform of PI3K to control endothelial cell migration." Nature **453**(7195): 662-6.

Graupera, M., J. Guillermet-Guibert, et al. (2008). "Isoform-selective role of the p110α PI 3-kinase in angiogenesis through regulation of endothelial cell migration." Nature **in press**.

Greenberg, J. I., D. J. Shields, et al. (2008). "A role for VEGF as a negative regulator of pericyte function and vessel maturation." Nature **456**(7223): 809-13.

Grishina, I. B., S. Y. Kim, et al. (2005). "BMP7 inhibits branching morphogenesis in the prostate gland and interferes with Notch signaling." Dev Biol **288**(2): 334-47.

Guan, J. L., J. E. Trevithick, et al. (1990). "Retroviral expression of alternatively spliced forms of rat fibronectin." J Cell Biol **110**(3): 833-47.

Hallmann, R., N. Horn, et al. (2005). "Expression and function of laminins in the embryonic and mature vasculature." Physiol Rev **85**(3): 979-1000.

Hamada, K., T. Sasaki, et al. (2005). "The PTEN/PI3K pathway governs normal vascular development and tumor angiogenesis." Genes Dev **19**(17): 2054-65.

Hammes, H. P., J. Lin, et al. (2002). "Pericytes and the pathogenesis of diabetic retinopathy." Diabetes **51**(10): 3107-12.

Hammes, H. P., J. Lin, et al. (2004). "Angiopoietin-2 causes pericyte dropout in the normal retina: evidence for involvement in diabetic retinopathy." Diabetes **53**(4): 1104-10.

Han, C., T. Y. Belenkaya, et al. (2004). "Distinct and collaborative roles of Drosophila EXT family proteins in morphogen signalling and gradient formation." Development **131**(7): 1563-75.

Han, M., L. H. Dong, et al. (2009). "Smooth muscle 22 alpha maintains the differentiated phenotype of vascular smooth muscle cells by inducing filamentous actin bundling." Life Sci **84**(13-14): 394-401.

Harrington, L. S., R. C. A. Sainson, et al. (2007). "Regulation of multiple angiogenic pathways by Dll4 and Notch in human umbilical vein endothelial cells." Microvasc Res.

Hayashi, H. and T. Kume (2008). "Foxc transcription factors directly regulate Dll4 and Hey2 expression by interacting with the VEGF-Notch signaling pathways in endothelial cells." PLoS ONE **3**(6): e2401.

Hayashi, H., H. Sano, et al. (2008). "The Foxc2 transcription factor regulates angiogenesis via induction of integrin beta3 expression." J Biol Chem **283**(35): 23791-800.

Hellstrom, M., H. Gerhardt, et al. (2001). "Lack of pericytes leads to endothelial hyperplasia and abnormal vascular morphogenesis." J Cell Biol **153**(3): 543-53.

Hellström, M., H. Gerhardt, et al. (2001). "Lack of pericytes leads to endothelial hyperplasia and abnormal vascular morphogenesis." J Cell Biol **153**: 543-553.

Hellstrom, M., M. Kalen, et al. (1999). "Role of PDGF-B and PDGFR-beta in recruitment of vascular smooth muscle cells and pericytes during embryonic blood vessel formation in the mouse." Development **126**(14): 3047-55.

Hellström, M., M. Kalén, et al. (1999). "Role of PDGF-B and PDGFR-beta in recruitment of vascular smooth muscle cells and pericytes during embryonic blood vessel formation in the mouse." Development **126**(14): 3047-55.

Hellstrom, M., L. K. Phng, et al. (2007). "VEGF and Notch signaling: the Yin and Yang of angiogenic sprouting." Cell Adhesion Migration **1**(3): 133-136.

Hellstrom, M., L. K. Phng, et al. (2007). "Dll4 signalling through Notch1 regulates formation of tip cells during angiogenesis." Nature **445**(7129): 776-80.

High, F. A., M. M. Lu, et al. (2008). "Endothelial expression of the Notch ligand Jagged1 is required for vascular smooth muscle development." Proc Natl Acad Sci U S A **105**(6): 1955-9.

Hirschi, K. K., J. M. Burt, et al. (2003). "Gap junction communication mediates transforming growth factor-beta activation and endothelial-induced mural cell differentiation." Circ Res **93**(5): 429-37.

Hirschi, K. K., S. A. Rohovsky, et al. (1998). "PDGF, TGF-beta, and heterotypic cell-cell interactions mediate endothelial cell-induced recruitment of 10T1/2 cells and their differentiation to a smooth muscle fate [published erratum appears in J Cell Biol 1998 Jun 1;141(5):1287]." J Cell Biol **141**(3): 805-14.

Hodivala-Dilke, K. M., K. P. McHugh, et al. (1999). "Beta3-integrin-deficient mice are a model for Glanzmann thrombasthenia showing placental defects and reduced survival." J Clin Invest **103**(2): 229-38.

Hodkinson, P. S., P. A. Elliott, et al. (2007). "Mammalian NOTCH-1 activates beta1 integrins via the small GTPase R-Ras." J Biol Chem **282**(39): 28991-9001.

Holderfield, M. T., A. M. Henderson Anderson, et al. (2006). "HESR1/CHF2 suppresses VEGFR2 transcription independent of binding to E-boxes." Biochem Biophys Res Commun **346**(3): 637-48.

Hosking, B. and T. Makinen (2007). "Lymphatic vasculature: a molecular perspective." Bioessays **29**(12): 1192-202.

Huang, L., W. Yu, et al. (2009). "Robo1/robo4: different expression patterns in retinal development." Exp Eye Res **88**(3): 583-8.

Huang, X. Z., J. F. Wu, et al. (2000). "Fatal bilateral chylothorax in mice lacking the integrin alpha9beta1." Mol Cell Biol **20**(14): 5208-15.

Hynes, R. O. (2007). "Cell-matrix adhesion in vascular development." J Thromb Haemost **5 Suppl 1**: 32-40.

Ibrahimi, O. A., F. Zhang, et al. (2004). "Kinetic model for FGF, FGFR, and proteoglycan signal transduction complex assembly." Biochemistry **43**(16): 4724-30.

Iivanainen, A., J. Kortesmaa, et al. (1997). "Primary structure, developmental expression, and immunolocalization of the murine laminin alpha4 chain." J Biol Chem **272**(44): 27862-8.

Im, E. and A. Kazlauskas (2006). "New insights regarding vessel regression." Cell Cycle **5**(18): 2057-9.
Inatani, M., F. Irie, et al. (2003). "Mammalian brain morphogenesis and midline axon guidance require heparan sulfate." Science **302**(5647): 1044-6.
Itoh, F., S. Itoh, et al. (2004). "Synergy and antagonism between Notch and BMP receptor signaling pathways in endothelial cells." Embo J **23**(3): 541-51.
Jakobsson, L., A. Domogatskaya, et al. (2007). "Laminin deposition is dispensable for vasculogenesis but regulates blood vessel diameter independent of flow." Faseb J.
Jakobsson, L., J. Kreuger, et al. (2007). "Building blood vessels--stem cell models in vascular biology." J Cell Biol **177**(5): 751-5.
Jakobsson, L., J. Kreuger, et al. (2006). "Heparan Sulfate in trans Potentiates VEGFR-Mediated Angiogenesis." Dev Cell **10**(5): 625-34.
Jiang, B., G. I. Liou, et al. (1994). "Astrocytes modulate retinal vasculogenesis: effects on fibronectin." Journal of Cell Science **107**: 2499-2508.
Jiang, B., G. I. Liou, et al. (1994). "Astrocytes modulate retinal vasculogenesis: effects on fibronectin expression." J. Cell Sci. **107**: 2499-2508.
Jiang, B. H., G. Jiang, et al. (2001). "Phosphatidylinositol 3-kinase signaling controls levels of hypoxia-inducible factor 1." Cell Growth Differ **12**(7): 363-9.
Jiang, B. H. and L. Z. Liu (2008). "AKT signaling in regulating angiogenesis." Curr Cancer Drug Targets **8**(1): 19-26.
Jiang, B. H. and L. Z. Liu (2008). "PI3K/PTEN signaling in tumorigenesis and angiogenesis." Biochim Biophys Acta **1784**(1): 150-8.
Jin, S., E. M. Hansson, et al. (2008). "Notch signaling regulates platelet-derived growth factor receptor-beta expression in vascular smooth muscle cells." Circ Res **102**(12): 1483-91.
Joyce, J. A., C. Freeman, et al. (2005). "A functional heparan sulfate mimetic implicates both heparanase and heparan sulfate in tumor angiogenesis and invasion in a mouse model of multistage cancer." Oncogene **24**(25): 4037-51.
Julich, D., R. Geisler, et al. (2005). "Integrinalpha5 and delta/notch signaling have complementary spatiotemporal requirements during zebrafish somitogenesis." Dev Cell **8**(4): 575-86.
Kamei, M., W. B. Saunders, et al. (2006). "Endothelial tubes assemble from intracellular vacuoles in vivo." Nature **442**(7101): 453-6.
Kaminski, W. E., P. Lindahl, et al. (2001). "Basis of hematopoietic defects in platelet-derived growth factor (PDGF)-B and PDGF beta-receptor null mice." Blood **97**(7): 1990-8.
Kaneko, Y., K. Kitazato, et al. (2004). "Integrin-linked kinase regulates vascular morphogenesis induced by vascular endothelial growth factor." J Cell Sci **117**(Pt 3): 407-15.
Kano, M. R., Y. Morishita, et al. (2005). "VEGF-A and FGF-2 synergistically promote neoangiogenesis through enhancement of endogenous PDGF-B-PDGFRbeta signaling." J Cell Sci **118**(Pt 16): 3759-68.
Karkkainen, M. J., P. Haiko, et al. (2004). "Vascular endothelial growth factor C is required for sprouting of the first lymphatic vessels from embryonic veins." Nat Immunol **5**(1): 74-80.
Karpanen, T. and T. Makinen (2006). "Regulation of lymphangiogenesis--from cell fate determination to vessel remodeling." Exp Cell Res **312**(5): 575-83.
Katsumi, A., T. Naoe, et al. (2005). "Integrin activation and matrix binding mediate cellular responses to mechanical stretch." J Biol Chem **280**(17): 16546-9.

Khaibullina, A. A., J. M. Rosenstein, et al. (2004). "Vascular endothelial growth factor promotes neurite maturation in primary CNS neuronal cultures." Brain Res Dev Brain Res **148**(1): 59-68.

Knoll, R., R. Postel, et al. (2007). "Laminin-alpha4 and integrin-linked kinase mutations cause human cardiomyopathy via simultaneous defects in cardiomyocytes and endothelial cells." Circulation **116**(5): 515-25.

Koh, W., R. D. Mahan, et al. (2008). "Cdc42- and Rac1-mediated endothelial lumen formation requires Pak2, Pak4 and Par3, and PKC-dependent signaling." J Cell Sci **121**(Pt 7): 989-1001.

Kreidberg, J. A., M. J. Donovan, et al. (1996). "Alpha 3 beta 1 integrin has a crucial role in kidney and lung organogenesis." Development **122**(11): 3537-47.

Kume, T. (2008). "Foxc2 transcription factor: a newly described regulator of angiogenesis." Trends Cardiovasc Med **18**(6): 224-8.

Kurup, S., A. Abramsson, et al. (2006). "Heparan sulphate requirement in platelet-derived growth factor B-mediated pericyte recruitment." Biochem Soc Trans **34**(Pt 3): 454-5.

Lamagna, C. and G. Bergers (2006). "The bone marrow constitutes a reservoir of pericyte progenitors." J Leukoc Biol **80**(4): 677-81.

Lampugnani, M. G. and E. Dejana (1997). "Interendothelial junctions: structure, signalling and functional roles." Curr Opin Cell Biol **9**(5): 674-82.

Lampugnani, M. G. and E. Dejana (2007). "The control of endothelial cell functions by adherens junctions." Novartis Found Symp **283**: 4-13; discussion 13-7, 238-41.

Lampugnani, M. G., F. Orsenigo, et al. (2006). "Vascular endothelial cadherin controls VEGFR-2 internalization and signaling from intracellular compartments." J Cell Biol **174**(4): 593-604.

Lan, Y., B. Liu, et al. (2007). "Essential role of endothelial Smad4 in vascular remodeling and integrity." Mol Cell Biol **27**(21): 7683-92.

Langley, R. R. and I. J. Fidler (2007). "Tumor cell-organ microenvironment interactions in the pathogenesis of cancer metastasis." Endocr Rev **28**(3): 297-321.

LeCouter, J., J. Kowalski, et al. (2001). "Identification of an angiogenic mitogen selective for endocrine gland endothelium." Nature **412**(6850): 877-84.

Lee, S., S. M. Jilani, et al. (2005). "Processing of VEGF-A by matrix metalloproteinases regulates bioavailability and vascular patterning in tumors." J Cell Biol **169**(4): 681-91.

Lee, T. H., S. Seng, et al. (2006). "Integrin regulation by vascular endothelial growth factor in human brain microvascular endothelial cells: role of alpha6beta1 integrin in angiogenesis." J Biol Chem **281**(52): 40450-60.

Lehti, K., E. Allen, et al. (2005). "An MT1-MMP-PDGF receptor-beta axis regulates mural cell investment of the microvasculature." Genes Dev **19**(8): 979-91.

Leiss, M., K. Beckmann, et al. (2008). "The role of integrin binding sites in fibronectin matrix assembly in vivo." Curr Opin Cell Biol **20**(5): 502-7.

Leong, K. G., X. Hu, et al. (2002). "Activated Notch4 inhibits angiogenesis: role of beta 1-integrin activation." Mol Cell Biol **22**(8): 2830-41.

Li, J., C. Yen, et al. (1997). "PTEN, a putative protein tyrosine phosphatase gene mutated in human brain, breast, and prostate cancer." Science **275**(5308): 1943-7.

Li, S., D. Harrison, et al. (2002). "Matrix assembly, regulation, and survival functions of laminin and its receptors in embryonic stem cell differentiation." J Cell Biol **157**(7): 1279-90.

Li, X., A. Ponten, et al. (2000). "PDGF-C is a new protease-activated ligand for the PDGF alpha-receptor." Nat Cell Biol **2**(5): 302-9.

Lian, J., X. Dai, et al. (2006). "Identification of an active site on the laminin alpha4 chain globular domain that binds to alphavbeta3 integrin and promotes angiogenesis." Biochem Biophys Res Commun **347**(1): 248-53.
Lin, T., S. B. Sandusky, et al. (2003). "A central nervous system specific mouse model for thanatophoric dysplasia type II." Hum Mol Genet **12**(21): 2863-71.
Lin, X. (2004). "Functions of heparan sulfate proteoglycans in cell signaling during development." Development **131**(24): 6009-21.
Lin, X., G. Wei, et al. (2000). "Disruption of gastrulation and heparan sulfate biosynthesis in EXT1-deficient mice." Dev Biol **224**(2): 299-311.
Lindahl, P., M. Hellstrom, et al. (1998). "Paracrine PDGF-B/PDGF-Rbeta signaling controls mesangial cell development in kidney glomeruli." Development **125**(17): 3313-22.
Lindahl, P., B. R. Johansson, et al. (1997). "Pericyte loss and microaneurysm formation in PDGF-B-deficient mice." Science **277**(5323): 242-5.
Lindblom, P., H. Gerhardt, et al. (2003). "Endothelial PDGF-B retention is required for proper investment of pericytes in the microvessel wall." Genes Dev **17**(15): 1835-40.
Liu, W. F., C. M. Nelson, et al. (2007). "Cadherins, RhoA, and Rac1 are differentially required for stretch-mediated proliferation in endothelial versus smooth muscle cells." Circ Res **101**(5): e44-52.
Lobov, I. B., R. A. Renard, et al. (2007). "Delta-like ligand 4 (Dll4) is induced by VEGF as a negative regulator of angiogenic sprouting." Proc Natl Acad Sci U S A **104**(9): 3219-24.
Lu, X., F. Le Noble, et al. (2004). "The netrin receptor UNC5B mediates guidance events controlling morphogenesis of the vascular system." Nature **432**(7014): 179-86.
Lu, Y., R. Zhou, et al. (2000). "The cellular and molecular mechanism of laminin-glycopeptides on anti-metastasis." Chin Med J (Engl) **113**(5): 466-70.
Luo, Y. and G. L. Radice (2005). "N-cadherin acts upstream of VE-cadherin in controlling vascular morphogenesis." J Cell Biol **169**(1): 29-34.
Mahabeleshwar, G. H., W. Feng, et al. (2007). "Mechanisms of integrin-vascular endothelial growth factor receptor cross-activation in angiogenesis." Circ Res **101**(6): 570-80.
Makinen, T., L. Jussila, et al. (2001). "Inhibition of lymphangiogenesis with resulting lymphedema in transgenic mice expressing soluble VEGF receptor-3." Nat Med **7**(2): 199-205.
Makinen, T., T. Veikkola, et al. (2001). "Isolated lymphatic endothelial cells transduce growth, survival and migratory signals via the VEGF-C/D receptor VEGFR-3." Embo J **20**(17): 4762-73.
Maniotis, A. J., R. Folberg, et al. (1999). "Vascular channel formation by human melanoma cells in vivo and in vitro: vasculogenic mimicry." Am J Pathol **155**(3): 739-52.
Marin-Padilla, M. (1995). "Prenatal development of fibrous (white matter), protoplasmic (gray matter), and layer I astrocytes in the human cerebral cortex: a Golgi study." J Comp Neurol **357**(4): 554-72.
Marti, H. J., M. Bernaudin, et al. (2000). "Hypoxia-induced vascular endothelial growth factor expression precedes neovascularization after cerebral ischemia." Am J Pathol **156**(3): 965-76.
Matsumoto, T., S. Bohman, et al. (2005). "VEGF receptor-2 Y951 signaling and a role for the adapter molecule TSAd in tumor angiogenesis." Embo J **24**(13): 2342-53.

May, T., P. P. Mueller, et al. (2005). "Establishment of murine cell lines by constitutive and conditional immortalization." J Biotechnol **120**(1): 99-110.
McCarty, J. H., R. A. Monahan-Earley, et al. (2002). "Defective associations between blood vessels and brain parenchyma lead to cerebral hemorrhage in mice lacking alphav integrins." Mol Cell Biol **22**(21): 7667-77.
Miao, H. Q. and M. Klagsbrun (2000). "Neuropilin is a mediator of angiogenesis." Cancer Metastasis Rev **19**(1-2): 29-37.
Miner, J. H., J. Cunningham, et al. (1998). "Roles for laminin in embryogenesis: exencephaly, syndactyly, and placentopathy in mice lacking the laminin alpha5 chain." J Cell Biol **143**(6): 1713-23.
Miquerol, L., B. L. Langille, et al. (2000). "Embryonic development is disrupted by modest increases in vascular endothelial growth factor gene expression." Development **127**(18): 3941-6.
Mitsi, M., Z. Hong, et al. (2006). "Heparin-mediated conformational changes in fibronectin expose vascular endothelial growth factor binding sites." Biochemistry **45**(34): 10319-28.
Moretti, F. A., A. K. Chauhan, et al. (2007). "A major fraction of fibronectin present in the extracellular matrix of tissues is plasma-derived." J Biol Chem **282**(38): 28057-62.
Naik, M. U., S. A. Mousa, et al. (2003). "Signaling through JAM-1 and alphavbeta3 is required for the angiogenic action of bFGF: dissociation of the JAM-1 and alphavbeta3 complex." Blood **102**(6): 2108-14.
Naik, M. U. and U. P. Naik (2006). "Junctional adhesion molecule-A-induced endothelial cell migration on vitronectin is integrin alpha v beta 3 specific." J Cell Sci **119**(Pt 3): 490-9.
Nikitenko, L. L. (2009). "Vascular endothelium in cancer." Cell Tissue Res **335**(1): 223-40.
Nikolopoulos, S. N., P. Blaikie, et al. (2004). "Integrin beta4 signaling promotes tumor angiogenesis." Cancer Cell **6**(5): 471-83.
Nilsson, I., M. Shibuya, et al. (2004). "Differential activation of vascular genes by hypoxia in primary endothelial cells." Exp Cell Res **299**(2): 476-85.
Nitta, T., M. Hata, et al. (2003). "Size-selective loosening of the blood-brain barrier in claudin-5-deficient mice." J Cell Biol **161**(3): 653-60.
Noguera-Troise, I., C. Daly, et al. (2006). "Blockade of Dll4 inhibits tumour growth by promoting non-productive angiogenesis." Nature **444**(7122): 1032-7.
O'Brien, L. E., T. S. Jou, et al. (2001). "Rac1 orientates epithelial apical polarity through effects on basolateral laminin assembly." Nat Cell Biol **3**(9): 831-8.
Ohlsson, R., P. Falck, et al. (1999). "PDGFB regulates the development of the labyrinthine layer of the mouse fetal placenta." Dev Biol **212**(1): 124-36.
Olivey, H. E., L. A. Compton, et al. (2004). "Coronary vessel development: the epicardium delivers." Trends Cardiovasc Med **14**(6): 247-51.
Olsson, A. K., A. Dimberg, et al. (2006). "VEGF receptor signalling - in control of vascular function." Nat Rev Mol Cell Biol **7**(5): 359-71.
Orecchia, A., P. M. Lacal, et al. (2003). "Vascular endothelial growth factor receptor-1 is deposited in the extracellular matrix by endothelial cells and is a ligand for the alpha 5 beta 1 integrin." J Cell Sci **116**(Pt 17): 3479-89.
Ozerdem, U., K. A. Grako, et al. (2001). "NG2 proteoglykan is expressed exclusively by mural cells during vascular morphogenesis." Dev. Dyn. **222**: 218-227.
Pan, Q., Y. Chathery, et al. (2007). "Neuropilin-1 binds to VEGF121 and regulates endothelial cell migration and sprouting." J Biol Chem **282**(33): 24049-56.
Phng, L. K. and H. Gerhardt (2009). "Angiogenesis: a team effort coordinated by notch." Dev Cell **16**(2): 196-208.

Phng, L. K., M. Potente, et al. (2009). "Nrarp coordinates endothelial Notch and Wnt signaling to control vessel density in angiogenesis." Dev Cell **16**(1): 70-82.
Pollard, S. M., M. J. Parsons, et al. (2006). "Essential and overlapping roles for laminin alpha chains in notochord and blood vessel formation." Dev Biol **289**(1): 64-76.
Poschl, E., U. Schlotzer-Schrehardt, et al. (2004). "Collagen IV is essential for basement membrane stability but dispensable for initiation of its assembly during early development." Development **131**(7): 1619-28.
Proweller, A., A. C. Wright, et al. (2007). "Notch signaling in vascular smooth muscle cells is required to pattern the cerebral vasculature." Proc Natl Acad Sci U S A **104**(41): 16275-80.
Purves, W. K., Orians G.H., Heller H.C., Sadava D (2002). Life: The Science of Biology, Sinauer Associates and WH Freeman.
Ray, J. L., R. Leach, et al. (2001). "Isolation of vascular smooth muscle cells from a single murine aorta." Methods Cell Sci **23**(4): 185-8.
Red-Horse, K., Y. Crawford, et al. (2007). "Endothelium-microenvironment interactions in the developing embryo and in the adult." Dev Cell **12**(2): 181-94.
Reynolds, A. R., L. E. Reynolds, et al. (2004). "Elevated Flk1 (vascular endothelial growth factor receptor 2) signaling mediates enhanced angiogenesis in beta3-integrin-deficient mice." Cancer Res **64**(23): 8643-50.
Reynolds, L. E., L. Wyder, et al. (2002). "Enhanced pathological angiogenesis in mice lacking beta3 integrin or beta3 and beta5 integrins." Nat Med **8**(1): 27-34.
Rider, C. C. (2006). "Heparin/heparan sulphate binding in the TGF-beta cytokine superfamily." Biochem Soc Trans **34**(Pt 3): 458-60.
Roberts, D. M., J. B. Kearney, et al. (2004). "The vascular endothelial growth factor (VEGF) receptor Flt-1 (VEGFR-1) modulates Flk-1 (VEGFR-2) signaling during blood vessel formation." Am J Pathol **164**(5): 1531-5.
Roca, C. and R. H. Adams (2007). "Regulation of vascular morphogenesis by Notch signaling." Genes Dev **21**(20): 2511-24.
Rossant, J. and L. Howard (2002). "Signaling pathways in vascular development." Annu Rev Cell Dev Biol **18**: 541-73.
Rudini, N., A. Felici, et al. (2008). "VE-cadherin is a critical endothelial regulator of TGF-beta signalling." Embo J **27**(7): 993-1004.
Ruhrberg, C., H. Gerhardt, et al. (2002). "Spatially restricted patterning cues provided by heparin-binding VEGF-A control blood vessel branching morphogenesis." Genes Dev **16**(20): 2684-98.
Sakai, T., S. Li, et al. (2003). "Integrin-linked kinase (ILK) is required for polarizing the epiblast, cell adhesion, and controlling actin accumulation." Genes Dev **17**(7): 926-40.
Sakurai, Y., K. Ohgimoto, et al. (2005). "Essential role of Flk-1 (VEGF receptor 2) tyrosine residue 1173 in vasculogenesis in mice." Proc Natl Acad Sci U S A **102**(4): 1076-81.
Sano, H., Y. Ueda, et al. (2002). "Blockade of platelet-derived growth factor receptor-beta pathway induces apoptosis of vascular endothelial cells and disrupts glomerular capillary formation in neonatal mice." Am J Pathol **161**(1): 135-43.
Sasaki, N., T. Sasamura, et al. (2007). "Polarized exocytosis and transcytosis of Notch during its apical localization in Drosophila epithelial cells." Genes Cells **12**(1): 89-103.
Sasaki, T., R. Fassler, et al. (2004). "Laminin: the crux of basement membrane assembly." J Cell Biol **164**(7): 959-63.
Sasisekharan, R., Z. Shriver, et al. (2002). "Roles of heparan-sulphate glycosaminoglycans in cancer." Nat Rev Cancer **2**(7): 521-8.

Sato, Y., R. Tsuboi, et al. (1990). "Characterization of the activation of latent TGF-beta by co-cultures of endothelial cells and pericytes or smooth muscle cells: a self-regulating system." J Cell Biol **111**(2): 757-63.

Saunders, W. B., K. J. Bayless, et al. (2005). "MMP-1 activation by serine proteases and MMP-10 induces human capillary tubular network collapse and regression in 3D collagen matrices." J Cell Sci **118**(Pt 10): 2325-40.

Sawano, A., S. Iwai, et al. (2001). "Flt-1, vascular endothelial growth factor receptor 1, is a novel cell surface marker for the lineage of monocyte-macrophages in humans." Blood **97**(3): 785-91.

Schoch, H. J., S. Fischer, et al. (2002). "Hypoxia-induced vascular endothelial growth factor expression causes vascular leakage in the brain." Brain **125**(Pt 11): 2549-57.

Schultz, K., B. L. Fanburg, et al. (2006). "Hypoxia and hypoxia-inducible factor-1alpha promote growth factor-induced proliferation of human vascular smooth muscle cells." Am J Physiol Heart Circ Physiol **290**(6): H2528-34.

Serini, G., L. Napione, et al. (2008). "Integrins team up with tyrosine kinase receptors and plexins to control angiogenesis." Curr Opin Hematol **15**(3): 235-42.

Shalaby, F., J. Rossant, et al. (1995). "Failure of blood-island formation and vasculogenesis in Flk-1-deficient mice." Nature **376**(6535): 62-6.

Siekmann, A. F. and N. D. Lawson (2007). "Notch signalling limits angiogenic cell behaviour in developing zebrafish arteries." Nature **445**(7129): 781-4.

Silva, R., G. D'Amico, et al. (2008). "Integrins: the keys to unlocking angiogenesis." Arterioscler Thromb Vasc Biol **28**(10): 1703-13.

Sima, A. V., C. S. Stancu, et al. (2009). "Vascular endothelium in atherosclerosis." Cell Tissue Res **335**(1): 191-203.

Soldi, R., S. Mitola, et al. (1999). "Role of alphavbeta3 integrin in the activation of vascular endothelial growth factor receptor-2." Embo J **18**(4): 882-92.

Song, S., A. J. Ewald, et al. (2005). "PDGFRbeta+ perivascular progenitor cells in tumours regulate pericyte differentiation and vascular survival." Nat Cell Biol **7**(9): 870-9.

Sorokin, L. M., M. A. Maley, et al. (2000). "Laminin alpha4 and integrin alpha6 are upregulated in regenerating dy/dy skeletal muscle: comparative expression of laminin and integrin isoforms in muscles regenerating after crush injury." Exp Cell Res **256**(2): 500-14.

Srinivas, S., T. Watanabe, et al. (2001). "Cre reporter strains produced by targeted insertion of EYFP and ECFP into the ROSA26 locus." BMC Dev Biol **1**: 4.

Stone, J., A. Itin, et al. (1995). "Development of retinal vasculature is mediated by hypoxia-induced vascular endothelial growth factor (VEGF) expression by neuroglia." J Neurosci **15**(7 Pt 1): 4738-47.

Suchting, S., C. Freitas, et al. (2007). "The Notch ligand Delta-like 4 negatively regulates endothelial tip cell formation and vessel branching." Proc Natl Acad Sci U S A **104**(9): 3225-30.

Taddei, A., C. Giampietro, et al. (2008). "Endothelial adherens junctions control tight junctions by VE-cadherin-mediated upregulation of claudin-5." Nat Cell Biol **10**(8): 923-34.

Takahashi, S., M. Leiss, et al. (2007). "The RGD motif in fibronectin is essential for development but dispensable for fibril assembly." J Cell Biol **178**(1): 167-78.

Takahashi, T., S. Yamaguchi, et al. (2001). "A single autophosphorylation site on KDR/Flk-1 is essential for VEGF-A-dependent activation of PLC-gamma and DNA synthesis in vascular endothelial cells." Embo J **20**(11): 2768-78.

Tallquist, M. D., R. A. Klinghoffer, et al. (2000). "Retention of PDGFR-beta function in mice in the absence of phosphatidylinositol 3'-kinase and phospholipase Cgamma signaling pathways." Genes Dev **14**(24): 3179-90.

Talts, J. F., T. Sasaki, et al. (2000). "Structural and functional analysis of the recombinant G domain of the laminin alpha4 chain and its proteolytic processing in tissues." J Biol Chem **275**(45): 35192-9.

Tammela, T., G. Zarkada, et al. (2008). "Blocking VEGFR-3 suppresses angiogenic sprouting and vascular network formation." Nature **454**(7204): 656-60.

Taverna, D. and R. O. Hynes (2001). "Reduced blood vessel formation and tumor growth in alpha5-integrin-negative teratocarcinomas and embryoid bodies." Cancer Res **61**(13): 5255-61.

Thurston, G., I. Noguera-Troise, et al. (2007). "The Delta paradox: DLL4 blockade leads to more tumour vessels but less tumour growth." Nat Rev Cancer **7**(5): 327-31.

Thyboll, J., J. Kortesmaa, et al. (2002). "Deletion of the laminin alpha4 chain leads to impaired microvessel maturation." Mol Cell Biol **22**(4): 1194-202.

Tillet, E., D. Vittet, et al. (2005). "N-cadherin deficiency impairs pericyte recruitment, and not endothelial differentiation or sprouting, in embryonic stem cell-derived angiogenesis." Exp Cell Res **310**(2): 392-400.

Tran, P. K., K. Tran-Lundmark, et al. (2004). "Increased intimal hyperplasia and smooth muscle cell proliferation in transgenic mice with heparan sulfate-deficient perlecan." Circ Res **94**(4): 550-8.

Trindade, A., S. R. Kumar, et al. (2008). "Overexpression of delta-like 4 induces arterialization and attenuates vessel formation in developing mouse embryos." Blood **112**(5): 1720-9.

Tzima, E., M. Irani-Tehrani, et al. (2005). "A mechanosensory complex that mediates the endothelial cell response to fluid shear stress." Nature **437**(7057): 426-31.

Uemura, A., S. Kusuhara, et al. (2006). "Tlx acts as a proangiogenic switch by regulating extracellular assembly of fibronectin matrices in retinal astrocytes." J Clin Invest **116**(2): 369-77.

Van den Akker, N. M., L. C. Winkel, et al. (2008). "PDGF-B signaling is important for murine cardiac development: its role in developing atrioventricular valves, coronaries, and cardiac innervation." Dev Dyn **237**(2): 494-503.

Vanhaesebroeck, B. and M. D. Waterfield (1999). "Signaling by distinct classes of phosphoinositide 3-kinases." Exp Cell Res **253**(1): 239-54.

Vardouli, L., E. Vasilaki, et al. (2008). "A novel mechanism of TGFbeta-induced actin reorganization mediated by Smad proteins and Rho GTPases." Febs J **275**(16): 4074-87.

von Tell, D., A. Armulik, et al. (2006). "Pericytes and vascular stability." Exp Cell Res **312**(5): 623-9.

Wagner, B., J. M. Ricono, et al. (2007). "Mitogenic signaling via platelet-derived growth factor beta in metanephric mesenchymal cells." J Am Soc Nephrol **18**(11): 2903-11.

Wang, J. F., X. F. Zhang, et al. (2001). "Stimulation of beta 1 integrin induces tyrosine phosphorylation of vascular endothelial growth factor receptor-3 and modulates cell migration." J Biol Chem **276**(45): 41950-7.

Weaver, V. M., O. W. Petersen, et al. (1997). "Reversion of the malignant phenotype of human breast cells in three-dimensional culture and in vivo by integrin blocking antibodies." J Cell Biol **137**(1): 231-45.

White, E. S., F. E. Baralle, et al. (2008). "New insights into form and function of fibronectin splice variants." J Pathol **216**(1): 1-14.

Wigle, J. T., N. Harvey, et al. (2002). "An essential role for Prox1 in the induction of the lymphatic endothelial cell phenotype." Embo J **21**(7): 1505-13.
Wijelath, E. S., J. Murray, et al. (2002). "Novel vascular endothelial growth factor binding domains of fibronectin enhance vascular endothelial growth factor biological activity." Circ Res **91**(1): 25-31.
Wijelath, E. S., S. Rahman, et al. (2006). "Heparin-II domain of fibronectin is a vascular endothelial growth factor-binding domain: enhancement of VEGF biological activity by a singular growth factor/matrix protein synergism." Circ Res **99**(8): 853-60.
Wilson, E., K. Sudhir, et al. (1995). "Mechanical strain of rat vascular smooth muscle cells is sensed by specific extracellular matrix/integrin interactions." J Clin Invest **96**(5): 2364-72.
Xie, S. Z., N. T. Fang, et al. (2008). "Differentiation of smooth muscle progenitor cells in peripheral blood and its application in tissue engineered blood vessels." J Zhejiang Univ Sci B **9**(12): 923-30.
Yang, J. T., B. L. Bader, et al. (1999). "Overlapping and independent functions of fibronectin receptor integrins in early mesodermal development." Dev Biol **215**(2): 264-77.
Yang, J. T., H. Rayburn, et al. (1993). "Embryonic mesodermal defects in alpha 5 integrin-deficient mice." Development **119**(4): 1093-105.
Yurchenco, P. D. and W. G. Wadsworth (2004). "Assembly and tissue functions of early embryonic laminins and netrins." Curr Opin Cell Biol **16**(5): 572-9.
Zeng, H., H. F. Dvorak, et al. (2001). "Vascular permeability factor (VPF)/vascular endothelial growth factor (VEGF) peceptor-1 down-modulates VPF/VEGF receptor-2-mediated endothelial cell proliferation, but not migration, through phosphatidylinositol 3-kinase-dependent pathways." J Biol Chem **276**(29): 26969-79.
Zhang, X., J. E. Groopman, et al. (2005). "Extracellular matrix regulates endothelial functions through interaction of VEGFR-3 and integrin alpha5beta1." J Cell Physiol **202**(1): 205-14.
Zhou, Z., M. Doi, et al. (2004). "Deletion of laminin-8 results in increased tumor neovascularization and metastasis in mice." Cancer Res **64**(12): 4059-63.